JOURNAL OF LIQUID CHROMATOGRAPHY

VOLUME 17 NUMBER 18 1994

Special Section on
CAPILLARY ZONE
ELECTROPHORESIS AND
RELATED TECHNIQUES

Edited by HALEEM J. ISSAQ
NCI-Frederick Cancer Research
& Development Center
Frederick, Maryland

JOURNAL OF LIQUID CHROMATOGRAPHY

November 1994

Aims and Scope. The journal publishes papers involving the applications of liquid chromatography to the solution of problems in all areas of science and technology, both analytical and preparative, as well as papers that deal specifically with liquid chromatography as a science within itself. Included will be thin-layer chromatography and all models of liquid chromatography.

Identification Statement. *Journal of Liquid Chromatography* (ISSN: 0148-3919) is published semimonthly except monthly in May, July, October, and December for the institutional rate of $1,350.00 and the individual rate of $675.00 by Marcel Dekker, Inc., P.O. Box 5005, Monticello, NY 12701-5185. Second Class postage paid at Monticello, NY. POSTMASTER: Send address changes to *Journal of Liquid Chromatography*, P.O. Box 5005, Monticello, NY 12701-5185.

Volume	Issues	Institutional Rate	Individual Professionals' and Student Rate	Foreign Postage		
				Surface	Airmail to Europe	Airmail to Asia
17	20	$1,350.00	$675.00	$75.00	$110.00	$130.00

Individual professionals' and student orders must be prepaid by personal check or may be charged to MasterCard, VISA, or American Express. Please mail payment with your order to: Marcel Dekker Journals, P.O. Box 5017, Monticello, New York 12701-5176.

CODEN: JLCHD8 17(18) i–vi, 3831–4064 (1994)
ISSN: 0148-3919

Printed in the U.S.A.

JOURNAL OF LIQUID CHROMATOGRAPHY

JOURNAL OF LIQUID CHROMATOGRAPHY

Indexing and Abstracting Services. Articles published in *Journal of Liquid Chromatography* are selectively indexed or abstracted in:

■ Abstracts Journal of the Institute for Scientific Information of the Russian Academy of Sciences ■ Analytical Abstracts ■ ASCA ■ Berichte Pathologie ■ BioSciences Information Service of Biological Abstracts (BIOSIS) ■ CAB International ■ Cambridge Scientific Abstracts ■ Chemical Abstracts ■ Chemical Reactions Documentation Service ■ Current Awareness in Biological Sciences ■ Current Contents/Life Sciences ■ Current Contents/Physical and Chemical Sciences ■ Engineering Index ■ Excerpta Medica ■ Physikalische Berichte ■ Reference Update ■ Saltykov-Shchedrin State Public Library ■ Science Citation Index

Manuscript Preparation and Submission. See end of issue.

This journal is also available on CD-ROM through ADONIS™ beginning with the 1991 volume year. For information contact: ADONIS, Marketing Services, P.O. Box 839, Molenwerf 1, 1000 AV Amsterdam, The Netherlands, Tel: +31-20-6842206, Fax: +31-20-6880241.

The Journals of Marcel Dekker, Inc. are available in microform form: RESEARCH PUBLICATIONS, 12 Lunar Drive, Drawer AB, Woodbridge, Connecticut, 06525, (203) 397-2600 or Toll Free 1-800-REACH-RP(732-2477). Outside North and South America: P.O. Box 45, Reading, RG1 8HF, England, 0734-583247.

Contributions to this journal are published free of charge.

Effective with Volume 6, Number 11, this journal is printed on acid-free paper.

CAPILLARY ZONE ELECTROPHORESIS AND RELATED TECHNIQUES

Edited by

Haleem J. Issaq
NCI-Frederick Cancer Research & Development Center
Frederick, Maryland

This is a special section of *Journal of Liquid Chromatography,*
Volume 17, Number 18, 1994.

MARCEL DEKKER, INC. New York, Basel, Hong Kong

JOURNAL OF LIQUID CHROMATOGRAPHY, 17(18), 3831-3846 (1994)

PERFORMANCE OF ZWITTERIONIC AND CATIONIC FLUOROSURFACTANTS AS BUFFER ADDITIVES FOR CAPILLARY ELECTROPHORESIS OF PROTEINS

Å. EMMER AND J. ROERAADE
Royal Institute of Technology
Department of Chemistry, Analytical Chemistry
S-100 44 Stockholm, Sweden

ABSTRACT

In this work, a study has been made of the performance of a zwitterionic fluorosurfactant and mixtures of a zwitterionic and a cationic fluorosurfactant, when used as buffer additives in capillary electrophoresis. Thus, it showed to be possible to change the direction of the electroosmotic flow by changing the pH of the buffer solution. Possible mechanisms for the behaviour of the electroosmotic flow at different pH and when using different surfactant combinations are suggested.
High efficiency separations of some model proteins can be obtained, when a mixture of a cationic and a zwitterionic fluorosurfactant is added to the running buffer solution. By changing concentration proportions between the surfactants, a change in separation selectivity is obtained. This procedure provides an alternative way for selectivity tuning in protein separations by capillary electrophoresis.

INTRODUCTION

Capillary electrophoresis has been recognized as a highly promising tool for separation of biomolecules, and a considerable effort has been made to improve the performance of this technique. In particular, separation of proteins has been a target object of several research groups (*e.g.*1). One of the most important problems recognized in this context has been the tendency of proteins to adhere onto the capillary inner wall. This leads to a severe degradation of the separation performance, and in some cases, even an irreversible adsorption of solutes can occur.

Several methods for suppression of protein adsorption have been proposed. A variety of permanent wall coatings, with the purpose of shielding the silanol groups of the silica surface have been presented (*e.g.* 2-10). However, the drawbacks of permanent wall coatings include time consuming and labourious procedures, sensitivity towards buffer pH extremes, and limited column life time.

An alternative to permanent coatings is the use of a running buffer with a high salt concentration, where the increased ionic strength leads to a competitive interaction with the negative sites of the wall (11). Other means to decrease adsorption problems are to use either a low buffer pH, resulting in a more neutral wall charge, as the silanols are protonized (12), or a high buffer pH, leading to a negative charge of both the wall and the solutes, which counteracts wall interactions by electrostatic repulsion (13). However, the use of extreme buffer pH values or buffers with a high ionic strength can cause either protein denaturation, or excessive electric currents and joule heating.

Previously, we have presented a concept where a cationic fluorosurfactant was employed as a buffer additive. The fluorosurfactant

forms an admicellar bilayer. This leads to a charge reversal and an electrostatic repulsion of positively charged proteins from the wall. A considerable improvement in protein bandshapes, separation efficiencies and reproducibility was obtained. (14, 15).

An interesting possibility to decrease adsorbtion, is by using of zwitterions as additives to the running buffer. Such compounds have a similar effect as adding salts, however without causing the drawback of an increased electrical conductivity (16-18). Zwitterions have also been incorporated in polyacrylamide layers of wall coated capillaries (19). The unique characteristics of zwitterions in addition to our encouraging earlier results obtained with fluorosurfactants, initiated the present study, where the behaviour of a zwitterionic fluorosurfactant as well as combinations of fluorosurfactants as a buffer additive was investigated.

EXPERIMENTAL

A custom made CZE apparatus, which is described elsewhere (14), was used. A UV-detector (Model 200, Linear Instruments, Reno, NV, USA), including a capillary cell (model 9550-0155, Linear Instruments) was employed for on-column detection. Injections were carried out by timer-controlled electromigration. Prior to use, new capillaries (fused silica, 50 μm ID, *ca.* 60 cm total length, and 50 cm length from the injection point to the detection window) were flushed with 0.4M NaOH for 30 min - 1 hour and then to neutrality with water, and finally with running buffer for 20 minutes. When a change between buffers of different compositions was made, the capillary was rinsed for 20 minutes with the new buffer. In some cases, a stabilization of the surface conditions was obtained by applying a voltage (20kV) across the capillary for 20 minutes. The cationic surfactant FC134 -

($C_8F_{17}O_2NH(CH_2)_3N^+(CH_3)_3I^-$) (3M Company, St. Paul, MN, USA) and the zwitterionic fluorosurfactant - ($F(CF_2CF_2)_{3-8}CH_2CH(OCOCH_3)CH_2N^+(CH_3)_2CH_2CO_2^-$) (Dupont, Wilmington, DE, USA) were added to the running buffer, either as individual additives or in different combinations, at concentrations ranging between 10 and 400 μm/ml. The model proteins myoglobin, ribonuclease, trypsinogen and lysozyme (Sigma, St. Louis, MO, USA) were used in concentrations between 0.02 mg/ml and 0.04 mg/ml each. The total protein concentration of the samples was kept below 0.2 mg/ml.

RESULTS AND DISCUSSION

The proposed mechanism, causing the effective reduction of protein adsorption, when a cationic fluorosurfactant (FC134) is added to the running buffer has been described earlier (14, 15). One of the important characteristics of this additive is the formation of an admicellar bilayer at the capillary wall surface. This leads to a positively charged wall , which will repell positively charged solutes. The use of a zwitterionic fluorosurfactant presents opportunities to change the magnitude and sign of the charge on the wall, by changing the buffer pH. This drastically influences the electroosmotic flow (EOF) and associated separation characteristics, as will be shown below.

To determine the pI of the zwitterionic fluorosurfactant, the electrophoretic migration time of a neutral compound (mesityl oxide) was determined in a series of experiments, where buffers with different pH values, containing the surfactant, were used. The pI showed to be around 8 (figure 1). When a negative potential is applied at the inlet side of the capillary, and the pH is kept below 8, the EOF is in the direction from the

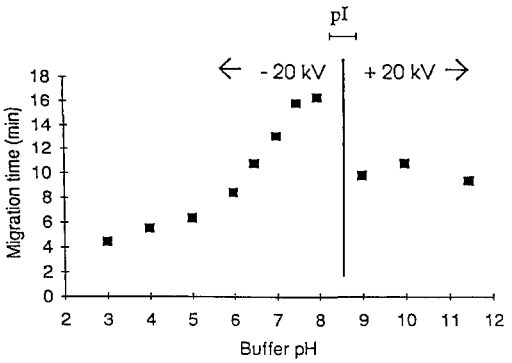

FIGURE 1. Migration time of mesityloxide *vs.* buffer pH.
200 µg/ml zwitterionic fluorosurfactant added to the running buffer.
Applied voltage: -20 kV (pH3-8), +20 kV (pH 9-11.5).

cathode to the anode. The EOF decreases with increased pH, since the positive charge of the zwitterion is decreasing. Above pH 8 , the zwitterion changes sign of charge, and the compound will then behave as an anionic additive. At this point the electroendosmotic flow reverses towards the direction of the cathode.

Recently, we observed that combinations of different fluorosurfactants added to the running buffer can be used to influence the separation selectivity between different proteins (20). This gave raise to the question how different mixtures of the zwitterionic and the cationic fluorosurfactant, used at different buffer pH, would influence the electroendosmosis, the separation selectivity and protein peak shapes.

In a first study, the migration time for mesityl oxide was measured as a function of the buffer pH, where a mixture of the cationic and the zwitterionic fluorosurfactant had been added. The results are shown in

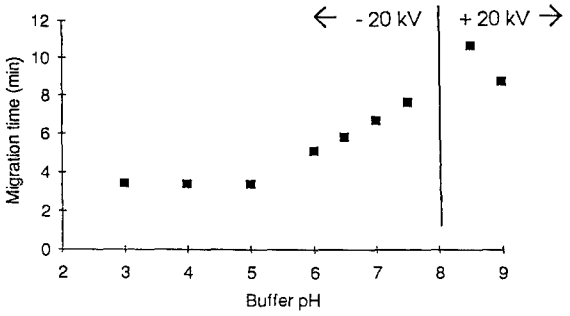

FIGURE 2. Migration time of mesityloxide *vs.* buffer pH.
100 µg/ml zwitterionic fluorosurfactant and 50 µg/ml cationic fluorosurfactant (FC 134) added to the running buffer.
Applied voltage: -20 kV (pH 3-8), +20 kV (pH 8.5-9).

figure 2, and it can be seen that the turnover pH for flow reversal is the same as in the case where only the zwitterion was added (*c.f.* fig. 1). However, in the range between pH 3 and pH 8, the use of the surfactant mixture resulted in a more constant and also higher electroosmotic flow rate (as can be observed from the migration data in fig. 2). It is fairly obvious that these results are related to the behaviour of the surfactant bilayer on the capillary wall. An increased charge density is obtained when the cationic compound is added to the zwitterion. This explains the differences in migration rates between the results shown in fig. 1 and 2. Also, the zwitterion rapidly loses charge, as the pH is raised from 3 to 8. In the case where the cationic surfactant is also present, the charge at the wall will be more dense and stable, until a pH is reached, where negative charges from the zwitterion begin to interact with the quarternary ammonium group of the cationic surfactant.

Figure 3 shows a proposed model for the appearance of the bilayers at different pH conditions.

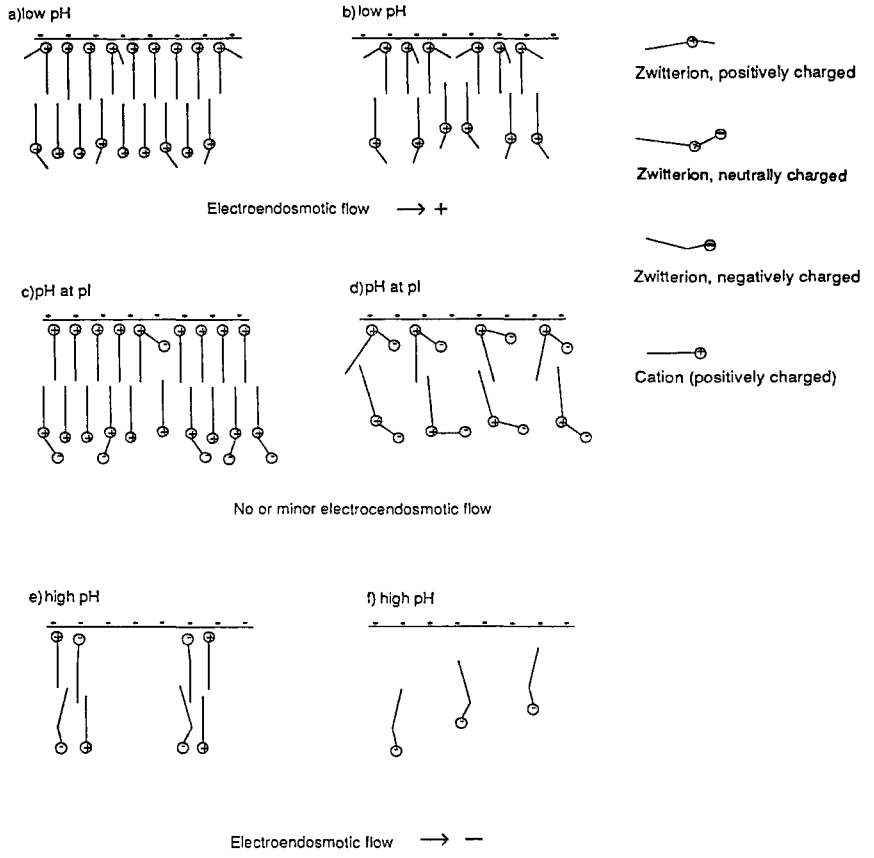

FIGURE 3. Proposed models for adhered layers of fluorosurfactants on a silica wall.
a, c and e) : buffer solution containing a cationic and a zwitterionic fluorosurfactant. b, d and f) : buffer solution where only a zwitterionic fluorosurfactant is added. a and b) : The pH of the buffer is below the isoelectric point of the zwitterion.
c and d: The pH of the buffer is at or near the isoelectric point of the zwitterion. e and f: The pH of the buffer is above the isoelectric point of the zwitterion.

In subsequent investigations, the influence of having different proportions of the two fluorosurfactants on the magnitude of the EOF was examined. In all experiments, a mixture of the two surfactants was employed, where the concentration of either one of the two compounds was varied, while the concentration of the other fluorosurfactant was kept constant. The migration speed of mesityl oxide was measured at pH 7, (where both surfactants are positively charged). At this pH value, an increased concentration of zwitterion surfactant resulted in longer migration times (a decrease of the EOF). On the other hand, a constant concentration of the zwitterion and a increase of the cationic surfactant FC134 resulted in shorter migration times. The results are shown in table 1. The obtained results can be explained in the following way: At pH 7, the cationic surfactant FC134 has a higher net positive charge then the zwitterion, which has lost a large part of its positive charge at this pH value. If the relative amount of cationic fluorosurfactant is increased, the positive charge of the bilayer at the wall will increase, which leads to an increased electroendosmotic flow.

At pH 9, the two surfactants are oppositely charged, which results in a more complex behaviour of the mixture. It has been suggested that cationic surfactants will co-adsorb together with anionic surfactants from such mixtures and form ion pairs onto a negatively charged surface (21-23, figure 3 e). Thus, when adding the cationic surfactant to a solution, containing the zwitterionic surfactant, a form of " charge-buffering" action is obtained. This suggestion corresponds well with the results obtained from the experiments (table 2 - upper part). A progressive increase of cationic surfactant did not influence the EOF to an appreciable extent, as long as a sufficient excess of the zwitterion was present.

When the concentration of the cationic surfactant was kept constant, and the concentration of the zwitterion was changed, the results obtained were

TABLE 1
Migration Times for Mesityl Oxide Using Different Concentrations of Fluorosurfactant Buffer Additives.

Concentration of cationic fluorosurfactant (μg/ml)	Migration time for mesityl oxide (min)
10	8.7
25	7.4
50	6.2
Concentration of zwitterionic fluorosurfactant (μg/ml)	**Migration time for mesityl oxide (min)**
25	5.6
100	6.2
400	7.0

Buffer pH = 7
Upper part of the table: Different cationic fluorosurfactant concentrations, while the zwitterionic fluorosurfactant concentration was 100 μg/ml in all experiments.
Lower part of the table: Different zwitterionic fluorosurfactant concentrations, while the cationic fluorosurfactant concentration was 50 μg/ml.
The applied voltage was- 20 kV.

significantly different (table 2 - lower part). At present, we have only a partial explanation for this behaviour. It is known that a mixture of oppositely charged fluorosurfactants behaves in a non-ideal way, which makes it difficult to predict the influences of surfactant concentration changes on the EOF. It is known for example (21) that the critical micellar concentration (CMC) for such mixtures is considerably lower than the average value, calculated from the CMC values of the individual components. Also, there can be a difference in composition between the micelles, the bilayer at the wall, and the free monomer solution (24-29).

TABLE 2
Migration Times for Mesityl Oxide When Different Concentrations of Fluorosurfactant were Added to the Running Buffer.

Concentration of cationic fluorosurfactant (μg/ml)	Migration time for mesityl oxide (min)
10	7.6
25	7.5
50	7.9
Concentration of zwitterionic fluorosurfactant (μg/ml)	**Migration time for mesityl oxide (min)**
25	9.2
100	7.9
400	10.2

Buffer pH=9
Upper part of the table: Different cationic fluorosurfactant concentrations, while the zwitterionic fluorosurfactant concentration was 100 μg/ml in all experiments.
Lower part of the table: Different zwitterionic fluorosurfactant concentrations, while the cationic fluorosurfactant concentration was 50 μg/ml.
The applied voltage was + 20 kV.

These differences in distribution of the surfactants can change, as the proportions between the individual surfactants are altered.

In view of the results obtained, it was of interest to investigate, how the presence of the fluorosurfactants would influence the CE separation behaviour of proteins. Thus, evaluations, using some model proteins (table 3) were carried out in presence of either the zwitterionic fluorosurfactant, or a combination of the cationic and the zwitterionic surfactant.

Figure 4a, b and c show the electropherograms recorded at pH 3, 4 and 5 respectively in presence of the zwitterionic fluorosurfactant. Significant differences in selectivity can be noted. However, the separation efficiency

TABLE 3
Characteristics of the Four Model Proteins.

Protein	Isoelectric point (pI)	Molecular weight (Mw)
Myoglobin	7.4	17 000
Trypsinogen	9	24 000
Ribonuclease	9.6	13 700
Lysozyme	11	14 300

does not exceed 60.000 theoretical plates, which is considerably below the efficiencies, that were obtained in an earlier study (14), where we used the cationic fluorosurfactant as an additive. We attribute the inferior efficiency to the lower density and charge of the admicellar bilayer of zwitterions. As the pH increases, the charge and bilayer density will be further reduced, and wall interactions become more pronounced. This can also be part of the cause for the decrease of the peak height for the most basic protein, lysozyme, at pH 5. (fig. 4 c)

Considerably improved results can be obtained when combinations of the zwitterionic and the cationic surfactant FC 134 are added to the running buffer. However, a concentration of not less then ca 50 µg/ml FC 134 is needed to obtain a sufficiently dense admicellar bilayer. An initial trial with a low FC 134 concentration (10 µg/ml) did not give satisfactory results (figure 5 a). The separation between the trypsinogen and ribonuclease was poor, and the separation efficiency was moderate. When the FC 134 concentration was increased to 50 µg/ml, a distinct improvement of both the selectivity and the efficiency was obtained (ca 200 000 theoretical plates). By changing the concentration of the zwitterion, the selectivity of the separation can be influenced, while the pH of the buffer is kept at a constant value (figure 5 b - d).

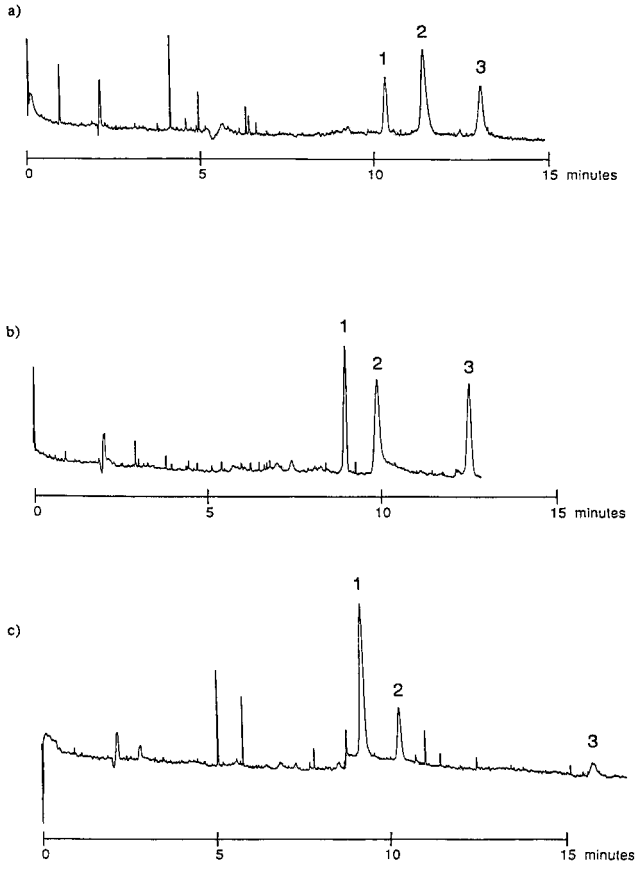

FIGURE 4. Electropherograms of model proteins in presence of the zwitterionic fluorosurfactant at different buffer pH.
a) pH 3, b) pH 4, c) pH 5. Zwitterion concentration: 200 μg/ml. Running buffer: 0.02 M phosphate. Applied voltage: -20 kV. Injection: Electromigration at 10 kV for 10 sec. Total protein concentration: 0.2 mg/ml. Wavelength: 210 nm.Compounds: 1. Myoglobin. 2. Ribonuclease. 3. Lysozyme.

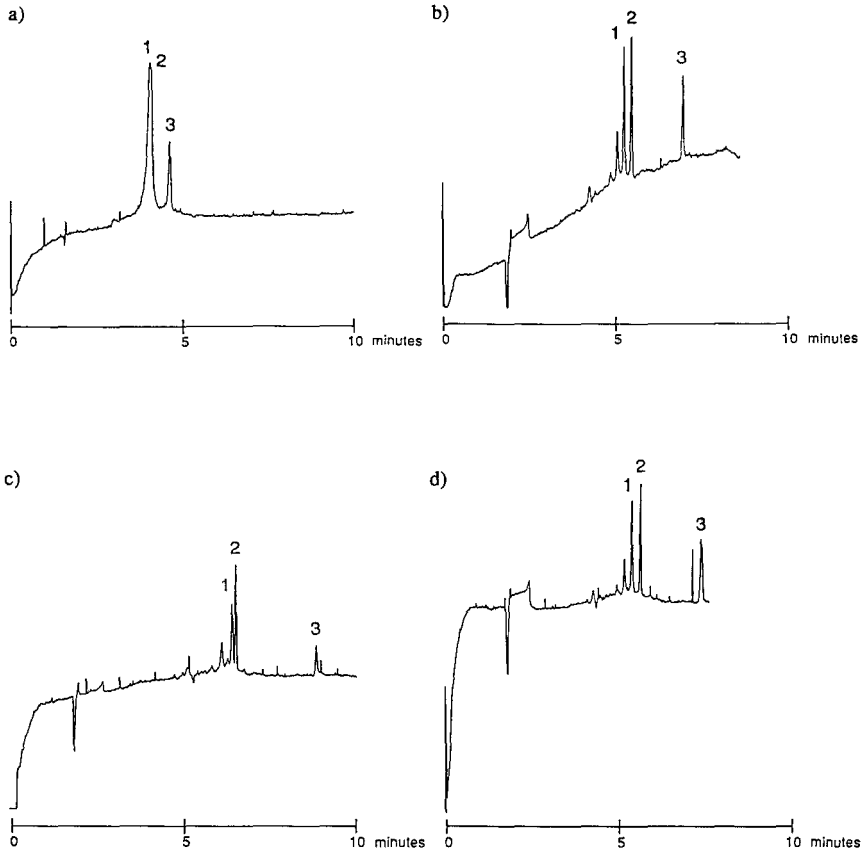

FIGURE 5. Electropherograms of model proteins in presence of a zwitterionic and a cationic fluorosurfactant
a) Concentration of the zwitterion: 100 µg/ml, Concentration of the cation: 10µg/ml. b) Concentration of the zwitterion: 25 µg/ml, Concentration of the cation: 50µg/ml. c) Concentration of the zwitterion: 100 µg/ml, Concentration of the cation: 50µg/ml. d) Concentration of the zwitterion: 400 µg/ml. Concentration of the cation: 50µg/ml. Running buffer: 0.01 M phosphate buffer at pH 4. Other conditions as in fig. 4. Compounds: 1. Trypsinogen. 2. Ribonuclease. 3. Lysozyme.

When comparing with results from our earlier work (14), where only the cationic fluorosurfactant FC 134 was added to the buffer, we found that the reproducibility of the migration times was lower, when surfactant mixtures were utilized. The migration time reproducibility of the separations in the present work are ca 2 - 3 % RSD. One of the reasons for this may be that the mixed systems are more sensitive to small pH changes. It should also be pointed out that the employed electrophoretic system did not have possibilities for temperature control or automated injection. It is likely, that the reproducibility can be improved by utilizing such facilities.

In conclusion, it showed to be possible to change the direction of the electroosmotic flow by a change of buffer pH, if a zwitterionic fluorosurfactant is added to the running buffer. This can also be accomplished when a mixture of a zwitterionic and a cationic fluorosurfactant are utilized.

A high separation efficiency and short migration times can be obtained for some basic proteins, when mixtures of the fluorosurfactants are employed as buffer additives zwitterionic fluorosurfactant. In this context, a number of issues, like quantitative aspects, interaction of the fluorosurfactants with the proteins etc. still need to be further investigated. However, we have shown that the separation selectivity can be tuned at a particular pH, by changing the individual concentrations of the additives. This charge-tuning method should provide new possibilities for optimization of protein separations.

ACKNOWLEDGEMENTS

Dr. Per Claesson from the Swedish Institute for Surface Chemistry, Stockholm, Sweden is greatfully acknowledged for valuable suggestions and stimulating discussions.

This work was financially supported by the Swedish Natural Science Research Council and the Swedish Board for Technical Development.

REFERENCES

1. Z. El Rassi and W. Nashabeh in Capillary Electrophoresis Technology, N.A. Guzman, ed., Marcel Dekker, New York, 1993, pp. 383-434.

2. S. Hjertén, J. Chromatogr., 347; 191-198 (1985).

3. Y.-F. Maa, K.J. Hyver and S.A. Swedberg, J. High Resolut. Chromatogr., 14; 65-67 (1991).

4. J.K. Towns and F.E. Regnier, J. Chromatogr., 516; 69-78 (1990).

5. J.W. Jorgenson and K.D. Lukacs, Science, 222; 266-272 (1983).

6. X.-W. Yao, D. Wu and F.E. Regnier, J. Chromatogr., 636; 21-29 (1993).

7. K.A. Cobb, V. Dolnik and M. Novotny, Anal. Chem., 62; 2478-2493 (1990).

8. J. Kohr and H. Engelhardt, J. Microcol. Sep., 3; 491-495 (1991).

9. J.T.Smith and Z. El Rassi, Electrophoresis, 14; 396-406 (1993).

10. A. Malik, Z. Zhao and M.L. Lee, J. Microcol. Sep., 5; 119-125 (1993).

11. J.S. Green and J.W. Jorgenson, J. Chromatogr., 478; 63-70 (1989).

12. R.M. McCormick, Anal. Chem., 60; 2322-2328 (1988).

13. H.H. Lauer and D. McManigill, Anal. Chem., 58; 166-170 (1986).

14. Å. Emmer, M. Jansson and J. Roeraade, J. Chromatogr., 547; 544-550 (1991).

15. Å. Emmer, M. Jansson and J. Roeraade, J. High Resolut. Chromatogr., 14; 738-740 (1991).

16. M.M. Bushey and J.W. Jorgenson, J. Chromatogr., 480; 301-310 (1989).

17. G. Mandrup, J. Chromatogr., 604; 267-281 (1992).

18. N.E. Astephen and T.E. Wheat, Poster M18 presented at HPCE'92, February 9-13, 1992, Amsterdam, The Netherlands.

19. M.A. Strege and A.L.Lagu, J. Liq. Chromatogr., 6; 51-68 (1993).

20. Å. Emmer, M. Jansson and J. Roeraade, Accepted for publication in J. Chromatogr.

21. J.H. Harwell and J.F. Scamehorn in Mixed Surfactant Systems, K. Ogino, M. Abe, eds., Marcel Dekker, New York, 1993, pp.263-281.

22. Z.Huang, Z. Yan and T. Gu, Colloids Surfaces, 36; 353-358 (1989).

23. M.J. Schwuger, Kolloid Z. Z. Polym., 243; 129-135 (1971).

24. P.K Jana and S.P. Moulik, J. Phys. Chem., 95; 9525-9532 (1991).

25. M. Abe and K. Ogino in Mixed Surfactant Systems, K. Ogino, M. Abe, eds., Marcel Dekker, New York, 1993, pp.1-21.

26. A.P. Graciaa, M.B. Ghoulam, G. Marion and J. Lachaise, J. Phys. Chem., 93; 4167-4173 (1989).

27. B.T. Ingram and R.H. Ottewill in Cationic Surfactants, Physical Chemistry, D.N.Rubingh, P.M. Holland, eds., Marcel Dekker, New York, 1991, pp.87-140.

28. P.M. Holland and D.N. Rubingh in Cationic Surfactants, Physical Chemistry, D.N.Rubingh, P.M. Holland, eds., Marcel Dekker, New York, 1991, pp.141-187.

29. J.F. Scamehorn in Phenomena in mixed surfactant systems, J.F. Scamehorn, ed., ACS Symposium Series vol. 311, 1986, pp.1-27.

Received: March 31, 1994
Accepted: April 5, 1994

JOURNAL OF LIQUID CHROMATOGRAPHY, 17(18), 3847-3857 (1994)

SEPARATION OF TAMOXIFEN AND METABOLITES BY CAPILLARY ELECTROPHORESIS WITH NON-AQUEOUS BUFFER SYSTEM

C. L. NG, H. K. LEE, AND S. F. Y. LI*
Department of Chemistry
National University of Singapore
Kent Ridge Crescent
Singapore (0511), Republic of Singapore

ABSTRACT

Tamoxifen and its metabolites were separated using a non-aqueous mobile phase consisting of ammonium acetate and a mixture of organic solvents, namely, methanol and acetonitrile. The effects of using other organic salts as the conducting medium and varying the composition of the mixture of acetonitrile and methanol on the separation were also investigated. Optimum separation was obtained by using 25 mM ammonium acetate in a 50:50 acetonitrile/ methanol mixture. High efficiency separations and short analysis times of less than 8 min were obtained. The reproducibility of migration time was better than 0.4 %. The detection limits of tamoxifen and its metabolites were less than 40 pg.

INTRODUCTION

Tamoxifen, a non-steroidal anti-estrogen, has been used extensively in the treatment of breast cancer in humans over a decade [1]. Tamoxifen forms several metabolites in the body, the major metabolite being N-desmethyltamoxifen. The structures of tamoxifen and its major metabolites are depicted in Fig 1.

The widespread use of tamoxifen has stimulated efforts to develop routine assays for this drug and its metabolites. Established HPLC assays involved the use of high percentage of

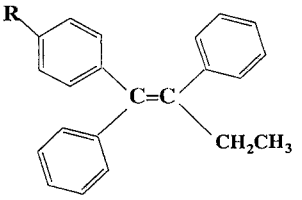

No.	COMPOUND	R
1	N-Desmethyltamoxifen	OCH_2CH_2NHMe
2	N-Desdimethyltamoxifen	$OCH_2CH_2NH_2$
3	Tamoxifen	$OCH_2CH_2NMe_2$
4	Metabolite Y	OCH_2CH_2OH
5	Metabolite E	OH

Fig 1 : Structures of tamoxifen and its metabolites.

organic solvents, high flow rates and long analysis times (> 50 min) owing to the hydrophobic properties of the analytes [2-6]. In some instances, ion-pairing reagents were added to improve selectivity [7]. Capillary gas chromatography with mass spectroscopic detection (GC-MS) was also used for the analysis of tamoxifens [8-9], but the major disadvantage was the need for analyte pre-derivatization before analysis.

Capillary electrophoresis (CE) has been used for pharmaceutical analysis such as the determination of components in drug formulations [10-11] and the monitoring of drugs in body fluids [12-13]. The use of CE for the analysis of tamoxifen and its metabolites has not been described previously and would pose as a challenge for the following reasons. Firstly, tamoxifen and its metabolites are very hydrophobic and hence there exists a solubility problem in aqueous buffers. Secondly, due to the similarity in structures between the tamoxifens, commonly used electrophoretic buffers would not be expected to provide adequate selectivity for their separation. Acetonitrile, methanol and ethanol have been added into the electrophoretic medium to increase the solubility of the analytes in the separation buffer as well as to increase the migration window in CE [14-15]. The disadvantage of using this type of system is the long analysis times attributable to the reduction in electroosmotic flow.

Recently, the use of a non-aqueous buffer solution for the separation of some anti-tumor agents has been reported by Naylor and co-workers [16]. In this approach, a totally organic

mobile phase such as methanol containing ammonium acetate as the electrolyte was used. An advantage of using CE with a non-aqueous medium for pharmacokinetic studies is the small sample requirement and the ability of such a system to perform sample preconcentration to increase sensitivity [16]. Furthermore, a totally organic mobile phase would allow the separation system to be conveniently coupled to a mass spectroscopic detector.

In this work, optimum conditions based on the use of a totally organic separation medium was determined for the separation of tamoxifen and some of its major metabolites. In addition, the effects of various organic salts and different compositions of organic mixtures used in the electrophoretic medium on the separation were investigated.

EXPERIMENTAL

A home-built CE system was used to conduct the experiments. An Isco Model CV^4 UV detector (Lincoln, NE, USA) with wavelength set at 254 nm was employed for the detection of peaks. Chromatographic data were collected with a Hewlett Packard Model 3394A integrator (Avondale, Palo Alto, USA) or a Perkin Elmer Model R100 chart recorder (Illinois, USA). A Spellman Model CZE1000R220 high power voltage supply (Plainview, NY, USA) capable of delivering up to 30 kV (with reversible polarity) and fused silica capillaries obtained from Polymicro Technologies (Phoenix, AZ, USA) of dimension 50 μm i.d., 44 cm effective length and 55 cm overall length were used in the experiments.

Tamoxifen ([Z]-1-[p-dimethylaminoethoxyphenyl]-1,2-diphenyl-1-butene) and its metabolites N-desdimethyltamoxifen, N-desmethyltamoxifen, metabolite E and metabolite Y were synthesized by colleagues from the same department. Standards were used without further purification. Sample solutions were prepared in the concentration range of 150-200 μg/mL. The structures of tamoxifen and the metabolites are shown in Fig 1.

Ammonium acetate, tetrabutylammonium bromide, tetrabutylammonium hydrogen sulphate and tetrapentylammonium bromide were obtained from Sigma Chemical Comapny (St Louis, MO, USA). The ammonium salts were first dissolved in methanol and appropriate volumes of acetonitrile were subsequently added to the required percentage (v/v). The two buffer reservoirs were capped to prevent evaporation. Methanol and acetonitrile of HPLC grade were purchased from BDH (Poole, England). Sample was injected at a height of 5 cm for 10 sec. The volume of injection was calculated to be 4 nL by using the equation [17] :

$$q = (\rho g \Pi r^4 \Delta h t_i) / (8 \eta L)$$

where q is the amount injected, ρ is the density of the sample solution, g is the acceleration due to gravity, r is the radius of the capillary column, Δh is the injection height (5 cm) raised and t_i is the time of injection, η is the viscosity of the sample solution and L is the length of the column.

RESULTS AND DISCUSSION

Since the tamoxifens are hydrophobic in nature and neutral at all pH conditions, they would not be expected to be separated by varying the buffer pH alone. In fact, even with the addition of SDS (MEKC) and γ-cyclodextrin to the micellar solution (γ-cyclodextrin modified MEKC), only a single peak was observed, as shown in Fig 2(a) and (b). This could be due to the similarity of the structures of tamoxifen and its metabolites. The addition of organic modifiers into the electrophoretic buffer has been shown to decrease electroosmotic flow and increase solubility of sample components in the electrophoretic buffer [14-15]. The effect of adding 10 % (v/v) of acetonitrile into a electrophoretic buffer consisting of SDS and γ-cyclodextrin is shown in Fig 2(c). Although there is an improvement in resolution, the peaks observed were broad and the total analysis time was increased to more than 20 mins.

Since tamoxifen and its metabolites are more readily soluble in organic solvents, the use of a non-aqueous separation buffer was considered. When 25 mM ammonium acetate was added to 100 % methanol to form the electrophoretic medium, the peaks were better resolved but analysis times were long (ca 30 min) and the peaks were broad. Based on the consideration that acetonitrile is a better solvent for the tamoxifens and its viscosity is less than methanol, the addition of acetonitrile was expected to shorten the migration times. The effect of varying the percentage of acetonitrile in methanol on the migration times of the tamoxifens is illustrated in Fig 3. From the plot, it can be observed that a marked decrease in migration times of the tamoxifens was observed after the addition of 5 % acetonitrile. The sharp decrease in migration time could be partly due to a drop in viscosity of the electrophoretic medium. Another reason could be that the solutes are more soluble in acetonitrile than in methanol, thus the addition of acetonitrile increased solubility of the analytes in the separation medium. Increase in acetonitrile concentration above 50 % resulted in a more gradual decrease in migration time. At 50 % acetonitrile, satisfactory separation was achieved. The use of 100 % acetonitrile as the separating medium was attempted without success since the solubility of ammonium acetate in acetonitrile was too low.

The effect of varying concentrations of ammonium acetate on the migration time and separation is shown in Fig 4. Increasing the concentration of ammonium acetate increased

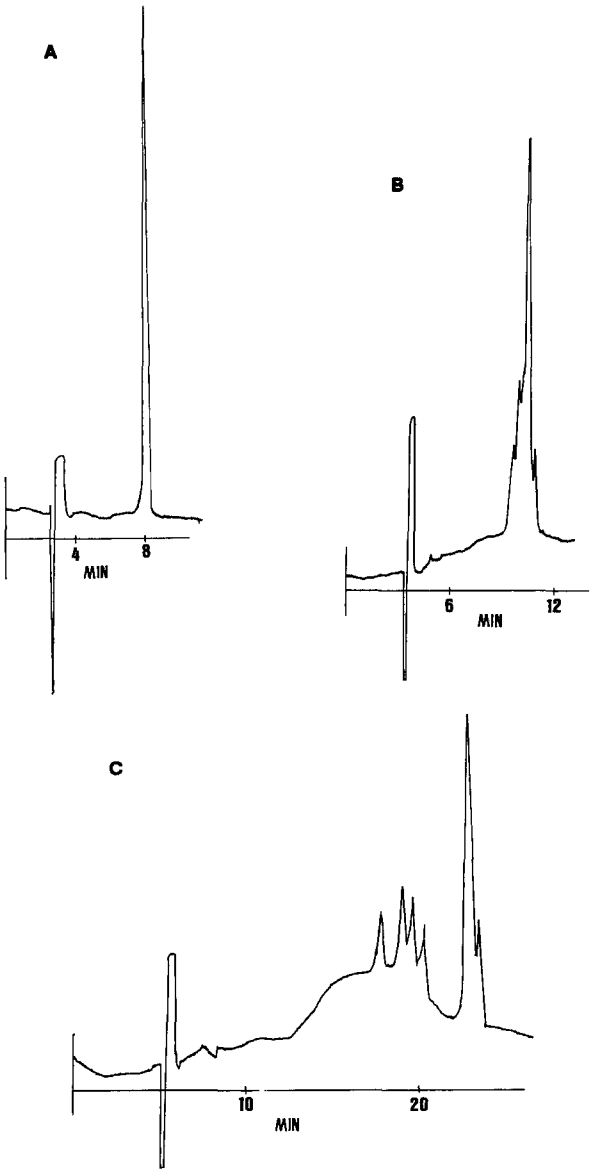

Fig 2 : Typical electropherogram of the separation of tamoxifen and its metabolites.
Electrophoretic conditions :
(a) 25 mM phosphate / borate at pH 8.0 and 50 mM SDS; voltage : 18 kV; detection wavelength : 254 nm; column : 50 µm i.d. fused silica, 44 cm effective length and 55 cm overall length.
(b) 25 mM phosphate / borate at pH 8.0, 60 mM SDS and 20 mM γ-cyclodextrin. Other conditions as in (a).
(c) 25 mM phosphate/ borate at pH 8.0, 60 mM SDS, 20 mM γ-cyclodextrin and 10 % acetonitrile; voltage : 14 kV. Other conditions as in (a).

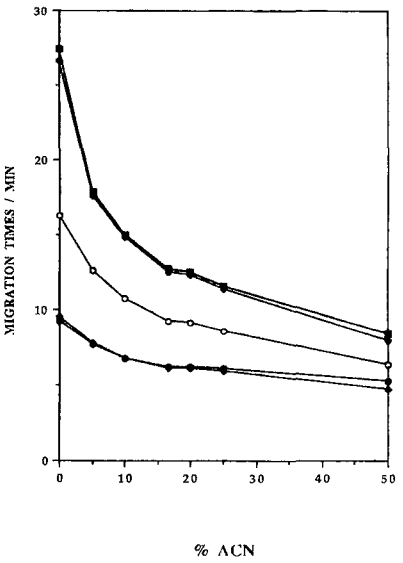

Fig 3 : Variation of migration time with percentage of acetonitrile in methanol
Legend : ♦ : N-desmethyltamoxifen; ● : N-desdimethyltamoxifen; o : tamoxifen; ◇ : metabolite Y; ■ : metabolite E.
Electrophoretic conditions : 25 mM ammonium acetate in organic buffer of varying acetonitrile in methanol. Other conditions as in Fig 2(a).

the ionic strength of the separation medium. It has been shown that electroosmotic flow decreased with increase in ionic strength [15], which subsequently led to longer migration times. No further improvement in resolution was obtained with the addition of more than 25 mM of ammonium acetate. Hence, the optimum separation condition of 25 mM ammonium acetate in 50:50 % acetonitrile / methanol was chosen which offered the best separation and shortest analysis time. A typical electropherogram obtained in such a condition is shown in Fig 5. Analytes which contain hydroxyl groups, such as metabolites E and Y, exhibited stronger interactions with methanol, and thus migrated out later. Efficiencies for this system ranged from 140 000 to 240 000 plates per meter whereas in typical HPLC analysis, the number of theoretical plates would be less than 4000. Another advantage of using the non-aqueous medium is the low current observed which resulted in reduced Joule heating, and consequently, less peak broadening. Reproducibilities in migration times was better than 0.4 % over 5 consecutive runs. The effect of various organic salts on the selectivity was also

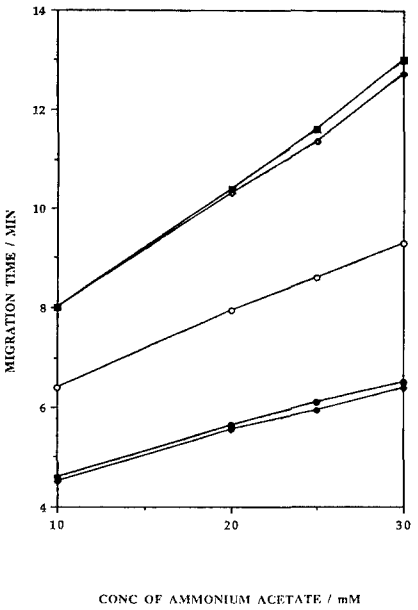

Fig 4 : Variation of migration time with concentration of ammonium acetate.
Legend : ♦ : N-desmethyltamoxifen; ● : N-desdimethyltamoxifen; ○ : tamoxifen; ◇ : metabolite Y; ■ : metabolite E.
Electrophoretic conditions : varying concentration of ammonium acetate in 25:75 (v/v) % acetonitrile:methanol mixture. Other conditions as in Fig 2(a).

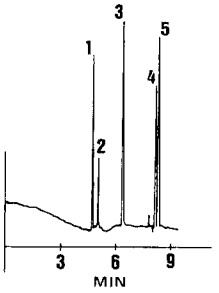

Fig 5 : A typical electropherogram of tamoxifen and its metabolites.
Electrophoretic conditions : 25 mM ammonium acetate in 50:50 acetonitrile:methanol. Other conditions as in Fig 2(a).
Peak identification : 1 : N-desmethyltamoxifen; 2 : N-desdimethyltamoxifen; 3 : tamoxifen; 4 : metabolite Y; 5 : metabolite E.

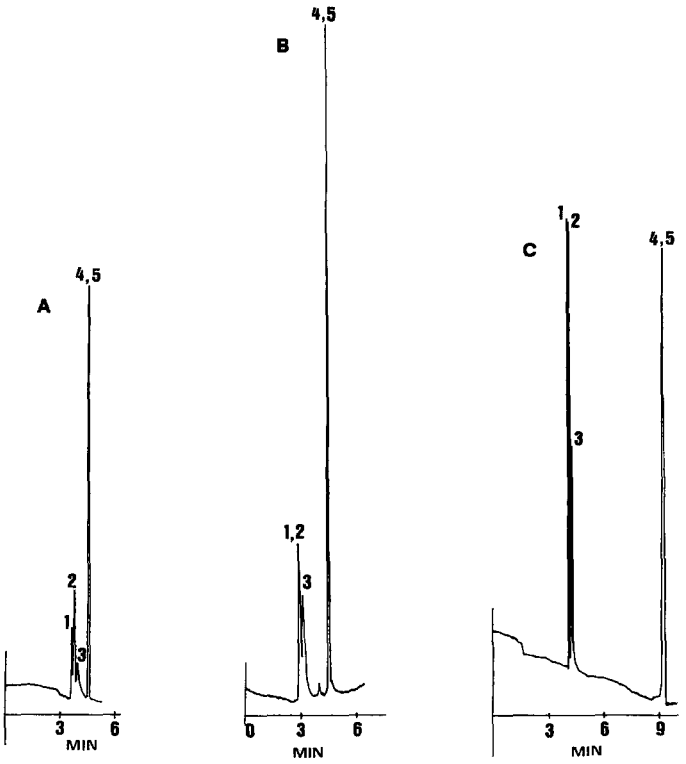

Fig 6 : Comparison of different organic salts on the selectivity and efficiency.
(a) tetrabutylammonium bromide
(b) tetrapentylammonium bromide
(c) tetrabutylammonium hydrogen sulphate
Electrophoretic conditions : 20 mM of the organic salts in 33:67 acetonitrile:methanol. Other conditions as in Fig 2(a). Peak identification as in Fig 5.

investigated. Instead of ammonium acetate, three other salts ie, tetrabutylammonium bromide, tetrabutylammonium hydrogen sulphate and tetrapentylammonium bromide were used. Typical electropherograms obtained using different salts are shown in Fig 6. Fig 6(a) and (b) show the electropherograms obtained using tetrabutylammonium bromide and tetrapentylammonium bromide. It was observed that although short analysis times were obtained, slight peak tailing and broadening were evident. In Fig 6(a) and (c), where the only difference is the presence of different anions in the buffer, tetrabutylammonium hydrogen

TABLE I

Detection Limits of Tamoxifen and Its Metabolites.

No.	Compound	Detection Limit*	
		pg	ppm
1.	N-desmethyltamoxifen	4	1
2.	N-desdimethyltamoxifen	20	5
3.	Tamoxifen	8	2
4.	Metabolite Y	40	10
5.	Metabolite E	8	2

* based on S/N = 2

sulphate seemed to offer slightly higher efficiency separations than tetrabutylammonium bromide. However, none of the tetra-alkylammonium salts provided selectivity as high as that obtained by ammonium acetate.

The detection limits for tamoxifen and it metabolites were determined and the results are tabulated in Table I. Although the concentration detection limit were only in the 1-10 ppm range, the mass sensitivity was higher than those obtained by HPLC with post column derivatization and fluorescence detection (50-500 pg) [2,3], UV detection (5 ng) [18], GC-MS (200 pg) [19] or recently, electrochemical detection (50-100 pg) [6].

CONCLUSION

A non-aqueous electrophoretic separation medium was employed for the separation of tamoxifen and its metabolites. Different organic solvents or a mixture of them and various organic salts could be used for the separation. High efficiencies, short analysis times and relatively low detection limits were obtained. The sensitivity and specificity of the system, the use of low volume of sample and the possiblity of coupling this technique to mass spectroscopic detection makes CE potentially a very powerful technique for the analysis of pharmaceuticals and their metabolites.

ACKNOWLEDGMENTS

The authors thank the National University of Singapore for financial support and Associate Professor K.Y. Sim for the supply of the tamoxifen samples.

REFERENCES

1. B.J.A. Furr, V.C. Jordan, Pharmacol. Ther., 25: 127-205 (1984)

2. R.R. Brown, R. Bain and V.C. Jordan, J. Chromatogr., 272: 351-358 (1983)

3. C.M. Camaggi, E. Strocchi, N. Canova and F. Pannuti, J. Chromatogr., 275: 436-442 (1983)

4. M. Nieder and H. Jaeger, J. Chromatogr., 413: 207-217 (1987)

5. F. Berthou and Y. Dreano, J. Chromatogr., Biomedical Applications, 616: 117-127 (1993)

6. S. Chamart, M. Hanocq and M. Helson, J. Chromatogr., Biomedical Applications, 496: 365-375 (1989)

7. Y. Golander and L.A. Sternson, J. Chromatogr., 181: 41-49 (1980)

8. C. Murphy, T. Fotsis, Pantzar, H. Adlercreutz and F. Martin, J. Steroid Biochem., 28: 609-618 (1987)

9. C. Murphy, T. Fotsis, P. Pantzar, H. Adlercreutz and F. Martin, J. Steriod Biochem., 26: 547-555 (1987)

10. Q.X. Dang, L.X. Yan, Z.P. Sun and D.K. Ling, J. Chromatogr., 630: 363-369 (1993)

11. M.T. Ackermans, F.M. Everaerts and J.L. Beckers, J. Chromatogr., 606: 229-235 (1992)

12. W. Thormann, S. Lienhard and P. Wernly, J. Chromatogr., 636: 137-148 (1993)

13. P. Lukkari, H. Siren, M. Pantsar and M.L. Riekkola, J. Chromatogr., 632: 143-148 (1993)

14. B.B. VanOrman, G.G. Liversidge and G.L. McIntire, J. Microcol. Sep., 2: 176-180 (1990)

15. H. Nishi, T. Fukuyama and S. Terabe, J. Chromatogr., 553: 503 (1991)

16. L.M. Benson, A.J. Tomlinson, J.M. Reid, D.L. Walker, M.M. Ames and S. Naylor, J. High Resolut. Chromatogr., 16: 324-326 (1993)

17. R.A. Wallingford and A.G. Ewing, Adv. Chromatogr., 29: 1 (1990)

18. D. Stevenson in E. Reid and I.D. Wilson (Editors), Drug Determination in Therapeutic and Forensic Contexts, Plenum, New York, 1984, pp 243-244

19. C.P. Daniel, S.J. Gaskell, H. Bishop and R.I. Nicholson, J. Endocrinol., 83: 401-408 (1979)

Received: April 20, 1994
Accepted: May 6, 1994

JOURNAL OF LIQUID CHROMATOGRAPHY, 17(18), 3859-3867 (1994)

SEPARATION OF TWO ISOFORMS (Ser^7/Thr^7) OF NATURAL SARAFOTOXIN-a BY CAPILLARY ELECTROPHORESIS: MASS SPECTROMETRY AND SYNTHESIS

H. LAMTHANH[1]*, A. BDOLAH[2], Z. WOLLBERG[2], AND J. L. GY[3]

[1]CEA, Département d'Ingénierie et Etudes des Protéines (DIEP)
CE Saclay, 91 191 Gif sur Yvette Cedex, France
[2]George S. Wise Faculty of Life Sciences
The Rose and Norman Lederer Chair in Experimental Biology
Ramat Aviv, 69 978 Tel Aviv, Israel
[3]Applied Biosystems (ABI)
B. P. 50 086
13 rue de la Perdrix
Paris Nord II
95 948 Roissy Charles de Gaulle Cedex, France

ABSTRACT

Each isoform was identified within the mixture in the natural sarafotoxin-a: Ser^7 and Thr^7-SRTX-a has been identified by chemical sequencing and recently by the sequencing of c-DNAs encoding for the sarafotoxins family. Mass spectrometry (MS) of the natural SRTX-a displayed the presence of two isoforms as noted by chemical and c-DNA sequencing. In order to evaluate the role of the 7 th residue in the bioactivity of SRTX-a , we carried out the separation of Ser^7 and Thr^7-SRTX-a from the natural SRTX-a isolated from the venom successicely by gel filtration, ion-exchange and reversed-phase HPLC. The capillary electrophoresis in micellar conditions (MECC) enabled us the separation of the Ser^7/ Thr^7-SRTX-a in an analytical range of peptide only. Due to the low range of the CE process in the quantitative recovery of two isoforms , each isoform was then synthesized

by solid phase for the bioassays and further spectroscopic studies. The MW and migration time of each synthetic isoform were found to fit with the corresponding natural product. Overall, CE (off-line in this study) with MS are the method of choice for the identification of natural products such as the SRTX-a isoforms because of its speed , nanogram scale sensitivity.

INTRODUCTION

The sarafotoxins(SRTX a,b,c,d) are a family of isopeptides (21 amino acids) , which were purified from the venom of the Israeli burrowing asp *Atractaspis engaddensis* (1) . These toxins have powerful cardiotoxic effects and induce the contraction of various smooth muscles.(2). A related family of cardiovascular and vasoconstrictor peptides, endothelins ET-1 , ET-2 , ET-3 , found in mammals and in other vertebrates (3) show a high degree of sequence homology with the sarafotoxin family.

The purification of SRTX-a from the venom successively by gel filtration, ion-exchange and reversed-phase HPLC and its sequencing by Edman degradation, enabled us to demonstrate the mixture of two isopeptides in the same HPLC peak: SRTX-a and SRTX-a1 which differ by only one residue (Thr/Ser) at the 7th position (4) (Figure 1). Furthermore, recent c-DNA cloning of the SRTXs family in our laboratory shows the existence of the two SRTX-a isopeptides namely SRTX-a1 or (Ser^7)-SRTX-a and SRTX-a or (Thr^7)-SRTX-a and also two SRTX-b isopeptides, namely SRTX-b1 or (Ser^7)-SRTX-b and SRTX-b or (Thr^7)-SRTX-b (5) . The different biological potencies of sarafotoxins have been attributed to the sequence heterogeneity in the N-ter region (4th to 7th residue) of the peptide (6), and specifically for the two most potent SRTXs (a and b) the difference between Ser^7 and Thr^7 raised a question on the role of the 7th residu on the biological potency of each isoform separately . Therefore, an attempt to isolate each natural isoform (SRTX-a / SRTX- a1) was carried out and the toxicity and bioactivity each isoform should be then tested to adress this question.

$Cys^{1}.Ser.Cys.Lys.Asp^{5}.Met.^{Ser}_{Thr}.Asp.Lys.Glu^{10}.Cys.Leu.Asn.Phe.Cys^{15}His.Gln.Asp.Val.Ile.Trp^{21}$

FIGURE 1

Amino-acid sequences of SRTX-a /(Thr^{7}) and a1 /(Ser^{7}) (disulfide bonds between Cys^{1} and Cys^{15}/ Cys^{3} and Cys^{11}) .

The analysis of the natural SRTX-a by mass spectrometry (MS) showed the presence of two isopeptides , as noted previously by chemical sequencing (4) . Capillary Electrophoresis (CE) only enabled us the separation of the two isopeptides. Due to the difficulty in scaling-up the separation of the two isoforms from the natural SRTX-a by CE , we decided to synthesize by solid phase the two isopeptides for the bioassays and further physico-chemical studies. In this paper, we wish to demonstrate 1/ the high resolving power and speed of the CE in the separation of two SRTX-isoforms and 2/ the usefulness of mass spectrometry and capillary electrphoresis in an off-line mode for the identification and characterization of the two SRTXs-a.

EXPERIMENTAL.

Purification of the mixture of two SRTX-a isoforms from the crude venom

The mixture of two SRTX-a isoforms was isolated and purified by column chromatography from the venom of *Atractaspis engaddensis* by gel filtration (Sephadex G-50) and ion-exchange (DEAE-cellulose) (4) . The fraction S6a of the DEAE-cellulose step was then purified by reversed phase chromatography on a Lichrosorb RP-18 column (250x4 mm, Merck, Damstadt, FRG) . The column was developed at 1 ml/min with a linear gradient of 0-80% acetonotrile in 0.1% trifluoroacetic acid using a Gilson model 303 HPLC system.

(^{252}Cf)-PDMS

Plasma desorption mass spectra were obtained with a DEPIL-(^{252}Cf)-time of flight mass spectrometer (7) at the Institut de Physique Nucléaire

(Orsay, France). The sample preparation method used is devised by Sundquist et al. (8). The peptide solution (10μL) was applied to a nitrocellulose target obtained by electrospraying a nitrocellulose solution onto an aluminized mylar foil. The nitrocellulose target was allowed to absorb the peptide solution (5 min.) and then spin dried. The concentration of peptide used for the PDMS analysis was estimated by UV spectra: 1μg/mL to 10 μg/mL. Therefore, the quantity of the analyzed peptide was 10 ng to 100 ng for the deposit of 10 μL. The target was then submitted to fission fragment in the mass spectrometer without being rinsed with water. The variable time of flight distance was set to 40 cm and the accelerating voltage to 15 kV. All spectra were collected for 15 min. in the positive mode, although the molecular peaks were clearly identifiable within a few seconds. Mass values are calculated from the centroids of time of flight peaks (7).

Capillary Electrophoresis (CE)

The separation of the two natural isopeptides and the elution of synthetic peptides were carried out on the ABI 270 A-HT apparatus (ABI, USA) with a 500 mm x 50 μm i.d. fused-silica capillary. Samples were introduced from the cathodic end of the capillary by 1 s. vacuum injection. Peptide solutions were prepared to be about 1 μg/ mL and the volume of one peptide solution injected corresponded approximately to a quantity of 10 ng of peptide. UV detection was at 200 nm. Before each run the capillary was washed with 1.0 M NaOH for 2 min followed by wash with buffer for 5 min.

Micellar electrokinetic capillary chromatography (MECC) conditions were based on the use of a surfactant concentration of 50 mM SDS in running buffer of 50 mM sodium tetraborate pH 8 (9). The experimental conditions are described in the legends of the figure.

Solid Phase Peptide Synthesis

SPPS was carried out on the automatic synthesizer (ABI 430 A) using the Boc-chemistry (10) and the two disulfide bonds were formed seqentially by using a specific chemistry : ferricyanide oxidation of Cys^3 and Cys^{11}

(11) and iodine oxidation of $Cys(Acm)^1$ and $Cys(Acm)^{15}$ (12). Boc-(L)-Trp(For)-Pam-Resin (0.66 mM/g) was used as the starting resin. The linear peptide $Cys^{3,11}$ and $Cys(Acm)^{11,15}$ was cleaved from the resin and purified by reversed phase HPLC. The mono-disulfide peptide was obtained after the ferricyanide oxidation and HPLC purification steps. The bi-disulfide-peptide or SRTX-a was obtained after the iodine oxidation and HPLC purification steps. The synthetic peptides were characterized by amino acid analysis , PDMS and CE.

RESULTS AND DISCUSSION

The mass spectrometry measurements of the purified natural SRTX-a displayed one protonated molecule (MH^+) observed at m/z 2511.79 corresponding to the (Thr^7)-SRTX-a (m/z calc 2512.90) and other protonated molecule (MH^+) observed at m/z 2497.62 corresponding to the (Ser^7)-SRTX-a (m/z calc. 2498.60). The difference in mass (14 a.m.u.) fit in with the substitution of one H atom from the serine side-chain by one CH_3 group for the threonine side-chain (Figure 2-A). Two other peaks with a minor intensity at m/z 2466.52 and m/z 2452.37 (difference of 45 a.m.u. respectively from the two major peaks) can not be assigned as a product of fragmentation from the two previous isoforms. The identity of these two peaks was not studied, but we thought that these two MH^+ values can likely correspond to the isoforms of the respective natural (Thr^7)-SRTX-a and natural (Ser^7)-SRTX-a.

In the first step, we tried to separate the two natural isopeptides by C.E. for bioassay measurements. Classical conditions of separation of (Ser^7)-SRTX-a and (Thr^7)-SRTX-a by C.E. were not successful. Different conditions were extensively investigated in the optimization of the resolution of the two natural isoforms: acidic, alkaline buffers, buffer concentration and applied voltage. C.E. in micellar conditions (MECC) e.g. in the presence of the detergent SDS, enabled the separation of the two components in the natural SRTX-a : the (Thr^7)-SRTX-a migration time is longer to that of (Ser^7)-SRTX-a (Figure 2 B). Two minor peaks at 7.92 min and 7.74 min are observed as in

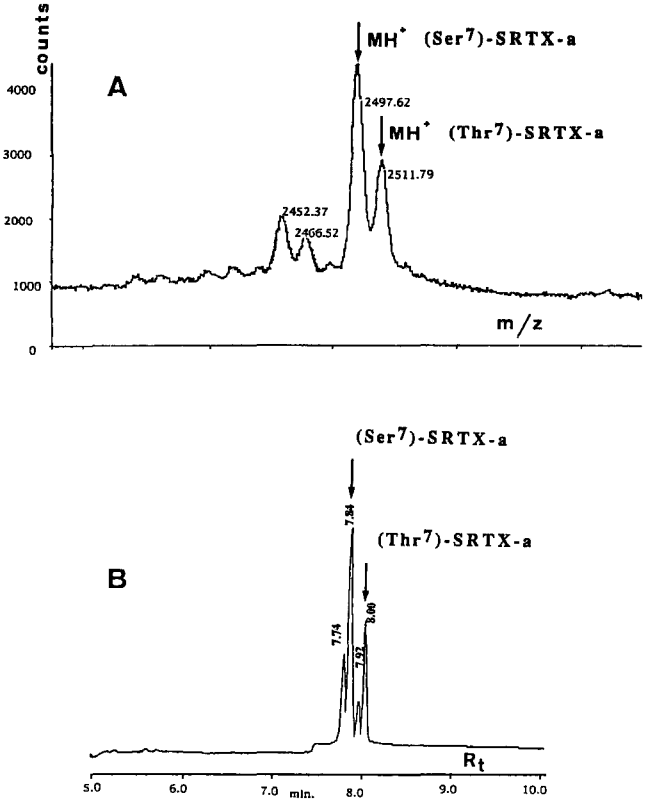

FIGURE 2

A- (^{252}Cf)-PDMS of natural SRTX-a purified from the *Atractaspis engaddensis* venom. The synthetic (Ser^7)-SRTX-a and (Thr^7)-SRTX-a positions' on the respective mass spectrum are indicated by the arrows.

B- CE in MECC conditions of natural SRTX-a purified from the *Atractaspis engaddensis* venom. The synthetic (Ser^7)-SRTX-a and (Thr^7)-SRTX-a positions' on the respective capillary electrophoregram are indicated by the arrows. The experimental conditions are : capillar lenght L=50 cm ; 15 kV ; 38 µA ; borate 50 mM pH 8.0 ; SDS 50 mM . Detector at 200 nm , 30°C. Samples are dissolved in 4 mM sodium citrate buffer at pH= 2.5.

the PDMS spectrum and can be likely assigned as the assumed isoforms of (Thr^7)-SRTX-a and (Ser^7)-SRTX-a (Figure 2B). This separation can be considered as the result of a difference in the partitioning of (Ser^7)/(Thr^7)-SRTX-a into the micelle (9) . At this point, it seems to us that the secondary structure of SRTX-a must be taken into account for the partitioning of the two isoforms into the micelle. The 6th-7th residues in the SRTX-b lying between the 3th-6th β-turn region and the helicoidal core (8th-15th region) are believed to have a β–sheet preference according to the NMR study of the SRTX-b (13) , an analog of the SRTX-a , peptide which has the same sequence from the 1st to the 12th residue (4). The Ser^7 or Thr^7 side-chain in SRTX-a should be exposed to the solvent and the detergent , which in turn facilitates the separation of the two isoforms : the greater the hydrophobicity of the side-chain , the longer the migration time (R_t) . The recovery of purified sample by CE for further studies is usually not quantitative. Therefore, we synthesized the two isopeptides SRTX-a and a1. The details of the solid-phase peptide synthesis will be published elsewhere. Mass spectrometry and the CE migration time of each synthetic isopeptide were compared individually to the natural product (Figure 2 A and B). Each synthetic peptide's MH^+ and R_t values are exactly at the same values to those of the corresponding natural product. The synthetic peptide's behaviour in MECC is identical to that of the natural product.

These CE results in MECC conditions demonstrate the high resolving power of the method :1/ good resolution of the 21 residues-peptide which differes only by one methyl group (serine / threonine side-chain) 2/ need of low quantity of natural product (nanogram scale). Used in combination with mass spectrometry, off-line in our study, the CE method seems to be ideal for the purification, identification and characterization of natural products on a nanogram scale.

The toxicity of each peptide was then measured. Preliminary results on the toxicity of each SRTX (a and a1) show an identical LD_{50} for both peptide (10 ng/g b.w. in mice) . This results suggest that the mutation of the 7th residue (Thr-Ser) didn't affect the toxicity of the SRTX-a. The bioactivity of each isoform is under study.

ACKNOWLEDGEMENTS

The authors are grateful to Dr. C. Deprun and Dr. Y. Le Beyec for the performance of the PDMS spectra at the Institut de Physique Nucleaire (Orsay , France).

ABBREVIATIONS

PDMS : plasma desorption mass spectrometry ; C E : capillary electrophoresis; MECC : micellar electrokinetic capillary chromatography ; SPPS : solid phase peptide synthesis ; acm : acetamidomethyl ; For : formyl ; Pam : phenylacetamidomethyl ; a.m.u.: atomic mass unit.

REFERENCES

1/ E. , Kochva, C.C. , Viljoen and D.P. , Botes , Toxicon , 20 , 581, 1982.

2/ Z. , Wollberg , R. , Shabo-Shina , N. , Intrator , A. , Bdolah , E. , Kochva , G. , Shavit , Y. , Oron, B.A. , Vidne and S. , Gitter , Toxicon , 26 , 525 ,1988.

3/ M. , Yanagisawa , H. , Kurihara , S. , Kimur , Y. , Tomobe , M. , Kobayashi , Y. , Mitsui , Y. , Yasaki , K. , Goto and T. , Masaki , Nature , 322 , 414 ,1988.

4/ C. , Takasaki , N. , Tamiya , A. , Bdolah , Z. , Wollberg and E. , Kochva , Toxicon , 26 , 543, 1988.

5/ F. , Ducancel , V. , Matre , C. , Dupont , E. , Lajeunesse , Z. , Wollberg , A. , Bdolah , E. , Kochva , J. C. , Boulain and A. Ménez , J. Biol. Chem. , 268 , 3052, 1993.

6/ Y. , Kloog and M. , Sokolovsky , Trends in Pharmacological Sci. , 10 , 212, 1989 .

7/ S. , Della-Negra , C. , Deprun and Y. , Le Beyec , Revue Phys. Appl. , 21 , 401, 1986 .

8/ G.P. Jonsson, A.B., Hedin, P.L. Hakansson, B.U.R., Sundquist, B.G.S., Save, P.S. , Nielsen, P. , Roepstorff, K.E. , Johansson, J. Kamensky and M.S.L. Lindberg, Anal. Chem. , 58 , 1084 ,1986.

9/ S. , Terabe , K. , Otsuka , K. , Ichikawa , A. ,Tsuchiya and T. , Ando, Anal. Chem. , 56 , 113 ,1984.

10/ R.B. , Merrifield , J. Am. Chem. Soc. , 85 , 2149, 1963.

11/ J.E. Rivier, R., Kaiser , and R. , Gaylean , Biopolymers , 17 , 1927 ,1978.

12/ D.F. , Veber, Milkowski , J.D., S.L. , Varga , R.G. , Denkewalter , R.G. and R. Hirschman, J. Am. Chem. Soc. , 94 , 5456 , 1972.

13/ A. , Aumelas , L. , Chiche , E. , Mahe , D. , Le-Nguyen , P. , Sizun , P. , Berthault and B. , Perly , Neurochem. Int. , 18 , 471, 1991.

Received: May 27, 1994
Accepted: June 14, 1994

JOURNAL OF LIQUID CHROMATOGRAPHY, 17(18), 3869-3888 (1994)

CAPILLARY ELECTROPHORESIS OF ALKALI AND ALKALINE-EARTH CATIONS WITH IMIDAZOLE OR BENZYLAMINE BUFFERS

PH. MORIN*, C. FRANÇOIS, AND M. DREUX
Université d'Orléans
Laboratoire de Chimie Bioorganique et Analytique
URA 499, BP 6759
45067 Orléans Cédex 2, France

Abstract

The separation of alkali, alkaline earth, and ammonium cations in several samples of water was achieved by capillary electrophoresis with indirect UV detection . A solution of imidazole (10^{-2} M, pH 4.5) was used as buffer to resolve a mixture of six cations (K^+, Na^+, Ca^{2+}, Ba^{2+}, Li^+ and Mg^{2+}) by capillary electrophoresis at 214 nm in less than 10 min. The addition of potassium cation to the running buffer has an influence on the resolution of Ca^{2+}/Na^+ and Na^+/Mg^{2+} peaks. A linear relationship between the corrected peak area and concentration was obtained in the 1-10 ppm range for these cations using a hydrodynamic injector. This electrophoretic system permitted the separation of these inorganic cations at a 50 ppb-level concentration with an hydrodynamic injection, thus making it possible to quantitatively determine their presence in mineral waters by capillary electrophoresis.

At pH 4.5, potassium and ammonium unfortunately have identical ionic mobilities causing them to comigrate in an imidazole buffer. Using an alkaline solution of benzylamine (10^{-2} M, pH 9) as carrier electrolyte, their separation can be successfully achieved with excellent resolution at 204 nm.

The analyses of tap water and several mineral waters have been achieved by capillary electrophoresis.

INTRODUCTION

Capillary electrophoresis, a recent analytical technique, is currently undergoing rapid development owing to its efficiency, high resolution, relative simplicity, UV detection with low wavelengths (190 nm), speed and automatization of separations, and low buffer consumption. Compared to liquid phase chromatography, one disadvantage, seems to be not only a rather weak reproducibility of the electroosmotic flow assuring the migration times, but also a lower concentration sensitivity. However, this technique is available not only for the separation of inorganic and organic anions and cations but also for the separation of ionizable and neutral organic molecules [1].

Until today, capillary electrophoresis had been studied more for the analysis of anions than of cations. Nevertheless, the analytical approach is similar, in that indirect detection is required because of the transparency of inorganic ions in the UV region (except for a few inorganic anions such as nitrate and bromide), and the operating conditions such as the electroosmotic flow must be in the same direction as the electrophoretic mobility of the ions analyzed in order to minimize their migration time. Table I shows some of the articles relative to the separation of cations by capillary electrophoresis [2-13].

Several types of detectors have been utilized for the separation of cations with the two major ones being the indirect UV detector and indirect fluorimetric detector. Initially, Aguilar et al. [2] separated the cations Fe^{2+}, Cu^{2+} and Zn^{2+} in the form of their cyano complexes in capillary electrophoresis; a phosphate buffer (20 mM) was used at pH 7 and cation detection was carried out at 214 nm. Then Foret et al. [5] separated fourteen lanthanides by capillary electrophoresis using an electrophoretic buffer consisting of an α-hydroxylisobutyric acid as complexing agent and creatinin as the indirect UV detector marker; in fact, the similarity between the electrophoretic mobilities of alkali and alkaline-earth, rare-earth and metal cations requires the addition of a water-soluble complexing reagent to the electrolyte. The electrophoretic mobility of each cation thus decreases following their complexation in-situ by α-hydroxylisobutyric acid and selectivity is largely improved. The factors affecting the separation of such cations were studied by Weston et al. [6,7]; the complexing agent was also α-hydroxylisobutyric acid and the compound allowing indirect UV detection was called UV Cat 1, a proprietary reagent developed at Waters. Very recently, Beck et al. [9] firstly proposed a nice alternative way for the separation of several alkali and alkaline earth cations by using an imidazole-based electrophoretic buffer and indirect UV detection at 214 nm. Finally, Swaile and Sepaniak [12] used a laser-based fluorimetric detector to detect cations Ca^{2+}, Mg^{2+} and Zn^{2+}, complexed by 8-hydroxyquinoline-5-sulfonic acid; this technique was applied to the detection of Ca(II) and Mg(II) in blood serum.

In order to use indirect photometric detection and to obtain symmetrical peaks, a UV absorbing cationic compound having similar electrophoretic mobility to that of the cations analyzed was chosen as main constituent of the buffer; several organic bases were considered among which was an aromatic amino (benzylamine) or a heterocyclic azote (imidazole).

Table I. A few examples of some inorganic cation separations by capillary electrophoresis.

Cations	Detection	Electrolyte	pH	Time	Sensitivity	Ref.
Zn^{2+}, Cu^{2+} Fe^{2+}	Direct UV 214 nm	phosphate 20 mM	7,0	5 min	-	2
$Au(CN)_2^-$ $Ag(CN)_2^-$	Direct UV 214 nm	$NaHCO_3$ 10 mM	9,6	-	2,82 µg/mL Au 3,48 µg/mL Ag	3
Al^{3+}, AlF^{2+}, AlF_2^+	Indirect UV 214 nm	imidazole 5 mM	3,5	5 min	10^{-5} M	4
lanthanides	Indirect UV 220 nm	acetate 30 mM - creatinine- HIBA 4 mM	4,8	5 min	10^{-7} M	5
alkali alkaline-earth lanthanides	Indirect UV 214 nm	UV Cat-1 5 mM HIBA 6,5 mM	4,4	10 min	0,05-0,1µg/mL 0,1-0,2 µg/mL	6,7
lanthanides	Indirect UV 214 nm	benzylamine 9 mM HIBA 4 mM CH_3COOH 20 mM	4,6	8 min	-	8
K^+, Na^+, Ba^{2+} Ca^{2+}, Mg^{2+}, Li^+	Indirect UV 214 nm	imidazole 5 mM	4,4	10 min	0,1 µg/mL	9
K^+, Ca^{2+}, Na^+, Mg^{2+}	Indirect UV 214 nm	UV Cat-1 5 mM- HIBA 6,5 -4,0 mM	4,0	10 min	5 µg/mL	10
alkali alkaline-earth	Indirect Fluorimetry	quinine sulfate H_2SO_4 0,58 mN	3,7	5 min	0,1-0,5fmol	11
Mg^{2+}, Ca^{2+} Zn^{2+}	Fluorimetry	HQS^- 2,5 mM λ_{exc} = 325 nm λ_{emis}= 425 nm	8,0	10 min	0,05-0,6 µg/mL	12
alkali alkaline-earth	Indirect Fluorimetry λ_{exc} = 251 nm λ_{emis}= 345 nm	Ce(III) 0,5 mM- 18-crown-6 2.5 mM	-	7 min	$1\text{-}3.10^{-6}$ M	13
K^+, Na^+, Rb^+, Li^+	conductimetry	MES 20 mM - histidine	6,0	8 min	2.10^{-6} M	14

HIBA: α-hydroxyisobutyric acid
HQS^-: 8-hydroxyquinoline-5-sulfonic acid
UVCat 1: UV background-providing component of the electrolyte (Waters product)

Several examples of cation separations are presented (K^+, Na^+, Ca^{2+}, Ba^{2+}, Li^+, Mg^{2+}, and NH_4^+) as well as their quantitative analyses.

EXPERIMENTAL

Capillary Electrophoresis Materiels

Different capillary electrophoresis systems were employed for this study; one was used in manual mode (Europhor), and the others in automatic mode with a thermostated capillary column (Spectra, Beckman).

Separations carried out on a Spectraphoresis 1000 apparatus (Spectra-Physics, San Jose, CA, USA) used a capillary column whose dimensions were 70 cm (or 44) total length, 63 cm (or 37) from the point of injection to the detector cell, and 50 μm I.D. Separations were achieved at an adjustable temperature (25-40°C) under positive power supply (15-30 kV) with a few tenths of microampers. Detector time constant was set at 0.1 s. The hydrodynamic injection was achieved in a short time (0.5 or 1 s). Data was kept in an IBM PS/2 computer model 70 386 using data acquisition software and electrophoretic data manipulation. This apparatus also contained a variable wavelength detector which allowed the recording of the UV-visible spectrum of the migrating compound.

Separations carried out on a P/ACE 2100 apparatus (Beckman Instruments Inc., Fullerton, CA, U.S.A.) equipped with a UV detector with wavelength filters (190, 200, 214, 254, 260, 280 nm). Fused silica capillaries (Beckman Intruments Inc.) of 75 μm I.D. x 375 μm O.D. and 57 cm long (50 cm to the detector) were used. The part of the capillary where separation takes place was kept at a constant temperature by immersion in a cooling liquid circulating in the cartridge with a detection aperture of 100 μm x 800 μm. The solutes were injected at the anode end of the capillary in the hydrodynamic mode by azote superpressure (0.5 psi). Data were collected using a IWT data acquisition system. Detector time constant was 0.1 s and data acquisition rate was 20 Hz.

Electrophoretic separations carried out on a Prime Vision apparatus (Europhor, Toulouse, France) utilized a fused-silica capillary tube with the following dimensions: total length, 96 cm; injector-detector length, 65 cm; I.D., 75 μm. Positive power supply (15 to 25 kV) delivered by a high-voltage generator (Prime Vision V) was applied between the two electrodes. The hydrodynamic injection times ranged between 1 and 10 s. The UV-visible detector (Prime Vision II) has variable wavelengths. A small section of polyimide was removed in order to carry out on-column UV detection with an optical length close to 75 μm; the detection wavelength was set at 214 and 204 nm for the imidazole and benzylamine buffers, respectively. The electropherograms were recorded on a Shimadzu C-R 5A integrator (Kyoto, Japan).

The pH of each solution was verified on a Beckman pH meter (Model ϕ10, Fullerton, CA, USA). The capillary tubing of fused silica was conditioned daily by rinsing with a solution of sodium hydroxide 1 N (10 min), then water (10 min), and finally with the

electrophoretic buffer (15 min). Between two consecutive analyses, the capillary was rinsed with water (3 min) then with the electrophoretic buffer (5 min) to improve reproducibility of the electroosmotic flow and migration times of the solutes.

Reagents and Products

All chemical products used were of analytical quality. Imidazole (99% purity) was obtained from Sigma (St Louis, MO, USA) whereas the tetrabutylammonium bromide (TBABr) (99% purity) and benzylamine (99% purity) were purchased from Aldrich (Milwaukee, WI, USA). The water used in the preparation of buffers as well as that necessary for dilutions was of HPLC quality (Fisons, Farmitalia, Milan, Italy). The electrophoretic buffer pH was adjusted with acetic acid 1M (Carlo Erba, Milan, Italy). Finally, each buffer or rinsing solution was filtered before use through a membrane filter having a diameter of 25 mm and porosity of 0.2 μm (Whatman, Maidstone, Great Britain).

RESULTS AND DISCUSSION

The electrophoretic buffer used for the separation of inorganic cations must contain an organic cation (stable within the 4-9 pH range to resolve cations K^+ and NH_4^+, particularly), which has an electrophoretic mobility close to that of the inorganic cations to be separated in order to obtain symmetrical and efficient electrophoretic peaks, and also an intense chromophore group in the UV region.

The imidazole (or 1,3-diaza-2,4-cyclopentadienyl ring) is a heterocyclic azote ($pKa_1 = 6.9$ and $pKa_2 = 14.5$) whose UV absorption spectrum maximum at pH 4.5 was set at 211 nm (Fig. 1). Moreover, the imidazole cation appears to have an electrophoretic mobility close to that of the calcium and sodium cations [9]. By using an imidazole buffer concentration of 10^{-2} M and a pH adjusted to 4.5, a mixture of five inorganic cations (K^+, Ba^{2+}, Ca^{2+}, Na^+ and Li^+) was nicely separated in 5 min (Fig. 2); separation voltage was equal to +20 kV (current 12 μA). The sample injection was carried out at the anodic end of the capillary and detection at the cathodic end; the electroosmotic flow (at 10.3 min) was in the same direction as the electrophoretic mobility of the cation. The number of theoretical plates was fairly high (from 377 000 for Ba^{2+}, 231 000 for Ca^{2+}, 257 000 for Na^+ to 102 000 for K^+) as mentionned in Table II. The migration order of Na^+ relative to Ca^{2+} and Mg^{2+} differs from that reported previously [9] but the buffer has not exactly the same composition. Besides, as already been reported, the co-ion buffer concentration may influence the migration of the analytes.

Addition of a Cation to the Electrolyte

A clear separation improvement of the sodium-magnesium cations was observed when the K^+ cation was added to the electrophoretic buffer (Fig. 3). Fig. 4 shows the

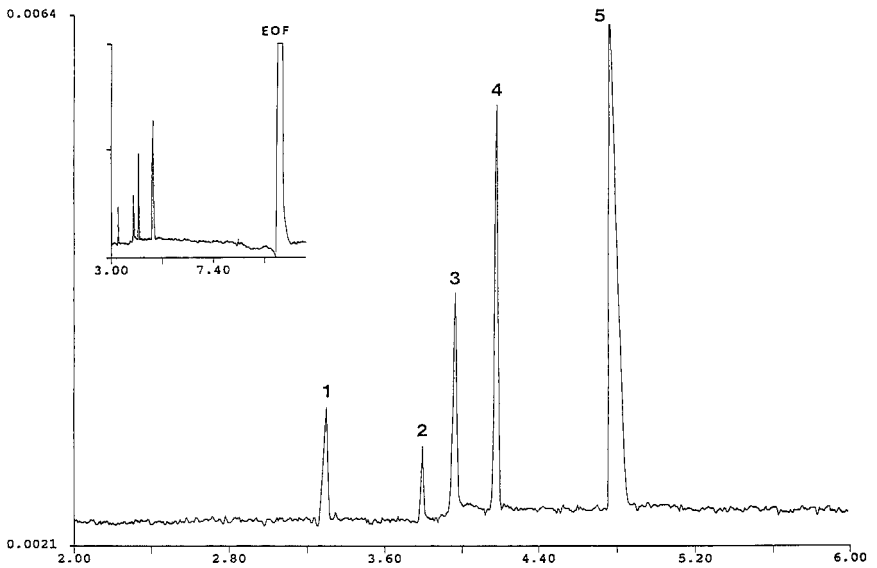

Figure 1. On-line UV spectra of selected buffers in the separation of cations by capillary electrophoresis.
1) imidazole (at pH 4.5); 2) benzylamine (at pH 9).

influence of the K^+ ions added to the buffer on the resolution of the Ca^{2+}/Na^+ and Na^+/Mg^{2+} peaks. The resolution of the Ca^{2+}/Na^+ peaks decreases for increasing potassium concentration added to the imidazole buffer and becomes smaller than 2.0 at potassium concentration greater than 10^{-3} M. At the opposite, the resolution of the Na^+/Mg^{2+} peaks increases for increasing potassium concentration in the running buffer. For a concentration of K_2SO_4 close to 0.5 mM, the resolution of Na^+-Mg^{2+} was greatly improved, and the separation of six cations was completed in less than 5 min (see Fig. 5a). However, the addition of a potassium cation to the buffer disturb indirect UV detection of the potassium cation, generally present in various samples (mineral water), by causing continually decreasing sensitivity loss for K^+ cation (Figs. 3a-e) and even a negative peak (Figs. 3d-e). An alternate solution would be to add to the electrophoretic buffer a cation not present in the sample to be analyzed; for example, the tetrabutylammonium cation added to the buffer at a concentration of 10^{-3} M avoided this detection drawback by maintaining the same resolution of cations Ca^{2+}, Na^+ and a slightly higher resolution of cations Na^+, Mg^{2+} (see Fig. 5b).

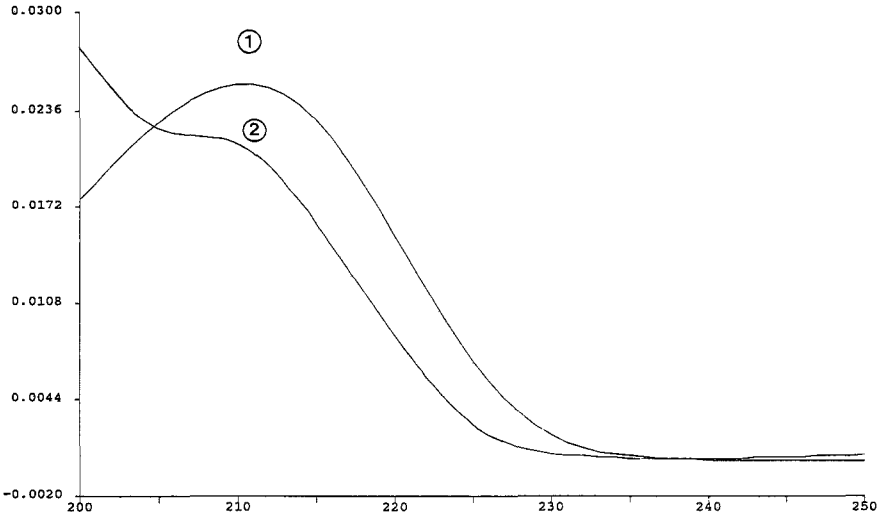

Figure 2. Separation of a standard mixture of five inorganic cations by capillary electrophoresis with imidazole as carrier electrolyte.
Buffer, 10^{-2} M imidazole (pH 4.5); applied voltage, + 19.8 kV; thermostatted capillary dimensions, 70 cm x 50 µm I.D.; wavelength detection, 214 nm; current, 12 µA; hydrodynamic injection, 5 s; temperature, 25°C; cation concentration, 4 ppm. Identification: 1) K^+; 2) Ba^{2+}; 3) Ca^{2+}; 4) Na^+; 5) Li^+.

Table II. Electrophoretic parameters of cations.
Applied voltage, + 19.8 kV; field strength, 283.5 v/cm; electroosmotic flow, $3.59.10^{-4}$ $cm^2/V^{-1}.s^{-1}$; experimental conditions: as the Figure 1.

cation	efficiency	asymetry factor	electrophoretic mobility (x 10^4 $cm^2.V^{-1}.s^{-1}$)
K^+	102 000	0.29	7.63
Ba^{2+}	377 000	0.79	6.18
Ca^{2+}	231 000	0.46	5.74
Na^+	257 000	0.53	5.25
Li^+	60 000	5.31	4.17

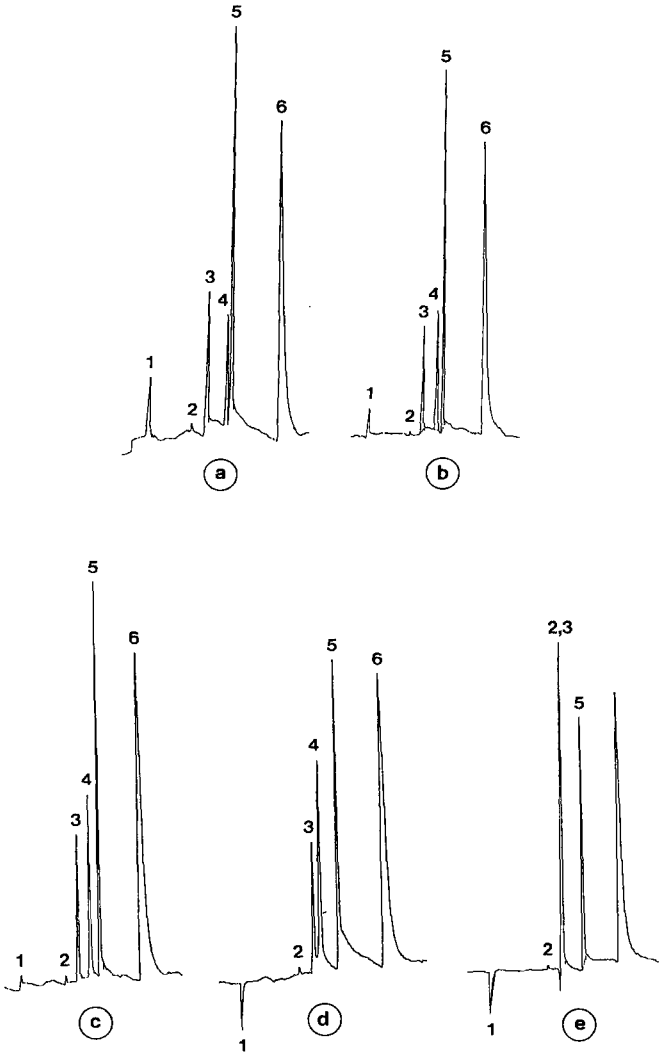

Figure 3. Addition of K^+ ions to the imidazole buffer.

Applied voltage, + 15 kV; capillary dimensions; 65 cm x 75 μm I.D.; wavelength detection, 214 nm; temperature 22 °C. Identification: 1) K^+; 2) Ba^{2+}; 3) Ca^{2+}; 4) Na^+; 5) Mg^{2+}; 6) Li^+.

Concentration of K^+ cation added to the imidazole buffer (10^{-2} M, pH 4.5): a) 0 mM; b) 0.25 mM; c) 0.5 mM; d) 1 mM; e) 1.5 mM

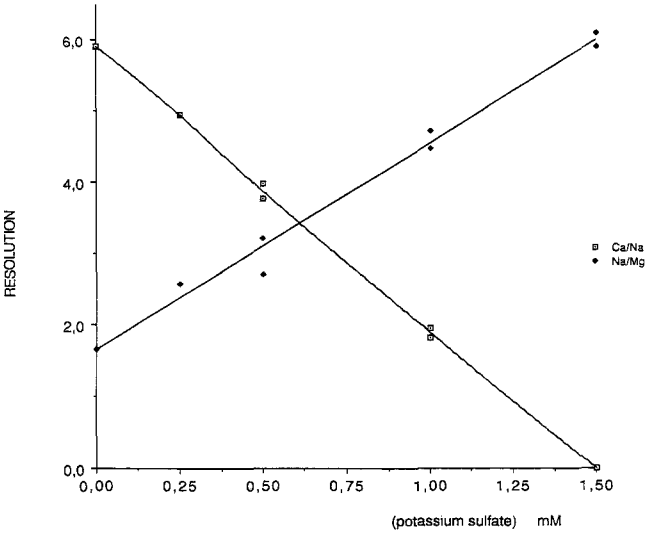

Figure 4. Influence of K_2SO_4 concentration added to the imidazole running buffer on the electrophoretic resolution of the Ca^{2+}/Na^{+} and Na^{+}/Mg^{2+} peaks.
Buffer, imidazole 10^{-2} M + K_2SO_4, pH 4.5. Capillary dimensions: 65 cm x 75 µm I.D. UV detection at 214 nm; hydrodynamic injection time, 3s. a) Ca^{2+}/Na^{+}; b) Na^{+}/Mg^{2+}.

Some of the experiments must be repeat with coated capillary with lower pH buffer or different inorganic and organic cations as buffers additives to gain additional insights into the role of cation/silica interactions.

Separation of Potassium and Ammonium Using Benzylamine Carrier

The simultaneous separation of ammonium and potassium cations is very useful in the analysis of food products or water. Unfortunately, these two cations have nearly identical electrophoretic mobilities (at 25°C, 73.5 and 73.4 mho-cm^2/eq for K^+ and NH_4^+, respectively), bringing about their comigration with the imidazole buffer (pH 4.5). In an alkaline medium, their separation is successful by partially transforming the ammonium cation to NH_3 (pKa = 9.25). Under these electrophoretic alkaline conditions, the mobility of the NH_4^+ cation decreases and the potassium cation migrates faster than the ammonium; on the other hand, the electroosmotic flow increases bringing about a shorter analysis time (see Fig. 6). The selected buffer chosen was benzylamine (pKa = 9.3) which has an high absorbance in the 200-204 nm UV range (Fig. 1b); its concentration was 10^{-2} M with the pH adjusted to 9.

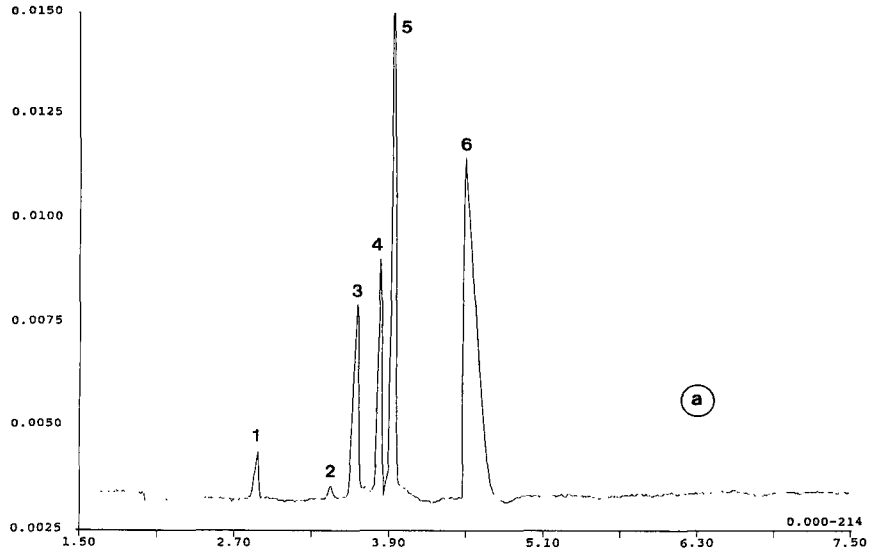
0.0150
0.0125
0.0100
0.0075
0.0050
0.0025
1
2
3
4
5
6
a
0.000-214
1.50
2.70
3.90
5.10
6.30
7.50

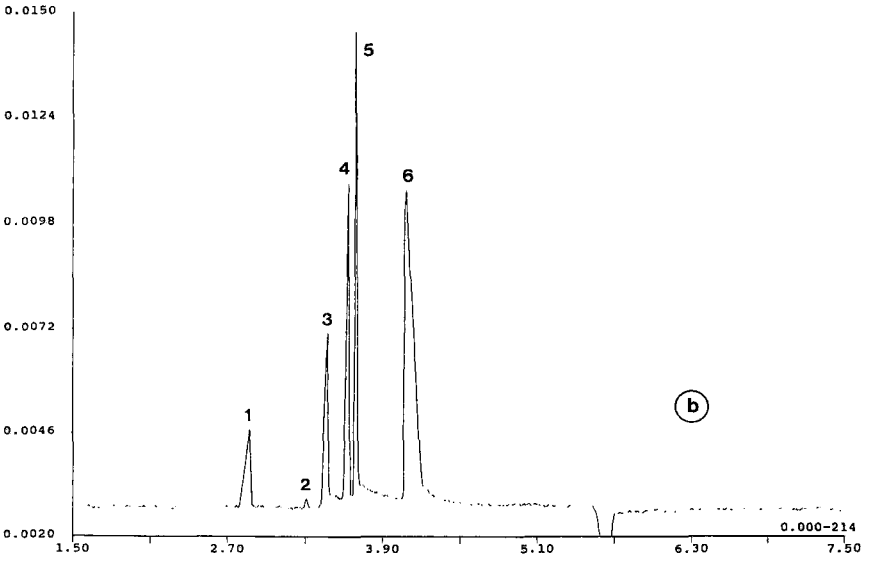
0.0150
0.0124
0.0098
0.0072
0.0046
0.0020
1
2
3
4
5
6
b
0.000-214
1.50
2.70
3.90
5.10
6.30
7.50

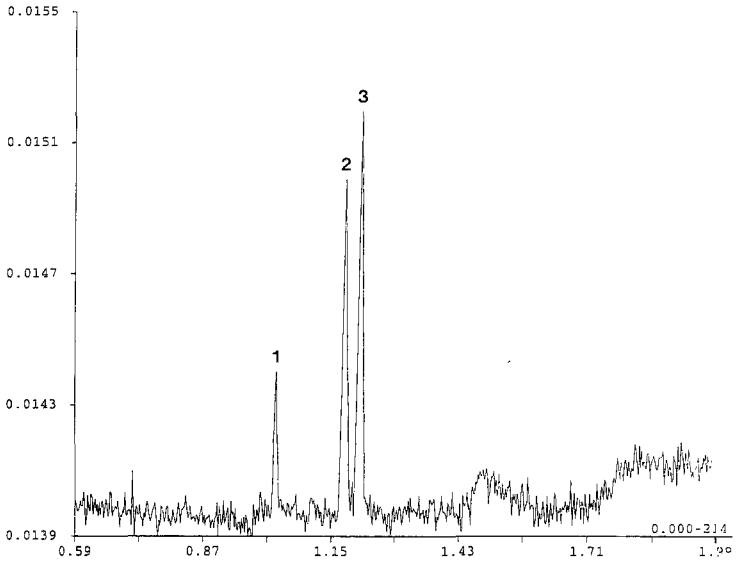

Figure 6. Separation of potassium and ammonium cations by capillary electrophoresis with benzylamine as carrier electrolyte.

Applied voltage, + 20 kV; thermostatted capillary dimensions, 44 cm x 50 μm I.D.; wavelength detection, 204 nm; temperature, 25°C; hydrodynamic injection time, 2 s; buffer; 10^{-2} M benzylamine (pH 9); solute concentration, 5 ppm. Cations: 1) K^+; 2) NH_4^+; 3) Na^+.

Determination of Electroosmotic Flow

The electroosmotic flow may be graphically determined by plotting for each cation the reciprocal migration time $t_m(i)$ versus the equivalent conductance limit λ_i^∞. Indeed, the migration speed of cation i in the capillary zone electrophoresis is expressed by the

---

Figure 5. Addition of K_2SO_4 or TBABr to the imidazole buffer

a) Buffer, 10^{-2} M imidazole + K_2SO_4 5 10^{-4} M (pH 4.5); applied voltage, + 25 kV; thermostatted capillary dimensions, 70 cm x 50 μm I.D.; wavelength detection, 214 nm; electromigration injection, 5 s at 10 kV; solute concentration, 10 ppm.

b) Buffer, 10^{-2} M imidazole + tetrabutylammonium bromide (TBABr) 1.10^{-3} M (pH 4.5); applied voltage, + 25 kV; thermostatted capillary dimensions, 70 cm x 50 μm I.D.; wavelength detection, 214 nm; electromigration injection, 5 s at 10 kV; solute concentration, 10 ppm. Cations: 1) K^+; 2) Ba^{2+}; 3) Ca^{2+}; 4) Na^+; 5) Mg^{2+}; 6) Li^+.

following equation:

$$v_m(i)=\left[m_{ep}(i)+m_{eo}\right].E \quad (1)$$

where $m_{ep}(i)$ is the electrophoretic mobility of cation i, m_{eo} the electroosmotic mobility, and E is the electric field. The reciprocal migration time may be expressed as a function of the electrophoretic mobility $m_{ep}(i)$ following equation 2:

$$\frac{1}{t_m(i)}=\frac{1}{t_0}+\frac{m_{ep}(i).V}{L_t.L_d} \quad (2)$$

where L_t represents the total column length, L_d the column length from the injector to the detector, V the electric voltage, t_o the migration time of a neutral compound, and $t_m(i)$ the migration time of cation i. Moreover, the electrophoretic mobility depends on the ionic strength I of the medium according to the Debye-Hückel theoretical equation 3:

$$m_{ep}(i)=m_{ep}^{\infty}(i)-\left(0.23Z_i^2.m_{ep}^{\infty}(i)+31.4.10^{-5}Z_i\right).I^{\frac{1}{2}} \quad (3)$$

where $m_{ep}^{\infty}(i)$ is the electrophoretic mobility of cation i at infinite dilution and Z_i its electrical charge. Suppose that only the strength of Coulomb and Stokes is exerted on cation i, then its equivalent conductance limit λ_i^{∞} is directly proportional to the electrophoretic mobility according to the Nernst-Einstein relationship 4:

$$\lambda_i^{\infty}=Fm_{ep}^{\infty}(i) \quad (4)$$

where F is the Faraday constant. For each cation i, we may assume that $m_{ep}(i)$ was close to $m_{ep}^{\infty}(i)$ due to the low ionic strength (I = 0.00965) of the imidazole buffer (10^{-2} M, pH 4.5). Thus, the value of time t_o, and consequently, of the electroosmotic flow can be determined by plotting the graph $1/t_m(i) = f(\lambda_i^{\infty}.V/F.L_d.L_t)$.

$$\frac{1}{t_m(i)}=\frac{1}{t_0}+\frac{\lambda_i^{\infty}.V}{F.L_d.L_t} \quad (5)$$

According to the experimental data related to the Fig.2 , the reciprocal migration time varies linearly with the quantity, $\lambda_i^{\infty}.V/F.\ L_d\ .\ L_t$., (see Fig. 7); the experimental slope is equal to 0.95 (close to theoretical value unity) and the time t_o is found to be equal to 9.9 min from the original ordinate value. The equivalent conductance limits λ_i^{∞} of alkali and alkaline-earth cations are sufficiently different for their separation to be achieved in free solution [15] as shown in Fig. 2. Migration times decrease with the equivalent conductance limit, according to the following decreasing migration time order for the cations: potassium (λ_{K^+} = 73.5 mho-

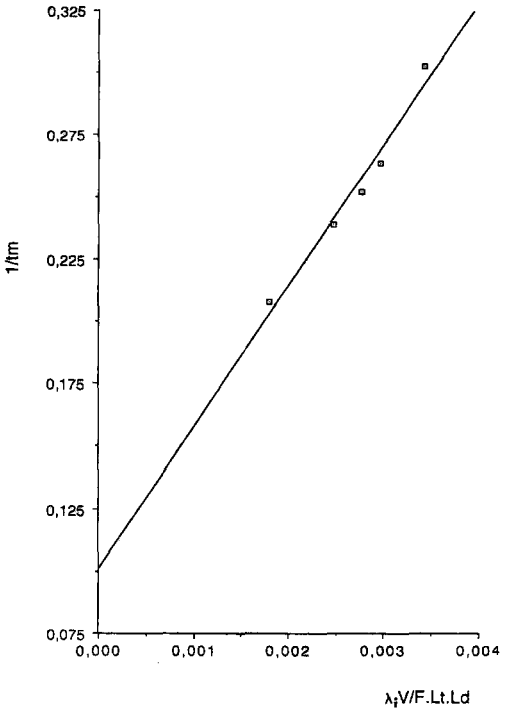

Figure 7. Determination of the electroosmotic flow plotted against the inversed migration time [$t_m(i)$] of each cation as a function of $\lambda_i^{\infty} V/FL_dL_t$, where λ_i^{∞} is the equivalent conductance limit (mho-cm^2/eq) of the cation i, L_t the total column length (cm), L_d the column length from the injector to the detector (cm), V the electrical voltage, and $t_m(i)$ the migration time of the cation (i).

Buffer, imidazole 10^{-2} M, pH 4.5. Capillary dimensions: 70 cm x 50 μm I.D; UV detection, 214 nm; hydrodynamic injection, 3 s; applied voltage, + 24.8 kV; temperature, 40°C; concentration of cations, 10 ppm.

cm^2), baryum ($\lambda_{Ba^{2+}}$ = 63.6), calcium ($\lambda_{Ca^{2+}}$ = 59.5), magnesium ($\lambda_{Mg^{2+}}$ = 53.1), sodium (λ_{Na^+} = 50.1), and finally lithium (λ_{Li^+} = 38.7). However, magnesium having the slowest migration time compared to that of sodium is contradictory to the order of their respective equivalent conductance limits unless we suppose a possible complexation of these cations by imidazole or a strong interaction of magnesium with the silica [11].

Dependence of Efficiency versus Injection Time and Solute Concentration

As would be expected for a capillary separation technique, the capacity of capillary electrophoresis is limited. The efficiency of the electrophoretic peaks was determined for these cations analyzed in different experimental conditions with a no-thermostatted capillary. The experimental influence of the injected cation concentration and of the hydrodynamic injection time on the number of theoretical plates, N, were studied with the imidazole buffer (10^{-2} M, pH 4.5).

Fig.8a shows the plots of the relative number of theoretical plates N/N_{max} as a function of cation concentration for sodium and lithium (N/N_{max} is the highest number observed for a concentration of 1 mg/L). The separation voltage (+12 kV) and the hydrodynamic injection time (2 s) were kept constant while the cation concentration varied froml 1 µg/mL to 10 µg/mL. The highest efficiency (200 300 for sodium and 177 100 for lithium) was observed at the lowest injected concentration. A notable decrease in efficiency was observed with the concentration (Fig.8), as already mentionned by ROW [16]; thus, there were a decrease in the number of theoretical plates for sodium peak (from 200 300 to 110 200) and for lithium peak (177 100 to 55 000) when the cation concentration rises up from 1 to 10 µg/mL

Just as, with a constant concentration, an increasing injected volume brings about a loss in efficiency of the electrophoretic peaks (see Fig. 8b); thus there was a 47% decrease in the number of theoretical plates for sodium peaks (from 175 000 to 93 000) when the injection time was increased from 1 to 5 s for a concentration of 1 ppm. This study confirms the rather limited column capacity in free zone electrophoresis.

Quantitation

By using hydrodynamic injection, the sample curves linking the corrected surface variations of the electrophoretic peaks to the analyzed cation concentrations are plotted for cations K^+ and NH_4^+, Na^+, Ca^{2+} and Mg^{2+} (Figs. 9a, 9b). The calibration curves were determined with either an imidazole buffer 10^{-2} M, pH 4.5 (experimental conditions: voltage, +18 kV; hydrodynamic injection time, 3 s), or with a benzylamine buffer 10^{-2} M, pH 9.0 (experimental conditions: voltage, +24 kV; hydrodynamic injection, 10 s). The linear

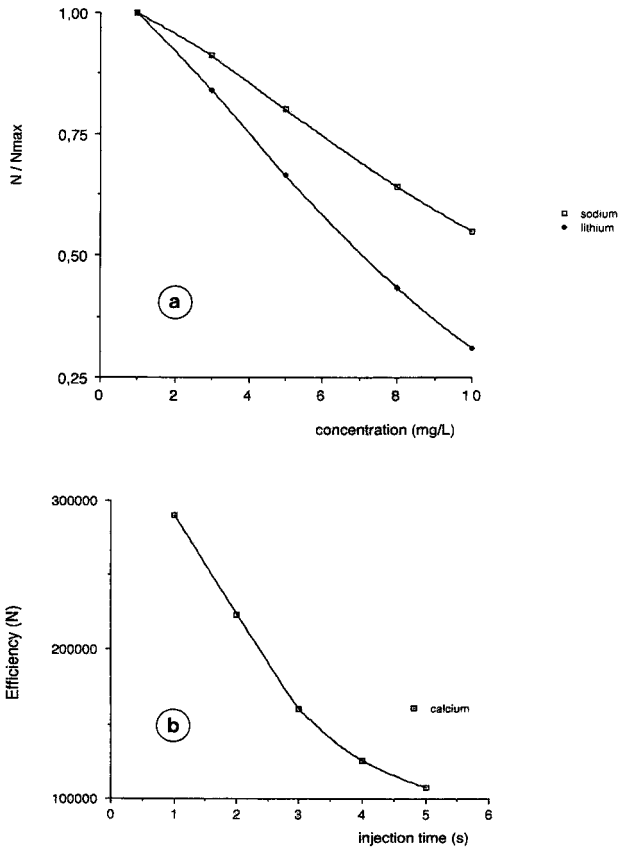

Figure 8. Effect of injected solute amount on peak efficiency.

a) at constant hydrodynamic injection time (2 s);

b) at constant solute concentration (10 ppm).

Buffer, imidazole 10^{-2} M (pH 4.5); capillary, 65 cm x 75 μm I.D; UV detection at 214 nm; hydrodynamic injection, 3 s; applied voltage, + 18 kV.

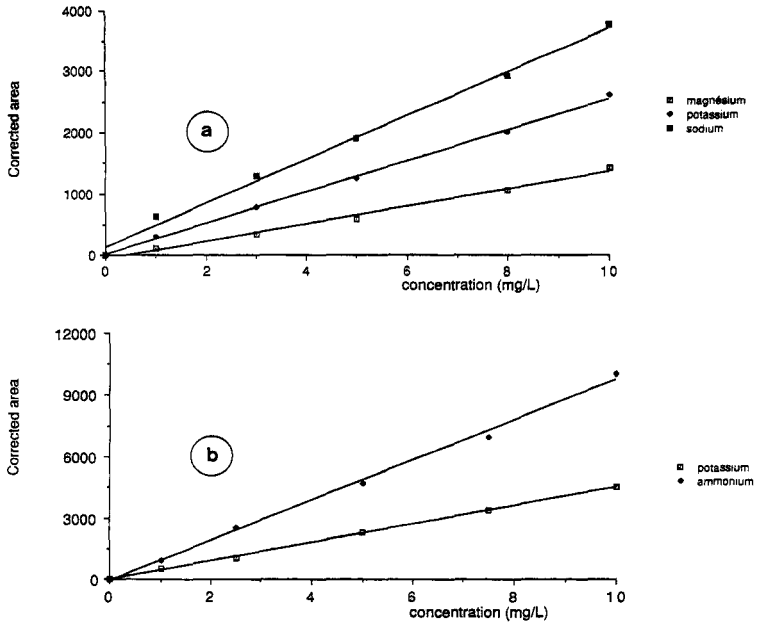

Figure 9. Relationships between concentrations (ppm) of the cations and corrected peak areas (arbitrary units).
a) buffer, imidazole 10^{-2} M (pH 4.5); capillary, 65 cm x 75 μm I.D.; UV detection at 214 nm; hydrodynamic injection, 3 s; applied voltage, + 18 kV. b) buffer, benzylamine 10^{-2} M (pH 9.0); capillary 65 cm x 75 μm I.D.; detection at 204 nm; hydrodynamic injection, 10 s; applied voltage, + 24 kV.

regression coefficients were equal to 0.999 for K^+ and NH_4^+. Using a longer hydrodinamic injection time, the separation of a 50 ppb-level cation mixture may be achieved without any resolution loss (Fig.10).

Analysis of mineral Waters

Fig. 11a shows the capillary electrophoresis separation of alkali and alkaline-earth cations found in tap water using an imidazole buffer (10^{-2} M, pH 4.5). The electrophoretic peaks correspond to potassium, sodium, calcium and magnesium, respectively. Generally, the alkali cations Na^+, Ca^{2+}, and Mg^{2+} present in mineral waters are of very different quantities

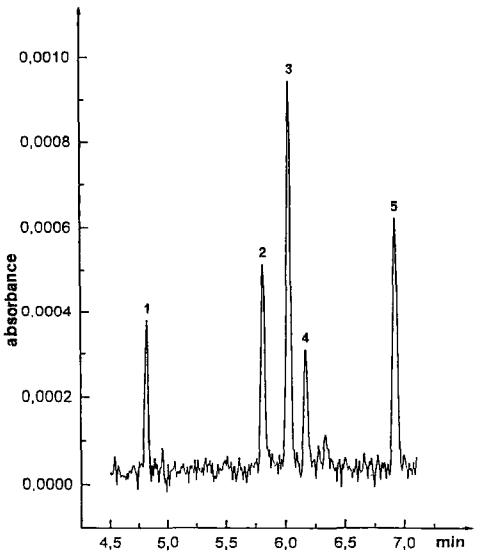

Figure 10. Separation of sub-ppm level cation mixtures by capillary electrophoresis.
Buffer, 10^{-2} M imidazole (pH 4.5); applied voltage, + 10 kV; thermostatted capillary dimensions, 57 cm x 75 μm I.D.; wavelength detection, 214 nm; current, 7 μA; hydrodynamic injection, 20 s (except for 5 s for 4 ppm); temperature, 25°C. Identification: 1) K^+; 2) Ca^{2+}; 3) Na^+; 4) Li^+.
Cation concentration: 50 ppb.

which make the quantitative analysis less accurate, especially in the case of the sodium cation. An alternative solution to maintain the resolution would consist by adding TBABr (Fig. 11b) or methanol to decrease the EOF value (Fig. 11c) to the electrolyte; the resolution of the Ca^{2+}/Na^+ and Ca^{2+}/Mg^{2+} peaks is improved at the small expense of an increase in analysis time. In particularly, Fig. 11c shows the analysis of mineral water by capillary electrophoresis using an imidazole buffer (10^{-2} M, pH 4.5) with 20% CH_3OH; the concentration ratio was nearly 70 between Ca^{2+} and Na^+, and 12 between Na^+ and Mg^{2+}.

CONCLUSION

The separation of alkali (sodium, potassium) and alkaline-earth (magnesium, calcium, barium) cations and also ammonium cation was achieved by capillary electrophoresis

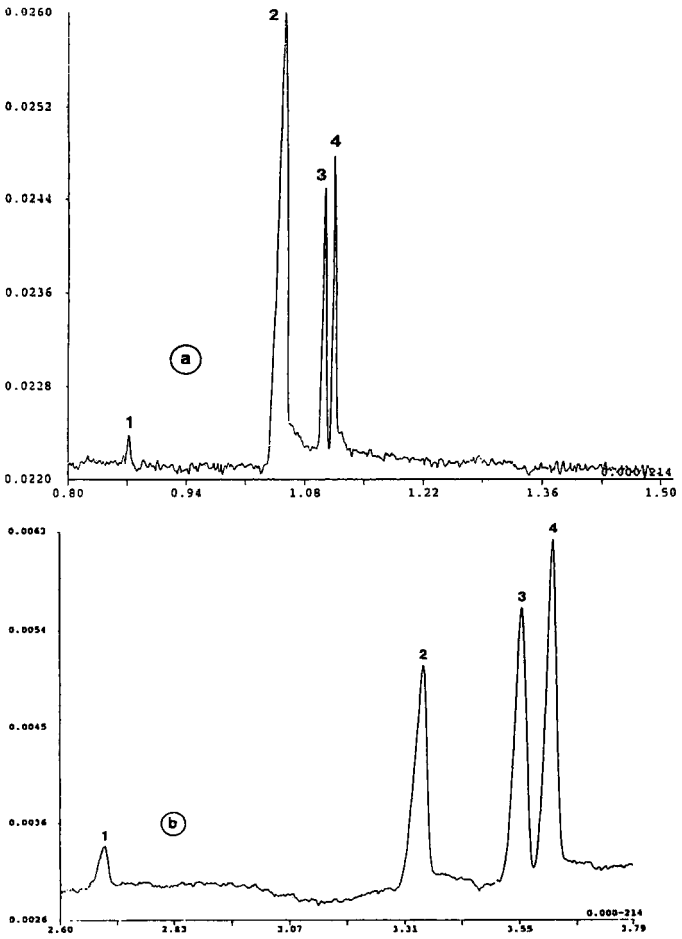

Figure 11 Separation of inorganic cations by CE in several waters.

a) Tap water; applied voltage, + 30 kV; thermostatted capillary dimensions 44 cm x 50 µm I.D.; wavelength detection, 214 nm; hydrodynamic injection time, 0.5 s; buffer 10^{-2} M imidazole (pH 4.5).

b) Mineral water; buffer, 10^{-2} M imidazole + TBABr 5.10^{-3} M (pH 4.5); applied voltage, 10 kV; capillary dimensions, 44 cm x 50 µm I.D.; wavelength detection, 214 nm; hydrodynamic injection time, 1 s.

c) Mineral water; buffer: 10^{-2} M imidazole + TBABr 10^{-3} M (pH 4.5) + 20% methanol; applied voltage, 8 kV; capillary dimensions, 44 cm x 50 µm I.D.; wavelength detection, 214 nm; hydrodynamic injection time, 1 s; temperature, 40°C.

Cations: 1) K^+; 2) Ca^{2+}; 3 Na^+; 4) Mg^{2+}.

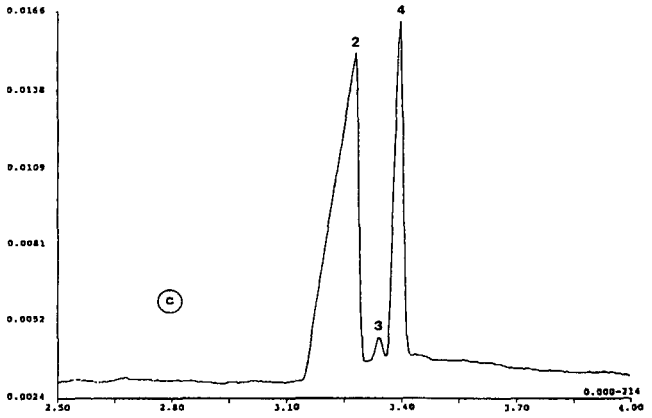

Figure 11 (continued)

using imidazole- or benzylamine-based electrophoretic buffers (pH 4.5 or 9.0, respectively) allowing indirect UV detection with carrier electrolytes.

Using an imidazole buffer (10^{-2} M, pH 4.5), the separation of cations K^+, Na^+, Ca^{2+}, Mg^{2+}, Ba^{2+} and Li^+ was carried out in a few minutes with excellent resolution (in particular for the Na^+/Ca^{2+} couple).

The separation of cations K^+ and NH_4^+ is possible using an alkaline electrophoretic buffer (pH 9.0) in order to decrease the electrophoretic mobility of the ammonium cation, hence differentiating it from the potassium cation.

The advantage of capillary electrophoresis over other separation techniques comes from its simple equipment, the use of a constant composition buffer and analysis speed compatible with routine analyses (especially for mineral waters).

ACKNOWLEDGEMENTS

This work has been supported by the Eurothermes Society (La Bourboule, France). Thanks are extended to Miss DEPERNET for technical assistance in the CZE analyses.

REFERENCES

1. S.F. Li: "Capillary electrophoresis. Principles, practice and applications". Elsevier, 1992.

2. M. AGUILAR, X. HUANG, R. ZARE, J. Chromatogr., 480, 427 (1989).

3. M. AGUILAR, A. FARRAN, M. MARTINEZ,J. Chromatogr., 635, 127 (1993).

4. N. WU, W. HORVATH, P. SUN, C. HUIE, J. Chromatogr., 635, 307 (1993).

5. F. FORET, S. FANALI, A. NARDI, P. BOCEK, Electrophoresis.,11,780 (1990).

6. A.WESTON, P. BROWN, P. JANDIK, W. JONES, A. HECKENBERG. J. Chromatogr., 593, 289 (1992).

7. A.WESTON, P. BROWN, A. HECKENBERG, P. JANDIK, W. JONES, J. Chromatogr., 602, 249 (1992).

8. M. CHEN, R. CASSIDY, J. Chromatogr., 602, 227 (1992).

9. W. BECK, H. ENGELHARDT, Chromatographia., 33 , 313 (1992).

10. M. KOBERDA, M. KONKOWSKI, P. YOUNBERG, W. JONES, A. WESTON., J. Chromatogr., 602, 235 (1992).

11. L. GROSS, E. YEUNG, Anal. Chem., 62, 427 (1990).

12. D. SWAILE, M. SEPANIAK, Anal. Chem., 63,179 (1991).

13. K.BÄCHMANN, J. BODEN, I. HAUMANN, J. Chromatogr., 626, 259 (1992).

14. X. HUANG, T. PANG, M. GORDON, R. ZARE, Anal. Chem., 59, 2747 (1987).

15. Handbook of Chemistry, Ed. 61, CRC Press: Boca Raton, FL, USA, 1991-1992.

16. K. ROW, W. GRIEST, M. MASKARINEC, J. Chromatogr., 409, 193 (1987) .

Received: March 31, 1994
Accepted: April 5, 1994

JOURNAL OF LIQUID CHROMATOGRAPHY, 17(18), 3889-3910 (1994)

DETERMINATION OF ANIONS IN WATER SAMPLES BY CAPILLARY ZONE ELECTROPHORESIS WITH INDIRECT UV DETECTION

K. LI AND S. F. Y. LI*
Department of Chemistry
National University of Singapore
Kent Ridge
Singapore (0511), Republic of Singapore

ABSTRACT

The separation of anions was performed by capillary zone electrophoresis with indirect UV detection. Optimum conditions for the separation of 12 anions, including the concentration of electroosmotic flow modifier, the concentration of the UV absorbing component and the pH etc. were obtained. This method was applied for the determination of anions in different water samples. The relative standard deviations for the analysis of anions were in the range of 1.2 to 6.9 percent. The detection limits were from 0.12 to 0.84 ppm for the 12 anions.

INTRODUCTION

Ion chromatography (IC) has been widely used to separate and analyze anions since it was introduced into the field of chromatography [1]. The most often and successful application of IC is to separate strong acid anions with conductivity detection [2]. Simultaneous separation of both strong and weak acid anions requires gradient elution to increase peak capacity [3] because of large affinity differences between the strong and weak acid anions to the ion exchange resin. Restrictions have resulted

from the specific columns and system complexicity. Inadequate selectivity and efficiency are also potential problems in some applications [1-2].

Capillary zone electrophoresis (CZE) is a relatively new separation method, which is based on the electrophoretic migration of the solutes. CZE has been widely used to separate ionic species with much better efficiency than HPLC and IC. The early application of CZE for the separation of inorganic anions was hampered mainly by the lack of universal detectors. A few studies have been performed using conductivity detector [4-6]. In the past few years, great progress has been made in the separation of inorganic anions using CZE method with indirect detection. The applicability of indirect detection for CZE has been discussed [7,8]. Some works dealing with the separation of organic and inorganic anion have been reported [9-19]. Because of the great influence of electroosmotic flow (EOF) on CZE separations [20], it is often necessary to use EOF modifier to control the EOF and to achieve optimal separation. Excellent separations of anions have been performed by Jones and coworkers [11] using chromate-based electrolyte systems. Optimal conditions for the separation of inorganic and organic anions have been discussed, but the detailed conditions and the EOF modifier were not revealed due to commercial reasons. Another excellent study performed by Harrold *et al* [15] reported on the separation of anions using pyromellitic acid as the UV background providing component and alkyl amine as the EOF modifier.

This paper presents results for the separation of anions using a chromate buffer system with cetyltrimethylammonium bromide as

EOF modifier. The optimum conditions for the separation of organic and inorganic anions were determined. The CZE method developed was applied to the determination of anions in various water samples.

EXPERIMENTAL

Chemicals and materials

Ca 10 mg/ml stock solutions for individual anions were prepared by dissolving a single weighed amount of analytical or better grade sodium or ammonium salt of the anions in deionized water. Standard mixtures at ppm level were prepared by stepwise dilution of the stock solutions fresh daily. Potassium chromate, used as the UV background-providing compound and electrophoresis buffer, was of analytical grade and was obtained from Aldrich (Milwaukee, WI, USA). 14.2 mM cetyltrimethylammonium bromide (CTAB) (Aldrich) solution was prepared by dissolving 0.1293 gram of analytical grade salt in 25 ml water. All solutions were prepared using 18 MΩ water from a Millipore water purification system. All other chemicals and reagents were analytical or better grade. The electrophoresis buffer was prepared from 0.58 M chromate and 14.2 mM CTAB stock solutions daily by stepwise dilutions. CTAB was used as an electroosmotic flow modifier to reverse the electroosmotic flow, so that an electroosmotic flow direction from the cathode to anode was obtained. 1:10 (v/v) high purity nitric acid and 100 mM sodium hydroxide were used to adjust the pH of the electrolyte in the pH study. All the buffers were passed through 0.45 μm membrane filters and degassed by ultrasonication prior to use.

Instrumentation

A home-made capillary electrophoresis system was used for the present investigation. A Spellman model RHR30PN10/RVC high voltage supply with reversible polarity and a maximum capacity of 30 kV was employed. A model UVIS 20 UV detector (Carlo Erba Instruments, Italy) and a piece of fused silica capillary tube of 550 mm total length and 450 mm effective length (from the injection end to the detection window) with 50 μm i.d., were used to perform the separation and determination of anions. On-line detection was carried out through a window by burning off 2 mm of polyimide coating from the capillary tube. Indirect UV detection was performed at 254 nm throughout the experiments. Samples were introduced into the column hydrodynamically by raising the sample vial to a height of 10 cm for 20 or 30 seconds. Samples were introduced into the capillary either from the cathode end when negative polarity power was applied or from the anode end when positive polarity was used. Electropherograms were recorded and processed with a Carlo Erba model PDP 700 integrator. The tap and rain water was passed through a 0.45 μm filter before injection. The mineral water samples were obtained from a supermarket and used for the determination without pretreatment.

RESULTS AND DISCUSSION

Separation of anions with CZE under different electroosmotic flow

When positive polarity power was used to separate anions, no peaks were recorded in the electropherograms except for the water peak. This could be explained by the fact that the electrophoretic flows for anions were in opposite direction to

and faster than the electroosmotic flow. In the case that the anions were injected from the anodic end, they could reach the detection cell only when electroosmotic flow overcomes the electrophoretic flows. Since simple anions have relatively large charge to radius ratios, their electrophoretic flows were greater than the electroosmotic flow and hence they would not migrate towards the detector. This is unlike the cases in most CE separations where the electroosmotic flow tends to be great than the electrophoretic flows [21].

When the polarity of the power supply was reversed, anions could reach the anode since their electrophoretic flows were greater than the electroosmotic flow. In such a CZE configuration, of the 12 anions injected into the column, i. e. thiosulphate, bromide, chloride, sulphate, nitrite, nitrate, molybdate, citrate, fluoride, phosphate, carbonate and acetate, the first eight anions were detected and separated within 24 min. The separation is illustrated in Figure 1A. The other anions could not reach the detection window within 1 hour, probably because the electrophoretic flows of these anions were slower than but close to and in opposite direction to the electroosmotic flow (if their electrophoretic flows were much slower than the electroosmotic flow, these anions would be expected to be detectable in a positive polarity CZE configuration [21]), and hence very slow migrations of these anions were expected. To speed up the migration of these anions, CTAB was added to the electrolyte buffer to modify the electroosmotic flow. CTAB concentration was found to affect the migration times of the anions significantly. Figure 1B and 1C show the separation of anions at different CTAB concentrations. At CTAB concentration of 2.0×10^{-5} M, 10 peaks,

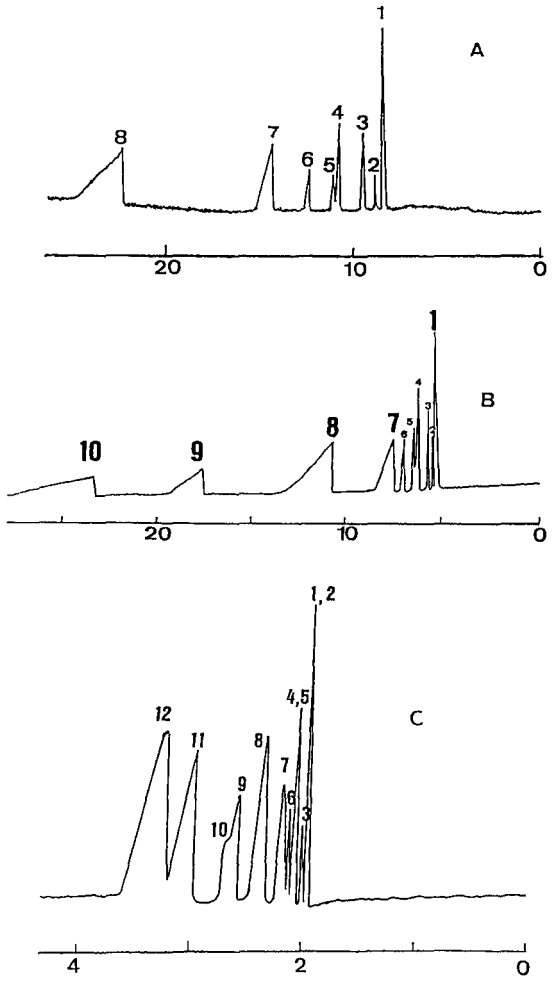

MIGRATION TIME / MIN.

Figure 1. CZE separation of anions at different CTAB concentrations. (A) CTAB = 0 (B) CTAB = 2.0 X 10^{-5} M (C) CTAB = 6.2 X 10^{-5} M. CrO_4^{2-} = 5.8 mM; pH = 8.5; 20 kV. CE column, 550 mm X 50 μm i.d. fused silica capillary column (effective length 450 mm). Peak identification. 1 = thiosulphate, 2 = bromide, 3 = chloride, 4 = sulphate, 5 = nitrite, 6 = nitrate, 7 = molybdate, 8 = citrate, 9 = fluoride, 10 = phosphate, 11 = carbonate, 12 acetate.

i.e. the eight peaks obtained in Fig. 1A and fluoride and phosphate, were detected within 25 min and the migration times for all the anions were shortened. At this CTAB concentration, the water peak, used as a marker of the electroosmotic flow, could not be detected in the electropherogram. This indicated that the EOF direction was still from the anode to the cathode, although its speed was hindered by the added CTAB cations which resulted in partial masking of the negative charges of the silanol group on the inner wall of the capillary tube. When CTAB concentration was further increased to 6.2×10^{-5} M, all the 12 anions could reach the detection cell, although 3 pairs of anions, i.e. thiosulphate and bromide, sulphate and nitrite as well as fluoride and phosphate, overlapped due to the fast but reversed electroosmotic flow (Fig. 1C). In Fig. 2, the effect of CTAB concentration on the migration times of the anions is shown. It can be seen that the migration times of the anions were greatly shortened by increasing the CTAB concentration to above 4 mM. In subsequent experiments, a CTAB concentration of 4.8×10^{-5} M was used to modify the electroosmotic flow and satisfactory separation for the 12 anions was achieved.

The influence of CTAB concentration on the migration times of anions could be explained as follows. At low concentrations of CTAB, the EOF was hampered by the added CTAB cations which reduced the negative charges of the silanol groups on the capillary tube. It was then reversed by the further increases in the CTAB concentration due to the positive charges of CTAB, and finally the reversed EOF reached a maximum when the capillary surface was completed covered by CTAB. This process resulted in the greatest increase in the migration velocities for the anions

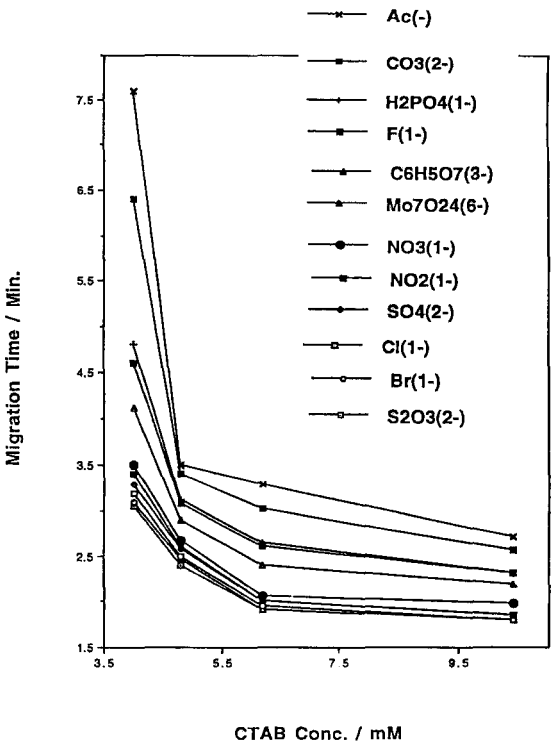

Figure 2. Effect of CTAB concentration on the migration times of anions. Conditions as in Fig. 1.

at low concentration of CTAB in buffer (see Fig. 2), and the increase in the migration velocities at higher concentrations was not so remarkable once the EOF reached a maximum when the surface of the silica capillary was saturated with CTAB.

Effects of chromate concentration on the separation of anions

The effect of chromate on the separation of anions could be attributed to two aspects. The first consideration is the UV

detection, which requires a low chromate concentration to achieve high sensitivity in the indirect UV mode. This is becasue the noise level in an indirect UV system is proportional to the concentration of the UV background-providing component [20]. In addition, chromate concentration affects the ionic strength of the electrophoresis buffer. A high chromate concentration increases the current passing through the column, resulting in a high noise level due to inadequate dissipation of the Joule heat. For these reasons, the chromate concentration should be kept low. On the other hand, a decrease in chromate concentration results in a decrease in the efficiency of displacement of the background ions by the sample ions [7], which is a function of the ratios of the analyte to the UV background component. As a result, a low sample loading capacity and narrow linear dynamic range would be expected [15]. Furthermore, if the concentration of chromate is too low, a decrease in the peak efficiency would be obtained, since the CZE efficiency is expected to increase with an increase in ionic strength [22], provided that effective heat dissipation can be achieved. Figure 3 shows the influence of the concentration of chromate on the migration times of the anions. The migration times of the anions increased with an increase in the concentration of chromate due to the slower EOF at higher chromate concentration.

From Fig. 3, the optimum concentration of chromate for the separation of the anions could be found. Although the separation for anions was generally improved at higher chromate concentration, particularly for fluoride and phosphate, as well as for sulphate and nitrate, at chromate concentration of 11.8 mM, the peaks for thiosulphate and bromide overlapped. Figure 4

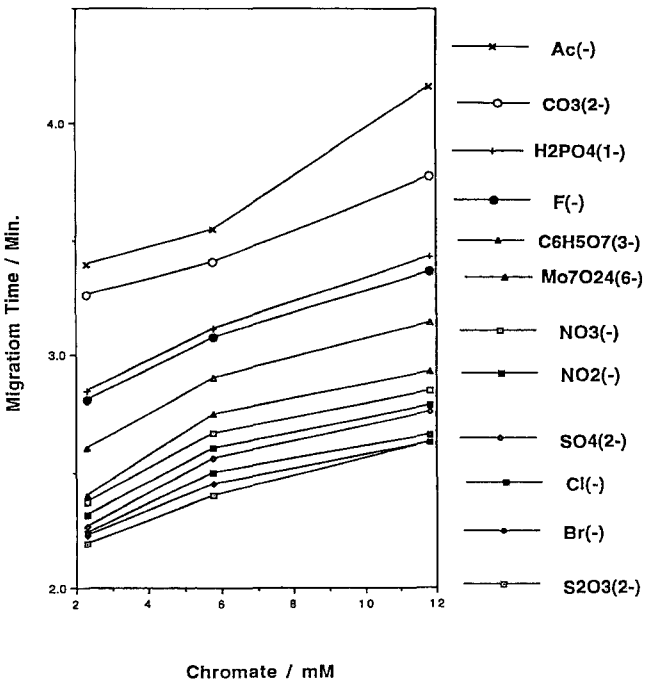

Figure 3. Effect of chromate concentration on the migration times of anions. CTAB = 4.8 X 10^{-5} M. Other conditions and peak identifications as in Fig. 1.

shows the electropherograms of anions at three different concentrations of chromate. It can be seen that the resolution and sharpness of the peaks were significantly affected by changes in the concentraction of chromate. In the present work, chromate buffers at concentrations in the range of 5.8 to 8.2 mM was used as electrophoresis buffers for the separation of anions which provided reasonably good efficiencies and sensitivities.

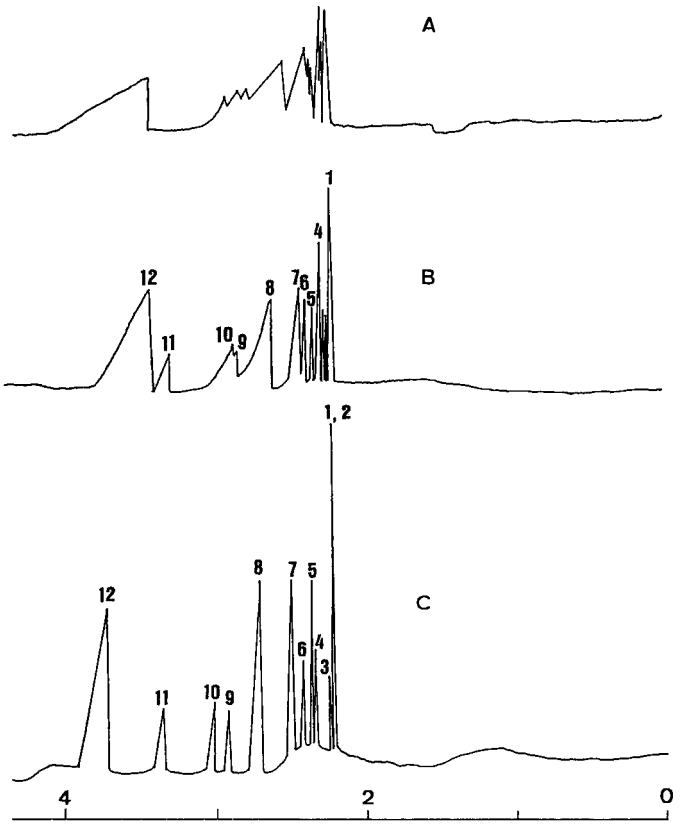

Figure 4. Separation of anions at different chromate concentrations. (A) CrO_4^{2-} = 0.85 mM (B) CrO_4^{2-} = 2.3 mM (C) CrO_4^{2-} = 10.8 mM. CTAB = 4.8 X 10^{-5} M. Other conditions as in Fig.2. Peaks in (A) were not identified, and peak identification in (B) and (C) as in Fig. 2.

Effect of pH of the electrolyte buffer on the separation of anions

The migration times of anions decreased with an increase in pH in the pH range of 7 to 12, mainly due to the slower electroosmotic flow at lower pH (Figure 5). This observation was consistent with an earlier investigation [9]. The 12 anions could be separated within the pH range of 6.5 to 11.5, but bromide comigrated with thiosulphate at pH 11.5 or higher. The migration order for strong acid anions was not changed in this pH range. However, the migration times for the weak acid anions, i.e. carbonate, phosphate and acetate, were affected significantly by changes in pH. This could be explained by the fact that these anions were progressively protonated as the pH of the electrophoresis buffer was decreased. As a result, their electrophoretic velocities became slower since the migration rates of the anions were mainly controlled by the charge to anion size ratio. Fluoride and phosphate, which overlapped with each other at pH higher than 11.5 due to the fast migration of the completely ionized phosphate at high pH, could be separated completely at lower pH. Migration rate of carbonate increased remarkably at pH higher than 9.5, and it migrated ahead of phosphate, fluoride and citrate and just after molybdate at pH 11.5. The migration time for acetate was relatively long in the pH range of 6.5 to 8.5. Figure 6 illustrates the separations of anions at pH 9.5 and 12.0. Since a pH value lower than 6.5 was not applicable because of the change of chemical form of chromate, and pH higher than 12.5 resulted in very noisy baseline, in this investigation, the pH range 7.5 to 10 was used to perform the determination of anions in water samples.

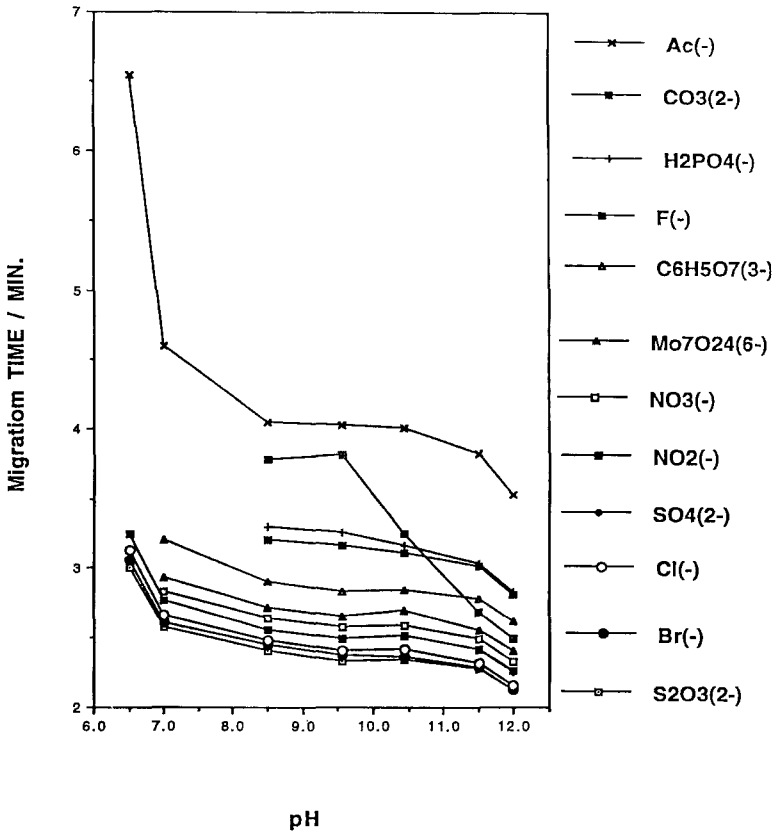

Figure 5. Effect of pH on migration times of anions. CTAB = 4.8 X 10^{-5} M, CrO_4^{2-} = 5.8 mM. Other conditions and peak identification as in Fig. 1.

Figure 7 illustrates a typical CZE separation of 12 anions using the optimal conditions obtained above. 12 anions were separated within a migration time window of 89 seconds.

APPLICATIONS

To demonstrate the usefulness of the CZE method developed, analyses of a variety of samples were performed. The

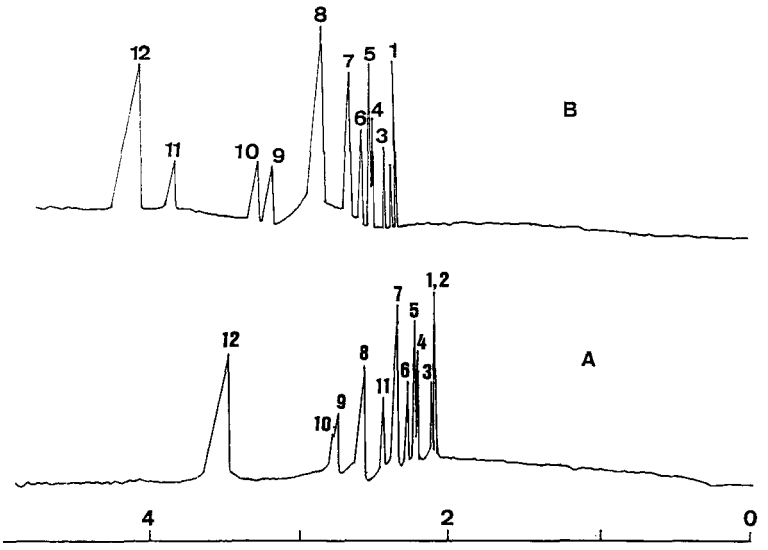

Figure 6. Separation of anions at different pH values. (A) pH =9.5 (B) pH = 12.0 CTAB = 4.8 X 10^{-5} M. Chromate = 5.8 mM. Other conditions and peak identification as in Fig. 1.

electropherograms obtained are shown in Figure 8 to Figure 12. Result of the quantitative analysis are included in Table 1 and II.

Figure 8 is an electropherogram of anions in tap water obtained using an applied voltage of 25 kV and a buffer containing 8.2 mM chromate as the UV absorbing component. Four anions, i.e. chloride, sulphate, nitrate and carbonate, were identified by spiking the sample with standards, and an unknown peak was observed. Figure 9 shows the CZE separation of anions in a commercial mineral spring water. In this and subsequent

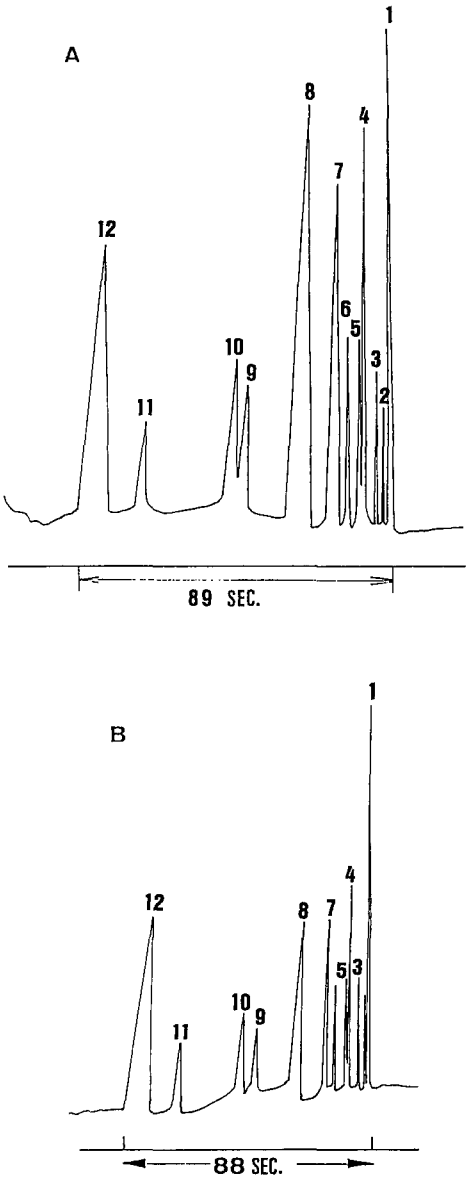

Figure 7. Typical CE separation of anions using the optimal conditions. Peak identifications as in Fig. 1.

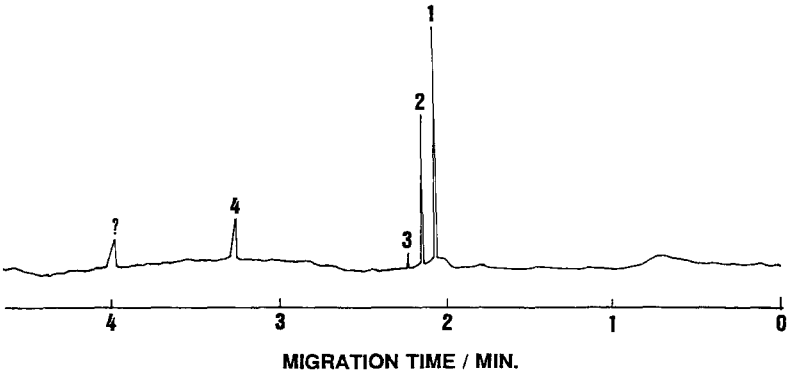

Figure 8. Electropherogram of anions in tap water. peak identification: 1 = chloride, 2 = sulphate, 3 = nitrate, 4 = carbonate, 5 = unknown. Other conditions as in Fig. 7.

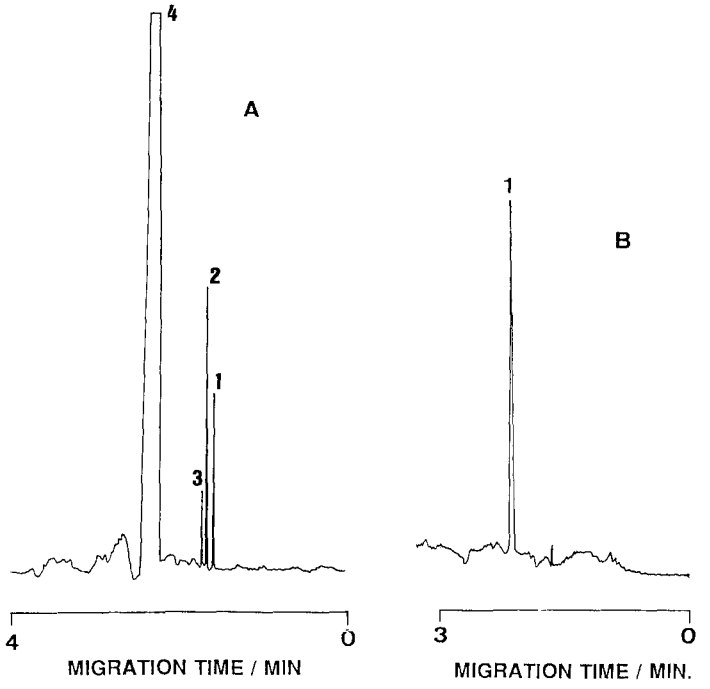

Figure 9. Electropherogram of anions in mineral spring water "Evian". 1=chloride; 2=sulphate; 3=nitrate; 4=bicarbonate. CZE conditions: 8.2 mM Chromate, 4.8 X 10-5 M CTAB, 25 KV applied voltage. Other conditions as in Fig. 1.

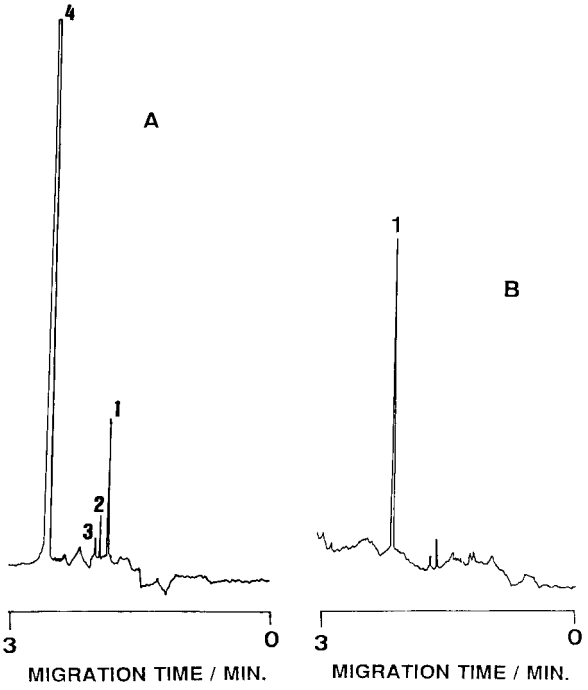

Figure 10. Electropherogram of anions in mineral spring water "Amust". 1=chloride, 2=sulphate, 3=nitrate, 4=bicarbonate. CZE conditions as in Fig. 9.

determinations, the applied voltage was 30 kV and a buffer containing 8.2 mM chromate was used to separate the anions. Very fast separation and high efficiencies for anions were obtained. Figure 10 is the electropherogram for anions in another mineral water sample, the concentrations of anions in the sample in Figure 10 are lower than those in sample in Figure 9. Figure 11 presents the separation of anions in a rain water sample.

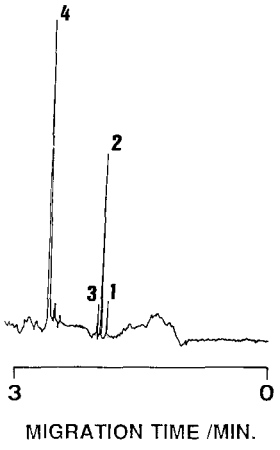

Figure 11. Electropherogram of anions in rain water sample. 1=chloride, 2=sulphate, 3=nitrate, 4=carbonate. CZE conditions as in Fig. 9.

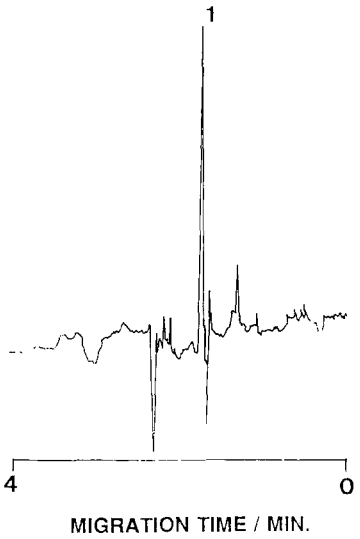

Figure 12. Electropherogram of anions in Pepsi-cola. 1=phosphate. Other conditions as in Fig. 9.

Table I. Analytical Results of anions in water samples.

	Concentration (ppm)				
	Cl^-	SO_4^{2-}	NO_3^-	CO_3^{2-}	PO_4^{3-}
1. tap water:					
Measured value	32.3	31.0		5.0	
R. S. D. (%)	3.6	4.5		2.7	
	(n=4)	(n=3)		(n=4)	
2. Mineral water "Evian":					
Reference value	4	10	1	357	NA
Measured Value	4.9	8.17	1.25	407	NA
RSD (%)	1.2	1.6	4.3	2.4	--
	(n=3)	(n=3)	(n=3)	(n=3)	--
3. Mineral water "Amust":					
Reference value	NA	0.94	0.11	59.1	NA
Measured value	4.0	1.24	ND	59.1	ND
RSD (%)	1.4	6.5	--	2.8	--
	(n=4)	(n=3)	--	(n=3)	--
4. Rain water					
Measured value	0.83	0.53	ND	ND	ND
RSD (%)	6.9	6.1	--	--	--
	(n=3)	(n=3)			
5. Pepsi-cola					
Measured value	--	--	--	--	1052
RSD (%)	--	--	--	--	5.62
					(n=3)

*: Chemical forms for carbonate and phosphate were not determined
NA: not available
ND: not detected

Table II. Detection limits of anions using CE method (ppm)[a].

thiosulphate	0.84
bromide	0.50
chloride	0.17
sulphate	0.16
nitrite	0.42
nitrate	0.25
molybdate	0.80
citrate	0.55
fluoride	0.13
phosphate	0.14
carbonate	0.27
acetate	0.37

[a]: based on 23.5 nl injection

Sulphate was quantitatively determined. It is suggested that the CZE method adopted here could be used for the monitoring of other anions of environmental interest. Figure 12 is the electropherogram of a soft drink (Pepsi-cola) after 40 times dilution. Phosphate was identified and quantitatively determined.

Table I summarizes the analytical results for the determination of anions in water samples with the CZE method. In Table II, the detection limits of the anions are listed. The detection limits were below 1 ppm, and are comparable to those typically obtained by ion chromatography (IC).

The results obtained in the present experiments showed that CZE provides a rapid and reliable method for the determination of anions in aqueous samples. Determination of anions in many different matrices can be readily carried out without the need to perform extensive sample preparations.

REFERENCES

[1] J. G. Tarter, Ion Chromatography, Marcel Dekker, New York, 1987

[2] J. S. Fretz, D. T. Gjerde and C. Pohlandt, Ion Chromatography, Huthig, New York, 1982.

[3] R. D. Rocklin, C.A. Pohl and J. A. Schibler, J. Chromatogr., 411, 107 (1987)

[4] X. Huang, J. A. Luckey, M. J. Gorden and R. Z. Zare, Anal. Chem., 61, 766-770 (1989)

[5] J. L. Beckers, Th. P. E. M. Verheggen and F. M. Everaerts, J. Chromatogr., 452, 591 (1988)

[6] F. Foret, M. Deml, V. Kahle and P. Bocek, Electrophoresis, 7, 430 (1986)

[7] E. S. Yeung, Acc. Chem. Rev., 22, 125-130 (1989)

[8] E. S. Yeung and W. G. Kuhr, Anal. Chem., 63, 275A-282A, (1991)

[9] W. G. Kuhr and E. S. Yeung, Anal. Chem., 60, 2642, (1988)

[10] B. J. Wildamn, E. Peter, E. Jackson, W. R. Jones and P. G. Alden, J. Chromatogr., 546, 456-466 (1991)

[11] P. Jandik and W. R. Jones, J. Chromatogr., 546, 433-443, (1991)

[12] W. R. Jones and P. Jandik, J. Chromatogr., 546, 445-458 (1991)

[13] M. T. Ackermans, F. M. Everaerts and J. L. Beckers, J. Chromatogr., 549, 345-355 (1991)

[14] J. P. Romano and J.Krol, J. Chromatogr., 640, 403-412 (1993)

[15] M. P. Harrold, M. J. Wojtusik, J. Riviello and P. Henson, J. Chromatogr., 640, 463-471, (1993)

[16] B. Kenney, J. Chromatogr., 546, 423-430 (1991)

[17] A. Nardi, M. Cristalli, C. Desiderio, L. Ossicini, S. K. Shukla and S. Fanali, J. Microcol. Sep., 4, 9-11 (1992)

[18] F. Foret, S. Fanali, L. Ossicini and P. Bocek, J. Chromatogr., 470, 299-308 (1989)

[19] K. Fukushi and K. Hiiro, J. Chromatogr., 518, 189-198 (1990)

[20] H. Small and T. E. Miller, Anal. Chem., 54, 462-469 (1982)

[21] S.F.Y. Li, Capillary Electrophoresis: principles, practice and applications, J. Chromatogr. Lib., Vol. 52, Elsevier Science Publishers, Amsterdam and New York, 1992.

[22] M. W. Nielen, J. Chromatogr., 542, 173 (1991)

Received: July 14, 1994
Accepted: July 26, 1994

JOURNAL OF LIQUID CHROMATOGRAPHY, 17(18), 3911-3923 (1994)

ANALYSIS OF A NEW DOXORUBICIN DERIVATIVE (FCE 23762) AND RELATED COMPOUNDS BY HIGH PERFORMANCE CAPILLARY ELECTROPHORESIS

M. G. QUAGLIA[1]*, A. FARINA[2], F. KILÁR[3], S. FANALI[4], E. BOSSÙ[1], AND C. DELL'AQUILA[1]

[1]*Dipartimento Studi Farmaceutici*
University of Rome "La Sapienza"
P.le A. Moro 5, 00185 Rome, Italy
[2]*Istituto Superiore di Sanità*
V.le Regina Elena 269, 00161 Rome, Italy
[3]*Central Research Laboratory*
Medical School, University of Pécs
Szigeti út 12, H-7643 Pécs, Hungary
[4]*Istituto di Cromatografia del C.N.R.*
Area della Ricerca di Roma
C.P. 10, 00016 Monterotondo Scalo, Rome, Italy

ABSTRACT:

High performance capillary electrophoresis was applied to analyse FCE 23762, a new antracycline analogue (doxorubicin derivative) with anti-tumor activity. It has been shown earlier that a FCE 23762 sample may contain two main impurities, one of the optical isomers of FCE 23762 and the most probable degradation product, adriamycinone. The pharmacologically active compound and its diastereomer were resolved in free zone electrophoresis experiments. Adriamycinone, a neutral compound, is baseline separated from the other two (cationic) compounds by micellar electrokinetic chromatography. The use of two different separation methods was advantageous for an efficient and sensitive analysis for the synthetic product of FCE 23762.

INTRODUCTION

Anthracycline antibiotics are chemotherapeutic agents with significant anti-tumor activity. Besides doxorubicin and daunorubicin a large number of analogue compounds have been synthesized with the aim to find anti cancer drugs with improved efficacy and minor toxicity. The clinical use of doxorubicin and other related compounds in cancer diseases, e.g., acute leukaemia, lymphoma and solid tumor, has been approved (1-5). The emergence of the resistance against these drugs observed in experimental conditions as well as in patients, however, initiated further research to develop (synthesize) new analogues. Among those, the class of morpholino anthracyclines and particularly a new compound, 3'-deamino-3'-[2-(S)-methoxy-4-morpholino]-doxorubicin (laboratory code FCE 23762), maintained good effect on doxorubicin-resistant tumor cells (6). FCE 23762 is a derivative of doxorubicin with a modified daunosamine moiety in position 3' synthesized and studied in the Chemical Research and Development Department of Farmitalia - Carlo Erba (Milan, Italy).

Figure 1. shows the structures of 3'-deamino-3'-[2-(S)-methoxy-4-morpholino]-doxorubicin (**I,** code: FCE 23762), 3'-deamino-3'-[2-(R)-methoxy-4-morpholino]-doxorubicin (**II,** named in this paper as "R-isomer") and adriamycinone (**III**). The "R-isomer" might appear as synthetic impurity in a FCE 23762 sample together with adriamycinone which is the most probable degradation product of both, FCE 23762 and "R-isomer".

The high toxicity and easy degradation of the doxorubicin derivatives require sensitive and selective analytical methods to perform stability tests and drug monitoring in biological fluids. HPLC techniques have been used widely for the analyses of anthracyclines (7-13), and among them two specific methods have been developed for stability studies of FCE 23762 and for its determination in

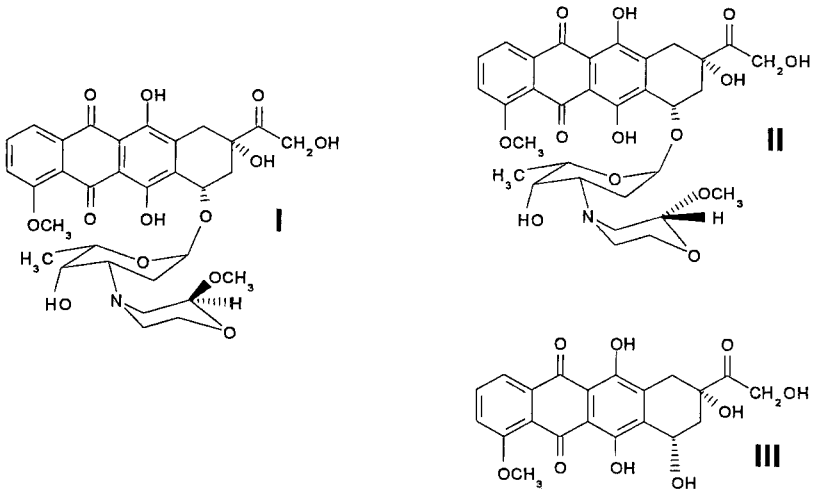

FIGURE 1. Chemical structures of (**I**) 3'-deamino-3'-[2-(S)-methoxy-4-morpholino]-doxorubicin, (**II**) 3'-deamino-3'-[2-(R)-methoxy-4-morpholino]-doxorubicin and (**III**) adriamycinone.

plasma (11,12). Some of the HPLC methods (13), however, showed low efficiency.

High performance capillary electrophoresis (HPCE) has also been employed to analyse daunorubicin, doxorubicin and epirubicin in human plasma (14). Since HPCE is a promising new separation method, providing high efficiency and sensitivity within short analysis time, we applied capillary electrophoretic methods for the determination of FCE 23762 and its related compounds.

EXPERIMENTAL

Chemicals

Samples (reference standards) of FCE 23762, "R-isomer" and adriamycinone were kindly supplied by the Chemical Research and Development Department of

Farmitalia - Carlo Erba (Milan, Italy). The purity of the FCE 23762 sample (considered as reference standard), attested by the Department, was: 3'-deamino-3'-[2-(S)-methoxy-4-morpholino]-doxorubicin 90.0 %, water 7.0 %, 3'-deamino-3'-[2-(R)-methoxy-4-morpholino]-doxorubicin 1.6 %, adriamycinone 0.4 % and unknown impurities 0.8 %.

Double distilled water was used for the separation of the electrolyte and the sample solutions. All common chemicals (acetic acid, sodium hydroxide, acetonitrile, etc.) were purchased from Merck. The solutions were degassed and kept at room temperature during the working day.

Stock solutions of the samples were prepared in water and diluted to the appropriate concentration before the electrophoretic analyses.

Capillary electrophoresis

Capillary zone electrophoresis (CZE) was performed in sodium phosphate (pH 2.5, 5.0, 6.0 or 7.0) or sodium acetate buffer (pH 4.2 or 5.0) without or with CH_3CN, as organic additive. Micellar electrokinetic chromatography (MEKC) experiments were made in a 15 mM phosphate - 6 mM borate buffer (pH 7) containing 20 mM SDS.

The analyses were carried out with a Spectra Phoresis 1000 Instrument (Thermo Separation Products, San José, CA, USA), equipped with a multiwavelength UV-VIS detector. Separations were performed in a CElect FS75 (75 μm ID) bare fused silica capillary (Supelco, Bellefonte, PA, USA) with a total length of 42 cm and effective length of 34 cm. Capillary conditioning were done every day (washing with 0.1 M NaOH for 30 min) and before every runs (washing with 0.1 M NaOH for 2 minutes, with water for 2 min and with background

electrolyte for 3 min). The samples were applied with vacuum for 1.5 s or 2 s (ca 3 nl/s). The temperature of the capillary cartridge was kept at 15 °C in the zone electrophoresis and 25 °C in the micellar electrokinetic chromatography experiments.

The SpectraPhoresis 1000 equipment was controlled and the data were evaluated with the SpectraPhoresis CE v.1.05B software (Thermo Separation Products). The samples were identified either with spiking or with the help of their spectra obtained by the multiwavelength detection.

RESULTS AND DISCUSSION

The purpose of this study was to obtain a fast capillary electrophoresis method to analyse the homogeneity and purity of FCE 23762, a new doxorubicin derivative with anti-tumor activity. In the synthetic procedure of FCE 23762 two other compounds might cause inhomogeneities, the "R-isomer", and a degradation product, adriamycinone (see Fig. 1). We have investigated the effect of separation mechanism (zone electrophoresis and micellar electrokinetic chromatography), pH and organic additive (modifier) in the background electrolyte on the resolution of the above three compounds.

The samples obtained from Farmitalia - Carlo Erba were considered as reference standards. At the same time, however, they were also regarded as "unknown" samples to be characterized by electrophoretic runs, because it was attested by the producer, that FCE 23762 sample contains also "R-isomer" and adriamycinone as impurities. The other two samples were not characterized in details by the supplier. In the electrophoretic experiments, therefore, mixtures of the samples (containing high amount of each compounds) were used to find

optimal conditions for the separations, but afterwards the stock solutions of the samples were investigated in the conditions, where the components had been best resolved.

FCE and "R-isomer" migrate in electric field as cations, while adriamycinone is a neutral compound. The separation of the two diastereomers, FCE 23762 and the "R-isomer", does not need, in principle, a chiral selector because they have different physico-chemical properties and therefore they could migrate with different electrophoretic mobilities. For resolving these compounds we used zone electrophoresis experiments in different buffer systems, such as, sodium phosphate at pH 2.5, 5, 6 or 7 and sodium acetate at pH 4.2 or 5.0. For the improval of the resolution different concentrations of acetonitrile, as organic additive, were tested.

Zone electrophoretic experiments, performed at acidic pH, showed, that an organic additive, acetonitrile, was always necessary for obtaining the resolution of the two diastereomers. This is probably due to the changes in the solvatation of the two diastereomers caused by the organic modifier which may influence the effective mobilities of the substances. Higher concentration of the acetonitrile, however, caused longer experimental runs (i.e., longer migration times of the substances in the same background electrolyte). In the phosphate buffer at pH 2.5 it was not possible to obtain baseline resolution of the two diastereomers, even an acetonitrile concentration as high as 70 % was applied (results not shown). Fig. 2a shows the baseline separation of FCE 23762 and "R-isomer" in 50 mM sodium acetate pH 4.2 in the presence of 70 % acetonitrile. Increasing the pH to 5.0 the acetonitrile concentration could be lowered to 30 % (Fig. 2b). Further increase of the pH was not useful, since the high electroosmotic flow (EOF) did not allow the separation of the two components because they were moving with the EOF (results not shown). Adriamycinone (neutral substance) in a mixture of all three

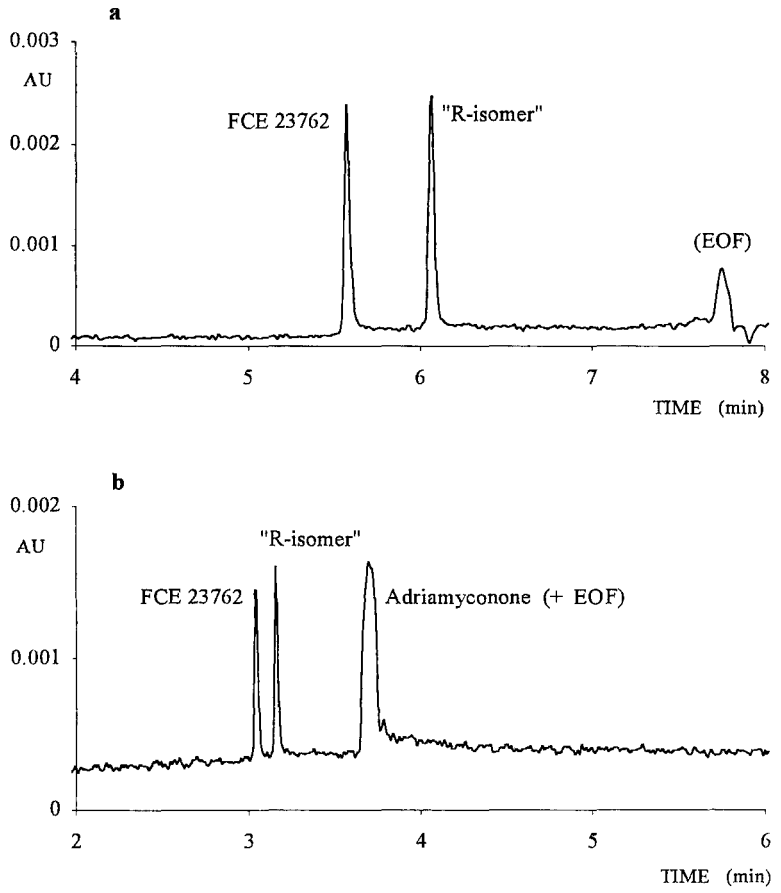

FIGURE 2. Capillary zone electrophoresis analyses of sample mixtures of (a) FCE 23762 (10 μg/ml) and "R-isomer" (10 μg/ml) and (b) FCE 23762 (5 μg/ml), "R-isomer" (5 μg/ml) and adriamycinone (8 μg/ml). Background electrolyte (a) 50 mM Na-acetate, pH 4.2, containing 70 % acetonitrile, (b) 50 mM Na-phosphate, pH 5.0, containing 30 % acetonitrile. Experimental conditions: capillary 75 μm ID x 42 cm (34 cm effective length); voltage 20 kV; current (a) 16 μA, (b) 30 μA; detection 225 nm; temperature 15 °C. Sample application was made by vacuum for 1.5 s. (EOF, electroosmotic flow).

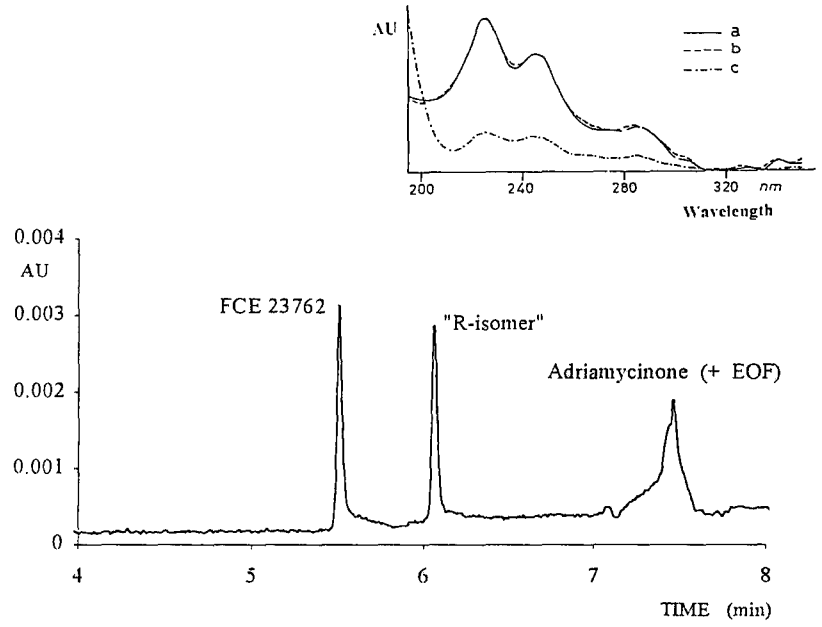

FIGURE 3. Capillary zone electrophoresis of a mixture of FCE 23762 (10 μg/ml; insert: a) "R-isomer" (8 μg/ml; insert: b) and adriamycinone (7 μg/ml; insert: c). Background electrolyte and experimental conditions are as in Fig. 2a. (EOF, electroosmotic flow). The spectra were obtained with multiwavelength detection.

compounds of interest (see Fig. 2b and Fig. 3) moved with the EOF forming an asymmetric peak.

For the separation of adriamycinone we used micellar electrokinetic chromatography in a phosphate-borate buffer containing 20 mM SDS. The two diastereomers of interest are not resolved in this condition (Fig. 4a), however, both, FCE 23762 and "R-isomer" were baseline separated from adriamycinone (Fig. 4b,c).

With the above two electrophoretic methods we analysed the original samples, as well. Using the experimental conditions in Fig. 2 and 3, the minimum detectable amount of "R-isomer" was obtained to be 0.5 % of the amount of FCE 23762 (using) in a mixture of both (the experimental error of the determination of the peak area ratio was found to be ± 0.3 % due to the baseline variations, probably caused by the influence of the organic additive or the other impurities). As it was expected from the purity testing attested by the producer, the FCE 23762 sample contained a small amount of the "R-isomer" (1.6 % of the sample that corresponds to ca. 1.8 % of the FCE 23762 content). The amount of the "R-isomer" was estimated from the electropherogram of the FCE 23762 stock solution (not shown) and found to be 2.0 % ± 0.3 % of the FCE 23762 content, which is in a good agreement of the previous characterization. However, the MEKC experiments did not show detectable amount of the adriamycinone in the sample (Fig. 5a), which means that our method has a detection limit of the related compound ca. 0.4 % of FCE 23762 or higher. Unexpectedly, the sample of the "R-isomer" showed the presence of adriamycinone detectable in the MEKC experiments (Fig. 5b) and estimated as 1.4 % ± 0.1 % of the "R-isomer" content. This impurity was also observed when the mixture of FCE 23762 and "R-isomer" was investigated (see Fig. 4a). The adriamycinone sample was found to be pure with either CZE or MEKC (results not shown).

CONCLUSIONS

Since we used two different separation mechanisms for the analysis of the anthracycline analogues, the impurities in the samples could be verified very efficiently. As a validation of the methods developed in this study we did not find

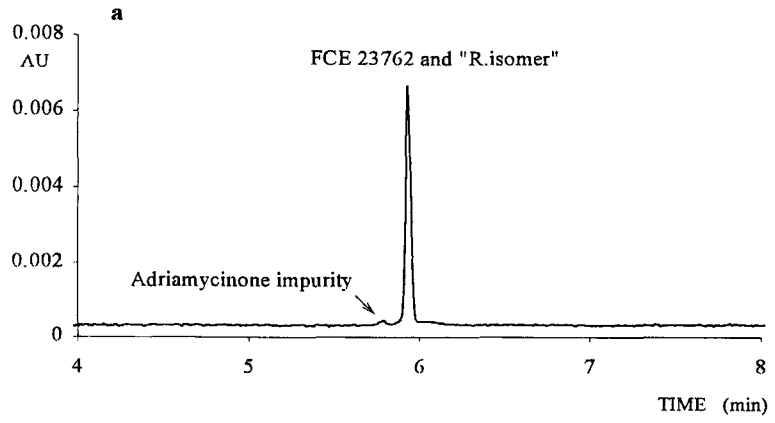
a
0.008
AU
0.006
0.004
0.002
0
FCE 23762 and "R.isomer"
Adriamycinone impurity
4
5
6
7
8
TIME (min)

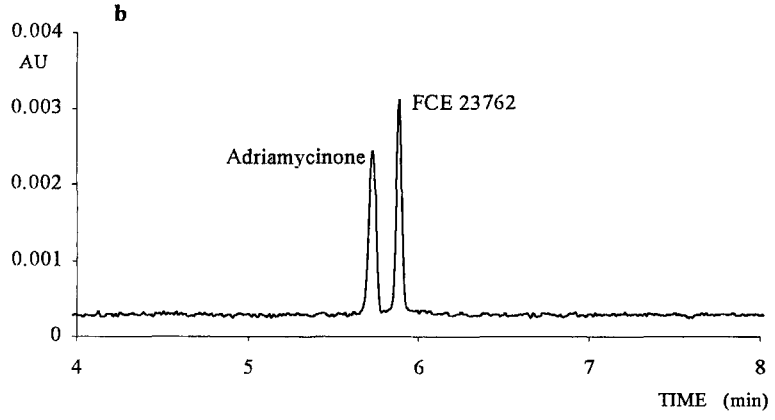
b
0.004
AU
0.003
0.002
0.001
0
FCE 23762
Adriamycinone
4
5
6
7
8
TIME (min)

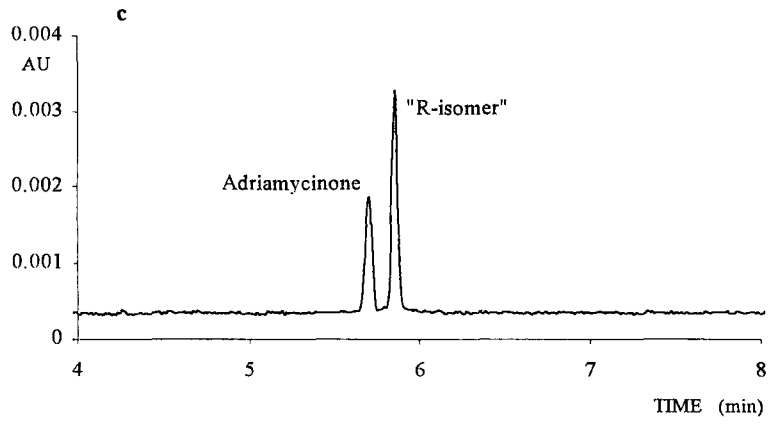
c
0.004
AU
0.003
0.002
0.001
0
"R-isomer"
Adriamycinone
4
5
6
7
8
TIME (min)

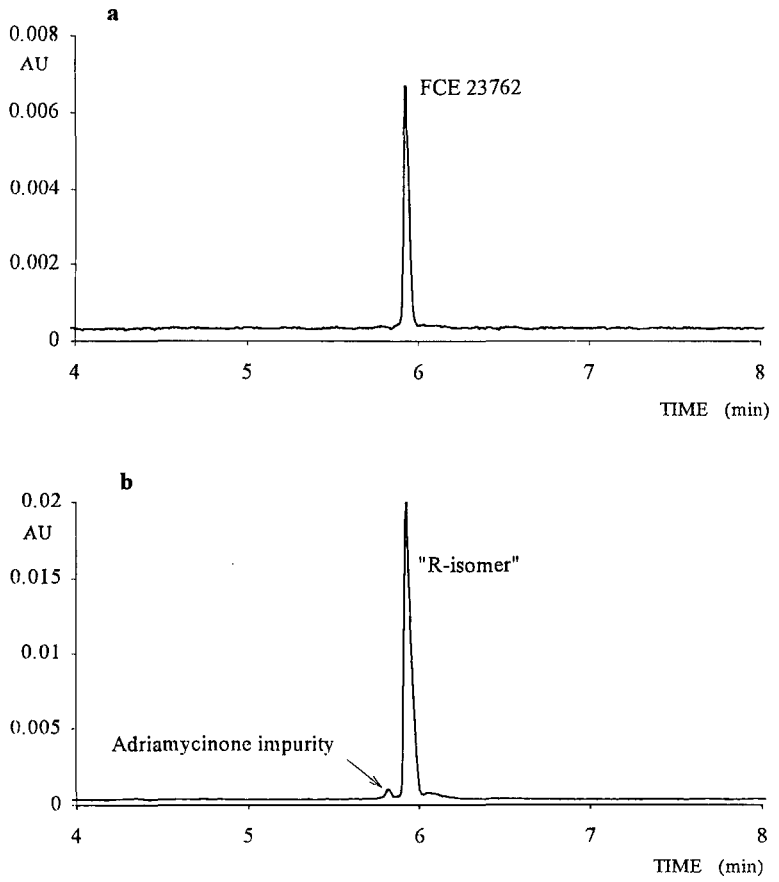

FIGURE 5. Micellar electrokinetic chromatography experiments of the (a) FCE 23762 (10 µg/ml) and (b) "R-isomer" (30 µg/ml) samples. Experimental conditions as in Fig. 4.

FIGURE 4. Micellar electrokinetic chromatography experiments of sample mixtures of (a) FCE 23762 (13 µg/ml) "R-isomer" (12 µg/ml), (b) FCE 23762 (8 µg/ml) and adriamycinone (7 µg/ml) and (c) "R-isomer" (9 µg/ml) and adriamycinone (6 µg/ml). Background electrolyte 15 mM Na-phosphate - 6 mM Na-borate, pH 7, containing 20 mM SDS. Experimental conditions: capillary 75 µm ID x 42 cm (34 cm effective length); voltage 20 kV; current 34 µA; detection 225 nm; temperature 25 °C. Sample application was made by vacuum for 1.5 s.

other impurities in the FCE 23762 sample than it was given by the producer. We were able to determine the impurities, determined by the other techniques above the detection limits of our methods. At the same time we characterized the sample of the "R-isomer" and described a small adriamycinone content in it.

The results demonstrate that the capillary electrophoresis analysis of FCE 23762, "R-isomer" and adriamycinone can be performed within short run time, and with high sensitivity. This makes the technique a potential complementary one to HPLC.

ACKNOWLEDGEMENT

The authors thank Thermo Separation Products who provided the possibility to use a SpectraPhoresis 1000 apparatus. This research was supported by grants from Ministero dell'Università e della Ricerca Scientifica e Tecnologica (MURST quota 40 %) and from Università "La Sapienza" (MURST-Ricerca di Ateneo, quota 60 %).

REFERENCES

1. F. Arcamone, Doxorubicin Anticancer Antibiotics, Academic Press, New York, 1981.

2. R. T. Dorrand, W. L. Frits, Cancer Chemotherapy Handbook, Elsevier, Amsterdam, 1980.

3. E. M. Acton, G. L. Tong, C. W. Mosher, R. L. Wolgemuth, Journal of Medical Chemistry, 27: 638-643 (1984)

4. J. R. Brown, Prog. Med. Chem., 15: 125-164 (1978)

5. W. B. Pratt, R. W. Ruddon, The Anticancer Drugs, Oxford University Press, Oxford, New York, 1979.

6. M. Ripamonti, G. Pezzoni, E. Pesenti, A. Pastori, M. Farao, A. Bargiotti, A. Suara, F. Spreafico, M. Grandi, British Journal of Cancer, 65: 703-707 (1992)

7. C. M. Camaggi, R. Comparsi, E. Strocchi, F. Testoni, F. Pannuti, Cancer Chemother. Pharmacol., 21: 216-220 (1988)

8. R. Mariani, M. Farina, W. Sfreddo, J. Pharm. Biomed. Anal., 7: 1877-1882 (1989)

9. R. Ficarra, P. Ficarra, M. L. Calabro, G. Alyavilla, T. Giacobello, V. Adamo, Boll. Chim. Farm., 130: 17-21 (1991)

10. A. Farina, M. G. Quaglia, E. Bossù, P. Melchiorre, J. Pharm. Biomed. Anal., 9: 1165-1168 (1992)

11. M. Breda, E. Pianezzola, M. Strolin Benedetti, J. Chromatogr., 578: 309-315 (1992)

12. M. L. Rossini, M. Farina, J. Chromatogr., 593: 47-53 (1992)

13. US Pharmacopeia, XXII Revision, US Pharmacopeial Convention, Rockville, MD, 1990.

14. N. J. Reinhoud, U. R. Tjaden, H. Irth, J. van der Greef, J. Chromatogr., 574: 327-334 (1992)

Received: April 19, 1994
Accepted: May 6, 1994

JOURNAL OF LIQUID CHROMATOGRAPHY, 17(18), 3925-3931 (1994)

CAPILLARY ELECTROPHORESIS OF STEROID CONJUGATES

JOSEPH C. TOUCHSTONE AND SIDNEY S. LEVIN
School of Medicine
University of Pennsylvania
Philadelphia, Pennsylvania 19104-6080

ABSTRACT

Capillary Electrophoresis of Steroid Conjugates

Advances in medical sciences have mandated increased separation efficiency and high level sensitivity. This is especially true when sample availability is in the ultra micro range. Because of this a study of capillary electrophoresis (CE for separation of steroid conjugates was carried out. There are few methods available to separate these molecules without first hydrolysis of the conjugates. The initial focus was on the estrogen conjugates since many of these are readily available for reference material. We avoided the use of derivative formation often necessary for optimal sensitivity.

The determination of steroids and their metabolites, the sulfates and glucuronides has been hampered for considerable time due to tedious methodology. Since this laboratory has been involved in this area for a number of years it seemed appropriate to investigate the utility of capillary electrophoresis (CE) for the separation of these substances. Only recently has there been reported investigation

on the use of CE for separation of small molecules; most of the prior work being with macromolecules and proteins. Chromatographic methods have been applied but required a high level of analytical skill. High performance liquid chromatography has been used but, has not been developed to a level of universal acceptance in this area.

Recent reports have indicated that CE can be successfully applied to smaller molecules. K.J. Lee, et al. have shown the separation of antiepileptic drugs in plasma, phenobarbital among them (1). Pleasance, et al. used CE for separation of sulfa type pharmaceuticals including sulfamethazine (2). Lukkari, et al. (3) were able to resolve ten β-blockers from urine by CE. Holland and Sepaniak (4) separated 10 mycotoxins in 45 minutes using micellar electrokinetic capillary chromatography. Wernly and Thormann (5) used this technique in analyses of drugs of abuse in human urine. Whang and Chen (6) separated riboflavin, thiamine, nicotinamide and pyridoxal using capillary zone electrophoresis. Smith and Khaledi (7) studied the effect of pH on separation of phenols.

CE thus has been indicated to be an attractive tool for pharmaceutical analysis because of ease of operation and high sensitivity. This report describes results obtained with CE of a number of steroid conjugates.

Experimental

Steroids

The steroids were obtained as follows: estriol-3-glucuronide and estriol-16α-glucuronide were obtained from Sigma Chemical Co. (St. Louis, MO); estriol-3-sulfate, estrone-sulfate, dehydroepiandiosterone-sulfate, equilenin sulfate, and equilin sulfate were generously supplied by Wyeth-Ayerst (Rouses Point, NY). All chemicals were EM Science (Gibbstown, NJ) reagent grade.

The biological samples were aliquots of samples collected from the clinic or from animals during the course of other experiments. All samples were filtered through 0.45 μm. Millipore filters prior to injection into the system. 2-4 nl. were injected by electromigration.

The instrument used was an ISCO Model 3850 (Lincoln, NB) capillary electrophoresis system. This provided variable current and voltage capabilities. The detection system was on column variable wavelength.

The capillary was an uncoated fused silica column of 50 μm. 1D and 50 cm length with the detection window at 31 cm. In the experiments reported the buffer used was a borate-sodium hydroxide solution of pH 10.2 and concentration of 0.2 mm. in borate. This was routinely degassed by filtering through a 0.45 μm. filter (Millipore). Urine samples were diluted 1:50 and the amniotic samples 1:25 with the buffer.

Results and Discussion

Table 1 shows that the steroid conjugates listed are readily separated. The estrogen conjugates are those present in urine or blood. These are present in larger quantities in the urine of pregnant women or pregnant mares. Because estriol-3-glucuronide did not separate completely from the 16-analogue, further investigation was carried out to improve the resolution. It was found that reducing the current increased resolution along with an increased retention time that resulted in a more complete separation of these two homologues as seen in Table II. Figure 1 indicates that the resolution provided by the conditions used was excellent for separation of the standard steroid conjugates studied. It is of interest that the sulfates have longer migration times than the glucuronides.

Figure 2 shows the separation of conjugates from amniotic fluid. The peak at 6.88 (13.7 mm) coincides with that of estriol-3-glucuronide. Figure 3 shows the

Table 1

Migration Times (min.) for Steroid Conjugates

44mA, 20kV, 210nm

Estriol-16α-Glucuronide	13.4	DHA* Sulfate	15.9
Estriol-3-Glucuronide	12.0	Equilin Sulfate	16.2
Estriol-3-Sulfate	14.55	Equilenin Sulfate	17.5
Estrone-Sulfate	16.60		

*dehydroepiandiosterone

Table II

Effect of Voltage on Separation

(Time in min.)

	44 mA / 20 kV	18 mA / 10 kV
Estriol-16α-Glucuronide	12.5	16.57
Estriol-3-Glucuronide	13.0	14.91

separation of estriol-16α-glucuronide from urine of term pregnancy. The peak at 17.85 min. has the migration shown by estriol-16α-glucuronide. Figure 4 shows the separation of conjugates in the urine of a rat with a bile fistula to which was administered phenobarbital. At present the separated peaks are not identified but some presumably are phenobarbital metabolites.

The results given in the foregoing discussions demonstrate that the conditions for capillary electrophoresis as described may provide means to separate steroid

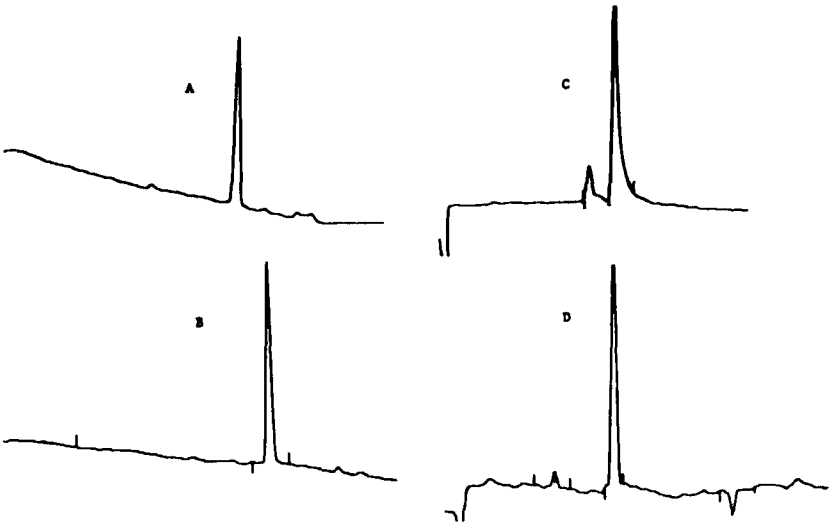

Figure 1 Resolution of Steroid Conjugates by Capillary Electrophoresis

a Estriol-3-glucuronide

b Estriol-16α-glucuronide

c Estrone-sulfate

d Estriol-3-sulfate

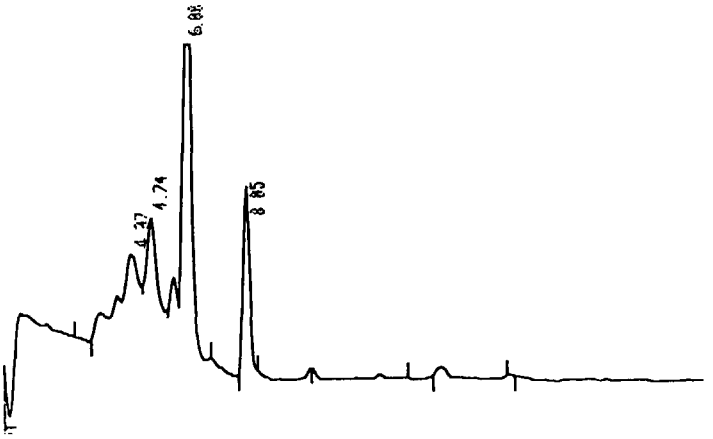

Figure 2 Separation of Components of Amniotic Fluid from Term Pregnancy. Peak at 13.0 min. coincides with E3-3-glucuronide.

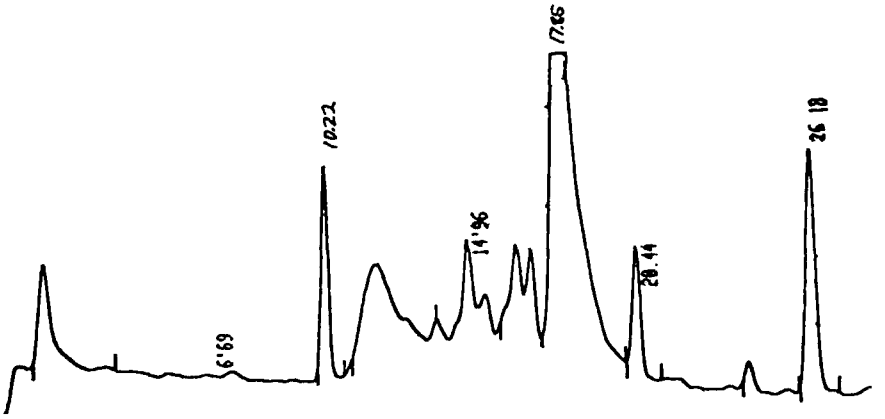

Figure 3 Separation of Components of Urine of Term Pregnancy. Peak at 17.85 is E3-16-glucuronide as noted by migration time.

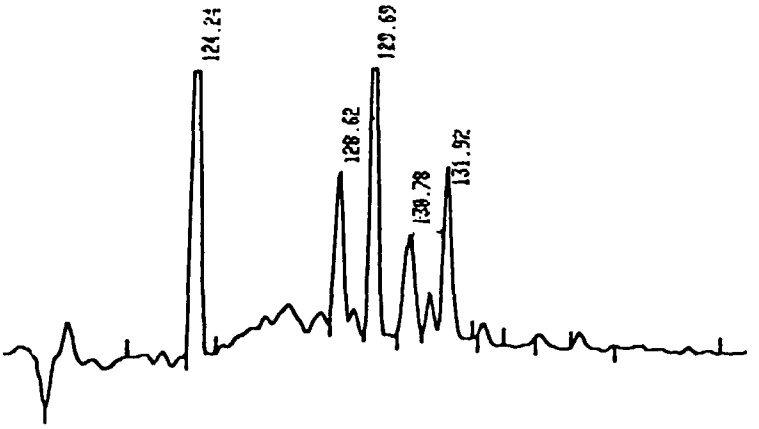

Figure 4 Separation of Components of Rat Urine. Separated Peaks as yet not Identified.

conjugates in biological media. Further work is in progress to evaluate the utility of this tool in metabolic studies.

References

1. Lee, K.J., Heo, G.S., Kim, N.J., and Moon, D.C., *J. of Chromatography*, 608, 243 (1992)
2. Pleasance, S., Thibault, P., and Kelly, J., *J. of Chromatography*, 591, 325 (1992)
3. Lukkari, P., Siren, H., Pantsor, M., and Riekkola, M.L., *J. of Chromatography* 632, 143 (1993)
4. Holland, R.D., and Sepaniak, M.F., *Anal. Chemistry* 65, 1140 (1993)
5. Wernly, P., and Thormann, W., *Anal. Chemistry*, 64, 2461 (1992)
6. Whang, C., and Chen, I., *Anal. Chemistry*, 64, 2461 (1992)
7. Smith, S.C., and Khaledi, M. *Anal. Chemistry*, 65, 193 (1993)

Received: July 24, 1994
Accepted: August 3, 1994

GENERAL PAPERS

JOURNAL OF LIQUID CHROMATOGRAPHY, 17(18), 3933-3949 (1994)

CORRELATION BETWEEN THE CHEMICAL STRUCTURES OF DIALKYL PEROXIDES AND THEIR RETENTION IN REVERSED-PHASE HIGH-PERFORMANCE LIQUID CHROMATOGRAPHY

STEFAN BAJ AND MAŁGORZATA DAWID
Institute of Organic Chemistry and Technology
Silesian Technical University
ul. Krzywoustego 4
44-101 Gliwice, Poland

ABSTRACT

High-performance liquid chromatographic capacity factors were determined on LiChrosorb RP 18 10 μm stationary phase for various organic peroxides. Studies of the quantitative structure-retention relationship (QSRR) employing non-empirical structural descriptors for the investigated compounds were performed by means of multiple regression analysis. Semi-empirical methods MINDO/3, MNDO, AM1, PM3 were employed to determine the structural descriptors which may influence the retention in a reversed-phase chromatographic system. Informative values of non-empirical structural descriptors determined with various semi-empirical methods have been compared.

INTRODUCTION

Organic peroxides are a group of organic compounds of considerable practical and theoretical importance [1-4]. Mixtures which contain organic peroxy substances are on the whole difficult to analyse by means of conventional techniques.

High-performance liquid chromatography (HPLC) is a versatile, efficient and relatively rapid method of separating non-volatile, thermally labile compounds, and it is

ideal for the separation and study of mixtures containing peroxy compounds [5-9]. The importance of HPLC in the analysis of peroxy compounds seems to be quite obvious.

The study of the relationship between retention indices and parameters describing the structure of molecules of the solute is one of the most intensively investigated question in modern chromatography [10]. These studies concern a set of various chemical compounds and various sets of structural parameters have been employed; no investigations of this type, however, have been carried out as far as organic peroxy compounds are concerne. Using this approach, it is possible to identify the dominant factors which define the interaction of solute molecules with chemical entities forming the chromatographic system. The assignment of retention factors for various substituents was suggested by Martin [11] and validated by Bate-Smith and Westall [12]. Horwath and co-workers [13.14] and others [15,16] have determined the quantitative structure-retention relationship (QSRR) for a variety of compounds and demonstrated the value of contribution of the functional group for both the prediction of retention and structural elucidation. Most QSRR reported in chromatographic literature were derived by means of multiple regression analysis. The dependent variable formed a set of retention data, while various empirical, semi-empirical and non-empirical structural parameters were assumed as independent variables. The selection of independent variables (structural descriptors) depends on numerous factors, among them the chromatographic techniques applied in the investigations. Retention differences related to the chemical structure have been discussed in adsorption liquid chromatography, where hydrogen bonding and π–π interaction are dominant as well as in reversed-phase and ion-exchange liquid chromatography, where the molecular interaction is probably related to solubility. One method of measuring this solubility in terms of the hydrophobic fragmental constant (log P) has been proposed by Rekker [17]. These QSRR have been discussed in detail by Kaliszan [18-20] who listed over 100 studies relating the partition coefficient (log P) factor to retention in HPLC.

Recent studies in reversed-phase chromatography have shown that both electrostatic and hydrophobic interactions make important contributions to retention [21-23]. The former is directly related to the solute charges and the latter to solute hydrophobicity.

In our study, the QSRR analysis a the variety of organic peroxides on RP HPLC was established through the simultaneous solution of a set of linear equations. As independent variables (structural descriptors) non-empirical parameters of the molecules were chosen which can be related to the hydrophobic or electrostatic properties of the molecules. These descriptors were calculated by means of semi-

empirical methods of quantum chemistry: PM3, AM1, MNDO i MINDO/3. Such an approach makes it possible to investigate also the application of this type of method for the prediction of retention.

The experiments described in this paper were designed to obtain some insight into the molecular mechanism of retention under reversed phase conditions and to evaluate the informative value of structural descriptors most often used in QSRR studies by means of different semi-empirical methods.

EXPERIMENTAL

Materials

Ethyl cumyl peroxide, n-propyl cumyl peroxide, iso-propyl cumyl peroxide, n-butyl cumyl peroxide, iso-butyl cumyl peroxide, sec-butyl cumyl peroxide, tert-butyl cumyl peroxide, n-hexyl cumyl peroxide, n-heptyl cumyl peroxide, n-oktyl cumyl peroxide , n-nonyl cumyl peroxide, allyl cumyl peroxide and benzyl cumyl peroxide were synthetized in the Institute of Organic Chemistry and Technology according to the method presented in reference [24].
Methyl alcohol, HPLC grade; Merck Darmstadt.

Instrumentation

The chromatographic system consists of a Philips LC XPD Chromatograph, a Reodyne Model 7125 syringe-loading injector with a 20 μl loop and a standard Cartrige Glass Column LiChrosorb RP 18 (10 μm). The mobile phase were methanol-water mixtures at a flow rate of 1.0 cm3/min. The compounds were detected at 257 nm with LC XPD UV-VIS Detector and integrated with a CDP4 integrator.

Determination of retention parameters

Chromatography was carried out using eluents with the following proportions (v/v) of methanol to water: 95 :5, 90 :10, 85 : 15, 80 : 20, 75 :25, 70 : 30. The capacity factors k' were calculated assuming a constant dead volume of the column,

taking the signal of water as the dead time marker. Logarithms of capacity factors (log k') for the respective compounds were plotted against the volume of methanol concentration.

Determination of structural descriptors

For each investigated peroxide the individual structural parameters which may influence retention, are: the total energy (E_{TOTAL}), the heat of formation, the net electron charges on individual atoms (O1, O2), the dipole moment, the square of the dipole moment (DIP^2), the torsion angle between some of the atoms in a molecule (C1-O1-O2-C2) (see Fig. 1.), the energy of LUMO (E_{LUMO}) and HOMO (E_{HOMO}) molecular orbitals. Molecular geometries were optimized and all the parameters mentioned above were calculated by means of the appropriate orbital package MOPAC procedures according to the methods PM3 [25], AM1 [26], MNDO [27] and MINDO/3 [28]. The structure of a methyl cumyl peroxide molecule, optimised according to the MNDO method is presented in Figure 1.

The values of structural descriptors obtained by means of all the applied methods are listed in tables I-IV.

RESULTS AND DISCUSSION

Logarithms of the capacity factors (log k') for the respective organic peroxides were plotted against the volume fraction of methanol in the eluent. The parameters derived from least squares regression for the investigated systems are given in Table V. Excellent linear relationships were obtained.

From the regression equations obtained (log k' = a*x + b), the log k' coefficients were calculated for all investigated compounds at the point corresponding to the proportion (v/v) 82 :12 methanol : water as eluent. The calculated values of log k' were then subjected to a correlated analysis with parameters describing the structure of the molecules of the organic peroxides.

In order to describe the relation between the retention indices of organic peroxides and the calculated structural parameters, a multiparameter regression analysis was performed. The QSRR equations were solved first by a stepwise regression analysis taking into consideration the significance of the respective descriptors. The setting up of such a preliminary correlation made it possible to

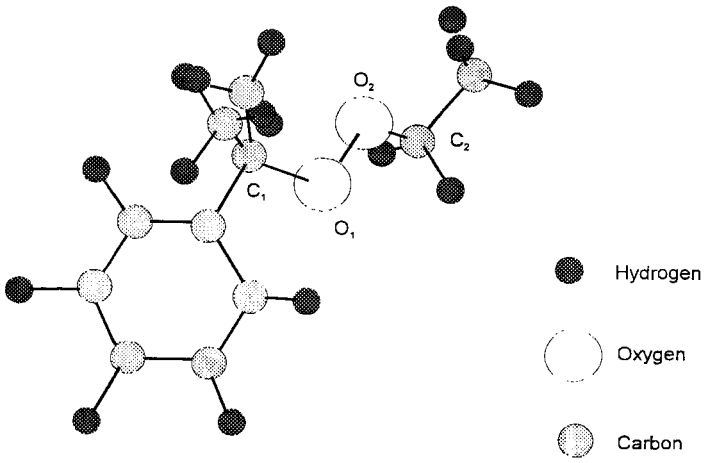

FIGURE 1. Molecular structure of ethyl cumyl peroxide calculated with MNDO semi-empirical method.

eliminate from them those descriptors which did not indicate a good correlation with log k'. Based on these calculations the following descriptors were eliminated: the heat of formation, the net charge on the atoms O1 and O2, the torsion angle between the atoms C1-O1-O2-C2, and the dipole moment. Multiple regression analysis, applying log k' as a dependent variable and the total energy (E_{TOTAL}), the values of LUMO and HOMO energy (E_{HOMO} and E_{LUMO}) and the square of dipole moment $(DIP)^2$ as dependent variables, was performed for each set of structural descriptors (MINDO/3, MNDO, AM1, PM3 results). The obtained QSRR equation are presented below:

MINDO3:

$$\log k' = -49.6814 - 0.0026\ (\pm 0.0002)E_{TOTAL} - 4.5693(\pm 1.65418)E_{HOMO} + 3.0164(\pm 0.92318)E_{LUMO} + 0.6366(\pm 0.13483)(DIP)^2 \quad (1)$$

$$R = 0.9900, \qquad F = 89.386, \qquad p < 1\ 10^{-5}$$

MNDO:

$$\log k' = -159.490 - 0.003\ (\pm 0.00035)E_{TOTAL} - 16.091(\pm 8.33871)E_{HOMO} + 11.512(\pm 4.21971)E_{LUMO} + 0.738(\pm 0.59894)(DIP)^2 \quad (2)$$

$$R = 0.9620, \qquad F = 24.801, \qquad p < 1.5\ 10^{-4}$$

TABLE 1

MOLECULAR STRUCTURE DESCRIPTORS DERIVED FROM OPTIMISED GEOMETRIC STRUCTURES OF ORGANIC PEROXIDES USING MINDO/3 METHOD.

Peroxide	E_{TOTAL} [eV]	Heat of formation [kcal/mol]	Torsion angle [deg]	Net Charge at O2 atom [*e*]	Net Charge at O1 atom	E_{HOMO} [eV]	E_{LUMO} [eV]	$(DIP)^2$ [Debye]
Ethyl cumyl peroxide	-2251.71	3.142	-130.792	-0.2272	-0.2376	-9.1755	0.6025	1.3456
***n*-Propyl cumyl peroxide**	-2408.40	-17.886	-129.044	-0.2290	-0.2366	-9.1755	0.5834	1.5092
***iso*-Propyl cumyl peroxide**	-2408.31	-15.644	-129.817	-0.2431	-0.2414	-9.1568	0.6102	1.0899
***n*-Butyl cumyl peroxide**	-2564.99	-22.089	-131.981	-0.2180	-0.2388	-9.0437	0.8365	0.7772
***iso*-Butyl cumyl peroxide**	-2564.60	-12.962	-132.167	-0.2393	-0.2162	-8.9996	0.9544	0.7807
***sec*-Butyl cumyl peroxide**	-2564.97	-21.447	-130.218	-0.2450	-0.2417	-9.1586	0.5990	1.0829
***tert*-Butyl cumyl peroxide**	-2564.50	-10.676	-177.302	-0.2682	-0.2576	-9.1319	0.6319	0.2642
***n*-Hexyl cumyl peroxide**	-2878.42	-36.004	-131.266	-0.2253	-0.2371	-9.1714	0.5840	1.3675
***n*-Heptyl cumyl peroxide**	-3034.99	-39.871	-132.438	-0.2255	-0.2375	-9.1726	0.5896	1.3718
***n*-Octyl cumyl peroxide**	-3191.78	-48.526	-131.719	-0.2373	-0.2255	-9.1713	0.5840	2.7386
***n*-Nonyl cumyl peroxide**	-3348.28	-50.743	-132.529	-0.2258	-0.2375	-9.1795	0.5815	1.4195
Allil cumyl peroxide	-2377.56	14.063	-130.700	-0.2257	-0.2417	-9.1447	0.5889	1.1881
Benzyl cumyl peroxide	-2913.85	29.983	-139.372	-0.2220	-0.2488	-8.9623	0.7062	0.4019

TABLE 2

MOLECULAR STRUCTURE DESCRIPTORS DERIVED FROM OPTIMISED GEOMETRIC STRUCTURES OF ORGANIC PEROXIDES USING MNDO METHOD.

Peroxide	E_{TOTAL} [eV]	Heat of formation [kcal/mol]	Torsion angle	Net Charge at O2 atom	Net Charge at O1 atom	E_{HOMO} [eV]	E_{LUMO} [eV]	$(DIP)^2$ [Debye]
Ethyl cumyl peroxide	-2274.55	0.611	-177.120	-0.1917	-0.1871	-9.3717	0.1823	0.3490
***n*-Propyl cumyl peroxide**	-2430.97	-3.606	-146.937	-0.1902	-0.1877	-9.3479	0.1946	0.5461
***iso*-Propyl cumyl peroxide**	-2430.85	-0.892	-207.634	-0.1926	-0.1865	-9.3403	0.2013	0.4879
***n*-Butyl cumyl peroxide**	-2587.42	-8.421	-147.855	-0.1893	-0.1908	-9.3413	0.1991	0.4529
***iso*-Butyl cumyl peroxide**	-2587.27	-4.982	-148.691	-0.1868	-0.193	-9.3736	0.1801	0.3181
***sec*-Butyl cumyl peroxide**	-2587.26	-4.779	-190.138	-0.1896	-0.1959	-9.3416	0.1992	0.0678
***tert*-Butyl cumyl peroxide**	-2586.98	26.877	-172.058	-0.1904	-0.1947	-9.3279	0.2112	0.0371
***n*-Hexyl cumyl peroxide**	-2900.31	-17.809	-140.786	-0.1888	-0.1901	-9.3430	0.1972	0.5255
***n*-Heptyl cumyl peroxide**	-3056.76	-22.038	-146.875	-0.1888	-0.19	-9.3446	0.1991	0.5423
***n*-Octyl cumyl peroxide**	-3213.21	-25.25	-145.042	-0.1882	-0.1896	-9.3420	0.1957	0.5844
***n*-Nonyl cumyl peroxide**	-3369.65	-31.928	-145.299	-0.1882	-0.1897	-9.3441	0.1968	0.5668
Allil cumyl peroxide	-2401.35	26.129	-150.207	-0.1870	-0.1929	-9.3336	0.2053	0.6439
Benzyl cumyl peroxide	-2940.95	34.859	-151.704	-0.1870	-0.1938	-9.3333	0.1075	0.3628

TABLE 3
MOLECULAR STRUCTURE DESCRIPTORS DERIVED FROM OPTIMISED GEOMETRIC STRUCTURES OF ORGANIC PEROXIDES USING AM1 METHOD.

Peroxide	E_{TOTAL} [eV]	Heat of formation [kcal/mol]	Torsion angle	Net Charge at O1 atom	Net Charge at O2 atom	E_{HOMO} [eV]	E_{LUMO} [eV]	$(DIP)^2$ [Debye]
Ethyl cumyl peroxide	-2266.68	-7.742	-113.369	-0.1524	-0.1504	-9.4725	0.4520	2.6050
***n*-Propyl cumyl peroxide**	-2422.49	-13.989	-113.224	-0.1527	-0.1498	-9.4721	0.4520	2.3104
***iso*-Propyl cumyl peroxide**	-2422.49	-12.258	-111.164	-0.1495	-0.1484	-9.4675	0.4568	2.7914
***n*-Butyl cumyl peroxide**	-2578.34	-21.309	-113.214	-0.1517	-0.1497	-9.4710	0.4530	2.7390
***iso*-Butyl cumyl peroxide**	-2578.24	-18.983	-113.249	-0.1524	-0.1499	-9.4709	0.4535	2.3482
***sec*-Butyl cumyl peroxide**	-2578.23	-18.717	-111.188	-0.1498	-0.1474	-9.4591	0.4650	2.7192
***tert*-Butyl cumyl peroxide**	-2578.00	-13.282	-177.268	-0.1623	-1.6130	-9.4460	0.4725	1.5409
***n*-Hexyl cumyl peroxide**	-2889.95	-33.558	-113.105	-0.1516	-0.1498	-9.4710	0.4541	2.8800
***n*-Heptyl cumyl peroxide**	-3045.75	-39.675	-113.086	-0.1516	-0.1498	-9.4715	0.4539	2.8900
n-Oktyl cumyl peroxide	-3201.68	-48.687	-113.172	-0.1517	-0.1498	-9.4720	0.4524	2.7822
n-Nonyl cumyl peroxide	-3357.36	-51.935	-110.773	-0.1496	-0.1475	-9.4744	0.4510	3.3966
Allil cumyl peroxide	-2393.80	17.673	-113.236	-0.1514	-0.147	-9.4290	0.4290	2.4766
Benzyl cumyl peroxide	-2933.63	26.555	-113.379	-0.1526	-0.1443	-9.4971	0.3419	2.0781

TABLE 4

MOLECULAR STRUCTURE DESCRIPTORS DERIVED FROM OPTIMISED GEOMETRIC STRUCTURES OF ORGANIC PEROXIDES USING PM3 METHOD.

Peroxide	E_{TOTAL} [eV]	Heat of formation [kcal/mol]	Torsion angle	Net Charge at O2 atom	Net Charge at O1 atom	E_{HOMO} [eV]	E_{LUMO} [eV]	$(DIP)^2$ [Debye]
Ethyl cumyl peroxide	-2134.92	-16.333	-216.187	-0.1498	-0.1594	-9.6393	0.1937	1.0323
***n*-Propyl cumyl peroxide**	-2284.29	-17.744	-215.464	-0.1471	-0.1528	-9.6236	0.2777	0.9819
***iso*-Propyl cumyl peroxide**	-2284.37	-19.59	-147.267	-0.1469	-0.1533	-9.6575	0.1890	0.6777
***n*-Butyl cumyl peroxide**	-2434.01	-27.211	-216.247	-0.1623	-0.1623	-9.6405	0.1949	1.1077
***iso*-Butyl cumyl peroxide**	-2434.04	-27.897	-211.134	-0.1641	-0.1641	-9.6394	0.1939	0.7428
***sec*-Butyl cumyl peroxide**	-2433.92	-25.263	-135.076	-0.1512	-0.1512	-9.6421	0.2123	1.1396
***tert*-Butyl cumyl peroxide**	-2433.89	-24.533	-144.481	-0.1475	-0.1475	-9.6432	0.2120	0.6338
***n*-Hexyl cumyl peroxide**	-2732.95	-34.924	-166.252	-0.1555	-0.1517	-9.6597	0.1777	0.0912
***n*-Heptyl cumyl peroxide**	-2882.49	-39.939	-156.688	-0.155	-0.151	-9.6687	0.1768	0.2414
***n*-Oktyl cumyl peroxide**	-3032.02	-45.761	-157.918	-0.1548	-0.1515	-9.6610	0.1778	0.1840
***n*-Nonyl cumyl peroxide**	-3181.54	-50.313	-145.067	-0.149	-0.1514	-9.6204	0.2706	0.7812
Allil cumyl peroxide	-2252.46	9.033	-212.289	-0.1604	-0.1604	-9.1769	0.3945	0.5293
Benzyl cumyl peroxide	-2757.19	20.607	-181.048	-0.1564	-0.1564	-9.6625	0.0178	0.0495

TABLE 5

STATISTICAL PARAMETERS OF LINEAR FIT OF LOG k' *VERSUS* METHANOL CONCENTRATION IN MOBILE PHASE

Number of calibration points for each compounds, n=5; number of replicates of each injection, m=7

Compounds	Intercept *b*	Slope *a*	R[a]	S.E[b]
Ethyl cumyl peroxide	7.291±0.205	-0.079±0.003	0.998	0.0405
n-Propyl cumyl peroxide	9.219±0.303	-0.098±0.004	0.998	0.0597
iso-propyl cumyl peroxide	9.912±0.402	-0.110±0.005	0.997	0.0792
n-Butyl cumyl peroxide	10.810±0.610	-0.076±0.008	0.993	0.1203
iso-Butyl cumyl peroxide	10.725±0.508	-0.113±0.006	0.995	0.0999
sec-Butyl cumyl peroxide	10.794±0.500	-0.115±0.006	0.996	0.0979
tert-Butyl cumyl peroxide	8.872±0.091	-0.097±0.001	0.999	0.0179
n-Hexyl cumyl peroxide	12.352±0.766	-0.124±0.087	0.995	0.0978
n-Heptyl cumyl peroxide	14.076±1.047	-0.147±0.012	0.993	0.1345
n-Oktyl cumyl peroxide	101.780±1.241	-6.596±0.534	0.993	0.9000
n-Nonyl cumyl peroxide	102.288±1.352	-5.794±0.496	0.993	0.9500
Allil cumyl peroxide	6.651±0.442	-0.071±0.006	0.991	0.0868
Benzyl cumyl peroxide	10.345±0.274	-0.111±0.003	0.998	0.0540

[a] R = correlation coefficient

[b] S.E. = standard error of regresion

AM1:

$$\log k' = -27.4426 - 0.0028\ (\pm 0.00045)E_{TOTAL} - 1.7695(\pm 9.77508)E_{HOMO} + 8.7019(\pm 4.71280)E_{LUMO} + 0.3789(\pm 0.33524)(DIP)^2 \quad (3)$$

$$R = 0.9492, \qquad F = 18.203, \qquad p < 4\ 10^{-4}$$

PM3:

$$\log k' = -37.4557 - 0.0028\ (\pm 0.00059)E_{TOTAL} - 3.2411(\pm 2.01671)E_{HOMO} + 6.5051(\pm 3.23314)E_{HOMO} - 0.5614(\pm 0.58134)(DIP)^2 \quad (4)$$

$$R = 0.9355, \qquad F = 14.041, \qquad p < 1\ 10^{-3}$$

TABLE 6
PARTIAL CORRELATION COEFFICIENTS DERIVED FROM MULTIPARAMETER REGRESSION OF LOG K' *VERSUS* STRUCTURAL DESCRIPTORS CALCULATED WITH MINDO/3, MNDO, AM1 AND PM3 METHODS.

Structural descriptor	Partial Correlation Coefficient			
	MINDO/3	MNDO	AM1	PM3
E_{TOTAL}	-0.9778	-0.9532	-0.9126	-0.8551
E_{HOMO}	-0.6987	-0.5637	-0.1201	-0.4940
E_{LOMO}	0.7661	0.6942	0.2056	0.5794
$(DIP)^2$	0.8578	0.4992	0.1574	0.3730

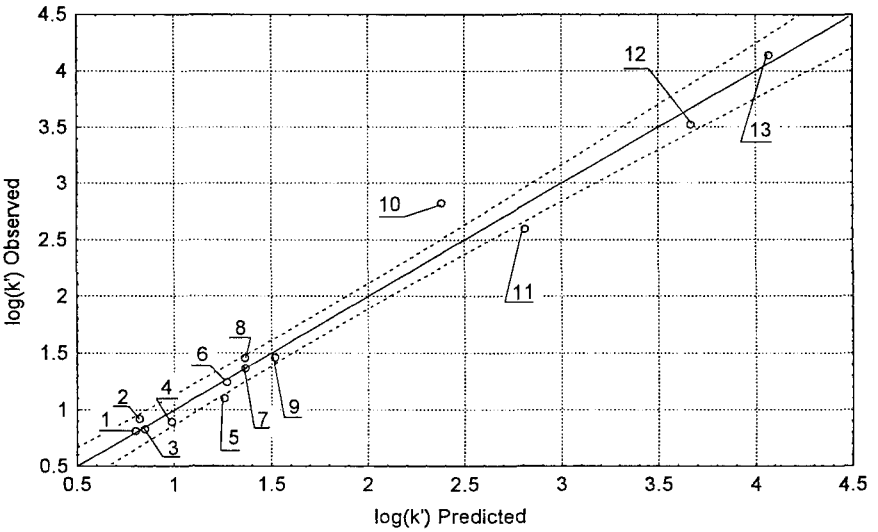

FIGURE 2. Relationship between the retention parameters of organic peroxide (log k') determined experimentally by RP HPLC (stationary phase: LiChrosorb RP 18 10 μm; mobile phase: methanol : water = 82 : 18 v/v) and calculated using eqn. 1 (MINDO/3). 1 - Ethyl cumyl peroxide; 2 - allyl cumyl peroxide; 3 - *iso*-propyl cumyl peroxide; 4 - *tert*-butyl cymyl peroxide; 5 - *n*-propyl peroxide; 6 - benzyl cumyl peroxide; 7 - *sec*-butyl cumyl peroxide; 8 - *n*-butyl cumyl peroxide; 9 - *iso*-butyl cumyl peroxide; 10 - hexyl cumyl peroxide; 11 - heptyl cumyl peroxide; 12 - octyl cumyl peroxide; 13 - nonyl cumyl peroxide.

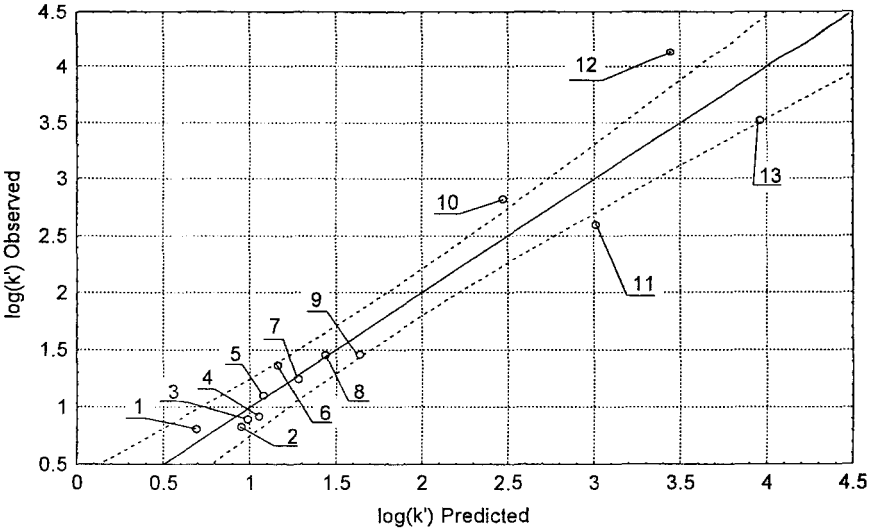

FIGURE 3. Relationship between the retention parameters of organic peroxide (log k') determined experimentally by RP HPLC (stationary phase: LiChrosorb RP 18 10 μm; mobile phase: methanol : water = 82 : 18 v/v) and calculated using eqn. 1 (MNDO). 1 - Ethyl cumyl peroxide; 2 - allyl cumyl peroxide; 3 - *iso*-propyl cumyl peroxide; 4 - *tert*-butyl cymyl peroxide; 5 - *n*-propyl peroxide; 6 - benzyl cumyl peroxide; 7 - *sec*-butyl cumyl peroxide; 8 - *n*-butyl cumyl peroxide; 9 - *iso*-butyl cumyl peroxide; 10 - hexyl cumyl peroxide; 11 - heptyl cumyl peroxide; 12 - octyl cumyl peroxide; 13 - nonyl cumyl peroxide.

The values in parentheses are the standard deviations of regression coefficients, R is the correlation coefficient, F is the f-test value, p is the significance level of the whole equation.

The correlation coefficients R obtained in all the calculation methods, applied to determine the structural descriptors, are good. The correlation coefficient R derived from equation (1) (MINDO/3 results) is excellent. The partial correlation coefficients between the respective variable and the dependent variable (log k') after controlling for all other independent variables in the equation are presented in Table VI. Negative values of these coefficients in the case of E_{TOTAL} and E_{HOMO} are the consequence of the fact thet relationship between dependent variable and structural descriptors mentioned above is described by a decreasing function. These coefficients indicate the

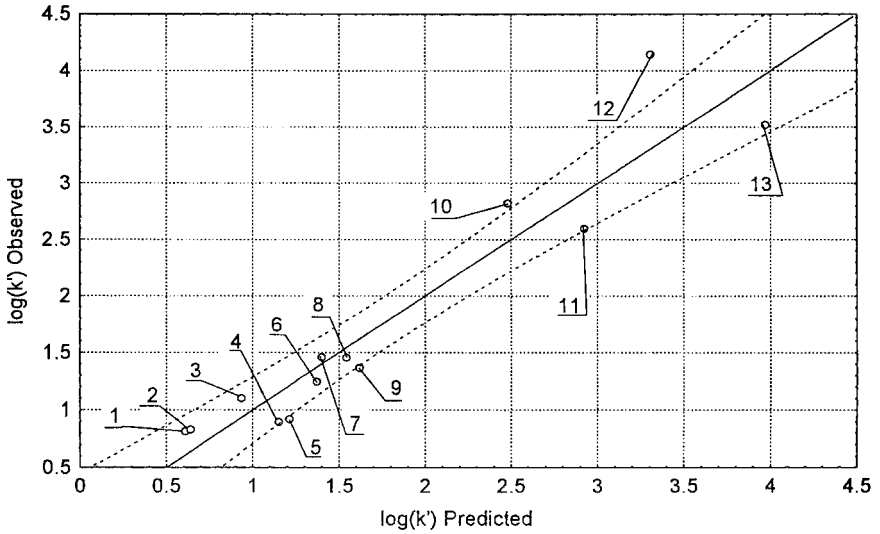

FIGURE 4. Relationship between the retention parameters of organic peroxide (log k') determined experimentally by RP HPLC (stationary phase: LiChrosorb RP 18 10 μm; mobile phase: methanol : water = 82 : 18 v/v) and calculated using eqn. 1 (AM1). 1 - Ethyl cumyl peroxide; 2 - allyl cumyl peroxide; 3 - *iso*-propyl cumyl peroxide; 4 - *tert*-butyl cymyl peroxide; 5 - *n*-propyl peroxide; 6 - benzyl cumyl peroxide; 7 - *sec*-butyl cumyl peroxide; 8 - *n*-butyl cumyl peroxide; 9 - *iso*-butyl cumyl peroxide; 10 - hexyl cumyl peroxide; 11 - heptyl cumyl peroxide; 12 - octyl cumyl peroxide; 13 - nonyl cumyl peroxide.

descriptor E_{TOTAL} as the most significant in each equation. The total molecular energy provides information about the bulkiness of the solute. This size-related descriptor may be related to the interaction between the solute molecule and the stationary phase occurring in reversed-phase liquid chromatography. The larger the solute molecule, the stronger the solute-adsorbent interaction. E_{HOMO} and E_{LUMO} descriptors are related to the ability of the solutes to participate in electron pair donor-acceptor interactions with eluent molecules. As may be concluded from the partial correlation coefficients, this kind of interaction is rather less importance for retention.

The last principal component $(DIP)^2$ determines the ability of the solute to participate in intermolecular interactions with the stationary and/or mobile phase of the dipole-dipole and dipole-induced dipole type. Their participation in the correlation equation is rather similar to E_{HOMO} and E_{LUMO}

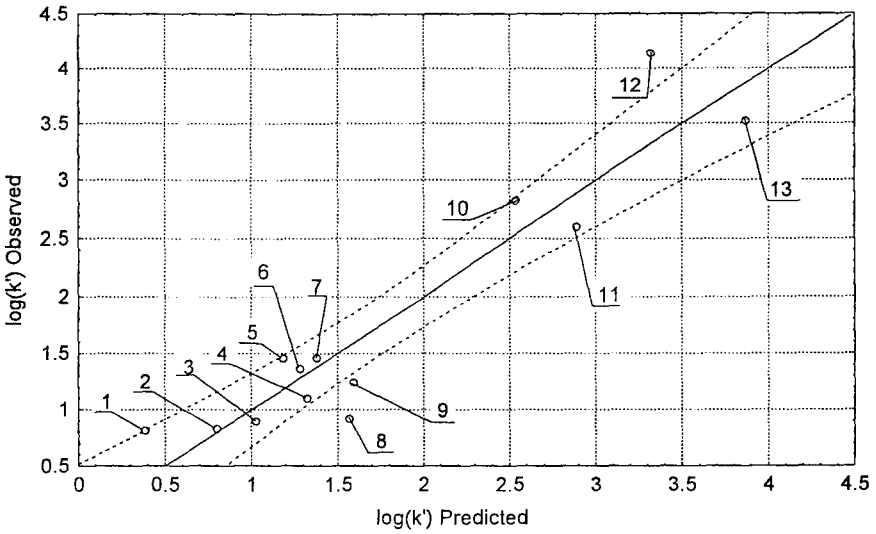

FIGURE 5. Relationship between the retention parameters of organic peroxide (log k') determined experimentally by RP HPLC (stationary phase: LiChrosorb RP 18 10 μm; mobile phase: methanol : water = 82 : 18 v/v) and calculated using eqn. 1 (PM3). 1 - Ethyl cumyl peroxide; 2 - allyl cumyl peroxide; 3 - *iso*-propyl cumyl peroxide; 4 - *tert*-butyl cymyl peroxide; 5 - *n*-propyl peroxide; 6 - benzyl cumyl peroxide; 7 - *sec*-butyl cumyl peroxide; 8 - *n*-butyl cumyl peroxide; 9 - *iso*-butyl cumyl peroxide; 10 - hexyl cumyl peroxide; 11 - heptyl cumyl peroxide; 12 - octyl cumyl peroxide; 13 - nonyl cumyl peroxide.

The remaining factors, i.e. torsion angle C1-O1-O2-C2, net charges at O1 and O2 atoms, the heat of formation and dipole moment are not essential for retention of organic peroxides in reversed phase liquid chromatography.

The correlation coefficient ***R*** is excellent in equation (1), where the structural descriptors were calculated according to the MINDO/3 method. The remaining equations do not provide such good results. The correlation between retention log *k'* and structural descriptors calculated according to the PM3 method is the worst one. The conclusion may be drawn that QSRR equations have different form depending on the method applied for calculating the structural descriptors. The best results were obtained using the MINDO/3 method to describe molecule parameters. The MINDO/3 method, applied to calculate the molecular parameter of organic peroxides, can in fact

yield more accurate results than much more recent semi-empirical methods like AM1 or PM3. One of the major assets of MINDO/3 was its demonstrated ability to reproduce *all* ground-state properties [29] of molecules of *all* kinds. Problems arise, however, in the case of molecules containing heteroatoms, such as nitrogen or sulphur, conjugated molecules, overcrowded molecules (e.g. neopentane) or molecules containing four-membered rings. This method can not be used to estimate activation energy, which tends to be too large. After several years of efforts these errors have been gradually corrected by means of the new methods MNDO, AM1 and PM3.

In the case of the organic peroxide molecules investigated in this paper, the ground-state parameters calculated with MINDO/3 methods are satisfactory and give the best correlation with the retention indices. The predictive potencies of eqns. 1 - 4 are illustrated in Figs 2-5.

CONCLUSIONS

The results of this study identify the structural factors which affect retention, and provide a quantitative estimation of the importance of these structural factors. Retention in reversed-phase chromatography was found to be a net effect of non-specific, dispersive, bulkiness-dependent interactions and electrostatic interactions involving solute molecules and molecules of both mobile and stationary phases. The E_{TOTAL} descriptors related to the first kind of interaction seem to be dominant in the retention mechanism. The correlation obtained between the selected set of structural descriptors and the retention indices for a variety of organic peroxides is very good and may be used to predict the retention properties of the investigated system of molecules.

Additionally, the present paper illustrates the applicability of semi-empirical calculations to investigations and to the understanding of the retention mechanism. This method can be used to predict the chromatographic properties of the investigated molecules. The relationship between log k' and the structural descriptors is different in the case of the semi-empirical methods employed. For organic peroxide molecules MINDO/3 method gives the most reliable values of E_{TOTAL}, E_{HOMO} and E_{HOMO} and $(DIP)^2$ parameters.

REFERENCES

1. H. Kropf, Organische Peroxo-Verbinddungen in Methoden de Organischen Chemie (Houben-Weyl), Band E 13, Teil 1-2, Georg Thieme Verlag, Stuttgart, 1988.

2. J. K. Kochi, Free Radicals Vol.1, John Wiley & Sons, New York 1973.
3. R. Hiatt, Organic Peroxides Vol. 3, Ed.: Swern, D. J., Wiley & Sons, New York 1983
4. R. A. Sheldon, "Synthesis and Uses of Alkyl Hydroperoxides and Dialkyl Peroxides" in Chem. Peroxides ,161 Ed.;Patai, S., John Wiley & Sons, New York, 1983.
5. L. Topolova, K. Dimitrov, and M. Aleksandrova, Izv. Akad. Nauk SSSR, Ser. Khim., 19: 520 (1986)
6. C. P. Patel, and V. Lilly, LC-GC, 6: 424 (1988)
7. J. B. Beltra, and B. de Havedia, Afinidad, 46: 185 (1989)
8. W. van Tilborg, J. Chromatogr., 115: 616 (1975)
9. S. Baj, and Z. Kulicki, J. Chromatogr., 588: 33 (1991)
10. T. Hanai, J. Chromatogr., 550: 313 (1991)
11. A. J. P. Martin, Biochem. Soc. Symp., 3: 4 (1949)
12. E. C. Bate-Smith, and R. G. Westall, Biochem. Biophys. Acta, 4: 427 (1950)
13. I. Molnar, and Cs. Horvath, J. Chromatogr., 145: 371 (1978)
14. B. K. Chen, and Cs. Horvath, J. Chromatogr., 171: 15 (1979)
15. C. M. Riley, E. Tomlinson, and T. M. Jefferies, J. Chromatogr., 185: 197 (1979)
16. E. Tomlinson, H. Poppe, and J. C. Kraak, Int. J. Pharmacol., 7: 225 (1981)
17. R. F. Rekker, The Hydrophobic Fragmental Constant, Elsevier, Amsterdam, 1977.
18. R. Kaliszan, Quantitative Structure-Chromatographic Retenrion Relationships (Chemical Analysis, Vol. 93), Ed. J. D. Winefordner, Wiley, New York, 1987.
19. R. Kaliszan, and K. Ośmiałowski, J. Chromatogr., 506: 3 (1990)
20. R. Kaliszan, A. Kaliszan, T. A. G. Noctor, W. P. Purcell, and I. W. Wainer, J.Chromatogr., 609: 68 (1992)
21. H. Zou, Y. Zhang, and P. Lu, J. Chromatogr., 265: 171 (1983)
22. P. Zou, H. Lu, and Y. Zhang, Microchim. Acta Part III, 35 (1990)
23. H. Liu, and F. F. Cantwell, Anal. Chem., 63: 2032(1991)
24. S. Baj, Pol. J. App. Chem., 35: 137 (1991)
25. J. J. P. Stewart, J. Comp. Chem., 10: 209 (1989)
26. M. J. S. Dewar, E. G. Zoebisch, E. F. Heal, and J. J. P. Stewart, J. Am. Chem. Soc., 107: 3902 (1985)
27. M. J. S. Dewar, and W. Thiel, J. Am. Chem. Soc., 99: 4899 (1977)

28. R. C. Bingham, M. J. S. Dewar, and D. H. Lo, J. Am. Chem. Soc., 97: 1285, 1294, 1302, 1307 (1975)
29. M. J. S. Dewar, and H. S. Rzepa, J. Am. Chem. Soc., 99: 7432 (1977)

Received: January 29, 1994
Accepted: June 27, 1994

JOURNAL OF LIQUID CHROMATOGRAPHY, 17(18), 3951-3968 (1994)

ANALYSES OF VEGETABLE OIL TRIACYLGLYCEROLS BY SILVER ION HIGH PERFORMANCE LIQUID CHROMATOGRAPHY WITH FLAME IONIZATION DETECTION

W. E. NEFF*, R. O. ADLOF,
G. R. LIST, AND M. EL-AGAIMY**
Food Quality and Safety Research
National Center for Agricultural Utilization Research
Agricultural Research Service, USDA
1815 North University Street
Peoria, Illinois 61604

ABSTRACT

Silver ion high performance liquid chromatography with a commercially available column with a simple isocratic mobile phase of acetonitrile in hexane and flame ionization detection was employed to separate and quantitate triacylglycerol species of vegetable oils. Coconut, palm, cottonseed, olive, safflower, sunflower, corn, pumpkinseed, linseed, soybean, and canola oils were analyzed, as well as randomized corn and soybean oils, and the blends and interesterified products of corn and soybean oil with cottonseed oil stearine. Fractionated triacylglycerol species were identified by gas chromatography of their methyl esters. Triacylglycerol composition was obtained by reversed phase and silver ion high performance liquid

**Visiting Scientist from Oils and Fats Research Section, Food Technology Research Institute, Agricultural Research Center, Giza, Egypt

chromatography of the same oil. Oil fatty acid composition was determined by gas chromatography of the transmethylated oil and correlated with that calculated from the triacylglycerol composition by silver ion chromatography of the same oil. The triacylglycerol separation was mostly based on the total unsaturation of the fatty acids attached to the glycerol moiety. However, partial separation of triacylglycerols with the same unsaturation content but different fatty acids indicates that other separation mechanisms, in addition to fatty acid complexation with silver ions, such as adsorption and partition, are involved. The flame ionization response (area percent) was determined to be proportional to weight percent for oil triacylglycerol composition. In addition to analyses of vegetable oils, the efficacy of the silver ion high performance liquid chromatography method with flame ionization detection for analyses of margarine base stocks produced from corn and soybean oils was demonstrated.

INTRODUCTION

Triacylglycerol (TAG) composition of seed oils has been determined by high temperature gas chromatography (GC) and reversed phase high performance liquid chromatography (RP-HPLC) (1-3). High temperatures of GC may adversely effect analysis of TAG with unsaturated fatty acids (FA) through thermal alteration. RP-HPLC avoids thermal alteration but the TAGs are resolved with respect to both FA unsaturation and chain length, which may give HPLC chromatograms that are difficult to interpret. Silver ion high performance liquid chromatography (Ag-HPLC) resolves TAG primarily by FA unsaturation, resulting in simpler chromatograms for TAG identification (2,4). Previously reported Ag-HPLC systems for TAG and FA separations use complex mobile phases (4,5). A simple isocratic mobile phase, acetonitrile in hexane, and a commercially available Ag-HPLC column were recently used to resolve

cis and trans FA methyl ester isomers (6) and TAG of *Crepis alpina oil* (7).

Several types of HPLC detectors have been used for TAG analysis. Light scattering and ultraviolet detectors have been used for semi-quantitative determination of TAG composition (5), but these lack linear response and require response factors. We have previously used the transport flame ionization detector (FID) with RP-HPLC analysis of vegetable oils (8-11), vegetable oil blends and interesterified products for margarine basestocks (12) and for the analysis of *Crepis alpina* and *Vernonia galamensis* oils (13). The FID detector was determined to give a linear response without the need for response factors for quantitative TAG analysis. Ag-HPLC with an FID detector was previously used for the quantitative determination of TAG of cocoa butter, palm oil, and soybean oil (14).

We used the Ag-HPLC FID system with the isocratic acetonitrile/hexane mobile phase for the analysis of TAG of *Crepis alpina* oil, an oil with an unusual fatty acid which contains an alkyne bond (7). Here we report the broad applicability of the technique in the analysis of fats and oils which have common fatty acids with alkene bonds.

EXPERIMENTAL

Material

A set of complex and varied oils and products were selected to illustrate the applicability of the Ag-HPLC-FID technique for TAG analysis. Vegetable oils (olive, soybean, sunflower, corn, cottonseed, pumpkinseed, peanut, safflower, canola, coconut, linseed, and palm) were obtained from either local

market or industrial sources as finished oils. Soybean and corn oil each was blended (1:1, wt/wt) with cottonseed stearine and then interesterified using 0.5% sodium methoxide catalyst. Also, soybean and corn oil were each randomized in the presence of 0.5% sodium methoxide catalyst.

Methods

Pure TAGS were prepared from the oils and products by solid phase extraction chromatography described previously (9).

Fatty acid location in the TAG was determined by the enzymatic lipolysis and capillary gas chromatography as reported previously (15) and was also used to verify vegetable oil randomization.

To verify the results of Ag-HPLC-FID, TAGS were resolved and quantitated by RP-HPLC-FID (8, 9). Quantitation was verified against weighed TAG standards (7).

For TAG analysis by Ag-HPLC-FID, a Chromosphere Lipids column (4.6 mm I.D. x 250 mm, 5 micron particle size) (Chrompack International, Middleburg, The Netherlands) was used. The TAG (10 μl; 50 mg solute per 2 ml hexane) were injected in triplicate. All TAG were eluted in 120 min by an isocratic mobile phase of 0.5% acetonitrile in hexane (v:v) at a flow rate of 1.0 ml/min. HPLC flame ionization detector (Tracor Model 945, Trimetrics, Houston, TX), response was monitored by a real time computer and calibrated against weighed TAG samples. Fractions were collected via a splitter between the column and detector as previously described (7).

TAGs were characterized and identified by gas chromatography flame ionization detection of methyl esters prepared by transmethylation of each Ag-HPLC

fraction. TAG identifications were confirmed by comparison of TAG composition obtained by Ag-HPLC with that obtained by RP-HPLC. Further, TAG identification was supported by comparison of the TAG fatty acid composition calculated from Ag-HPLC fractions with the fatty acid composition determined experimentally for the starting TAG mixture (10).

Transmethylation was performed on the TAG by heating the sample in 0.5 N KOH in methanol at 50°C for 30 min. The reaction was stopped with acetic acid and the mixture was extracted with 5 ml petroleum ether:diethylether (1:1 v/v), water washed to neutral Ph and dried with 5 ml acetone azeotrope under helium.

Fatty acid methyl esters (FAME) samples were analyzed by direct injection capillary-GC utilizing an SP2380 column (30 m, 0.25 mm ID and 0.2 micron film thickness (Supelco, Inc., Bellefonte, PA) in a Varian 3400 Gas Chromatograph (Walnut Creek, CA) equipped with a flame ionization detector. The column was operated isothermally at 150°C for 35 min and then programmed to 210°C at 3°C/min with helium head pressure 10 psi. The injector and detector temperature were 240°C and 280°C respectively. GC chromatogram peak integration was by computer. The FAME were identified by matching their retention times with respect to authentic standards.

RESULTS AND DISCUSSION

Quantitative analyses of vegetable oil TAG are presented in Tables 1-3. The methyl ester quantitation by GC-FID was used to characterize the TAG species with respect to amount of saturated (S), monenoic (M), dienoic (D), and trienoic (T) fatty acids per TAG components represented by the Ag-HPLC chromatogram

TABLE 1

Vegetable Seed Oil Triacylglycerol Composition by Silver Ion and Reversed-Phase High Performance Liquid Chromatography with Flame Ionization Detection[a]

Resolution			Quantitation (Area Percent)[c]									
			Coconut		Palm		Cottonseed		Olive		Peanut	
Triacylglycerol saturated, monenoic, dienoic, trienoic fatty acid species[b]	Number of Double Bonds	Triacylglycerol Molecular Species Reversed Phase[d,e]	Reversed Phase	Silver Ion	Reversed Phase	Silver Ion	Reversed Phase	Silver Ion	Reversed Phase	Silver Ion	Reversed Phase	Silver Ion
SSS	0	PPP,PPS,PSS,SSS	39.3	86.9	7.7	7.2	0.3	1.1			3.9	3.1
SSM	1	POP,SOP,SOS	0.1	0.2	41.8	38.7	2.0	2.6	3.2	3.2	1.7	1.4
SSD	2	PLP,SLP,SLS	0.3	0.3	6.8	7.8	12.5	11.5	2.3	2.1	4.0	5.7
SMM	2	POO,SOO	0.6	0.4	27.6	28.5	3.8	3.6	26.4	27.5	9.2	9.3
SMD	3	LOP,LOS	0.5	1.5	8.3	9.0	13.3	12.3	11.0	10.9	17.6	16.5
MMM	3	OOO	0.4	1.0	2.0	4.4	0.7	1.5	33.1	34.1	15.5	14.0
SDD	4	LLS,LLP	2.3	2.3	1.5	1.9	30.0	30.1	5.1	2.3	5.4	6.9
MMD	4	LOO	1.4	1.6	1.3	1.9	2.6	4.3	14.4	14.4	21.6	20.3
DDM,TMM	5	LLO,LNOO	2.1	2.3	0.3	0.6	11.4	13.4	3.4	4.4	14.1	14.5
DDD	6	LLL	3.0	3.4			21.3	19.8	1.0	1.0	2.7	4.6
TDD	7	LNLL					0.1	0.1			0.1	0.8
UNIDENTIFIED			0.0	0.1	2.7	0.0	0.0	0.7	0.1	0.1	4.2	2.8

[a]HPLC and Flame Ionization Conditions given in Experimental Section.
[c]Area percent standard deviation ± 01. to 0.2%.
[d]S,M,D,T = saturated (palmitic and stearic acids except for coconut, which also contains caprylic, capric, lauric and myristic acids (19)); monoenoic (oleic); dienoic (linoleic) and trienoic (linolenic) acids, respectively, attached to the triacylglycerol glycerol moiety.
[e]S,P,O,L and Ln = stearic, palmitic, oleic, linoleic and linolenic acids, respectively, attached to the triacylglycerol moiety.
[f]Coconut oil also contains saturated triacylglycerols with caprylic, capric, lauric and myristic acids (19).

TABLE 2

Vegetable Seed Oil Triacylglycerol Composition by Silver Ion and Reversed-Phase High Performance Liquid Chromatography with Flame Ionization Detection[a]

Resolution			Quantitation (Area percent)[b]							
			Safflower		Sunflower		Corn		Pumpkinseed	
Triacylglycerol saturated, monenoic, dienoic, trienoic, fatty acid species[c]	Number of Double Bonds	Triacylglycerol Molecular Species Reversed Phase[d]	Reversed Phase	Silver Ion	Reversed Phase	Silver Ion	Reversed Phase	Silver Ion	Reversed Phase	Silver Ion
SSS	0	PPP,PPS,PSS,SSS	0.8	0.1	0.3	0.4	0.2	0.4	0.3	0.1
SSM	1	POP,SPO,SOS	0.6	0.6	0.7	1.1	0.5	1.3	2.2	1.2
SSD	2	PLP,SLP,SLS	1.4	1.6	1.7	1.4	2.3	2.9	8.3	8.1
SMM	2	POO,SOO	0.9	1.4	1.8	1.4	3.0	3.8	3.2	3.8
SMD	3	LOP,LOS	5.3	6.3	8.1	7.9	11.9	10.8	13.9	14.7
MMM	3	OOO	0.8	0.7	1.5	1.4	3.0	3.8	4.2	4.5
SDD	4	LLS,LLP	17.6	18.7	20.4	20.8	18.7	17.8	20.6	20.7
MMD	4	LOO	3.5	4.5	6.0	6.0	10.0	11.8	9.6	10.5
DDM	5	LLO	19.6	19.8	23.4	23.3	23.3	23.7	17.7	18.9
DDD	6	LLL	47.4	46.1	35.9	35.8	26.3	22.8	18.9	16.7
TDD	7	LNLL	0.2	0.2	0.3	0.3	0.7	0.9	0.3	0.4
UNIDENTIFIED			1.9	0.0	0.0	0.2	0.1	0.0	0.9	0.4

See notes in Table 1

TABLE 3
Vegetable Seed Oil Triacylglycerol Composition by Silver Ion and Reversed-Phase High Performance Liquid Chromatography with Flame Ionization Detection[a]

Resolution			Quantitation (Area Percent)[c]					
			Linseed		Soybean		Canola	
Triacylglycerol saturated, monenoic, dienoic, trienoic, fatty acid species[c]	Number of Double Bonds	Triacylglycerol molecular species reversed phase[d]	Reversed Phase	Silver Ion	Reversed Phase	Silver Ion	Reversed Phase	Silver Ion
SSS	0	PPP, PPS, PSS, SSS	0.1	0.1	0.5	0.4	0.5	0.1
SSM	1	POP, SOP, SOS	0.8	0.8	0.7	1.4	0.9	0.7
SSD	2	PLP, SLP, SLS	1.0	0.3	3.7	3.9	0.7	1.0
SMM	2	POO, SOO	2.2	2.3	3.8	4.2	5.7	6.5
SMD	3	LOP, LOS	4.3	3.3	12.9	11.6	8.0	7.0
MMM	3	OOO	2.1	2.1	2.9	3.4	21.1	21.9
SDD	4	LLS, LLP	2.1	4.8	16.9	15.5	3.9	5.1
MMD	4	LOO	1.9	5.2	11.1	9.4	22.4	21.7
DDM, TMM, SMT	4-5	LLO, LNOO, LNOP	12.1	14.2	17.7	21.2	20.1	21.2
DDD, TDS, TDM	5-6	LLL, LNLO, LNLP	14.9	17.9	21.8	20.5	11.7	9.8
TDD	7	LNLL	16.8	12.4	6.8	6.7	3.5	3.1
TTM	7	LNLNO	6.5	5.7			0.1	0.0
TTD	8	LNLNL	12.7	11.7	1.0	0.9	0.6	0.8
TTT	9	LNLNLN	22.2	19.2				
UNIDENTIFIED			0.3	0.0	0.2	0.9	0.8	1.1

See notes in Table 1

peaks. Some linolenic acid containing TAG eluted with linoleic TAG during Ag-HPLC of linolenic acid containing vegetable oils. (Christie, using a different Ag-HPLC column and a more complex mobile phase system, also observed that TAG containing T and D were unresolved with linolenic acid rich oils like linseed [16].) The GC-FID procedure was particularly useful for analysis of fractions which contained both dienoic and trienoic acid containing TAG. GC analysis was previously demonstrated by Christie for identification of TAG components represented by Ag-HPLC chromatogram peaks (16).

The retention volumes of the vegetable oil TAG increased as the number of double bonds increased from zero to nine (by the total number of fatty acid double bonds in the triacylglycerol). TAG containing the same number of double bonds (for example, SSD vs. SMM and SDD vs. MMD) showed partial resolution, perhaps due to secondary partition or adsorption mechanisms. However, computer integration of the TAG chromatogram peaks allowed estimation of the amount of each TAG. Other TAG with the same number of double bonds, like the pair MDD and TMM and the pair DDD and TDM showed no resolution and estimation of these components was based on GC-FID analysis of the TAG fraction after transmethylation.

The accuracy of the TAG quantitation by Ag-HPLC-FID with 0.5% acetonitrile/hexane system relative to TAG standards known by weight was previously reported (7). We found area percent compared well to weight percent without having to apply response factors for tristearoyl (SSS), trioleoyl (MMM), trilinoleoyl (DDD), triarachidonoyl (tetraenoic fatty acids), and tricrepenynoyl (monenoic alkynoic fatty acids) glycerols. Also, FID linear response had been demonstrated for another Ag-HPLC column with a

different mobile phase, for tripalmitoyl and trilauroylglycerols (14). Unlike TAG analyses obtained by Ag-HPLC systems with light scattering and ultraviolet detectors which required response factors for quantitation (5, 16), the TAG quantitation reported for the vegetable oil TAG resolved by Ag-HPLC-FID in Tables 1-3 gave good quantitation without response factors of the oil composition.

Previously, good TAG quantitation without response factors was demonstrated for the HPLC FID detector in combination with reversed phase HPLC (RP-HPLC FID) analyses of vegetable oils (8, 17). TAG quantitation by RP-HPLC-FID, which resolves TAG based on both fatty acid carbon number and unsaturation is also presented in Tables 1-3. Quantitative results for many of the TAG resolved by Ag-HPLC-FID were in agreement with those for RP-HPLC-FID analysis of the same oil. Thus, identification of the TAG resolved by Ag-HPLC is further supported by RP-HPLC analyses.

Fatty acid composition calculated from the quantitation of resolved TAG (10,16) by Ag-HPLC-FID and the experimental GC analysis of the methyl esters of the same oil are presented in Table 4. These results further confirm the TAG identity and quantitation determined by Ag-HPLC FID analyses.

In a previous study of margarine basestock formulations, we used the RP-HPLC-FID method for TAG analyses of interesterified blends of fully hydrogenated soybean oil with nine commonly used vegetable oils (12). TAG composition data obtained by Ag-HPLC-FID and by RP-HPLC-FID of corn oil and the basestocks produced by randomization of corn oil, the corn oil blend with cottonseed stearine and its interesterified product are presented in Table 5.

TABLE 4
Fatty Acid Composition of Selected Vegetable Oils as Calculated from Triacylglycerol Composition and as determined by Gas Chromatography of the Respective Oils after Transmethylation[a]

Vegetable Oil	Method	Area Percent Fatty Acid Composition			
		Saturated	Oleic	Linoleic	Linolenic
Coconut	HPLC	88.7	3.4	7.9	0.0
	GC	88.3	2.9	8.8	0.0
Palm	HPLC	49.3	40.8	9.8	0.0
	GC	48.9	41.1	9.9	0.0
Cottonseed	HPLC	25.7	15.9	58.2	0.2
	GC	25.1	16.1	58.6	0.2
Olive	HPLC	16.5	70.0	13.3	0.3
	GC	16.8	69.9	12.3	1.0
Peanut	HPLC	16.7	49.2	33.3	0.8
	GC	19.8	48.0	31.9	0.3
Safflower	HPLC	9.2	14.9	75.1	0.8
	GC	9.3	14.8	75.2	0.2
Corn	HPLC	13.9	26.1	59.6	0.4
	GC	13.8	26.4	59.0	0.8
Pumpkinseed	HPLC	21.0	24.6	54.1	0.3
	GC	18.7	25.7	54.8	0.8
Linseed	HPLC	9.4	17.3	31.2	42.1
	GC	9.6	19.3	29.9	41.2
Soybean	HPLC	14.3	24.8	53.3	7.6
	GC	14.9	25.1	52.8	7.2
Canola	HPLC	8.7	57.3	27.4	6.6
	GC	8.5	56.3	26.2	9.0

[a]Conditions given in Experimental Section.

Composition data for soybean oil, randomized soybean oil, soybean oil blend with cottonseed stearine and its interesterified product are given in Table 6. Ag-HPLC chromatograms of the corn oil products are given in Fig. 1 and for the soybean oil products in Fig. 2.

There is good agreement between the composition data obtained by RP-HPLC FID or by Ag-HPLC FID (Tables 5 and 6). These results show Ag-HPLC FID is a suitable method for analyses of the TAG composition changes

TABLE 5
Triacylglycerol Composition of Corn Oil, Randomized Corn Oil, Corn Oil and Cottonseed Stearine (CSOST) Blend and Interesterified Product, by Silver Ion and Reversed-Phase HPLC with Flame Ionization Detection[a]

Resolution		Area Percent[b]							
		Corn Oil		Randomized Corn Oil		Blend Corn Oil + CSOST		Interesterified Corn Oil + CSOST	
Triacylglycerol saturated, monenoic, dienoic, trienoic fatty acid species silver ion[c]	Triacylglycerol molecular species reversed phase[d]	Reversed Phase	Silver Ion	Reversed Phase	Silver Ion	Reversed Phase	Silver Ion	Reversed Phase	Silver Ion
SSS	PPP,PPS,PSS,SSS	0.2	0.4	0.2	0.1	19.8	20.5	2.3	3.0
SSM	POP,SOP,SOS	0.5	1.3	0.5	0.7	0.5	1.2	5.6	5.0
SSD	PLP,SLP,SLS	2.3	2.9	2.8	1.9	2.3	2.5	10.9	12.8
SMM	POO,SOO	3.0	3.8	2.5	4.5	2.7	3.3	4.1	4.0
SMD	LOP,LOS	11.9	10.8	13.0	9.8	10.2	8.8	20.7	18.9
MMM	OOO	3.0	3.8	2.3	5.1	2.3	3.2	0.7	0.7
SDD	LLS,LLP	18.7	17.8	17.9	14.2	15.4	13.2	21.6	22.4
MMD	LOO	10.0	11.8	10.1	14.2	8.0	9.9	4.7	4.9
DDM	LLO	23.3	23.7	24.1	24.8	17.1	17.9	14.5	15.4
DDD	LLL	26.3	22.8	24.4	22.7	20.3	17.7	12.0	12.5
TDD	LNLL	0.7	0.9	0.8	0.9	0.6	0.9	0.6	0.4
UNIDENTIFIED		0.1	0.0	1.4	1.1	0.8	0.9	2.3	0.0

See notes in Table 1

TABLE 6

Triacylglycerol Composition of Soybean Oil, Randomized Soybean Oil, Soybean Oil and Cottonseed Stearine (CSOST) Blend and Interesterified Product, by Silver Ion and Reversed-Phase HPLC with Flame Ionization Detection[a]

Resolution		Area Percent[b]							
				Randomized		Blend		Interesterified	
		Soybean Oil		Soybean Oil		Soybean Oil + CSOST		Soybean Oil + CSOST	
Triacylglycerol saturated, monenoic, dienoic, trienoic, fatty acid species silver ion[c]	Triacylglycerol molecular species reversed phase[d]	Reversed Phase	Silver Ion	Reversed Phase	Silver Ion	Reversed Phase	Silver Ion	Reversed Phase	Silver Ion
SSS	PPP,PPS,PSS,SSS	0.5	0.4	0.6	1.6	16.1	16.6	2.3	3.1
SSM	POP,SOP,SOS	0.7	1.4	1.4	2.2	1.0	1.5	5.8	2.5
SSD	PLP,SLP,SLS	3.7	3.6	3.4	1.1	3.5	2.8	1.3	2.2
SMM	POO,SOO	3.8	4.2	6.0	5.9	3.4	3.9	13.4	16.0
SMD	LOP,LOS	12.9	11.6	14.5	8.8	11.6	9.1	20.5	18.6
MMM	OOO	2.9	3.4	1.4	6.1	2.4	3.0	0.5	0.4
SDD	LLS,LLP	16.9	15.5	13.4	9.0	13.2	13.3	19.3	22.5
MMD	LOO	11.1	9.4	8.4	14.8	6.5	7.8	3.9	3.6
MDD,SMT,MMT	LLO,LNOP,LNOO	17.7	21.2	22.9	23.9	14.9	17.3	12.5	14.1
DDD,TDS,TDM	LLL,LNLP,LNLO	21.8	20.5	18.8	19.6	20.6	16.9	13.3	10.7
TDD	LNLL	6.8	6.7	6.2	5.4	5.7	5.2	3.5	3.2
TTD	LNLNL	1.0	0.9	0.9	0.8	0.8	1.2	0.0	0.4
UNIDENTIFIED		0.2	1.2	2.1	0.8	0.3	1.3	3.7	2.7

See notes in Table 1

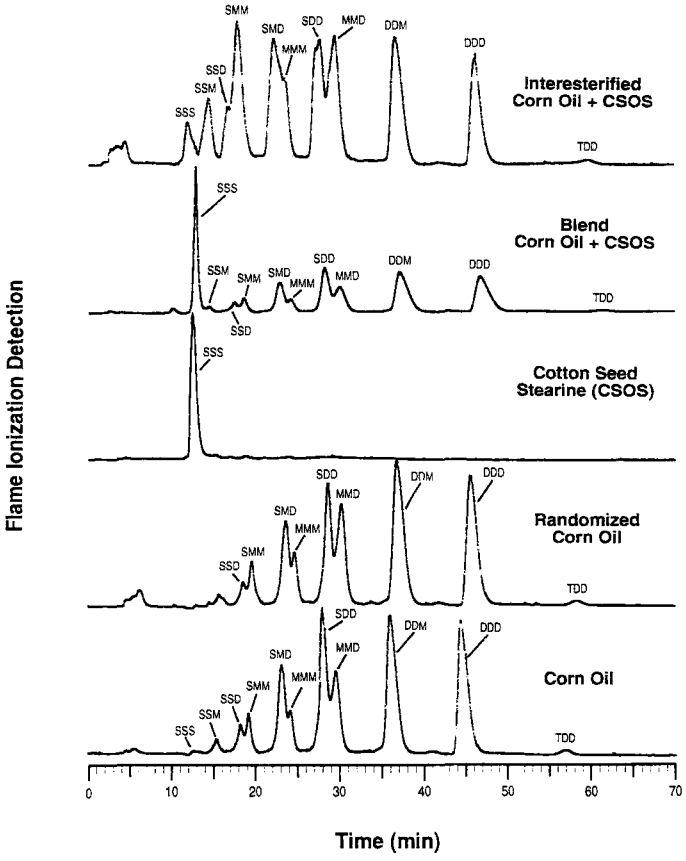

FIGURE 1. Triacylglycerol analyses by Ag-HPLC-FID of corn oil and randomized corn oil, blend of corn oil and cottonseed oil stearine and its interesterified product. See notes in Table 1.

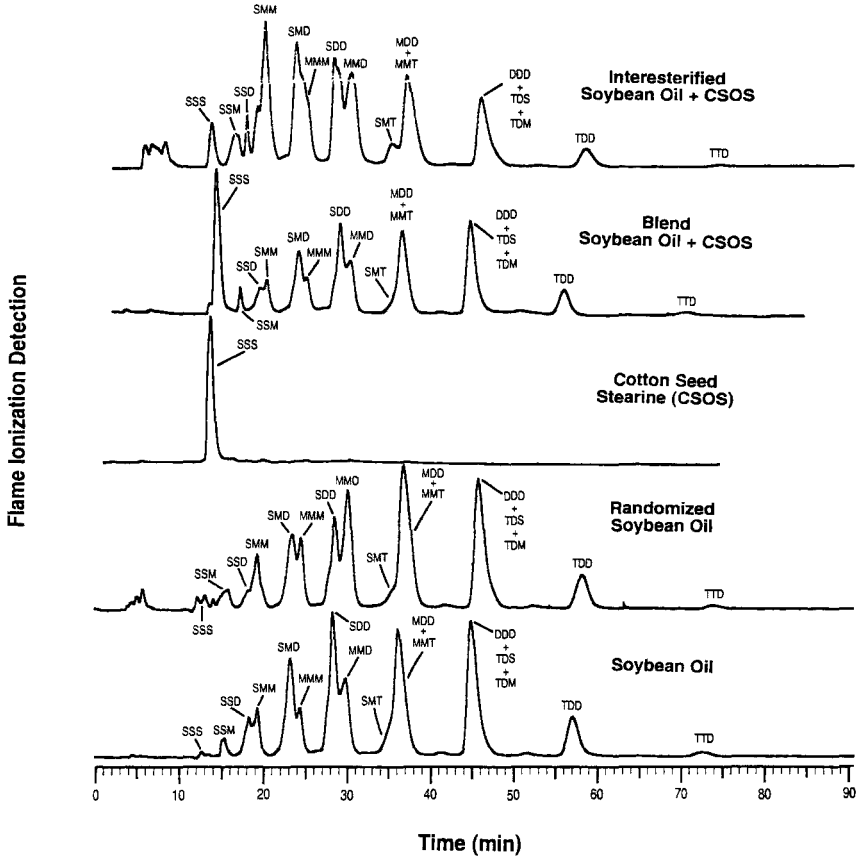

FIGURE 2. Triacylglycerol analyses by Ag-HPLC-FID of soybean oil and randomized soybean oil, blend of soybean oil and cottonseed oil stearine and its interesterified product. See notes in Table 1.

obtained by randomization, blending and interesterification of fats. For example, in Table 5, TAG composition of randomized corn oil relative to that of the starting oil showed slight decrease in SMD compared to MMM and slight increase in MMD compared to SDD. The blend of corn oil and cottonseed oil stearine showed the high concentration of SSS which was greatly reduced with increase in other TAG after interesterification. Similar results were obtained from the soybean oil study. TAG composition of randomized soybean oil relative to that of the starting oil showed a decrease in SMD compared to MMM and an increase in MMD compared to SDD. The blend of soybean oil showed a high initial concentration of SSS, which was greatly reduced after interesterification.

Ag-HPLC FID, with isocratic mobile phase of acetonitrile/hexane, is thus a suitable method for vegetable oil TAG analysis, yielding chromatograms which are easy to interpret and to quantitate. The chromatograms for TAG eluted by Ag-HPLC compared to RP-HPLC are less complex due to TAG elution with respect to fatty acid double bond number as opposed to both unsaturation and carbon chain length for TAG eluted by RP-HPLC (8,9,12,18).

ACKNOWLEDGEMENT

We are grateful to Ray K. Holloway for capillary gas chromatography analyses. This research was conducted with the support and cosponsorship of San Diego State University Foundation, San Diego, CA, and INTSOY/University of Illinois, Urbana, IL.

REFERENCES

1. W. W. Christie, in Lipid Analysis, 2nd Edition, Pergamon Press, New York, NY, 1982, p. 135.
2. W. W. Christie, in High-Performance Liquid Chromatography and Lipids, Pergamon Press, New York, NY, 1987, p. 169.
3. W. W. Christie, in Gas Chromatography and Lipids, The Oily Press, Ayr, Scotland, 1989, p. 186, 242.
4. B. Nikoloua-Damyanova, in Advances in Lipid Methodology-One, W. W. Christie, ed., The Oily Press, Ayr, Scotland, 1992, p. 181.
5. W. W. Christie, *Ibid.* p. 239.
6. R. O. Adlof, J. Chromatogr. 659:95 (1994).
7. W. E. Neff, R. O. Adlof, M. El-Agaimy, J. Am. Oil Chem. Soc. (In press) (1994).
8. M. A. M. Zeitoun, W. E. Neff, E. Selke, T. L. Mounts, J. Liquid Chromatogr. 14, 2685 (1991).
9. W. E. Neff, E. Selke, T. L. Mounts, W. M. Rinsch, E. N. Frankel, M. A. M. Zeitoun, J. Am. Oil Chem. Soc. 69: 111 (1992).
10. H. Konishi, W. E. Neff, T. L. Mounts, J. Chromatogr. 629: 237 (1993).
11. W. E. Neff, T. L. Mounts, W. M. Rinsch, H. Konishi, J. Am. Oil Chem. Soc., 70: 163 (1993).
12. M. A. M. Zeitoun, W. E. Neff, G. R. List, T. L. Mounts, *Ibid.* 70: 467 (1993).
13. W. E. Neff, R. O. Adlof, H. Konishi, D. Weisleder, *Ibid.* 70: 449 (1993).
14. B. S. J. Jeffrey, *Ibid.* 68: 289 (1991).
15. W. E. Neff, M. A. M. Zeitoun, D. Weisleder, J. Chromatogr. 589: 353 (1992).
16. W. W. Christie, *Ibid.* 454: 273 (1988).

17. F. C. Phillips, W. L. Erdahl, J. A. Schmit, O. S. Privett, Lipids 19: 880 (1984).

18. W. E. Neff, T. L. Mounts, W. M. Rinsch, H. Konishi, and M. El-Agaimy, J. Am. Oil Chem. Soc. (In press) (1994).

19. M. A. M. Zeitoun, W. E. Neff, G. R. List, T. L. Mounts, *Ibid.* 70: 467 (1993).

Received: April 2, 1994
Accepted: June 20, 1994

JOURNAL OF LIQUID CHROMATOGRAPHY, 17(18), 3969-3982 (1994)

A MODIFIED SIMPLE AND RAPID REVERSED PHASE HIGH PERFORMANCE LIQUID CHROMATOGRAPHIC METHOD FOR QUANTIFICATION OF AMITRIPTYLINE AND NORTRIPTYLINE IN PLASMA

J. ATTA-POLITOU, K. TSARPALIS, AND A. KOUTSELINIS
Department of Forensic Medicine and Toxicology
School of Medicine, University of Athens
M. Asias 75-Goudi, Athens 11527, Greece

ABSTRACT

A simple and rapid reversed-phase liquid chromatographic method for the determination of amitriptyline and nortriptyline in plasma is described. Protriptyline was used as internal standard. Plasma samples were extracted from alkaline pH with hexane-isoamylalcohol 98:2 v/v for 60 sec on a vortex apparatus. The organic phase was back extracted with HCl 0.1N and the aqueous phase was injected directly and monitored at 240nm. Samples were chromatographed on a 5 μm Kromasil 100-C8 column (25 cm x 4 mm id) using acetonitrile/0.04M KH_2PO_4 40:60 v/v as the mobile phase. The lower limit of detection was 5 ng/ml for amitriptyline and nortriptyline while the lower limit of quantification was 10 ng/ml for both compounds. Peak height and plasma amitriptyline or nortriptyline concentrations were linearly related from 25 to 300 ng/ml. No potential sources of interference have been identified. The methodology was used to monitor plasma amitriptyline or nortriptyline concentrations in patients receiving therapeutic doses of these drugs as well as for qualitative determination of several tricyclic antidepressants in plasma in cases of emergency toxicology.

INTRODUCTION

Tricyclic antidepressants are widely used in the treatment of patients suffering from depression. Therapeutic monitoring of tricyclic antidepressants plasma levels can be important in determining clinical efficacy, predicting side effects and monitoring compliance (1-4). Various methods have been described for the measurement of tricyclic antidepressants in plasma and have been extensively reviewed (5-7). High performance liquid chromatographic (HPLC) approaches for the determination of tricyclic antidepressants in plasma have been reported in the literature (8-23).

The most widely used tricyclic antidepressant is amitriptyline (AT). Its main metabolite nortriptyline (NT), formed by mono-N-demethylation, also contributes towards the pharmacological activity and is also marketed as a therapeutic agent.

Many analytical methods have been described for the determination of AT and NT, in plasma. Among these methods several are based on normal phase (10,11,24,25), reversed-phase (12-15,26,27) and ion-pair reversed-phase (16,28) high performance liquid chromatography as well as on gas chromatography (29-32).

This report describes a relatively simple, specific and accurate reversed-phase liquid chromatographic method, which allows quantification of AT and NT in plasma. The method developed modifies previously described methods (12-16,26) in several aspects offering convenience and rapidity in analysis. These modifications include the use of C-8 column with a simpler mobile phase, in which no pH adjustment or addition of amines are required , two rapid extraction steps and a direct injection of the aqueous acidic phase onto the HPLC system. Preliminary data suggests that the method is equally suitable for quantification of clomipramine in plasma as well as for qualitative determination of several tricyclic antidepressants and their metabolites in plasma, in cases of emergency toxicology.

MATERIALS AND METHODS

Apparatus

Chromatography was performed with an HPLC system consisting of a JASCO (Japan Spectroscopic Co. LTD) Model 880PU pump fitted with a model 880-02 Ternary Gradient Unit which was used under isocratic conditions on manual mode. The system

fitted with a Model 7125 manual injector (Cotati, Rheodyne, California, U.S.A.) and a 50 µl sample loop.

A Jasco Model 875 UV variable wavelength UV/VIS detector was operated at 240 nm. Samples were chromatographed on a 5 µm Kromasil 100-C8, 25 cm x 4 mm (i.d) reversed-phase column (MZ Analysentechnic D-6500 Mainz). A Hewlett Packard HP3394A integrator was used to record chromatograms, at peak height mode (chart speed 0.5 cm/min). A Millipore filtration system (Millipore, Bedford, M.A. USA) with type HV Millipore filters (pore size 0.45 µM) was used, for degassing mobile phase under vacuum.

Reagents and chemicals

Acetonitrile and water were HPLC grade (Lichrosolv®) and were obtained from Merck. Hexane and isoamylalcohol were analytical grade and were obtained from Ferak-Berlin. Amitriptyline, nortriptyline and protriptyline were gifts from local representatives.

Chromatographic Conditions

The mobile phase consisted of acetonitrile/0.04M KH_2PO_4 40:60 v/v. A flow rate of 1.0 ml/min was used at ambient temperature, resulting in a pressure of about 130 kg/cm^2. Mobile phases were degassed by vacuum through filtration, after mixing. Analysis was performed at 240 nm with the detector set at 0.004 absorbance units full-scale.

Standards for calibration graphs

Stock standard solutions of AT, NT, and protriptyline (Pro), which was used as an internal standard, were prepared in methanol to give final concentrations of 1 mg/ml. Standards stored at 4°C have been stable for 8 months. Standard solutions of final concentration of 100 µg/ml were prepared by diluting the stock standards 10-fold with distilled water. An aqueous reference solution containing both AT and NT to final concentration 10 µg/ml was prepared from a 100 µg/ml standard solution of each compound. Working solutions were prepared containing 0.25, 0.50, 0.75, 1.0, 1.5, 2.0, 2.5,

3.0 μg/ml of AT and NT by appropriate dilutions of the reference solution with water. Plasma standards for calibration curves were prepared by spiking 1.0 ml aliquots of pooled drug free plasma with 100 μl of the above mentioned working solutions, to make AT and NT plasma standards ranging from 25 to 300 ng/ml. A working solution of internal standard (0.3 μg/ml) was prepared by dissolving 300 μl of a 10 μg/ml aqueous solution into 10ml of distilled water. Calibration graphs of the recovered standards were prepared for each day of analysis to establish linearity and reproducibility of the HPLC system. Graphs were constructed of the peak-height ratio of each compound to internal standard against drug concentration.

Extraction procedure

In 10-ml glass conical tube with glass stopper, 1.0 ml of plasma, 100 μl of internal standard aqueous solution 0.3 μg/ml (30ng), and 200 μl of 1.5M solution NaOH were added and mixed briefly for 15 sec on vortex. Each sample was extracted with 6.0 ml of hexane-isoamylalcohol 98:2 v/v on vortex for 60 sec at speed 4 (Vortex-Genie, Model K-550 GE, Scientific Ind. Spingfield Mass 01103). The sample tube was centrifuged for 5 min at 2000rpm. The upper (organic) layer was then transferred into a 10-ml conical glass tube and reextracted with 200 μl HCl 0.1N on vortex for 60 sec at speed 4 and then centrifuged for 5 min at 2000rpm. An aliquot of about 80 μl of the aqueous phase was injected onto the HPLC system.

Analytical variables

Absolute recovery was calculated at 50, 150, 300 ng/ml spiked plasma samples by comparing the peak heights from extracted samples with those obtained from a direct injection of the corresponding unextracted aqueous standards.

Relative recovery was calculated at 50, 150, 300 ng/ml spiked plasma samples by comparing peak heights of extracted analytes with peak heights of extracted internal standards.

Within run and between run precision was determined by extracting plasma supplemented with AT and NT to 50, 150, 300 ng/ml.

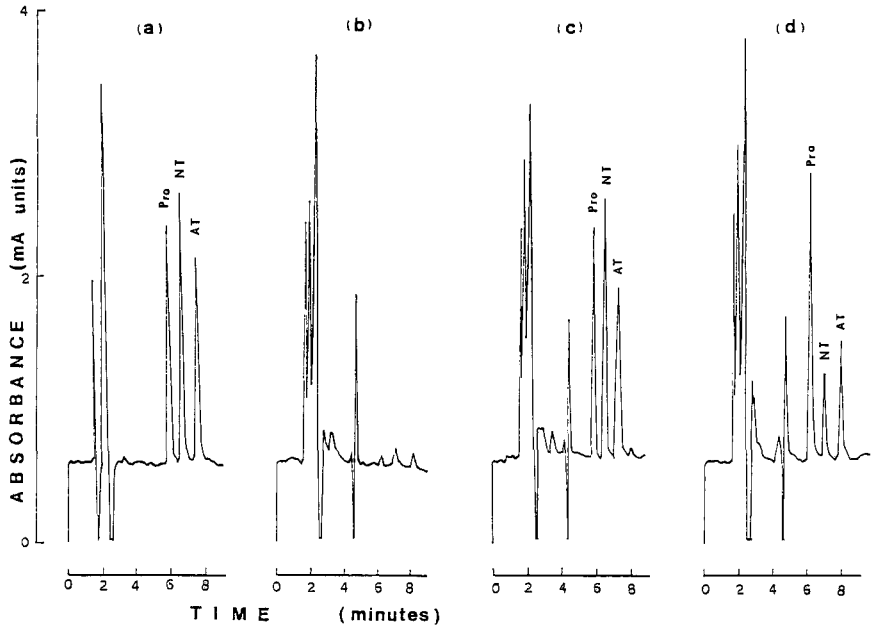

Figure 1: Chromatograms obtained from:
(a)a direct injection of an aqueous test solution containing 1μg/ml of AT,NT and 0.15μg/ml of Pro. Injected volume 50μl, corresponding to 50ng AT,NT and 7.5ng Pro
(b)an extracted drug free plasma
(c)an extracted drug free plasma supplemented with AT,NT,Pro to 200, 200, 30ng/ml respectively and
(d)an extracted plasma sample of a patient receiving 150mg amitriptyline daily for 5 days.
AT: 101.7ng/ml NT: 42.8ng/ml
Amitriptyline (AT), Nortriptyline (NT), Protriptyline-Internal standard (Pro).

Assay versatility

The method was also evaluated for qualitative analysis of several tricyclic antidepressants and their metabolites in plasma, in cases of emergency toxicology (screening method). Preliminary data suggests that the method is equally suitable for quantification of clomipramine in plasma.

Analysis of plasma samples

The overall precision of the assay was evaluated by analysing plasma samples spiked by three different concentrations of AT and NT, as well as in plasma samples of 10 patients who were receiving different oral doses of SAROTEN® (amitriptyline) daily. Patients samples were centrifuged immediately after collection and plasma stored at -20°C until analysis.

RESULTS

Retention times for Pro (internal standard), NT and AT were 5.87, 6.64, and 7.53 minutes, respectively. Figure 1a shows a chromatogram obtained from a direct injection of an aqueous test solution containing 1 μg/ml of AT and NT and 0.15 μg/ml Pro (injected volume 50 μl corresponding to 50 ng AT, 50 ng NT and 7.5 ng Pro). Figure 1b shows a chromatogram obtained from an extracted drug free plasma, while Figure 1c of an extracted drug free plasma supplemented with AT, NT to 200 ng/ml each and internal standard to 30 ng/ml. Figure 1d shows a chromatogram obtained from extracted plasma of a patient receiving AT for five days (150 mg/day). No interfering peaks were observed in several samples of drug free plasma. Figure 2 shows chromatograms obtained from a direct injection of an aqueous solution containing a mixture of several tricyclic antidepressants and their metabolites (a) and an extracted drug free plasma spiked with this mixture of compounds (b).

Recovery

Absolute and relative extraction recovery data from plasma samples supplemented with AT and NT to 50, 150, 300 ng/ml are referred in Tables 1 and 2 respectively (means of five experiments).

Linearity and Sensitivity

The peak height ratios for AT/internal standard and NT/ internal standard were linearly related to plasma concentrations of AT and NT, respectively, from 25 to at least 300 ng/ml.

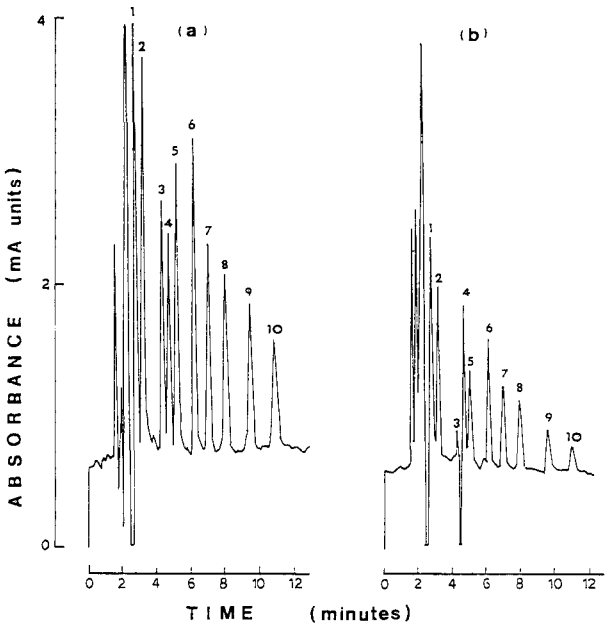

Figure 2. Chromatograms obtained from a direct injection of an aqueous solution containing 1µg/ml of compounds 1,2,3,4,5,7,8,9,10 and 0.20µg/ml of coumpound 6 (injected volume 50µl, corresponding to 50ng of each of compounds 1,2,3,4,5,7,8,9,10 and 10ng of compound 6) [a] and an extracted drug free plasma supplemented with compounds 1,2,3,4,5,7,8,9,10 to 100ng/ml and compound 6 to 20ng/ml [b].

1:E-10-OH-nortriptyline(Rt=2.67), 2:Z-10-OH-nortriptyline(Rt=3.11), 3:8-OH-desmethylclomipramine.HCl(Rt=4.19), 4:8-OH-Clomipramine(Rt=4.57), 5:Doxepine(Rt=5.04), 6:Protriptyline(Rt=6.04), 7:Nortriptyline(Rt=6.86), 8:Amitriptyline(Rt=7.84), 9:Desmethylclomipramine.HCl(Rt=9.32), 10:Clomipramine(Rt=10.71)

TABLE 1.

Absolute Extraction Recoveries and Coefficient of Variation(CV) of nortriptyline, amitriptyline and protriptyline from spiked plasma samples.

	Nortriptyline		**Amitriptyline**		**Protriptyline***	
Spiked plasma standards (ng/ml)	Rec% ± SD	CV	Rec% ± SD	CV	Rec% ± SD	CV
50 (n = 5)	88.7 ± 7.7	8.7	93.4 ± 11.8	12.6	96.0 ± 4.3	4.5
150 (n = 5)	95.7 ± 4.2	4.4	89.4 ± 4.2	4.7	95.8 ± 2.5	2.6
300 (n = 5)	87.0 ± 7.6	8.7	83.8 ± 7.3	8.7	92.5 ± 6.0	6.5

* All spiked plasma standards contained protriptyline (internal standard) to 30ng/ml.

TABLE 2.

Relative Extraction recoveries and Coefficient of variation (CV) of nortriptiline and amitriptyline from spiked plasma samples

	Nortriptyline			Amitriptyline		
Spiked plasma standards(ng/ml)	PHR	± SD	CV	PHR	± SD	CV
50 (n=5)	0.29	± 0.01	3.4	0.24	± 0.01	4.2
150 (n=8)	0.82	± 0.04	4.9	0.56	± 0.03	5.4
300 (n=5)	1.59	± 0.05	3.1	1.11	± 0.04	3.6

PHR: Peak height of extracted analyte to peak height of extracted internal standard.

The slopes of 15 calibration curves of AT in plasma, prepared over a period of four months, had a CV of 7.96%. The average regression equation was: $y = 0.00345x + 0.044$, where y = peak height ratio of AT /internal standard and x = plasma concentration of AT (ng/ml). The correlation coefficients for each standard curve constructed invariably exceeded 0.996.

The slopes of 15 calibration curves for NT in plasma over a period of four months had a CV of 5.63%. The average regression equation was: $y = 0.00519x + 0.064$ where y = peak height ratio of NT/internal standard and x = plasma concentration of NT (ng/ml). Correlation coefficients for each standard curve exceeded 0.994.

The lower limit of detection was 5 ng/ml for AT and NT while the lower limit of quantification was 10 ng/ml for both compounds.

Reproducibility and Accuracy

Within-run reproducibility and accuracy data for AT and NT are referred in Table 3. Between-run CVs were 7.3% and 8.5% for AT and NT respectively at 150 ng/ml spiked plasma (n=15), over a period of 4 months.

Interferences

Twenty compounds were studied for possible interference, including several drugs that might be administered to anxious or depressed patients (Table 4). Propoxyphene

TABLE 3.

Within-run accuracy and reproducility data of amitriptyline and nortriptyline from spiked plasma samples.

	Amitriptyline			**Nortriptyline**		
Conc Added (ng/ml)	50	150	300	50	150	300
Conc Found g/ml(x)	54.18	151.72	307.60	41.41	145.64	293.50
SD	6.38	9.95	12.90	5.02	6.88	9.53
CV%	11.77	6.56	4.19	12.12	4.72	3.24
Rr (Rel.range)	0.31	0.20	0.12	0.34	0.14	0.10
Er (Rel.error)	0.08	0.01	0.02	-0.17	-0.03	-0.02
n	5	10	5	5	10	5

TABLE 4.

Compounds studied for interference.

	Rt(min)		**Rt(min)**
Lorazepam (a)	-	Phenobarbital (c)	4.49
Oxazepam (a)	-	Chlorpromazine (c)	9.10
Bromazepam (a)	-	Chlordiazepoxide(c)	8.66
Triazolam (a)	-	Chlorpheniramine(c)	3.61
Diazepam (a)	-	Propanolol (c)	4.25
Nitrazepam (a)	-	Propoxyphene (b)	7.62
Alprazolam (a)	-	Maprotiline (b)	7.60
Artane (a)	-	Imipramine (b)	7.20
Theophylline (a)	-	Phenytoin (b)	6.75
Pseudoephedrine (a)	-		
Haloperidol (a)	-		

(a) = Not detected
(b) = Interfered, see text.
(c) = Detected but not interfered.

produced peak at 7.62 min; resolution was insufficient for quantification of AT. Phenytoin peak (Rt=6.75) was overlapping with that of NT. Maprotiline and imipramine (Rt 7.60 and 7.20 respectively) cannot be separated from AT by the described method, but in clinical practice they are not administered with AT.

Most of the benzodiazepines, which are commonly coadministered to depressed patients, were studied in spiked plasma samples and did not interefere to the analysis since they are not coextracted through the procedure described in this methodology. All the other compounds shown in Table 4 were tested for possible interference as aqueous solutions.

DISCUSSION

A number of analytical methods using reversed-phase high performance liquid chromatography have been reported for quantification of AT and NT in plasma (12-15,26,27). The methodology developed in this report modifies previously reported methods (12-15,26).

In this study several solvent mixtures were tested for the extraction of AT, NT and Pro (internal standard) from plasma samples. Hexane-isoamylalcohol 98:2 v/v, which has been used for the extraction procedure in previously reported methods (11,14,16,25) showed satisfactory extraction recovery (Tables 1,2). Since both solvents of the extraction mixture have relatively high boiling points, analysis is prolonged because of the time which is required for the evaporation step. For this reason, back extraction of the organic phase into 200 µl HCl 0.1N and direct injection of the aqueous phase onto the HPLC system was found preferable, making the analysis more rapid. Furthermore, in the present study, plasma samples were extracted in both steps of the extraction procedure, on a vortex apparatus for only 60 sec, while previously reported methods suggested gentle shaking for 10 min (15) or 60 min (14) and rotate-mix for 5 min (16). Our efforts to increase sensitivity using 100 µl instead of 200 µl HCl 0.1N for the back extraction of the organic phase proved to be unsuccessful because extraction recovery of the analytes was decreased.

During the preliminary phase of this study C-18 and C-8 columns (25 cm x 4 mm i.d., 5 µm) were tested for the analysis at ambient temperature. When the

C-18 (Lichrospher RP-18, MZ Analysentechnic D-6500 Mainz) column was tested, which has been used in previous studies (14-16,26) and the aqueous acidic phase was injected directly onto the HPLC system, unsatisfactory chromatograms were obtained, in regard to peak shape and resolution, after 50 injections of extracted plasma samples. On the contrary, the C-8 material was far more favourable with respect to column efficiency and peak shape. Moreover the C-8 column proved to be more resistant in our hands, being used for the analysis of more than 20 plasma samples per day. The use of acetonitrile / 0.04M KH_2PO_4 40:60 v/v as the mobile phase resulted in an excellent separation of the substances which were studied. In this methodology, pH adjustment of the mobile phase, used in other methods (13-16) has been avoided. Furthermore, the addition of aliphatic amines in the eluent, as competing bases for silica sites to decrease chemisorption which causes peak tailing, reported in other studies (13,26), has also been avoided. Therefore, it can be concluded that the method developed is more convenient, in comparison with previously reported ones.

The methodology used in this study, proved to be precise and accurate for the determination of AT and NT in spiked plasma samples (Table 3). Moreover plasma AT and NT levels in 10 patients included in this study, who received different oral doses of AT daily, are in accord with those reported in relevant studies (1,2).

Although the method has not been extensively used for the determination of clomipramine and its metabolites desmethylclomipramine, 8-OH-clomipramine and 8-OH-desmethylclomipramine, it appears to have sufficient specificity, sensitivity and precision using protriptyline as internal standard.

The methodology developed in this study can also be used as a screening procedure for the qualitative determination of several tricyclic antidepressants and their metabolites in plasma (Fig.2), being extremely useful in cases of emergency toxicology, as a part of the general toxicological analysis.

In conclusion, the analytical methodology developed in this report is simple, rapid, accurate, sensitive and specific. It can be used for monitoring plasma AT and NT steady-state concentrations as well as the subtherapeutic concentrations encountered during the initial start-up phase of AT therapy. The present methodology also provides the possibility for qualitative determination of several tricyclic antidepressants in plasma; this is certainly of value in cases of emergency toxicology.

REFERENCES

1. Orsulak, P.J., Schildkraunt, J.J.. Guidelines for therapeutic monitoring of tricyclic antidepressant plasma levels. Ther. Drug. Monit. 1 , 199-208, 1979.

2. Preskorn, S.H., Dorey, R.C., Jerkovich G.S.. Therapeutic drug monitoring of tricyclic antidepressants. Clin. Chem. 34/5, 822-828, 1988.

3. Feighner, J.P.. Clinical efficacy of the newer antidepres-sants. Clinical Psychopharmacology 1, (6 Suppl.), 23S-26S, 1981.

4. Sjöqvist, F., Bertilsson, L., Asberg, M.. Monitoring tricyclic antidepressants, p.p.93-91. In: Frontiers in Therapeutic Drug Monitoring, ed. by Tognoni, G., Latini, R. and Jusko, W.J., Raven Press, New York, 1980.

5. Norman, T.R., Maguire, K.P.. Analysis of tricyclic antidepressant drugs in plasma and serum by chromatographic techniques. J. Chromatogr. (Biomedical Applications) 340, 173-197, 1985.

6. Scoggins, B.A., Maguire, K.P., Norman, T.R., Burrows, G.D. Measurement of tricyclic antidepressants. Part I. A review of methodology. Clin. Chem. 26 /1, 5-17, 1980.

7. Scoggins, B.A., Maguire, K.P., Norman, T.R., Burrows, G.D. Measurement of tricyclic antidepressants. Part II. Applications of methodology. Clin. Chem. 26 /7, 805-815, 1980.

8. Suckow, R.F., Cooper, T.B.. Simultaneous determination of amitriptyline, nortriptyline, and their respective isomeric 10-hydroxy metabolites in plasma by liquid chromatography. J. Chromatogr. 230 (2), 391-400, 1982.

9. Beierle, F.A., Hubbard, R.W.. Liquid chromatographic separation of antidepressant drugs: I. Tricyclics. Ther. Drug. Monit. 5 , 279-292, 1983.

10. Streator, J.T., Eichmeier, L.S., Caplis, M.E.. Determination of tricyclic antidepressants in serum by high pressure liquid chromatography on a silica column. J. Anal. Toxicol. 4, 58-62, 1980.

11. Vandemark, F.L., Adams, R.F., Schmidt, G.J.. Liquid-chromatographic procedure for tricyclic drugs and their metabolites in plasma. Clin. Chem. 24 /1, 87-91, 1978.

12. Koteel, P., Mullins, R.E., Gadsden, R.H.. Sample preparationand liquid-chromatographic analysis for tricyclic antidepressants in serum. Clin. Chem. 28 /3, 462-466, 1982.

13. Kabra, P.M., Mar, N.A., Marton, L.J.. Simultaneous liquid chromatographic analysis of amitriptyline, nortriptyline, imipramine, desipramine, doxepin and nordoxepin. Clin. Chim. Acta 111, 133-146, 1981.

14. Preskorn, S.H., Leonard, K., Hignite, C.. Liquid chromatography of amitriptyline and related tricyclic compounds. J. Chromatogr. 197, 246-250, 1980.

15. Brodie, R.R., Chasseaud, L.F., Hawkins, D.R.. Separation and measurement of tricyclic antidepressant drugs in plasma by highperformance liquid chromatography. J. Chromatogr. (Biomedical Applications) 143, 535-539, 1977.

16. Proelss, H.F., Lohmann, H.J., Miles, D.G.. High-performance liquid-chromatographic simultaneous determination of commonly used tricyclic antidepressants. Clin. Chem. 24/11, 1948-1953, 1978.

17. Dorey, R.C., Preskorn, S.H, Widener, P.K.. Results compared for tricyclic antidepressants as assayed by liquid chromatography and enzyme immunoassay. Clin. Chem. 34 (11), 2348-51, 1988.

18. Rop, P.P., Viala, A., Durand, A., Conquy, T.. Determination of citalopram, amitriptyline and clomipramine in plasma by reversed-phase high-performance liquid chromatomotography. J.Chromatogr. 338 (1), 171-178, 1985.

19. Jensen, K.M.. Determination of amitriptyline-N-oxide, amitriptyline and nortriptyline in serum and plasma by high-performance liquid chromatography. J. Chromatogr. 183 (3), 321-329, 1980.

20. Matsumoto, K., Kanba, S., Kubo, H., Yagi, G., Iri, H., Yuki, H.. Automated determination of drugs in serum by column-switching high-performance liquid chromatography. IV. Separation of tricyclic and tetracyclic antidepressants and their metabolites. Clin. Chem. 35 (3), 453-456, 1989.

21. Dadgar, D., Power, A.. Applications of column-switching technique in biopharmaceutical analysis. I. High-performance liquid chromatographic determination of amitriptyline and its metabolites in human plasma. J. Chromatogr. 416 (1), 99-109, 1987.

22. Kiel, J.S., Abramson, R.K., Smith, C.S., Morgan, S.L. Development of a rapid extraction and high-performance liquid chromatographic separation for amitriptyline and six biological metabolites. J. Chromatogr. 383 (1), 119-27, 1986.

23. Dixon, R., Marin, D.. Tricyclic antidepressants:a simplified approach for the routine clinical monitoring of parent drug and metabolites in plasma using HPLC. Res. Commun. Chem. Pathol. Pharmacol. 33 (3), 537-45, 1981.

24. Watson, I.D., Stewart, M.J.. Quantitative determination of amitriptyline and nortriptyline in plasma by high-performance liquid chromatography. J. Chromatogr. 132, 155-159, 1977.

25. Edelbroek, P.M., De Haas E.J.M., De Wolff, F.A.. Liquid-chromatographic determination of amitriptyline and its metabolites in serum, with adsorption onto glass minimized. Clin. Chem. 28, 2143-2148, 1982.

26. Kraak, J.C., Bijster, P.. Determination of amitriptyline and somc of its metabolites in blood by high-pressure liquid chromatography. J. Cromatogr.(Biomedical Applications) 143, 499-512, 1977.

27. Härtter, S., Hiemke, C.. Column switching and high-performance liquid chromatography in the analysis of amitriptyline, nortriptyline and hydroxylated metabolites in human plasma or serum. J. Chromatogr.(Biomedical Applications) 578, 273-282, 1992.

28. Mellström, B., Braithwaite, R.. Ion-pair liquid chromatography of amitriptyline and metabolites in plasma. J. Chromatogr. 157, 379-385, 1978.

29. Burch, J.E., Roberts, S.G., Raddats, M.A.. Amitriptyline and its basic metabolites determined in plasma by gas chromatography. J. Chromatogr. 308, 165-179, 1984.

30. Jones, D.R., Lukey, B.J., Hurst, H.E.. Quantification of amitriptyline, nortriptyline and 10-hydroxy metabolite isomers in plasma by capillary gas chromatography with nitrogen-sensitive detection. J. Chromatogr. 278 (2), 291-299, 1983.

31. Vinet, B.. Column deactivation in analysis for underivatized tricyclic antidepressants by gas chromatography with use of nitrogen detector. Clin. Chem. 29 (3), 452-455, 1983.

32. Vandel, S., Vincent, F., Prudhon, F., Nezelof, S.,Bonin,B., Bertschy, G.. Etude comparative de deux techniques de dosage de l'amitriptyline et nortriptyline: EMIT et chromatographie gazeuse. Therapie, 47 (1), 41-45, 1992.

Received: March 12, 1994
Accepted: June 27, 1994

JOURNAL OF LIQUID CHROMATOGRAPHY, 17(18), 3983-3988 (1994)

HIGH PERFORMANCE LIQUID CHROMATOGRAPHIC ASSAY FOR ISOSORBIDE 5-MONONITRATE AND IMPURITIES OF INORGANIC NITRATES IN PHARMACEUTICALS

DANICA AGBABA[1], VALENTINA JANJIC[2], DOBRILA ZIVANOV-STAKIC[1], AND SOTE VLADIMIROV[1]

[1]*Faculty of Pharmacy*
Department of Pharmaceutical Chemistry
Vojvode Stepe 450, 11000 Belgrade
P.O. Box 146, Serbia
[2]*Quality Control Department*
"Zdravlje" Leskovac, Serbia

ABSTRACT

A simple and reliable high performance liquid chromatographic (HPLC) method for the quantification of isosorbide 5- mononitrate and inorganic nitrate impurity in raw material and dosage formulations has been developed and validated. The procedure which simultaneously resolves active organic nitrates : isosorbide 5-mononitrate, isosorbide 2-mononitrate and isosorbide 2.5-dinitrate , and main impurities (including related nitrate and acetate esters) , may be used as a control of purity of raw material and dosage forms.

INTRODUCTION

Coronary vasodilator isosorbide dinitrate (ISDN) was found to metabolize the following active mononitrates : isosorbide 5-mononitrate (5-ISMN) and isosorbide 2-mononitrate (2-ISMN). The former one has been recently found to be more active or less toxic and therefore predominantely used in the treatment of angina pectoris.

Stability studies (1-4), identification or determination (5-24) of mono- and dinitrate esters in raw material, as well as in dosage formulations, have been mostly performed by using HPLC (1,3,5-10,24), GC (2,4,11-12) or TLC (13-17). Colorimetry (18-19) and polarography (20-22) have also been used for quantification of organic nitrates in dosage forms. Isosorbide 2-acetate (IS-2A), 5-acetate (IS-5A) and diacetate (ISDA), 2-nitrate-5-acetate (IS-2N5A) or 2-acetate-5-nitrate (IS-2A5N) could be traced as impurities originated from the synthesis of parent nitrates. The above mentioned mixture was isolated and identified by GC(23).

According to British Pharmacopoeia (18) it is required to analyse the presence of inorganic nitrates in raw material and dosage forms.Inorganic nitrates can derive as impurities either from the synthesis of organic nitrates or as a product of degradation.

However, there are no published reports on the quantification assay of inorganic nitrates impurities. Therefore, the present paper will focus on assay of 5-ISMN and the isolation and quantification of the residue of inorganic nitrates in raw material and dosage forms by HPLC.

EXPERIMENTAL

Reagents

Isosorbide 5-mononitrate (5-ISMN), isosorbide 2-mononitrate (2-ISMN) and isosorbide 2.5-dinitrate (ISDN) , isosorbide (IS), isosorbide 2-acetate (IS-2A), isosorbide 2.5-diacetate (IS-2.5DA), isosorbide 2-acetate-5-nitrate (IS-2A5N) were obtained from Kali Chemie Pharma (Hanover,FRG). Sodium nitrate was of analytical grade. Water and methanol were of HPLC grade. Ancorbid^{R} sustained release pellets, containing 40 mg and 60 mg 5-ISMN, were obtained from "Zdravlje" Leskovac (Serbia) .

Instruments

HPLC system Spectra Physics (San Jose ,CA,USA) Model 8100 was used equipped with a UV detector Model 8440 (wavelength set up at 220 nm) and an integrator Model 4200. The analytical column (250 x 4 mm) was packed with 5 μm Lichrosorb RP 18 (Merck, Darmstadt,FRG). The mobile phase of methanol-water (30 : 70) was filtered through a 0.45 μm membrane filter and degassed in an ultrasonic bath prior to use. The flow rate was 1 ml/min.

5-ISMN and Inorganic nitrates impurity assays.

A stock solution of 1 mg/ml 5-ISMN was prepared in water; calibration solutions were prepared by diluting the stock solution to obtain 0.1-0.25 mg/ml. Working standard solution of 5-ISMN was diluted to the concentration of 0.2 mg/ml.

A stock solution of 0.5 mg/ml sodium nitrate was prepared in water; calibration solutions were prepared by diluting the stock solution to obtain 0.25 - 2.5 μg/ml.

Sample solutions - The amounts of raw material or powdered pellets containing 50 mg of 5-ISMN were dissolved in 100 ml water. After filtration, the aliquots of 50 μl sample solution were subjected to HPLC for an inorganic nitrates assay. 50 μl of the diluted sample solution to 0.2 mg/ml were subjected to HPLC for 5-ISMN assay.

RESULTS AND DISCUSSION

Separation of 5-ISMN from active nitrates 2-ISMN, ISDN, and potential impurities, arose from different sources such as :IS (starting material in the synthesis), IS-2A, ISDA, IS-2A5N (intermediates in the synthesis), and inorganic nitrates (degradation products), is shown in Fig.1. It can be observed that under the conditions of the procedure, IS and inorganic nitrates have similar retention time (about 1.6 and 1.7 min., respectively). However, inorganic nitrate has a lower detection limit (factor 10^3) than IS and its determination from diluted samples cannot be interfered by IS.

Validation of the method

Linearity

The response (peak area) was proportional to the concentrations over the range tested; between 0.1 and 0.25 mg/ml for 5-ISMN and 0.1 to 5 μg /ml for inorganic nitrates (equivalent to 0.1 -2 % of the 5-ISMN concentration). The regression equations were $y= 4.3 +1944x$ with a correlation coefficient of $r=0.999$ ($n=5$), where $x=$mg/ml and $y= 4 + 224x$, and $r=0.998(n=5)$, where $x=\mu$g/ml for 5-ISMN and inorganic nitrates,respectively.

Precision

The repeatability of the analytical system was determined by using two samples of 5-ISMN found to contain 0.176 and 0.5% of inorganic nitrates impurities. Six consecutive replicate injections of each sample gave a relative standard deviation (RSD) of 2.7 and 0.9%. The repeatability of 5-ISMN assay running the concentrations of 0.1, and 0.2 mg/ml, gave a RSD of 1.5 and 0.7%.

Recovery

The accuracy of the method was proved by determination of 5-ISMN from laboratory-made tablet excipient mixture spiked with a 5.3, 14.8 and 24.4 mg of 5-ISMN: recoveries were 100.26, 100.67 and 100.09, respectively. A solution containing 5-ISMN with no detectable amount of inorganic nitrates was spiked with aliquots of the impurity solution

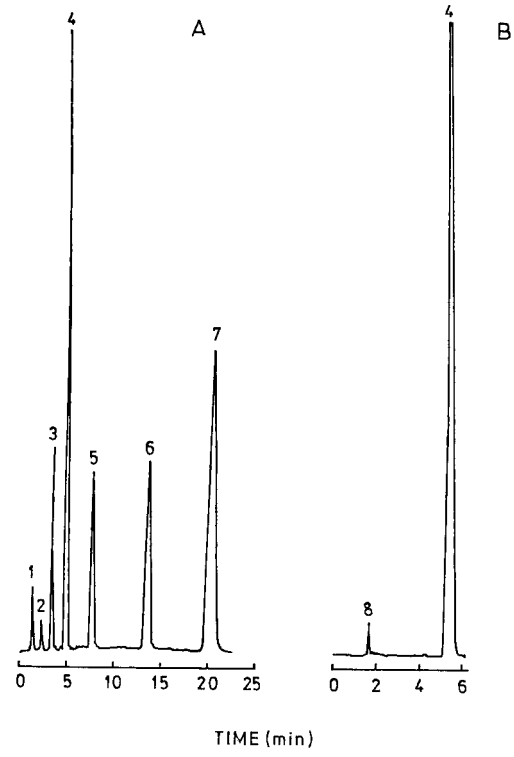

FIGURE 1. HPLC chromatogram of: A - mixture of IS (1), 2-ISMN (2), IS-2A (3), 5-ISMN (4), IS-2.5DA (5), IS-2A5N (6) and ISDN (7), B - sample of Ascorbid 40 mg pellets containing inorganic nitrates (8) at a concentration of 0.18%. The retention times were 1.60, 2.20, 3.42, 5.03, 7.95, 14.30, 21.50 and 1.70 for compounds 1,2,3,4,5,6,7 and 8 respectively,

TABLE 1.

Assay of 5-ISMN and Inorganic Nitrates

	5-ISMN		Inorganic Nitrates	
	Taken (mg)	Found mg ± s. d.	%	RSD[a]
Raw Material	50	49.2 0.75	0.11	4.5
Ascorbid 40 mg tbl.	40	38.9 0.75	0.17	4.7
Ascorbid 60 mg tbl.	60	58.9 0.97	0.20	3.5

[a]Relative Standard Deviation

at two concentrations of 1.25 and 5 μg/ml (equivalent to 0.5 and 2%). Recoveries obtained were 102.5% and 100.5%. Detection limit of the method was 1.5 μg/ml for 5-ISMN and 0.065 μg/ml (equivalent to 0.024%) for inorganic nitrates.

Application

The method was used to screen the raw material and dosage forms on inorganic nitrates impurities. The results obtained for 5-ISMN and inorganic nitrates assay are shown in Table 1. The results obtained for inorganic nitrates of 0.11% for raw material and 0.17 - 0.2% for dosage forms meet the requirements of USP not exceeding 2%.

The results suggest that because of its sensitivity and reproducibility, the method may be suitable for the simultaneous determination of 5-ISMN and inorganic nitrates impurities in raw material and dosage formulations.

Simple isocratic system used for separation is found to be suitable for routine purity control of active nitrates.

ACKNOWLEDGEMENT

The authors wish to thank Miroslav Nikolic and Verica Nikolic for the kind contribution in experimental part of the work.

REFERENCES

1. N.Mizuno, C.Shimizu, E. Morita, D.Shinkuma, Y.Yamanaka, J.Chromatogr.,264: 159-163 (1983)
2. N.Ruseva, N.Dimova, Farmatsiya (Sofia) 35: 1-4 (1985)
3. K.Nieminen, R.Aaltonen, P.Kahela, Acta Pharm. Fenn., 97: 2 1- 27 (1988)
4. W.Y.Lu, Yanxue Xuebeo, 24: 797-800 (1989)
5. C.Cavazzutti, L.Gagliardi, A.Amato, E.Gattavecchia, D.Tonelli, J.Chromatogr.,244: 391-395 (1982)
6. K.Kral, G.Kainz, Z.Anal. Chem., 316: 497-500 (1983)
7. C.S.Olsen, H.S.Scroggins, J.Pharm.Sci., 73: 1303-1304 (1984)
8. I.Torok, T.Paal, C.Koszeng,P.Kesaru, Acta Pharm.Hung.,55: 154-162 (1985)
9. M.Carlson, R.D. Thompson,R.P.Snell, J.Chromatogr. Sci.,26: 574-578 (1988)
10. D.G.Prue,R.N.Johnson, B.T.Kho, J.Assoc. Off. Anal. Chem. 60: 1341-1344 (1977)
11. L.Nobil, M.A.Raggi, V.Cavrini, A.M.Di Pietra, J.Pharm.Belg., 44: 210-214 (1989)
12. D.L.Hayward, R.Kitchen, D.Livingstone, Can.J.Chem.,40: 434-440 (1962)
13. A.J.Jr.Dietz, Biochem.Pharmacol., 16: 2447-2448 (1967)
14. D.A.Sherber, M.Marcus, S.Kleinberg , Biochem Pharmacol., 19: 607-612 (1970)
15. M.Carlson, R.Thompson, J.Chromatogr., 368: 472-475 (1986)
16. T.Azcona, A.Martin-Gonzales, P.Zamorano, C.Pascual, C.Graul,M.Garcia De Mirasierra, J.Pharm.Biomed.Anal.,9: 725-729 (1991)
17. H.L.Bhalla, J.E.Khenolkar, Indian Drugs, 21: 158-159 (1984)

18. British Pharmacopoeia, HMSO, London, (1993), p.366
19. S.Silvestri, Pharm.Acta Helv., 50: 304-307 (1975)
20. W .Turner, R.S. Lenhiewicz, J.Pharm.Sci., 65:118-121 (1976)
21. P.Kazandzhieva, N.Firkova, M.Yakowich, Farmatsya, 37: 1-7 (1987)
22. S.Pinzauti, E.La Porta, P.Gratteri, G.Papeschi, V.Giannellini, Pharm.Acta Helv.,64: 125-128 (1989)
23. N.Russeva, N.Dimova, G.Spyrov, M.Jurovska, J.Chromatogr.,295: 255-258 (1984)
24. United States Pharmacopeia, 22nd rev. Mack Publishing, Co.Easton,PA, (1991), p.740

Received: February 18, 1994
Accepted: May 24, 1994

JOURNAL OF LIQUID CHROMATOGRAPHY, 17(18), 3989-3997 (1994)

DETERMINATION OF ALFUZOSIN IN HUMAN PLASMA BY HIGH-PERFORMANCE LIQUID CHROMATOGRAPHY WITH COLUMN-SWITCHING

GIUSEPPE CARLUCCI*, ENRICO DI GIUSEPPE, AND PIETRO MAZZEO
Dipartimento di Chimica
Ingegneria Chimica e Materiali
Università dell'Aquila
Via Vetoio 67010 Coppito - L'Aquila, Italy

ABSTRACT

A high - performance liquid chromatographic method for the determination of alfuzosin in human plasma has been developed and validated. A column-switching procedure without extraction was used to isolate the drug from biological matrix prior to the quantitative analysis. The lower limit of detection for the analyte was 1 ng/ml. The method was linear from 2 to 150 ng/ml for human plasma. Within- and between-assay precision and accuracy were all found to be <5.2% at the eight concentrations evaluated. This procedure, simple and rapid, is suitable for pharmacology studies on alfuzosin.

INTRODUCTION

Alfuzosin is a selective antagonist of α_1-adrenergic receptors [1], active as antihypertensive agent [2], recently introduced in therapeutics for the treatment

of benign prostatic hypertrophy [3]. Its chemical name is N-[3-[(4-amino-6,7-dimethoxy-2-quinazolinyl) methylamino] propyl] tetrahydro-2-furancarboxamide; its formula is shown in Fig.1.

Some HPLC assays for alfuzosin have been recently described. Three of these methods [4-6] were developed for the determination of the enantiomers of the drug in rat and human plasma on a chiral protein column of human α_1-acid glycoprotein; one used a liquid-liquid extraction and a large volume injection technique for the quantitation of alfuzosin in biological fluids [7].

This paper describes a direct injection method, using column- switching without extraction, for the determination of alfuzosin in human plasma, providing accurate and precise results. The analysis of plasma samples from volunteers was carried out using this procedure.

EXPERIMENTAL

Chemicals and Materials

HPLC-grade acetonitrile and methanol were obtained from Farmitalia-Carlo Erba (Milan, Italy). Orthophosphoric acid (85% m/m) and potassium dihydrogenphosphate (analytical grade) were purchased from Fluka Chemika - BioChemika (Buchs, Switzerland). Alfuzosin hydrochloride was kindly supplied by LIRCA S.p.A. (Milan, Italy). Water (HPLC-grade) was obtained by distillation in glass and purification through a Milli-Q water purification system (Millipore Corporation, Bedford, MA, USA). Phosphate buffer was filtered through an HA 0.45 μm filter, while acetonitrile and methanol were filtered through an FA 0.5 μm filter (Millipore, Bedford, MA, USA).

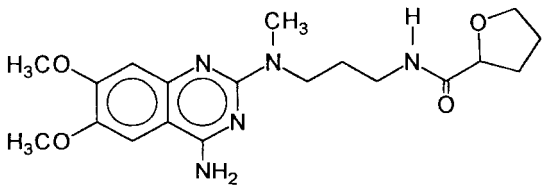

Figure 1 Chemical structure of alfuzosin.

Chromatographic System and Conditions

The chromatographic apparatus consisted of a model 510 and a model M-45 solvent delivery systems (Waters Associates, Milford, MA, USA). The luminescence detector model LS 30 (Perkin-Elmer, Rome, Italy) was set at 265 nm (excitation wavelength) and 400 nm (emission wavelength). The chromatograms were recorded on a model HP-3296-II integrator (Hewlett-Packard, Rome, Italy). A model 7125 sample injector and a six-port switching valve model 7000 (Rheodyne, Cotati, CA, USA) were used. The chromatographic arrangement (Fig.2) included a clean-up column (50 x 4.6 mm i.d.) filled with LiChrosorb C_{18} (10 µm) reversed-phase material (Merck, Darmstadt, Germany) and a guard column (20 x 4.6 mm i.d.) (not shown in Fig.2), packed with Pellicular-CN (40 µm) (Supelco, Bellefonte, PA, USA), placed between the switching valve and the analytical column. This was a cyanopropyl column Spherisorb S5W (25cm x 4.6 mm i.d., 5 µm particle size) (Phase Separations, UK). The clean-up solvent from pump A consisted of methanol-water (5:95, v/v). The analytical solvent from pump B was a mixture of acetonitrile-methanol-0.05M phosphate buffer (38:2:60, v/v/v). The pH of the phosphate buffer was adjusted to 2.5 with orthophosphoric acid. The mobile

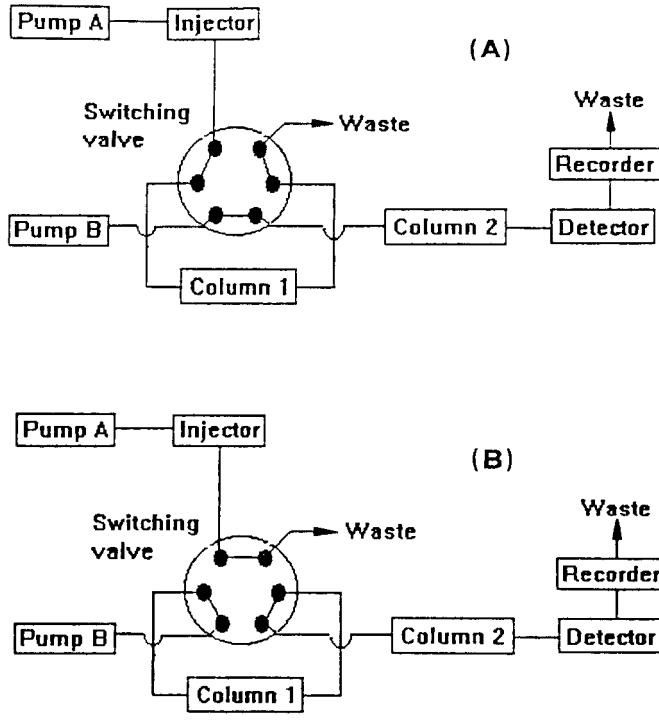

Figure 2 Column-switching system for direct injection of plasma and on-line HPLC analysis of alfuzosin: (A) Sample application; (B) Sample elution.

phase was prepared daily, filtered, sonicated before use, and delivered at a flow-rate of 1.0 ml/min.

Standard Solutions

A stock solution of alfuzosin hydrochloride was prepared by dissolving 10 mg of this compound in 10 ml of water. This solution could be stored at -20°C for over two weeks with no evidence of decomposition. Standard solutions, containing alfuzosin in the concentration range 2-150 ng/ml, were prepared by

diluting the stock solution with control human plasma. Calibration curve was obtained by plotting the peak-area of alfuzosin against the drug concentration.

Analysis of Samples

After injection of 50 µl of plasma sample into the clean-up column, which had been previously equilibrated with clean-up solvent (methanol-water 5:95, v/v), the column was washed for 1 min with this solvent at a flow-rate of 1.0 ml/min. The substance adsorbed on the clean-up column was then introduced into the analytical column with the analytical mobile phase, by switching the six-port valve to back-flush mode for 2 min. The six-port valve was then returned to its initial position. The analytical column was disengaged from the clean-up column, and the latter was equilibrated with clean-up solvent ready for the next injection. The separation was carried out with analytical solvent at a flow-rate of 1.0 ml/min, and the analysis was achieved by using the above calibration curve.

RESULTS AND DISCUSSION

Under the chromatographic conditions described, the alfuzosin peak is well resolved. Fig. 3 shows typical chromatograms of blank plasma, blank plasma spiked with alfuzosin, and plasma of a volunteer treated with alfuzosin. No endogenous component or metabolite was observed near the retention time corresponding to alfuzosin. The retention time for alfuzosin was 6.2 min. The equation obtained through regressional analysis of data for the above standard solutions was $y=6\cdot10^4 + 1.5\cdot10^4x$ with correlation coefficient $r=0.998$, where y= peak-area in the arbitrary units of the HP-3396-II system used and x=alfuzosin concentration (ng/ml). The assay was validated by analysing seven alfuzosin

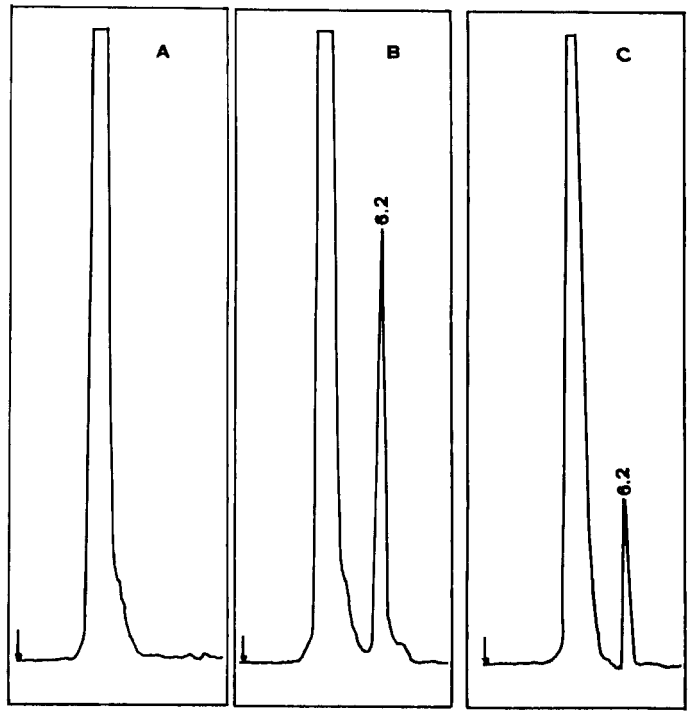

Figure 3 Chromatograms after column-switching: (A) Blank plasma; (B)Blank plasma spiked with alfuzosin (2.0 ng/ml); (C) Plasma of a volunteer treated with 5 mg of alfuzosin (4.4 ng/ml).

standards. Each datum was the average of a minimum of five determinations. The calibration curve for alfuzosin in human plasma was linear over the range 2.0 -150ng/ml. Reproducibilities for witin-day and between-day were evaluated to assess the precision and accuracy of this analytical method. The results are shown in Tables 1-2. The coefficients of variation (CVs) of the five independent samples at each concentration in the within-day assay were between 2.0 and 5.2% with relative errors (REs) of 2.1 -4.1% and in the between-day assay were

TABLE 1
Within - day precision and accuracy in the calibration standard of alfuzosin in human plasma.

Theoretical concentration (ng/ml)	Measured concentration* (ng/ml)	CV (%)	RE (%)
2.0	1.92±0.10	5.2	4.1
3.0	2.90±0.18	5.2	3.4
5.0	4.89±0.22	4.4	2.2
10	9.70±0.48	4.9	3.0
20	19.20±0.67	3.5	4.1
50	48.30±1.50	3.1	3.5
100	97.50±1.96	2.0	2.5
150	149±0.8	2.0	2.1

* Mean of five assays±SD; CV = Coefficient of Variation; RE = Relative Error.

TABLE 2
Between - day precision and accuracy in the determination of alfuzosin in human plasma

Theoretical concentration (ng/ml)	Measured concentration* (ng/ml)	CV (%)	RE (%)
2.0	1.92±0.64	3.3	3.7
3.0	2.84±0.12	2.8	3.4
5.0	4.95±0.05	2.1	2.0
10	9.7±0.04	4.1	3.1
20	19.50±0.70	3.6	2.5
50	49.15±1.50	3.0	2.7
100	98.30±1.30	3.3	2.7
150	148±1.70	4.2	3.4

*Mean of five assays±SD; CV = Coefficient of Variation; RE = Relative Error.

between 2.1 and 4.2% with relative errors of 2.0-3.7% in the concentration range 2.0-150ng/ml. Using a signal-to-noise ratio of 3, the detection limit of alfuzosin in human plasma was 1.0 ng/ml. The alfuzosin extraction efficiency, determined by comparing peak-area of plasma extracts versus the corresponding aqueous standards, was approximately 87%. This simple HPLC method should be of value for monitoring the alfuzosin concentration in plasma in patients, for assessing the patient compliance in assuming prescribed alfuzosin regimes and for examining the relationship between alfuzosin concentration in plasma and its efficacy in patients with benign prostatic hypertrophy. The HPLC method described in this paper is rapid, sensitive, and allows accurate and precise results, using a simple column switching extraction technique.

Acknowledgements

This research was supported by a grant from the Ministero dell'Università e della Ricerca Scientifica e Tecnologica (quota 40%), and the Consiglio Nazionale delle Ricerche.

REFERENCES

[1] A. H. Deering, J. G. Riddell, D.W.G. Harron, R.G. Shanks, *Br. J. Clin. Pharmacol.*, **25**: 417-424 (1988).

[2] M. G. Scott, A. H. Deering, M. T. McMahon, D. W. G. Harron, R. G. Shanks, *Eur. J. Clin. Pharmacol.*, **37**: 53-58 (1989).

[3] A. Jardin, H. Bensadoun, M. C. Delauche-Cavallier, P. Attali, *The Lancet*, **337**: 1457-1461 (1991).

[4] A. M. Krstulovic, *J. Pharm. Biomed. Anal.*, **6**: 641-656 (1988).

[5] A. M. Krstulovic, J. L. Vende, *Chirality*, **1**: 243-245 (1989).

[6] A. Rouchouse, M. Manoha, A. Durand, J. P. Thénot, *J. Chromatogr.*, **506**: 601-610 (1990).

[7] P. Guinebault, M. Broquaire, C. Colafranceschi, J. P. Thénot, *J. Chromatogr.*, **353**: 361-369 (1986).

Received: February 18, 1994
Accepted: June 20, 1994

JOURNAL OF LIQUID CHROMATOGRAPHY, 17(18), 3999-4017 (1994)

HPLC WITH FLUORESCENCE DETECTION FOR THE STUDY OF BENOMYL DISSIPATION ON TREATED LETTUCES

J. J. JIMÉNEZ[1], J. ATIENZA[1], AND J. L. BERNAL[2]

[1]*Agronomial Research Service*
Junta de Castilla y León
P.O. Box 172
E-47080 Valladolid, Spain

[2]*Department of Analytical Chemistry*
Faculty of Sciences
University of Valladolid
E-47005 Valladolid, Spain

ABSTRACT

Benomyl is determined as carbendazim by using an analytical procedure that involves a previous lyophilization of the sample, then an extraction with ethyl acetate and after that a liquid-liquid partition. Carbendazim is evaluated by reversed-phase high performance liquid chromatography with fluorescence detection. The degradation rate of benomyl added on lettuces grown in greenhouses is strongly dependent on the temperature, which stablishes the security times for their trading.

INTRODUCTION

Benomyl and carbendazim are two related fungicides widely used on fruits and vegetables. Several authors have assigned to both fungicides a carcinogenic and mutagenic activity [1, 2], so their maximum residual levels allowed on vegetables are regulated in many countries in order to avoid potential toxic hazards. In order to know these levels and also the duration from the fungicide addition to that moment in which the residue concentrations are under the allowed limit, it is necessary to carry on studies about their persistence and degradation. There are several works about this theme, studying particular aspects such as the low penetration of the fungicides in the pulp of refrigerated fruits such as pears [3] and apples [4]. Their residual levels and accumulation in monarda and peppermint aromatic oils [5], strawberries [6], blueberries [7], and fruits as peaches and apples [8] have also been studied. Benomyl and carbendazim residues were also determined in liquid samples: wine, grape juice and water [9-11].

In most of the papers mentioned above, benomyl, due to its quick degradation rate, is usually

determined as carbendazim, introducing an acid hydrolisis step on the analytical procedure. Such procedure usually has an extraction step with organic solvents, one or more liquid-liquid partitions and then a HPLC determination with ultraviolet or fluorescent detection [6, 7, 9], but they have also been proposed other non-chromatographic techniques such as fluorescence, spectrophotometry, differential pulse polarography and inmunoassay among others [12-19].

In this work the dissipation of benomyl on treated lettuces growing in greenhouse has been studied, trying to relate such dissipation with the temperature and with the intensity of fungicide treatment. To this aim, an ordinary clean-up procedure with HPLC-fluorescence detection, adecuated for evaluating high levels of carbendazim, has been used; it has also been included a previous step of lyophilization of the sample [20]. The suitability of the analytical procedure has been tested on fortified samples of lettuce and tomato. Some considerations about the mobile phase composition, the wavelength selection and the stability of benomyl in aqueous solution have been made.

EXPERIMENTAL

Reagents

Residue analysis grade ethyl acetate, methanol, and *n*-hexane, and HPLC grade acetonitrile were purchased from Panreac (Barcelona, Spain) and SDS (Peypin, France). Ultrapure water was supplied by a Milli-Q plus apparatus from Millipore (Milford, Ma). Benomyl and carbendazim certified purity standards were supplied by Promochem (Wesel, Germany). Hydrochloric acid and sodium hydroxide were obtained from Panreac, and cellulose powder from Aldrich (Steinheim, Germany).

Apparatus

Fluorescence measurements were made on a Perkin-Elmer LS-5 computer-controlled spectrofluorimeter (Norwalk, Co).

Lyophilization equipment, furnished with a vacuum pump and a freezing system, was purchaded from Telstar (Barcelona, Spain) .

Turbo-vap evaporator system furnished with a thermostated water bath and nitrogen sweeping was

obtained from Zymark (Hopkinton, Ma). Kokusan centrifuge (Tokyo, Japan), universal food cutters and mechanic stirrers were also employed.

Sample preparation

Prior to extraction, an amount of 100 g of vegetable sample (lettuce leaves or tomato pulp and peel) was minced and blended with 20 g of powdered cellulose. Optionally, a known volume of a benomyl solution was added for spiking the sample. The mixture was then homogenized by shaking and frozen at -35°C for subsequent lyophilization.

Extraction

A lyophilized vegetable sample (0.2-2 g) was extracted by mechanical stirring with 10 ml of ethyl acetate for 10 min. The mixture was then centrifuged at 3000 rpm for 5 min and the organic phase was collected. The solid residue was extracted with another 10 ml of ethyl acetate, stirring for 10 min, and the liquid phase separated through centrifugation. The two organic phases collected were mixed and treated with 5 ml of 0.01 M HCl. After

stirring for 5 min, 5 ml of 0.1 M NaOH were added. The resulting phases were separated by centrifugation and the lower aqueous layer was discarded. The organic phase was evaporated to dryness under a nitrogen stream at 40°C. The extract was dissolved by shaking in 2 ml of methanol and 5 ml of *n*-hexane. After separation, the methanol extract was collected, filtered through a PTFE filter (0.5 μm pore size) and analysed by HPLC.

HPLC system

The HPLC system consisted of a ConstaMetric 4100 quaternary pump, an AutoMetric 4100 autosampler, a membrane degasser and a SpectroMonitor 3200 UV-visible detector, all of which was supplied by LDC Analytical (Riviera Beach, Fl), in addition to a Waters 470 fluorescence detector (Milford, Ma). Data were acquired and processed by means of a computerized system.

The chromatographic conditions used for the determination of carbendazim in the lettuce extracts were as follows: 150 × 4.6 mm Spherisorb ODS-2 column from Phenomex (Torrance, Ca), acetonitrile-water 30:70 as mobile phase at a flow-rate of 1.5 ml/min,

injected volume: 25 μl, excitation and emission wavelengths for fluorescence detection: 285 and 317 nm, respectively. Carbendazim from tomato samples was eluted with acetonitrile-water 20:80 at a flow-rate of 1.5 ml/min. Benomyl was determined using acetonitrile-water 50:50 as mobile phase at a flow-rate 1 ml/min and UV detection at 220 nm. The chromatographic column and the mobile phase were both thermostated at 25°C.

RESULTS AND DISCUSSION

Stability of benomyl in solution

A preliminary study about the stability of benomyl in aqueous solution was carried out by HPLC with UV detection in order to determine its degradation rate. The experiment was performed with the commercially available formulation Benlate, a preparation containing 50% benomyl, from Du Pont de Nemours (Wilmington, De) and a certified standard, all of which gave rise to a degradation profile such as that shown in Fig. 1. Benomyl peak area decreased by 50% within 7 h after preparation and by 70% after 15 h. The degradation rate was somewhat higher in the first hours.

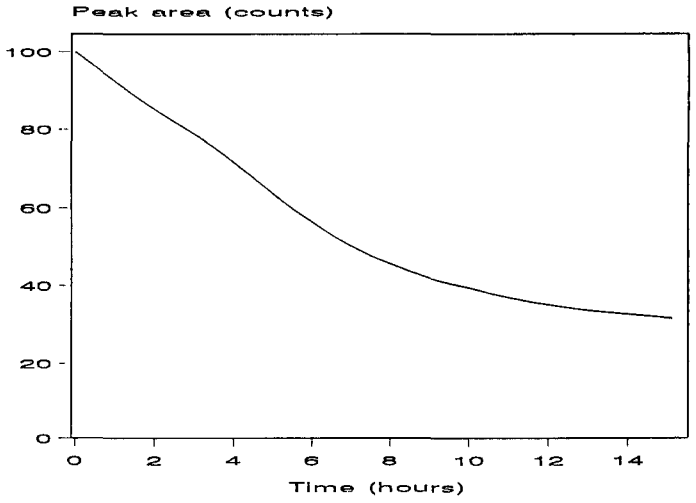

Figure 1: Degradation of benomyl in aqueous solution.

Since the degradation rate of benomyl is higher in organic solvents in relation to aqueous solutions [10, 21], laboratory determination is usually avoided. This led to evaluate the fungicide via its most common metabolite, carbendazim. The concentration of carbendazim analytically determined on vegetables will have two origins: the hydrolysis of benomyl and the carbendazim yielded by natural degradation under the prevailing environmental radiation, temperature and moisture conditions.

Selection of wavelengths

Figure 2 shows a three-dimensional representation, fluorescence intensity-excitation wavelength-emission wavelength, and its matching contour diagram for a methanol solution of carbendazim. The maximum fluorescence intensity was achieved at a excitation wavelength of 285 nm and a emission wavelength of 317 nm.

It is interesting to note that benomyl dissolved in methanol initially exhibits no fluorescence, only after a few hours a three-dimensional spectrum similar to that observed for carbendazim is obtained.

Analysis of fortified samples

Table 1 lists the results obtained by applying the extraction and clean-up procedure on fortified lettuce and tomato samples for proving the suitability of the method. The recoveries achieved for different matrices and fortification levels were all acceptable (above 95%), with a good relative standard deviation that ranged from to 3.3% to 3.8%.

The appropiate mobile phase varied as a function of the matrix due to the presence of different

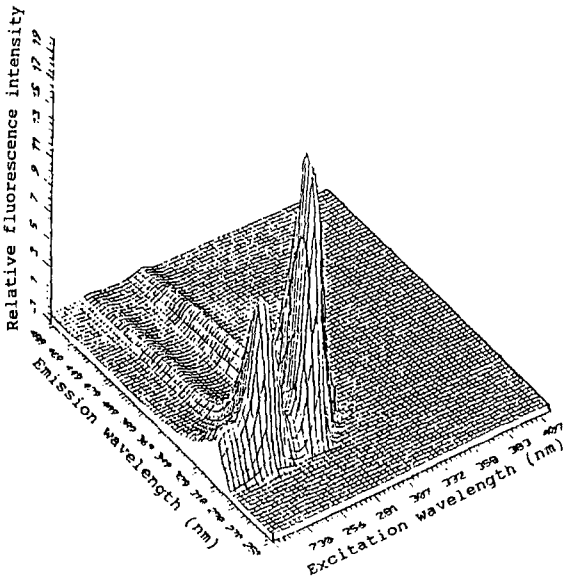

Tridimensional fluorescence spectrum

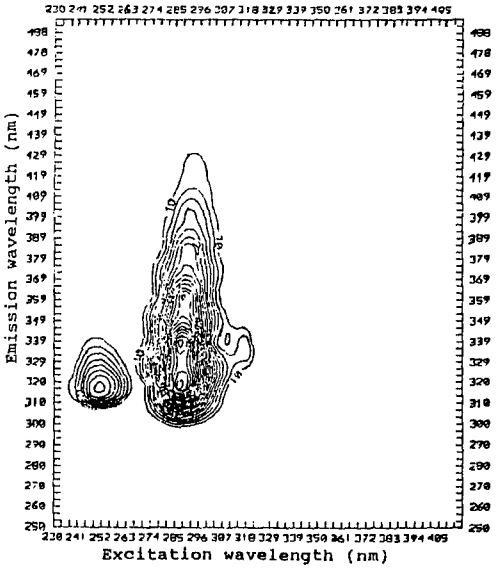

contour map

Figure 2: Tridimensional fluorescence spectrum and contour map of a carbendazim standard dissolved in methanol.

TABLE 1

Recovery (%) of benomyl on fortified vegetable samples (n=5). Lyophilized sample amount: 2 g.

SAMPLE	FORTIFICATION LEVEL (mg/Kg)	RECOVERY (%)	σ_{n-1}
Tomato	6.0	95.3	3.4
Tomato	0.3	97.4	3.8
Lettuce	6.0	96.5	3.5
Lettuce	0.3	99.6	3.9

σ_{n-1}: standard deviation

coextracted substances. No such substances were found in the lettuce extracts, which mobile phase yielded a peak for carbendazim at a retention time of 2.8 min. On the other hand, tomato extracts contained unknown compounds whose chromatographic peaks overlapped with that of carbendazim under the conditions used for the lettuce extracts. The chromatographic peaks were isolated by using a different mobile phase, the elution of carbendazim was delayed to 5.7 min (Figure 3). Table 2 lists the retention times for carbendazim obtained with mobile phases of different composition.

The detection limit of carbendazim provided by the fluorescence detector was obtained by successive dilutions of a standard and found to be 0.07 mg/l. In consequence, the detection limit for the lettuce

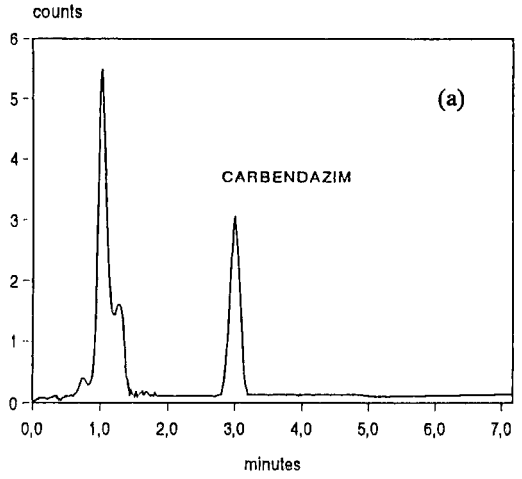

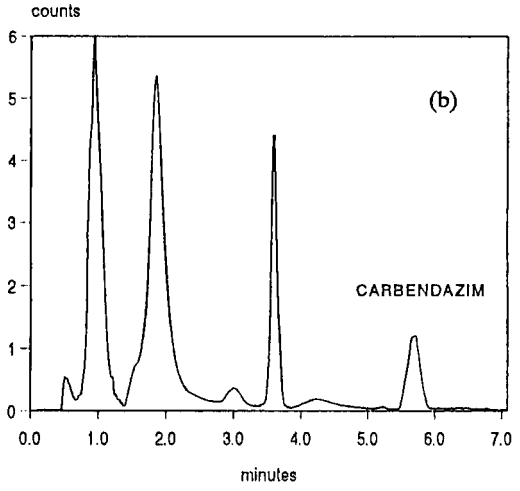

Figure 3: Chromatograms obtained by the proposed procedure.
3 a) Lettuce extract. Mobile phase: acetonitrile-water 30:70.
3 b) Tomato extract. Mobile phase: acetonitrile-water 20:80.

TABLE 2

Retention time (in minutes) of carbendazim on a 150 x 4.6 mm Spherisorb ODS-2 column. Flow-rate 1 ml/min.

ACN (%)	RETENTION TIME	
	ACN-WATER	ACN-BUFFER*
50	2.3	1.4
30	3.5	1.9
25	5.5	3.0
20	7.7	5.4

*Buffer: Na_2HPO_4/KH_2PO_4, 1/1 in volume, 0.03M each one.

samples was 0.03 mg/kg while the detection limit for the tomato analysis was somewhat higher, 0.05 mg/kg. Spanish legislation allows a maximum value of 5 mg/kg for leafy vegetables such as lettuces and 2 mg/kg for tomatoes, so the method complies with the legal limits for both products.

Dissipation of benomyl on lettuces

The above method has been applied to the determination of benomyl on greenhouse lettuce samples that were treated with a suspension (1 g/l) of Benlate, which was evenly spread on the vegetables.

Three randomly chosen individual lettuce heads were cut off at ground level, placed in plastic bags

and stored at -20°C in the dark, daily for 30 days.

The greenhouse was equipped with temperature sensors that allowed the average daily temperature to be known.

Figure 4 shows three dissipation curves of benomyl, in equivalent units of carbendazim, and the greenhouse temperature. As can be seen from one of the curves in the Fig. 4a, the initial concentration, 36.3 mg/kg, dropped off to 2.5 mg/kg in 30 days. The dissipation rate in the first week was quite low, in coincidence with prevailing low temperatures; later, the higher temperature seems to increase the dissipation rate. Finally, a virtually constant residual concentration is observed as a result of a slow dissipation rate observed although the high temperatures.

A similar behaviour was observed in the Fig. 4a, in the other experiment performed at similar temperatures and higher phytosanitary treatment intensity. The difference between the concentration levels of each experience decreased gradually, attaining a similar residual concentration, 2.5-3.0 mg/Kg, after 30 days.

As can be observed from Fig. 4b, the higher ambient temperature increased the dissipation rate.

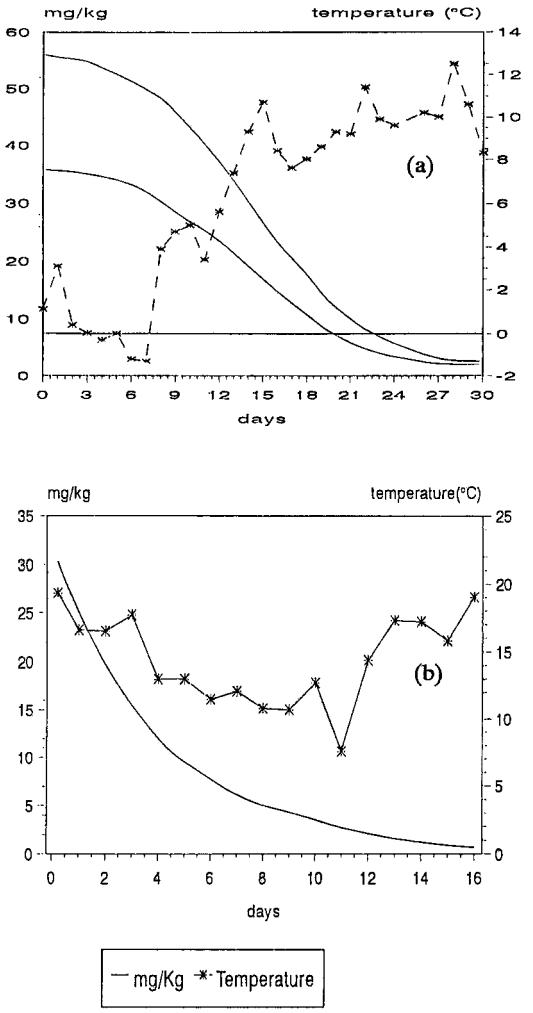

Figure 4: Dissipation of carbendazim on lettuces.
4 a) Low ambient temperature.
4 b) High ambient temperature.

In this case, the curve was not asymptotical in the first days after treatment; rather, the carbendazim concentration dropped off quickly from the beginning, from 30.3 to 0.7 mg/kg in 16 days.

The temperature can influence the dissipation rate in vegetables in two ways: through the dilution resulting from growth of the plant and through the rate of decay of the fungicide on the vegetable. Both are favoured by high temperatures.

On the basis of the maximum allowed carbendazim concentration (5 mg/kg), the vegetables studied would be fit for human consumption 22 and 24 days after treatment at low temperatures, and only 9 days after treatment at high temperatures. The interval of time for safe human consumption varies with the ambient temperature and the fungicide concentration used in the treatment.

CONCLUSIONS

The degradation rate of benomyl used on lettuces is strongly related to the environmental temperature, so higher is the temperature higher is the rate of degadation, which is very low at temperatures near 5 °C.

The degradation rate of benomyl is also affected by the intensity of fungicide treatment nevertheless its impact is lower than the temperature impact.

The use of lyophilizated sample simplifies the laboratory assays reducing the size of the necessary sample and the volume of organic solvents used.

ACKNOWLEDGEMENT

We thank to *Instituto Nacional de Investigaciones Agrarias* (project No 9075) for financial support.

REFERENCES

1.- J. Van Damme, B. de Ryckel and M. Galoux, J. Chromatogr., 518, 375-384 (1990).

2.- R. Wiles, "Regulating Pesticides in Food", in "The Delaney Paradox". National Academy Press, Washington DC, 1987, pp. 199.

3.- U. Kiigemagi, D.D. Inman, N.M. Mellenthin and M.L. Deinzer, J. Agric. Food Chem., 39, 400-403 (1991).

4.- A. Monico-Pifarre and M. Xirau-Vayreda, J. Assoc. Off. Anal. Chem., 70, 596-598 (1987).

5.- A. Bélanger, Acta-Horticulture, 249, 67-73 (1989).

6.- A. Monico-Pifarre and M. Xirau-Vayreda, J. Assoc. Off. Anal. Chem., 73, 553-556 (1990).

7.- R.J. Bushway, H.L. Hurst, J. Kugabalasooriar and L.B. Perkins, J. Chromatogr., 587, 321-324 (1991).

8.- C.H. Liu, G.C. Mattern, X. Yu and J.D. Rosen, J. Agric. Food Chem., 38, 167-171 (1990).

9.- C.H. Marvin, I.D. Brindle, R.P. Singh, C.D. Hall and M. Chiba, J. Chromatogr., 518, 242-249 (1990).

10.- C.H. Marvin, I.D. Brindle, C.D. Hall and M. Chiba, J. Chromatogr., 555, 147-155 (1991).

11.- C. Sánchez-Brunete, A. de Cal, P. Melgarejo and J.L. Tadeo, Int. J. Environ. Anal. Chem., 37, 35-43 (1989).

12.- X. Jiang and M. Ding, Fenxi Huaxue, 17, 823-825 (1989).

13.- F. García Sánchez and C. Cruces Blanco, Anal. Chem., 60, 323-328 (1988).

14.- J.R. Rangaswamy, Y.N. Vijayashankar and S.R. Prakash, J. Food Sci. Technol., 24, 309-310 (1987).

15.- P. Hernández, S. García and L. Hernández, Anal. Chem. Acta, 259, 325-331 (1992).

16.- L.F. López, A. G. López and M.V. Riba, J. Agric. Food Chem., 37, 684-687 (1989).

17.- R.J. Bushway, A.S. Savage and B.S. Ferguson, J. Agric. Food Chem., 35, 51-58 (1990).

18.- W.H. Newsome and P.G. Collins, J. Assoc. Off Anal. Chem., 70, 1025-1027 (1987).

19.- C. Bicchi, F. Belliardo, L. Cantamessa, G Gasparini, M. Icardi and E. Sesia, Pestic. Sci., 25, 355-360 (1989).

20.- J.J. Jiménez, J. Atienza, J.L. Bernal and L. Toribio, Chromatographia, 38, 395-399 (1994).

21.- R.P. Singh, I.D. Brindle, C.D. Hall and M. Chiba, J. Agric. Food Chem., 38, 1758-1762 (1990).

Received: February 15, 1994
Accepted: May 24, 1994

JOURNAL OF LIQUID CHROMATOGRAPHY, 17(18), 4019-4030 (1994)

RAPID ANALYSIS OF FREE AMINO ACIDS IN INFANT FOODS

M. L. ALONSO*[1], A. I. ALVAREZ[2], AND J. ZAPICO[2]
[1]*Dpto de Bioquímica*
B. M. y Fisiología
Facultad de Ciencia y Tecnología de los Alimentos
Burgos, Spain
[2]*Dpto Fisiología, Farmacología y Toxicología*
Universidad de León
León, Spain

ABSTRACT

A new approoch to the analysis of free amino acids from infant foods is described. The method is based on reaction of the free amino acids with phenylisothiocyanate to form stable derivatives which are subsequently separated by liquid chromatography. Sample preparation procedures are described. Separation of all amino acids using this method was completed in 20 min. This method was much faster than the traditional Ion-exchange methods (2-3 h). Variability of the method (expressed as coefficients of variation) for the determination (including preparation of samples, derivatization and liquid chromatography) of all amino acid was less than 10%.

INTRODUCTION

The used of phenylisothiocyanate (PITC, or Edman's reagent) for amino acid analysis was first described by Heinrickson and Meredith (1) and developed

* Dra. Mª Luisa Alonso: Author who correspondence would be addressed

commercially by Waters (Milford, MA) as the Pico-Tag method (2,3). In the Pico-Tag method, PITC is used for derivatization of amino acids. Reverse-phase gradient elution liquid chromatography is used to separate the phenylthiocarbamyl (PTC) derivatives (normally in less than 20 min), which are then detected by their UV absorbance at a 254 nm. The PITC derivatization method has been reported to be rapid, efficient, and reproducible and to provide results with most amino acids comparable to those obtained by conventional ion-exchange methods (4,5).

The PTC methodology was applied to the analysis of insulin β-chain, human insulin, trypsin and oxytocin (2,6) and has since been applied to several hundred proteins and peptides.

Applications of the PTC derivatization methodology are beginning to appear, such as the analysis of amino acid composition of low levels of growth factors isolated from bovine neural tissue (7), the characterization of angiogenin from human carcinoma cells (8,9). This method has been used to the determination of free amino acids in serum and other phisiological samples such as liver, brain and heart (10).

With some minor modifications in sample preparations and chromatography, the Pico-Tag method has been applied to the determination of amino acids in food matrixes (11,12,13).

EXPERIMENTAL

The Pico-Tag method for sample preparation and analysis was used (Liquid chromatografic analysis of aminoacids in foods using a modification of the Pico-Tag method, revision 1987, Millipore Corp.), with some modifications as described below.

Reagents and Apparatus

(a) Reagents.- Potasium hidroxide, sodium acetate trihydrate, glacial acetic acid, phosphoric acid and ethanol was obtained from Merck (Barcelona, Spain). Disodium hydrogen phosphate and perchloric acid was obtained from Panreac (Barcelona, Spain). All of them were of analytical-reagent grade. Acetonitrile and triethylamine (LC grade) were obtained from Scharlau (Barcelona, Spain).

Phenylisothiocyanate solution (PITC) (Protein sequencing grade) and amino acid standard were purchased from Sigma Chemical Co. (St. Louis, MO).

(b) Equipment.- High purity water generated by a Milli-Q-Water System from Millipore Corp. (Bedford, MA, USA) was used in the preparation of buffers and solutions.

An LC gradient system consisting of a ternary Model SP-8800 pump, a Spectra-physics multiwavelenght detector (Spectra-Chrom 200), a integrator Chromjet (Spectra-physics), a Rheodyne Model 7125 injector with 20 µl loop and a temperature control module was used.

Analyses was performed on a C_{18} Ultrabase (5µm particle size) reversed-phase column (25cm x 0.46cm I.D.) purchased from Scharlau (Barcelona, Spain).

Samples

The study was performed on prepared infant foods which were vacuum packed and are commercially called pots. Four varieties were analysed: vegetable, meat, fish and dessert with six different fruit. These products were supplied for Nestle, S.A. The amino acids content of the samples are shown in Table 1.

Preparation of Samples

Samples of 5 g were dissolved in 50 mL perchloric acid 0.6N, homogeinized in Sorvall. The mixture was then centrifuged at 3500 r.p.m. for 20 min. After that, the supernadant was filtered through a 0.45 mm filter (Millex-GS Millipore) and pH was adjustment with potasium hidroxide (30%) to 7.0 ± 0.2 measured with a pHmeter (CRISON micropH 2001). The filtered was placed the fridge for 5 min. The extracts obtained were frozen for later analysis by HPLC, prior to the measuring of the volume.

Derivatization of Amino Acids with PITC

Extract (1mL) was evaporated to dryness at 37 °C under liquid nitrogen. The derivatizing solution was prepared just before use, by mixing 70 µL ethanol, 10µL water, 10 µL TEA and 10 µL PITC obtained from Sigma Chemical Co. All amino

TABLE 1
Values obtained from Manufacturer

Amino acid	Vegetable	Meat	Fish	Fruit
Asp	225	100	230	115
Glu	265	500	370	105
Ser	90	90	110	30
Gly	70	90	80	35
His	40	100	60	25
Arg	120	190	130	45
Thr	70	140	100	25
Ala	85	136	110	40
Pro	35	140	20	35
Tyr	50	80	90	20
Val	90	75	30	35
Met	20	80	50	15
Cys	15	25	20	10
Ile	75	100	110	25
Leu	130	125	80	45
Phe	85	140	90	30
Trp	25	40	30	10
Lys	120	250	190	35

acids were derivatizing by adding 20 μL derivatizing solution. The samples were mixed, and the tubes were covered with Parafilm and let to stand for 20 min at room temperature (18 ± 1 °C) for completion of derivatization. The excess reagent was evaporated under liquid nitrogen at 37 °C. The residual which corresponds to derivatized dried samples was redissolved in 200 μL sample diluent. This diluent was prepared by dissolving 710 mg disodium hydrogen phosphate in 1 L of mixed water-acetonitrile (19+1) and by adjusting the pH to 7.40 with phosphoric acid. Finally, 20 μL of sample was then injected into the chromatographic system.

Chromatography

The LC procedures are briefly outline below.

(a) Solvents- Solvent A was prepared by mixing 19 g sodium acetate trihydrate in 1 L water. To this solution 500μL TEA was added. The pH was then adjusted to 6.40 with glacial acetic acid. Finally, 760 mL of this solution was mixing with 60 mL pure acetonitrile.

Solvent B was prepared by adding 600mL acetonitrile to 400mL water followed by mixing and degassing.

Both solvents were degassed in a ultrasonic bath (Sonorex), and filtered using a vacuum pump through 0.45 mash filters (Millipore)

(b) Gradient conditions.-The gradient conditions used are shown in Table 2.

Column temperature was maintained at 38±1 °C. The detection was at 254 nm.

Calculations.

The amounts of free amino acids in the pots were calculated using peak area values. These values yielded concentration values by applying calibration curves obtained from known amino acid concentration.

RESULTS AND DISCUSSION

Four infant formulas (vegetables, meat, fish and fruits) were analyzed using the LC methods described in this report. This method allowed for the separation of essential amino acids.

The amino acid elution profiles of samples of vegetables, meat, fish and fruits are shown in Figures 1, 2, 3 and 4, respectively. In general, all amino acids were satisfactorily resolved and the separation was completed in 20 min.

The gradient shape was chosen to optimize the spacing of the separated peaks in the minimun analysis time.

Normally, hydrolyzed samples are redried with methanol-water-TEA before derivatization (4, 14). Other researches only used methanol for redrying since the use of methanol-water-TEA result in the loss of ammonia (13). But in this work, once the samples were evaporated to dryness, they were resuspended into the derivatization reagent.

Moreover, the commonly used composition of the derivatization reagent (methanol-TEA-water-PITC, 7+1+1+1) (4, 10, 13) was modified (ethanol-TEA-water-PITC, 7+1+1+1) because the resolution of amino acids obtained was better. The resolution of Ser/Gly obtained in this investigation was significantly better than that reported by other authors (10,15).

Lavi et al (16) reported some difficulty in determing lysine, threonine, cysteine and histidine by derivatization with PITC and separation of the derivatized amino

TABLE 2
Gradient Table. The gradient was lineal in all cases.

Time (min)	A(%)	B(%)	Flow (ml/min)
0	100	0	1.00
14.5	54	46	1.00
15.0	0	100	1.00
17.0	100	0	1.50
20.0	100	0	1.50
20.5	100	0	1.00

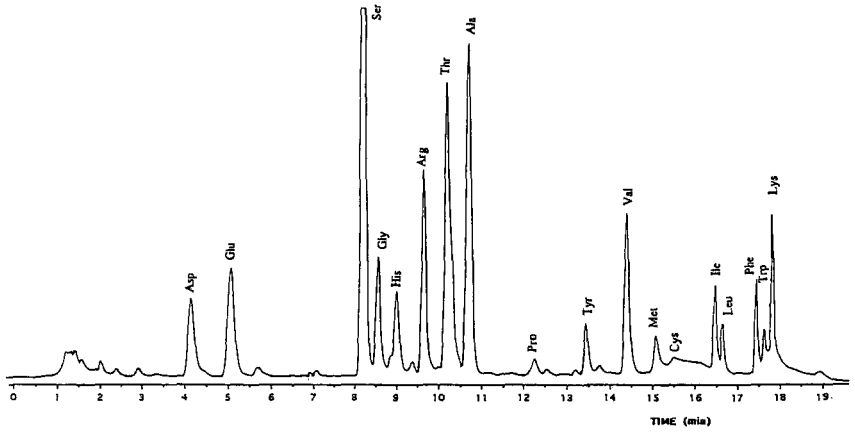

FIGURE 1. Elution profile of vegetable sample showing resolution of PTC-amino acids by liquid chromatography

acids by reverse-phase chromatography. These researches (16) used methanol as deproteinization agents which have been reported (3) to cause considerable losses and reduced yield of many PTC-amino acids. More recently, ultrafiltration has been used for deproteinizing samples prior to analysis by liquid chromatography and selection of appropiate membrane are important in recoveries obtained of 90% or more (10).

Although the resolution of Cys was not ideal, it was adequate for the calculation of this amino acid in most samples.

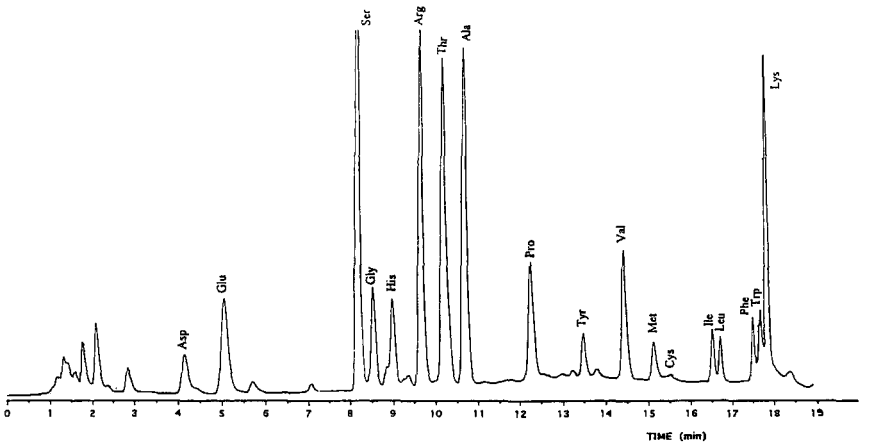

FIGURE 2.-Elution profile of meat sample showing resolution of PTC-amino acids by liquid chromatography

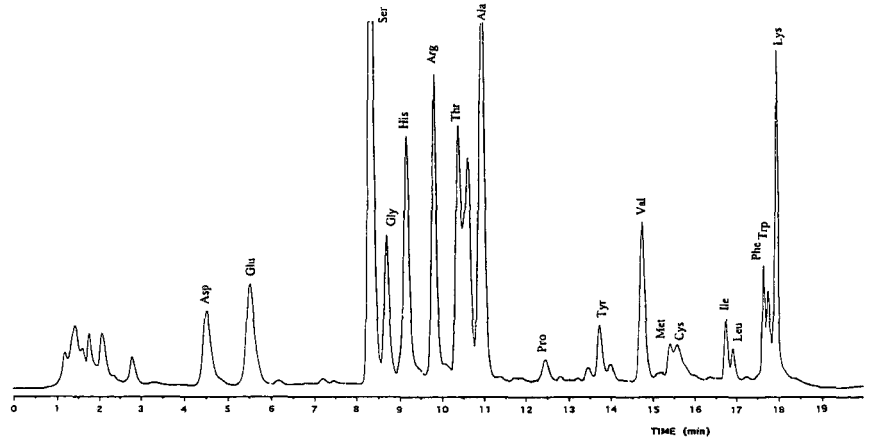

FIGURE 3.- Elution profile of fish sample showing resolution of PTC-amino acids by liquid chromatography

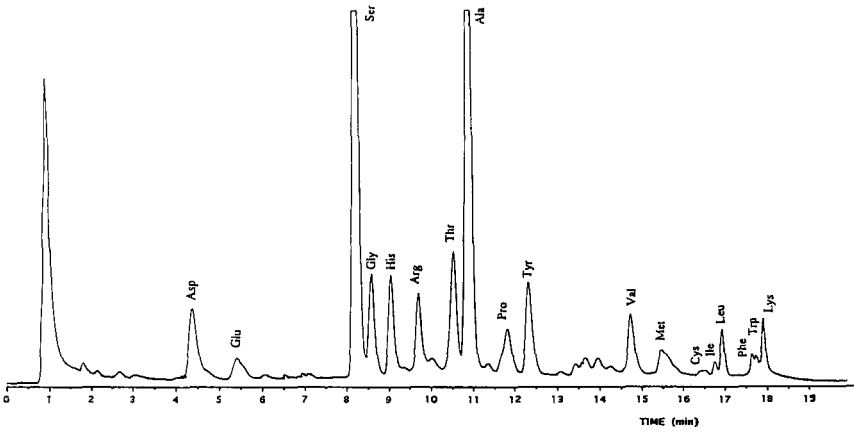

FIGURE 4.- Elution profile of dessert sample showing resolution of PTC-amino acids by liquid chromatography .

Three samples of each infant food were analyzed to estimate the variation of the liquid chromathography method. Moreover, three replicates of the sample extract were analyzed to estimate the variation of the chromatography. The reproducibility data for each sample are shown in table 3, 4, 5 and 6. The variability expressed as coefficient of variation (CV) of the entire analytical procedure, including extraction, derivatization and chromatography, for all amino acids was less than 10%. Variability was highest for cysteine (Cys), tyrosine (Tyr), threonini (Thr) and lysine (Lys) (although never greater than 10% CV).

The coefficient of variation of the entire analytical procedure indicate this method seem to be very precise for amino acid analysis in infant foods. These experimental results can not be compared to those by other authors since research into similar products has not been found in bibliography. Only, Grün et al (17) give lysine values for baby vegetable and beef foods between 173.1-246.4 mg lysine/ 100 g of food and between 24.7-13.7 mg lysine/ 100 g of food for banana samples. The lysine content of baby food samples was determined by Grün et al (17) by using a trinitrobenzenesulfonic acid (TNBS) method, adapted from Hall et al (18). Trinitrophenillysine was measured spectrophotometrically at 415 nm.

TABLE 3

Means and Coefficients of Variation (CV) of Amino Acids in Vegetable Samples determined by LC Methods

Amino acid	Concentration found[a]	CV(%)[b]
Asp	220.39±10.30	4.67
Glu	360.34±5.90	1.91
Ser	91.62±3.65	3.98
Gly	70.92±2.46	4.17
His	80.27±3.59	4.47
Arg	79.46±2.07	2.60
Thr	62.31±3.29	5.28
Ala	76.91±3.32	4.32
Pro	19.12±1.12	5.86
Tyr	63.03±3.49	5.53
Val	66.88±3.40	5.08
Met	38.64±2.04	5.28
Cys	11.38±0.78	6.75
Ile	115.02±2.40	2.09
Leu	83.34±1.93	2.32
Phe	144.17±2.90	2.01
Trp	39.39±1.77	4.49
Lys	81.57±7.85	9.62

[a]Mean ± S.D. (n=6)

[b]Coefficient of variation

TABLE 4

Means and Coefficients of Variation (CV) of Amino Acids in Meat Samples determined by LC Methods

Amino acid	Concentration found[a]	CV(%)[b]
Asp	137.77±7.16	5.19
Glu	351.54±12.75	3.63
Ser	56.65±2.92	5.15
Gly	67.35±3.28	4.87
His	85.36±2.21	2.59
Arg	140.12±5.62	4.01
Thr	65.45±3.43	5.24
Ala	96.40±4.25	4.41
Pro	138.61±5.68	4.09
Tyr	53.19±3.16	5.95
Val	46.34±2.11	4.55
Met	45.27±2.36	5.21
Cys	7.22±0.35	4.85
Ile	64.41±2.02	3.14
Leu	65.44±3.04	4.65
Phe	92.77±2.55	2.75
Trp	60.18±2.91	4.83
Lys	317.07±16.12	5.09

[a]Mean ± S.D. (n=6)

[b]Coefficient of variation

TABLE 5

Means and Coefficients of Variation (CV) of Amino Acids in Fish Samples determined by LC Methods

Amino acid	Cocentration found[a]	CV(%)[b]
Asp	234.60±9.88	4.21
Glu	271.78±15.73	5.79
Ser	110.69±3.72	3.36
Gly	80.33±3.84	4.79
His	126.96±3.95	3.11
Arg	131.13±1.61	1.23
Thr	57.50±3.75	6.52
Ala	122.58±7.32	5.97
Pro	22.11±1.21	5.47
Tyr	65.44±2.60	3.97
Val	52.72±2.27	4.30
Met	40.89±2.26	5.52
Cys	5.21±0.13	2.49
Ile	84.14±2.23	2.65
Leu	43.05±1.41	3.27
Phe	160.37±4.05	2.52
Trp	78.92±3.96	5.02
Lys	214.94±8.69	4.04

[a]Mean ± S.D. (n=6)

[b]Coefficient of variation

TABLE 6

Means and Coefficients of Variation (CV) of Amino Acids in dessert with six different Fruit Samples determined by LC Methods

Amino acid	Concentration found[a]	CV(%)[b]
Asp	103.13±3.87	3.75
Glu	45.62±1.27	2.79
Ser	29.35±1.34	4.56
Gly	28.14±1.22	4.33
His	54.96±2.06	3.75
Arg	19.08±0.90	4.72
Thr	10.25±0.36	3.51
Ala	68.19±3.15	4.62
Pro	32.06±1.16	3.62
Tyr	11.15±0.86	7.71
Val	13.79±0.47	3.41
Met	17.37±0.73	4.20
Cys	5.07±0.21	4.14
Ile	12.24±0.24	1.96
Leu	39.91±1.97	4.94
Phe	19.60±0.87	4.44
Trp	10.05±0.19	1.89
Lys	24.74±1.34	5.44

[a]Mean ± S.D. (n=6)

[b]Coefficient of variation

Amino acids values obtained for us agree well with the values supplied from manufacturer (Table 1).

Other authors have reported PTC-amino acid method agree well with those from the ion-exchange analysis for different foods (4,13).

CONCLUSIONS

This liquid chromatographic method reported in the present study can be used for accurate, rapid (20 min) and reproducible determination of most nutritionally important amino acids in this foods including tryptophan.. Moreover, this method can be used for rapid determination of available lysine.

ACKNOWLEDGMENT

The authors are indebted to the Comision Interministerial de Ciencia y Tecnologia (project ALI88-0103) for financial support.

We are grateful to NESTLE, S.A. for the supply of samples.

REFERENCES

(1) Heinrickson, R.L., & Meredith, S.C., Anal. Biochem, 136, 65, 1984.

(2) Bidlingmeyer, B.A., Cohen, S.A., & Tarvin, T.L., J. Chromatogr., 336, 93, 1984.

(3) Cohen, S.A., Tarvin, T.L., & Bidlingmeyer, B.A., Am. Lab., 16, 48, 1984.

(4) Bidlingmeyer, B.A., Cohen, S.A., Tarvin, T.L., & Frost, B. J., Assoc. Off. Anal. Chem., 70, 241, 1987.

(5) White, J.A., Hart, R.J., & Fry, J.C. J.,Automatic Chem., 8, 170, 1986.

(6) Bidlingmeyer, B.A., Cohen, S.A., & Tarvin, T.L., Int. Symp. HPLC Biol. Sci., Meibourne, Australia, 20, 1984..

(7) Lobb, R.R., & Fett, J.W., Biochemistry 23, 6296, 1984.

(8) Fett, J.W., Strydom, D.J., Lobb, R.R., Alderman, E.M., Bethune, J.L., Riordan, J.F., & Vallee, B.L., Biochemistry, 24, 5480, 1985.

(9) Strydom, D.J., Fett, J.W., Lobb, R.R., Alderman, E.M., Bethune, J.L., Riordan, J.F., & Vallee, B.L., Biochemistry,24, 5486, 1985.

(10) Sarwar, G., & Botting, H.G., J. Assoc. Off. Anal. Chem., 73, 470, 1990.

(11) White, J.A., Hart, R.J., & Fry, J.C., J. Auto. Chem,. 8, 170, 1986.

(12) Elkin, R.G., & Wasynczuk, A.M., Cereal Chem,. 64, 226,1987.

(13) Sarwar, G., Botting, H.G., & Peace, R.W., J. Assoc. Off. Anal. Chem., 71, 1172,1988.

(14) Beaver, R.W.; Wilson, D.M.; Jones, H.M. & Haydon, K.D., J. Assoc. Off. Anal. Chem., 70, 241, 1987.

(15) Early, R.J., & Ball, R.O. J., Anal. Purifications, 2, 47, 1987.

(16) Lavi, L.E., & Holcenberg, J.S., J. Chromatogr., 377, 155, 1986.

(17) Grün, I.U., Barbeau, W.E., Mc Chrisley, B. & Driskell, J.A., J. Agric. Food Chem., 39, 102, 1991.

(18) Hall, R.J., Trinder, N. & Wood, M.R., Analyst, 100, 68, 1975.

Received: February 10, 1994
Accepted: June 20, 1994

JOURNAL OF LIQUID CHROMATOGRAPHY, 17(18), 4031-4056 (1994)

CHARACTERIZATION OF BRANCHING-CHARACTERISTICS OF STARCH-GLUCANS BY MEANS OF COMBINED APPLICATION OF COMPLEXATION, ENZYMATICALLY CATALYZED MODIFICATION, AND LIQUID-CHROMATOGRAPHY

A. HUBER[1] AND W. PRAZNIK[2]
[1]*Institut für Physikalische Chemie*
KF-Universität
Heinrichstrasse 28
A-8010 Graz, Austria
[2]*Institut für Chemie*
Universität für Bodenkultur
Gregor-Mendelstrasse 33
A-1180 Vienna, Austria

ABSTRACT

Molecular characteristics, especially the branching-structure, of glucans from starch granules isolated from tubers of potato species Ukomo are determined. Granule-fraction with different mean-diameters are provided by sedimentation as inital separation step for further investigations. Then aqueous/DMSO dissolved starch glucans were separated into a non-branched/long-chain-branched and a short-chain-branched fraction by precipitation with n-butanol and methanol, respectively. By means of preparative SEC glucan pools of these fractions were collected and as well analyzed by means of methylation/GC-MS as checked for their individual potential to complex with polyiodide anions. Additionally equivaalents of these fractions were debranched by the catalytic action of pullulanase to determine the constituting glucan chain distribution by means of analytical SEC. Results of branching characteristics in terms of average number of monomers between two adjacent branching positions (bp→bp), average

percentage of branching (b%) and E_{640}/E_{525}(nb/lcb / scb)-ratio from different techniques are in good agreement and yield significantly different values for glucans from large and small starch-granules.

INTRODUCTION

Multiple and superimposed heterogeneity is a basic quality of polymers[1], especially of biopolymers like polysaccharides[2,3]. Properties such as monomer composition, molecular weight (degree of polymerization) and branching-characteristics are examples for molecular properties which are controlling macroscopic material qualities. For this reason there is a strong effort to determine appropriate parameters at the molecular level to get reliable selection- and processing-critera[4,5]. Strategies to gain such characteristic parameters include purification of the material of interest without artefacts and the application of separation-techniques combined with suitable methods for identification and quantification[6,7,8]. Due to the fact that polymers show a range of distributions, separation-techniques are a most proper tool to increase the quality of information because they enable access onto the range and shape of distributions, whereas only average values can be achieved from bulk-characterizations[9,10]. But also the actually applied mode of separation has to be selected solemnly, stongly depends on the parameter of interest, and either is ΔH- or ΔS-controlled considering that any separation is attained by energy-differences in terms of delta Free Enthalpy (ΔG) which includes as well Enthalpy-(ΔH) as Entropy-($T\Delta S$) contributions. Generally, entropy-controlled ($\Delta H \rightarrow 0$) separation techniques enable the determination of size-/shape-distributions, whereas enthalpy-controlled ($\Delta H >> T\Delta S$) techniques, even refered as non-exclusion techniques, are applied to achieve distributions according to different chemical potentials ($\Delta\mu$)[11].

A key-subject in the analysis of biopolymers is the dependence of material-characteristics on the history of particle-genesis, on specific catalytic mechanisms

and on the influence of global (environmental) conditions[12,13]. The actual studies deal with this topic by investigating molecular characteristics, especially the branching-structure, of different fractions of potato-starch which will be determined by means of combined application of several preparative and analytical separation-steps, modification-procedures, complexation/precipitation-techniques and extended data analysis. Therefore starch granules from tubers of potato species Ukomo got fractionated yielding two initial pools of particles with different mean-diameter. Both granule-fractions were dissolved in aqueous DMSO and splitted into a non-branched/long-chain-branched and a short-chain-branched glucan fraction by precipitation with n-butanol and methanol, respectively. Preparative SEC of each of these four glucan-species provided glucan-pools which were enzymatically debranched and yielded the constituting glucan-chain distributions. Analysis of these hydrolization-products was performed by means of analytical SEC and included transformation of mass distribution into number distribution of molecular weights as an essential procedure.

MATERIALS AND METHODS

Starch

Starch granules were purified from ripe tubers of potato species Ukomo. The tubers were washed, peeled, smashed and suspended in pure water. The slurry was sieved to separate the starch components from fibers and then got centrifuged to remove water soluble components with the supernatant.

Sedimentation

For the pooling of starch granules according to their size the aqueous starch-slurry was applied at the top of a water-filled column (ID=63 mm, l=340 mm). Separation was achieved by different sedimentation times (t_s) of large (t_s: short) and small (t_s: long) particles. Fractions of decreasing particle size

were collected, a specimen of large granules (Fr.I: t_s=2-5 min) and another one of small granules (Fr.II: t_s>30 min) were utilized for further investigations.

Dissolution

Starch particles from different pools were dissolved in 90% aqueous DMSO with a concentration of 1% (wt/v). Dissolution was completed by stirring over night at 70°C. Clear solutions were obtained either immediately or after centrifugation (3000 rpm, 15 min). Analysis of the non-dissolved residues proved to be non-starchy materials. Dissolution of starch in DMSO, different to aqueous sodium hydroxid, represented an essential purification step because accompanying proteins and lipids were insoluble. DMSO dissolved starch samples could be stored for several weeks without significant aging-effects such as degradation, aggregation or retrogradation.

Precipitation

Fractionation of native starch into non-branched/long-chain-branched (nb/lcb) and short-chain -branched (scb) components was achieved by complexation of aqueous DMSO dissolved starch with n-butanol: nb/lcb glucans were precipitated, whereas the scb components remained in solution[14]. 450 ml of an aqueous 0.15% (wt./v) NaCl-solution was added to 100 ml of the 1% (wt./v) DMSO-starch-solution and mixed 10:1 with n-butanol. This solution was stored 2 days at 4°C and the resulting precipitate was centrifuged, washed with methanol, dried in vacuum and yielded a dry white powder. The scb-starch fraction which remained in the supernatant after the n-butanol complexation can be precipitated by adding an excess of methanol, i.e. by mixing 1:4 with methanol and storing over night at 4°C. This precipitate was centrifuged, washed two times with methanol and dried in vacuum. As well the nb/lcb-glucan-fraction as the scb-fraction easily can be redissolved in 90% aqueous DMSO for further investigations.

Staining:

Total carbohydrates in the eluate from the semi-preparative SEC-system have been determined by mixing 1 ml of the sample solution with 2 ml anthron reagent (200 mg cristalline anthron p.A. dissolved in 100 ml H_2SO_4 96 % p.A.) and heating the mixture for 10 min in a boiling water bath. After cooling the solution and degassing it by means of ultrasound, absorption at 540 nm has been measured and the concentration of total carbohydrates is read from a calibration curve obtained from D-glucose[15,16].

For the determination of nb/lcb- and scb-glucan-complexes with polyiodide anions 125 mg freshly sublimated iodine was dissolved in the presence of 400 mg potassium iodide in 1000 ml demineralized water and diluted 1:1 with 0.1 M acidic acid to ensure a final pH between 4.5 and 5 when mixed with the alkaline eluate from size-exclusion chromatography. λ_{max} for the iodine-glucan-complex is known to depend on both, the degree of polymerization (dp) and the branching structure of the glucan chains: at wavelengths above 600 nm nb/lcb-glucans give strong absorption (the typical blue amylose colour), below 600 nm the scb-glucans are absorbing (the typical violett amylopectin colour)[17,18]. Best results were obtained by vis-detection at 640 nm (nb/lcb) and 525 nm (scb), respectively. The reliability of the detection of scb-glucan-iodine-complexes at 525 nm is supported by the corresponding maxima in ORD/CD-spectra for α1-4-glucan-chains with dp-values smaller than 40[19,20].

Vis-absorption was detected by means of a Spectrophotometer 550, Perkin-Elmer/UK.

Methylation/GC-MS-analysis

Methylation/GC-MS-analysis was applied to the starch samples for the determination of branching characteristics[21]. Therefore aqueous/DMSO-dissolved starch was mixed with solid sodium-hydroxide and methyljodid. After shaking with chloroform, the organic phase got dried and the procedure performed a second time to ensure total methylation. For GC-MS-analysis the glucans were

hydrolized with trifluoroacidic acid, reduced with Na BH_4 and acetylated with acidic acid anhydrid.

Such treatment yields reaction products from starch-glucans with different retention-times at GC-MS-analysis, depending on the kind of monomer: glucose from the non-reducing end → 1,5-di-O-Ac 2,3,4,6-tetra-O-Me-D-sorbit, α1-4-linked glucose within the polymer-chain → 1,4,5-tri-O-Ac 2,3,6-tri-O-Me-D-sorbit and α1-4 linked glucose with α1-6-linked branches → 1,4,5,6-tetra-O-Ac 2,3-di-O-Me-D-sorbit[22].

Enzymatically catalized debranching

For the enzymatically supported branching analysis the starch-samples were dissolved in DMSO and diluted 1:2 with aqueous buffer and mixed with aqueous pullulanase-solution (purified NOVO Promozym 200 L, Novo, DK; EC 3.2.1.41), an alternative approach to the application of isoamylase[23,24]. Debranching action was performed for 48 h at 37°C with additional incubation of pullulanase after 24 h to ensure total hydrolysis of α1-6-glycosidic linkages.

Size-exclusion Chromatography

For **preparative SEC** a series of two columns S-1000 Superfine (l=850 mm, ID=16 mm, $M_{excl}=10^8$ g mol^{-1}) and S-200 Superfine (l=940 mm, ID=16 mm, $M_{excl}=10^5$ g mol^{-1}) with 0.005 N Na OH and a flow rate of 1.6 m min^{-1} were utilized.

For **semipreparative/analytical SEC of native glucan** samples a Sephacryl-system consisting of a S-1000 Superfine column (l=1290 mm, ID=16 mm, $M_{excl}=10^8$ g mol^{-1}), a S-400 Superfine column (l=900 mm, ID=16 mm, $M_{excl}=10^6$ g mol^{-1}) and a S-200 Superfine column (l=940 mm, ID=16 mm, $M_{excl}=10^5$ g mol^{-1}) were utilized in series with 0.005 N Na OH as eluent at a flow rate of 0.75 ml min^{-1}.

For **analytical SEC of debranched glucan-chains** a system of Superose 6 TM (Pharmacia, Uppsala/S) (l=290 mm, ID=10 mm, $M_{excl}=5.10^6$ g mol^{-1}),

Fractogel (Merck, Darmstadt/FRG) HW50 S (l=290 mm, ID=10 mm, M_{excl}=20 000 g mol^{-1}) and HW40 S (l=290 mm,ID=10 mm,M_{excl}=7000 g mol^{-1}) were utilized with 0.05 M KCl as eluent at a flow rate of 0.6 ml min^{-1}.

Mass of eluted glucans was detected by a differential refractometer R503, Waters/UK. Fractions for iodine and anthron staining were collected with a fraction collector Ultrorac type 7000, LKB/UK.

Branching Analysis

A well working technique to check the branching characteristics of glucans is their enzymatic debranching, that means selective hydrolysis of α1-6-glycosidic linkages combined with succeeding SEC-separation and analysis of the resulting glucan-chain distribution. Detection of SEC-separated glucan chains by means of a differential refractive index detector initially yields the mass-distribution (w(M)) which has to be transformed into number distribution (n(M)) for branching analysis in terms of percentage of branching positions within a glucan (b%) and an average number of monomers between two adjacent branching points (bp→bp). Transformation of mass distribution (w(M): eq.(1a)) into number distribution (n(M): eq.(1b)) can be achieved according eq.(1a), eq.(1b) and eq.(2)[25], where N(M) is defined as the number fraction, W(M) as the weight fraction of molecules in the molecular weight range dM.

(1a) $$n(M) = \frac{d\,N(M)}{dM}$$

(1b) $$w(M) = \frac{d\,W(M)}{dM}$$

(2) $$n(M) = \frac{w(M)}{M}$$

In the analysis of the n(M)-functions up to three peaks in the differential number distribution (Mp_I, Mp_II, Mp_III) were taken as representative glucan-chain

populations. Contributions for the different populations were estimated corresponding to their approximate percentage of area (n%_I, n%_II, n%_III) in the n(M)-function. An average number of monomers between two adjacent branching points (bp→bp) can be calculated according eq.(3) with i=I, II, III:

$$bp \rightarrow bp = \frac{\sum_i dp_{(Mp)_i} \cdot n\%_i}{100} \quad (3)$$

Introducing an norm-glucan with a reference degree of polymerization of $ref_{dp}=1000$, an average number of branching points within such a glucan with ref_{dp} (av_b) can be calculated according eq.(4):

$$av\_b = \frac{ref_{dp}}{bp \rightarrow bp} \quad (4)$$

Application of eq.(5) yields an average percentage of branching (b%) for a glucan with $dp=ref_{dp}$ yielding an average percentage of monomers with branching positions:

$$b\% = \frac{av\_b \cdot 100}{ref_{dp}} \quad (5)$$

RESULTS AND DISCUSSION

Starch-glucans from tubers of potato species Ukomo were investigated for their branching-chararacteristics by applying a range of separation-, identification- and quantification-methods (Table 1). The main topic of interest was the question whether granules with different biological history contain glucans with different branching-structure, and if so, can these dissimilarities be specified. For starch, in a first approach, different biological history was set identical with different

TABLE 1

Applied Techniques and Methods for the Characterization of Starch-glucans from Tubers of Potato Species Ukomo.

Method	Glucan -Fractions applied analytical techniques / glucan-component			
sedimentation	Fraction I: Fr.I		Fraction II: Fr.II	
preparative SEC: iodine-staining anthron-staining	**Iodine-staining:** E_{640} nb/lcb-quantification E_{525} scb-quantification E_{640}/E_{525} starch composition **Anthron-Chromogen:** E_{550} total carbohydrates		**Iodine-staining:** E_{640} nb/lcb-quantification E_{525} scb-quantification E_{640}/E_{525} starch composition **Anthron-Chromogen:** E_{550} total carbohydrates	
precipitation	**n-butanol:** Fr.Ibut	**methanol:** Fr.Imet	**n-butanol:** Fr.IIbut	**methanol:** Fr.IImet
preparative SEC-pools: enzymatically catalized debranching	Fr.Ibut_a	Fr.Imet_a	Fr.IIbut_a	Fr.IImet_a
	Fr.Ibut_b	Fr.Imet_b	Fr.IIbut_b	Fr.IImet_b
	Fr.Ibut_c	Fr.Imet_c	Fr.IIbut_c	Fr.IImet_c
analysis	**de-branching:** pullulanase catalyzed hydrolysis of α1-6-glycosidic linkages **iodine-staining:** E_{640} non-branched/long-chain branched glucan-quantification E_{525} short-chain branched (scb) glucan quantification E_{640}/E_{525} starch composition: (nb/lcb / scb)-ratio **anthron-chromogen:** E_{550} total carbohydrates after acid-catalized total-hydrolysis **analytical SEC:** molecular weight distribution: weight w(M) → number n(M) **branching analysis:** average number of branching points within dp=ref_{dp}: av_b percentage of branching points within dp=ref_{dp}: b% average number of monomers between adjacent bp: bp→bp			

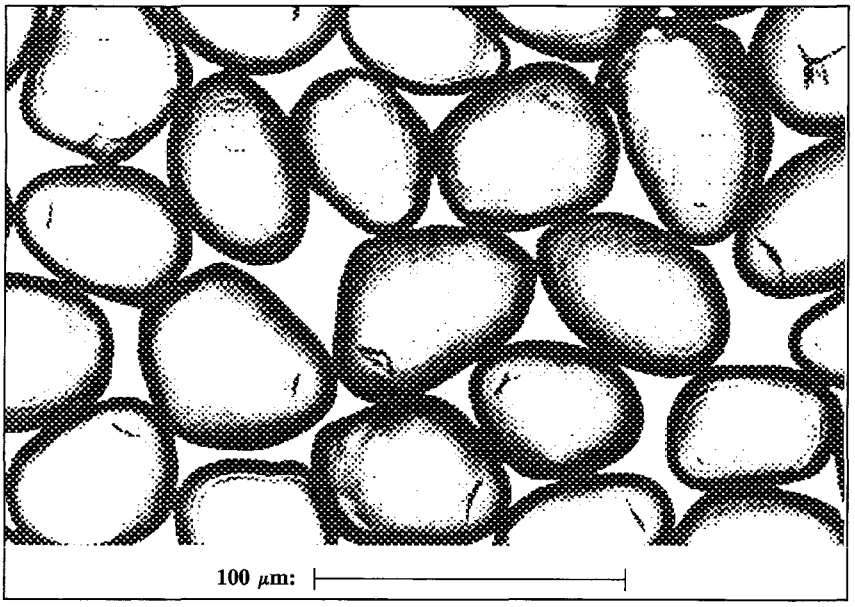

FIGURE 1 Starch granules fraction I (Fr.I) from sedimentation of aqueous starch slurry from tubers of potato species Ukomo. Particle diameters range between 45-70 μm.

granule-sizes[26,27] and thus, the starch particles initially were pooled according to increasing sedimentation times, i.e. with decreasing particle mean-diameters. Two of these granule-fractions, Fr.I: d=45-70 μm (Fig.1) and Fr.II: d=20-40 μm (Fig.2), were utilzed for further investigations. As well Fr.I as Fr.II were dissolved in aqueous 90% DMSO and got separated on the semi-preparative/analytical SEC-system. The amount of carbohydrates in each of the fractions was determined by means of vis-detection at 550 nm as the amount of anthron-coupled-glucose, previously produced by acidic hydrolysis of the glucans. Vis-detection at 640 nm (E_{640}) and 525 nm (E_{525}) for each of the fractions from SEC-separation enabled the determination of chromatograms for non-branched/long-chain-branched (nb/lcb) and short-chain-branched (scb) polyiodide-complexed glucans. Consequently, these E_{640}- and E_{525}-chromatograms enabled the

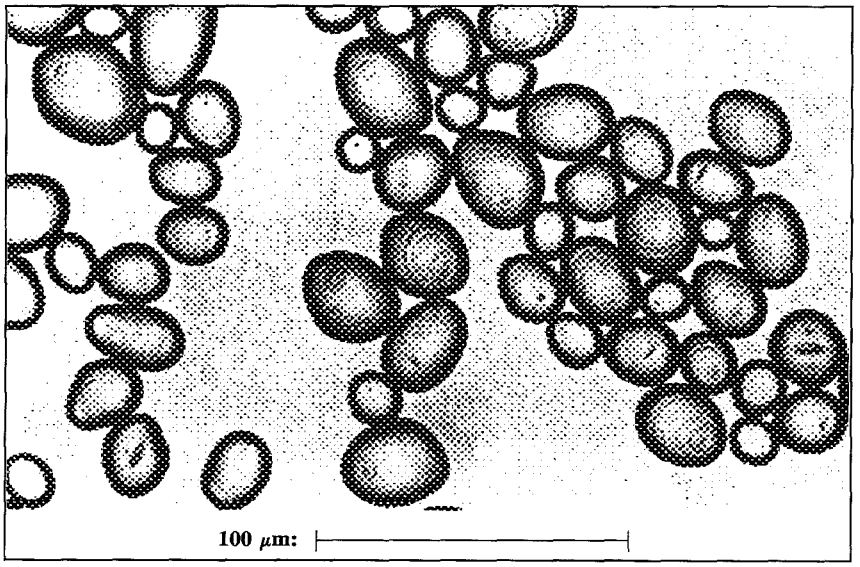

FIGURE 2 Starch granules fraction II (Fr.II) from sedimentation of aqueous starch slurry from tubers of potato species Ukomo. Particle diameters range between 20-40 μm.

computation of qualitative starch composition factors over the range of eluted fractions as the ratio of E_{640}/E_{525} (nb/lcb / scb). For both fractions (Fr.I: Fig.3; Fr.II: Fig.4) glucans at low-retention volumes show E_{640}/E_{525}-values close to and below 1.0, indicating a main-amount of scb-glucans, whereas high-retention-volume-glucans show E_{640}/E_{525}-values in the range of 2.0, an evidence for mainly nb/lcb-glucans. The midrange domain of eluted glucans with E_{640}/E_{525}-values rising from 1.0 up to 2.0 obviously indicates the transition from nb/lcb-majority to scb-majority of the eluted glucans. At this state of analysis no significant differences between starch from granules of Fr.I and Fr.II could be identified.

In a next step of differentiating the starch-glucans, the aqueous DMSO dissolved fractions Fr.I and Fr.II were mixed with n-butanol to precipitate the non-branched/long-chain branched components. The short-chain-branched glucans

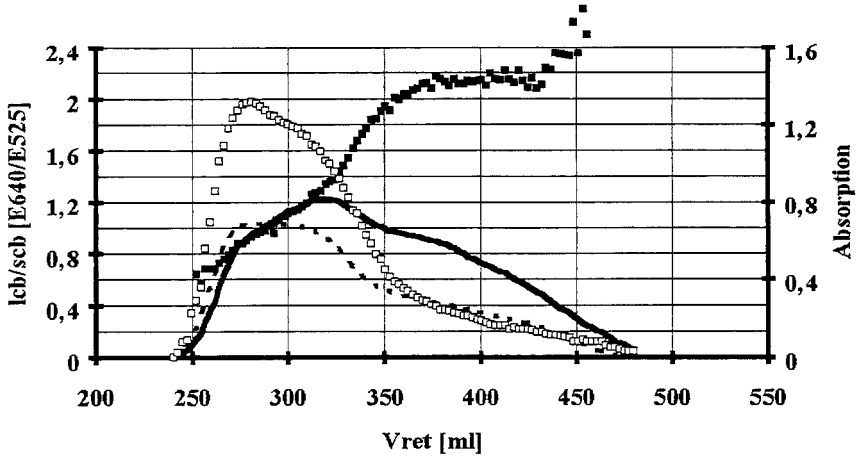

FIGURE 3 Large starch granules (Fr.I): dissolved in aqueous 90% DMSO and separated on semi-preparative/analytical SEC; fractions complexed with polyiodide anions: detection of non-branched/long-chain-branched (nb/lcb) glucans at 640 nm (————), detection of short-chain-branched glucans at 525 nm (— — —); starch composition ratio E_{640}/E_{525} (nb/lcb / scb)-ratio (■■■); total carbohydrates by detection at 550 nm of anthron-coupled glucose after acidic hydrolysis of glucans (□□□).

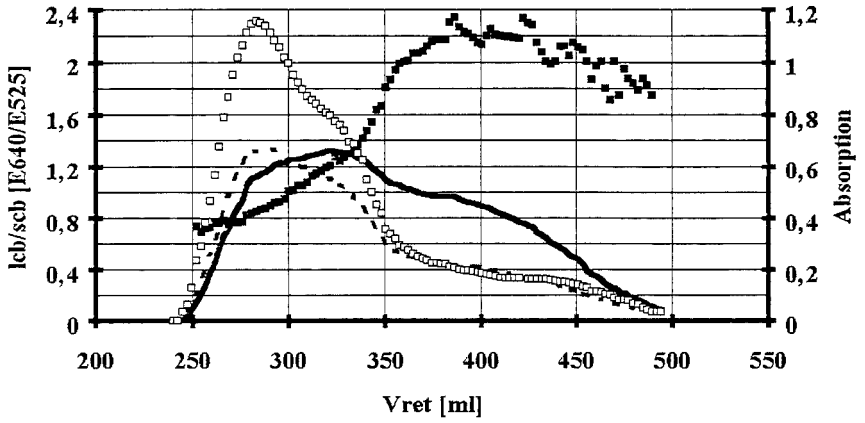

FIGURE 4 Small starch granules (Fr.II): dissolved in aqueous 90% DMSO and separated on semi-preparative/analytical SEC; fractions complexed with polyiodide anions: detection of non-branched/long-chain-branched (nb/lcb) glucans at 640 nm (————), detection of short-chain-branched glucans at 525 nm (— — —); starch composition ratio E_{640}/E_{525} (nb/lcb / scb)-ratio (■■■); total carbohydrates by detection at 550 nm of anthron-coupled glucose after acidic hydrolysis of glucans (□□□).

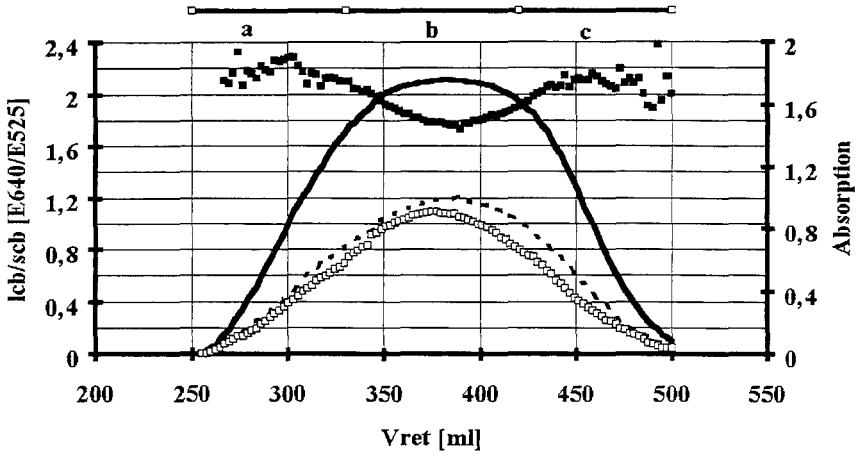

FIGURE 5 Large starch granules (Fr.I): n-butanol precipitated fraction from aqueous DMSO dissolved starch expected to represent a non-branched/long-chain-branched glucan fraction; separation on semi-preparative/analytical SEC; fractions complexed with polyiodide anions: detection of non-branched/long-chain-branched (nb/lcb) glucans at 640 nm (————), detection of short-chain-branched glucans at 525 nm (— — —); starch composition ratio E_{640}/E_{525} (nb/lcb / scb)-ratio (■■■); total carbohydrates by detection at 550 nm of anthron-coupled glucose after acidic hydrolysis of glucans (□□□); ranges of components which were pooled (Fr.Ibut_a, Fr.Ibut_b, Fr.Ibut_c) for enzymatically catalyzed debranching.

in the supernatant subsequently got precipitated by an excess of methanol. The four fractions (Fr.Ibut, Fr.Imet, Fr.IIbut, Fr.IImet) were washed, dried, redissolved in aqueous DMSO and again analyzed on the semi-preparative SEC-system. The starch composition factor computed as the E_{640}/E_{525}-ratio with values between 1.8 and 2.2 for the n-butnol-precipitates indicated as well for the large granules (Fr.Ibut: Fig.5) as for the small granules (Fr.IIbut: Fig.7) a majority of nb/lcb-glucans. The same procedure yields for the methanol-precipitates (Fr.Imet: Fig.6, Fr.IImet: Fig.8) E_{640}/E_{525}-values close to 0.8, indicating an expected majority of short-chain-branched glucans. Again, no significant difference between the nb/lcb-glucans of Fr.I and Fr.II could be identified at this state of analysis. The scb-glucans slightly differ in the tendency of their E_{640}/E_{525}-values

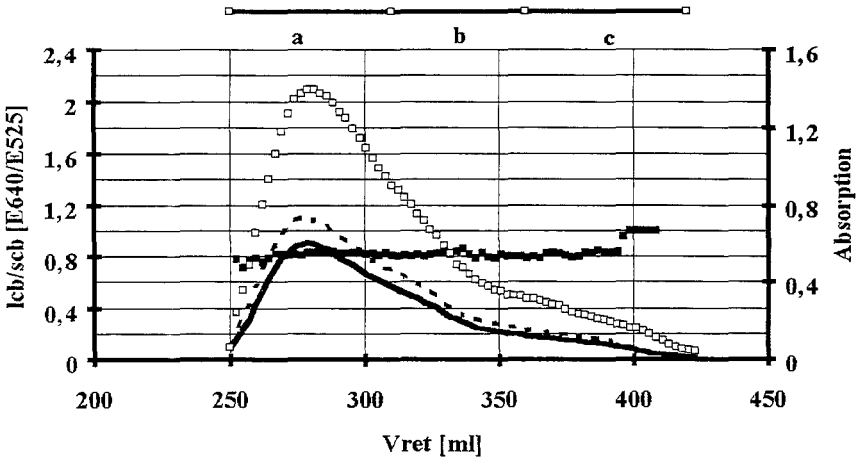

FIGURE 6 Large starch granules (Fr.I): methanol precipitate from the supernatant of the previous n-butanol precipitatation of aqueous DMSO dissolved starch expected to represent a short-chain-branched glucan fraction; separation on semi-preparative/analytical SEC; fractions complexed with polyiodide anions: detection of non-branched/long-chain-branched (nb/lcb) glucans at 640 nm (————), detection of short-chain-branched glucans at 525 nm (— — —); starch composition ratio E_{640}/E_{525} (nb/lcb / scb)-ratio (■■■); total carbohydrates by detection at 550 nm of anthron-coupled glucose after acidic hydrolysis of glucans (□□□); ranges of components which were pooled (Fr.Imet_a, Fr.Imet_b, Fr.Imet_c) for enzymatically catalyzed debranching.

in the midrange domain of elution: scb-glucans from large granules (Fr.I: Fig.6) keep values close to 0.8, whereas scb-glucans from small granules (Fr.II: Fig.8) tend toward even lower values.

In a next step each of the four glucan-fractions were fractionated on the preparative SEC-system into glucan-pools at low- (a), midrange- (b) and high- (c) retention-volumes (fractions indicated in Fig.5-8, according Table 1). The glucans in each of these pools got debranched by catalytic action of pullulanase and the reaction-products were analyzed by means of analytical SEC and extended data analysis. As separation of the debranched glucans on the analytical SEC-system initally yields the mass-modulated molecular weight distribution (w(M)) application of eq.(2) to the w(M)-distributions is required to transform the w(M)- into

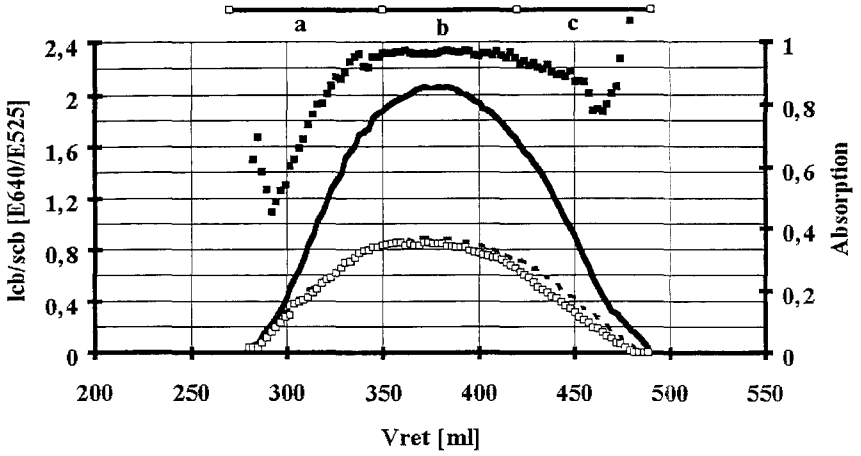

FIGURE 7 Small starch granules (Fr.II): n-butanol precipitated fraction from aqueous DMSO dissolved starch expected to represent a non-branched/long-chain-branched glucan fraction; separation on semi-preparative/analytical SEC; fractions complexed with polyiodide anions: detection of non-branched/long-chain-branched (nb/lcb) glucans at 640 nm (————), detection of short-chain-branched glucans at 525 nm (— — —); starch composition ratio E_{640}/E_{525} (nb/lcb / scb)-ratio (■■■); total carbohydrates by detection at 550 nm of anthron-coupled glucose after acidic hydrolysis of glucans (□□□); ranges of components which were pooled (Fr.IIbut_a, Fr.IIbut_b, Fr.IIbut_c) for enzymatically catalyzed debranching.

n(M)-distributions to give weight to the glucan-chains by their number and not by their mass. For each of the analyzed debranched glucan-pools both distributions (n(M) and w(M)) are illustrated in the indicated Figures 9-12. Peaks in the differential molecular weight distributions (Mp_x) were classified to be representative for a glucan-chain-population with specified degree of polymerization $dp_{(Mp)}$. The contribution of each of these populations was estimated from the percentage of area in the n(M)-function. By means of such $dp_{(Mp)}$- and n%-data average values of branching characteristics were calculated according to eqs.(3)-(5).

At this state of analysis the non-branched/long-chain-branched glucans from large (Fr.I) and small (Fr.II) granules showed significantly different branching characteristics. The average number of monomers between two adjacent

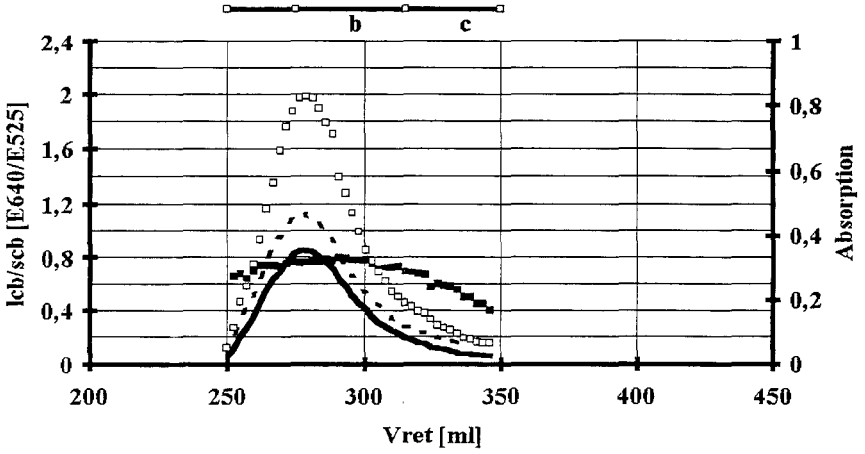

FIGURE 8 Small starch granules (Fr.II): methanol precipitate from the supernatant of the previous n-butanol precipitatation of aqueous DMSO dissolved starch expected to represent a short-chain-branched glucan fraction; separation on semi-preparative/analytical SEC; fractions complexed with polyiodide anions: detection of non-branched/long-chain-branched (nb/lcb) glucans at 640 nm (————), detection of short-chain-branched glucans at 525 nm (— — —); starch composition ratio E_{640}/E_{525} (nb/lcb / scb)-ratio (■■■); total carbohydrates by detection at 550 nm of anthron-coupled glucose after acidic hydrolysis of glucans (□□□); ranges of components which were pooled (Fr.IImet_b, Fr.IImet_c) for enzymatically catalyzed debranching.

branching positions results with bp→bp=94.5 for the initial (Fr.Ibut_a: Fig.9a, Tab.2a) and bp→bp=172.5 for the midrange (Fr.Ibut_b: Fig.9b, Tab.2a) preparative SEC-fraction of large granules. This average distance is significantly larger than that for nb/lcb-glucans from small granules: bp→bp=19 for the inital fraction of preparative SEC (Fr.IIbut_a: Fig.11a, Tab.3a), more indicating scb-glucans than a nb/lcb-fraction; bp→bp=52 for the midrange fraction (Fr.IIbut_b: Fig.11b, Tab.3a) and bp→bp=37 for the final fraction of preparative SEC (Fr.IIbut_c: Fig.11c, Tab.3a). Obvious dissimilarities between glucans from large and small granules, already documented by different average values for the parameters of branching characteristics, even more explicitely are illustrated by the absence of extremely high-dp glucan-chains in nb/lcb-glucan-fractions of small granules (large granules :Figs.9a-b, small granules: Figs.11a-c).

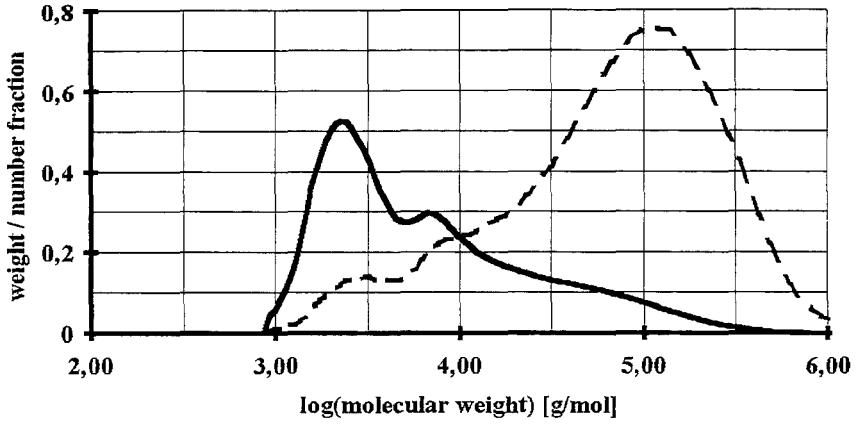

FIGURE 9a Large starch granules (Fr.I): n-butanol precipitated nb/lcb-glucan fraction; pool Fr.Ibut_a from preparative SEC, debranched by catalytic action of pullulanase; (- - -) mass distribution from DRI-detection of analytical SEC of debranched glucans; (———) number distribution according eq.(1). Results of branching analysis in Tab.2a.

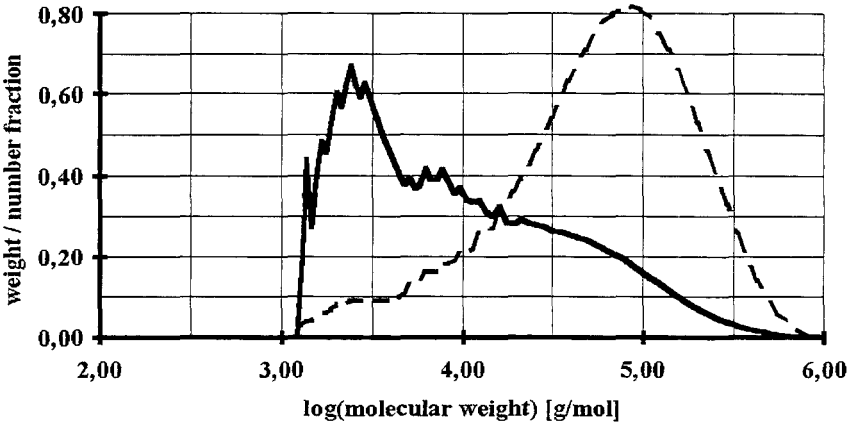

FIGURE 9b Large starch granules (Fr.I): n-butanol precipitated nb/lcb-glucan fraction; pool Fr.Ibut_b from preparative SEC, debranched by catalytic action of pullulanase; (- - -) mass distribution from DRI-detection of analytical SEC of debranched glucans; (———) number distribution according eq.(1). Results of branching analysis in Tab.2a.

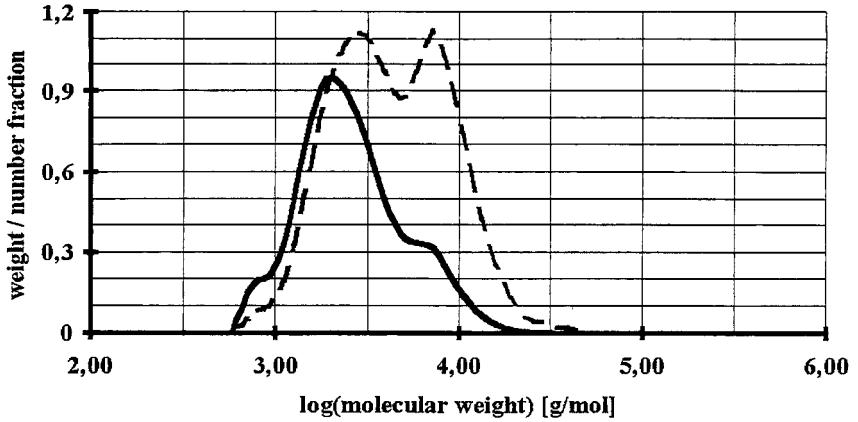

FIGURE 10 Large starch granules (Fr.I): methanol precipitate from supernatant of previous n-butanol precipitatation of aqueous DMSO dissolved starch expected to be a scb-glucan fraction; identical for pools Fr.Imet_a, Fr.Imet_b, Fr.Imet_c from preparative SEC, debranched by catalytic action of pullulanase; (- - -) mass distribution from DRI-detection of analytical SEC of debranched glucans; (———) number distribution according eq.(1). Results of branching analysis in Tab.2b.

Table 2a

Branching Analysis of Large Starch-granules (Fr.I) from Tubers of Potato Species Ukomo. (abbreviations in the text; illustrations for number and mass distributions of glucan chains: Figure 9a (Fr.Ibut_a) and Figure 9b (Fr.Ibut_b))

glucan-fraction	Mp [g mol^{-1}]	$dp_{(Mp)}$	n_%	branching characteristics		
				av_b	bp→bp	b%
Fr.Ibut_a: Mp_I	2 500	15	~ 70	**10.58**	**94.5**	**1.06**
Fr.Ibut_a: Mp_II	7 400	45	~ 20			
Fr.Ibut_a: Mp_III	122 000	750	~ 10			
Fr.Ibut_b: Mp_I	2 500	15	~ 45	**5.80**	**172.5**	**0.58**
Fr.Ibut_b: Mp_II	7 400	45	~ 35			
Fr.Ibut_b: Mp_III	122 000	750	~ 20			

Table 2b

Branching Analysis of Large Starch-granules (Fr.I) from Tubers of Potato Species Ukomo. (abbreviations in the text; illustrations for number and mass distributions of glucan chains: Figure 10 (identical for Fr.Imet_a, Fr.Imet_b, Fr.Imet_c))

glucan-fraction	Mp [g mol^{-1}]	$dp_{(Mp)}$	n_%	branching characteristics		
				av_b	bp→bp	b%
Fr.Imet_a: Mp_I	2 000	12	~ 80			
Fr.Imet_a: Mp_II	7 400	45	~ 20	**53.76**	**18.6**	**5.38**

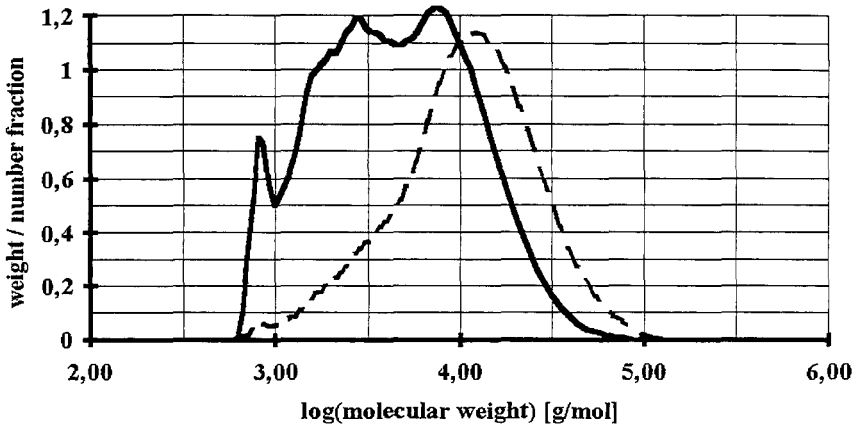

FIGURE 11a Small starch granules (Fr.II): n-butanol precipitated nb/lcb-glucan fraction; pool Fr.IIbut_a from preparative SEC, debranched by catalytic action of pullulanase; (- - -) mass distribution from DRI-detection of analytical SEC of debranched glucans; (———) number distribution according eq.(1). Results of branching analysis in Tab.3a.

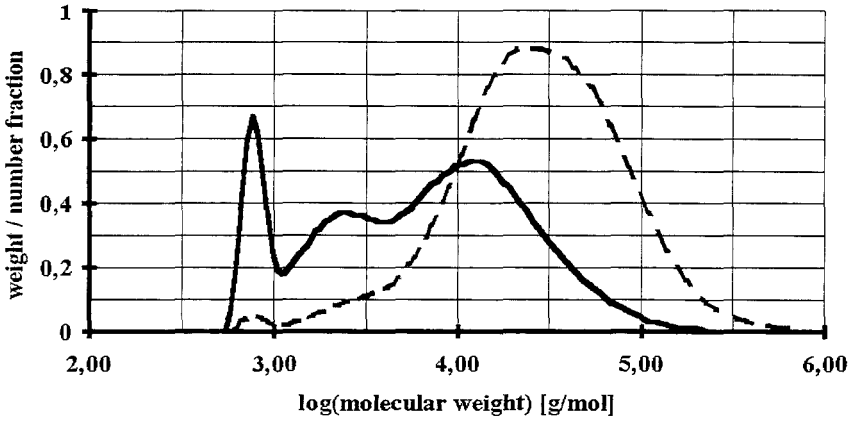

FIGURE 11b Small starch granules (Fr.II): n-butanol precipitated nb/lcb-glucan fraction; pool Fr.IIbut_b from preparative SEC, debranched by catalytic action of pullulanase; (- - -) mass distribution from DRI-detection of analytical SEC of debranched glucans; (———) number distribution according eq.(1). Results of branching analysis in Tab.3a.

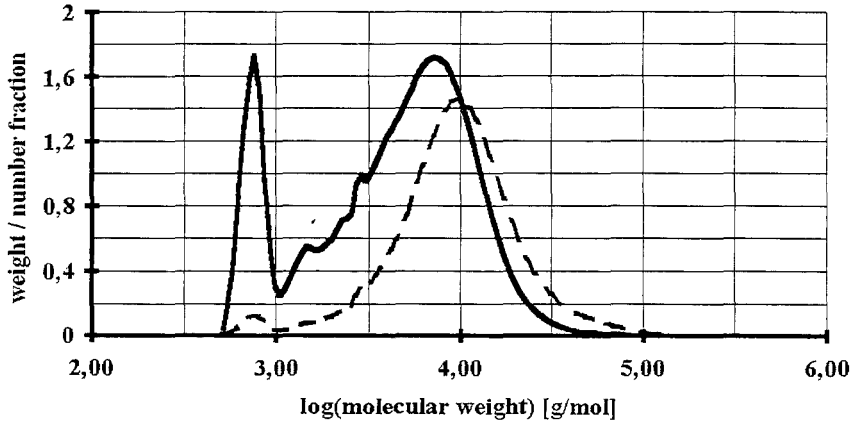

FIGURE 11c Small starch granules (Fr.II): n-butanol precipitated nb/lcb-glucan fraction; pool Fr.IIbut_c from preparative SEC, debranched by catalytic action of pullulanase; (- - -) mass distribution from DRI-detection of analytical SEC of debranched glucans; (———) number distribution according eq.(1). Results of branching analysis in Tab.3a.

Table 3a

Branching Analysis of Large Starch-granules (Fr.II) from Tubers of Potato Species Ukomo. (abbreviations in the text; illustrations for number and mass distributions of glucan chains: Figure 11a (Fr.IIbut_a), Figure 11b (Fr.IIbut_b) and Figure 11c (Fr.IIbut_c))

glucan-fraction	Mp [g mol^{-1}]	$dp_{(Mp)}$	n_%	branching characteristics		
				av_b	bp→bp	b%
Fr.IIbut_a: Mp_I	800	5	~ 5	**52.63**	**19.0**	**5.26**
Fr.IIbut_a: Mp_II	2 500	15	~ 80			
Fr.IIbut_a: Mp_III	7 400	45	~ 15			
Fr.IIbut_b: Mp_I	800	5	~ 20	**19.23**	**52.0**	**1.92**
Fr.IIbut_b: Mp_II	2 500	15	~ 20			
Fr.IIbut_b: Mp_III	13 000	80	~ 60			
Fr.IIbut_c: Mp_I	800	5	~ 20	**27.03**	**37.0**	**2.70**
Fr.IIbut_c: Mp_II	7 400	45	~ 80			

Table 3b

Branching Analysis of Large Starch-granules (Fr.II) from Tubers of Potato Species Ukomo. (abbreviations in the text; illustrations for number and mass distributions of glucan chains: Figure 12a (Fr.IImet_b), Figure 12b (Fr.IImet_c))

glucan-fraction	Mp [g mol^{-1}]	$dp_{(Mp)}$	n_%	branching characteristics		
				av_b	bp→bp	b%
Fr.IImet_b: Mp_I	2 500	15	~ 85	**49.38**	**20.3**	**4.94**
Fr.IImet_b: Mp_II	8 200	50	~ 15			
Fr.IImet_c: Mp_I	800	5	~ 20	**83.33**	**12.0**	**8.33**
Fr.IImet_c: Mp_II	1 600	10	~ 70			
Fr.IImet_c: Mp_III	6 500	40	~ 10			

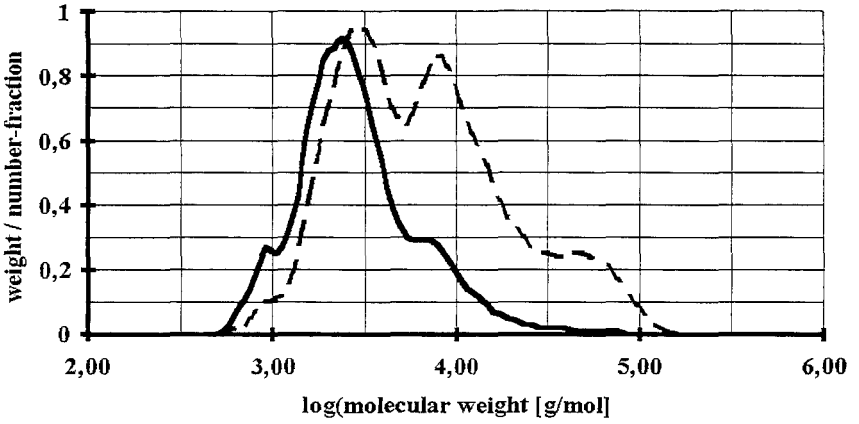

FIGURE 12a Small starch granules (Fr.II): methanol precipitate from supernatant of previous n-butanol precipitatation of aqueous DMSO dissolved starch expected to be a scb-glucan fraction; pool Fr.IImet_b from preparative SEC, debranched by catalytic action of pullulanase; (- - -) mass distribution from DRI-detection of analytical SEC of debranched glucans; (———) number distribution according eq.(1). Results of branching analysis in Tab.3b.

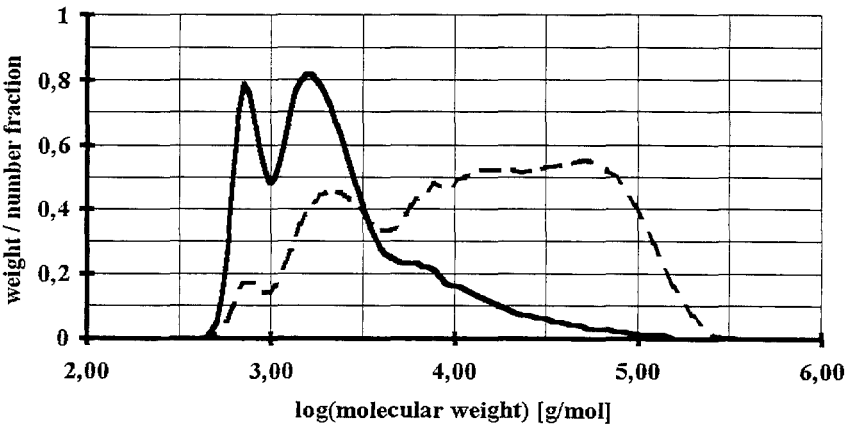

FIGURE 12b Small starch granules (Fr.II): methanol precipitate from supernatant of previous n-butanol precipitatation of aqueous DMSO dissolved starch expected to be a scb-glucan fraction; pool Fr.IImet_c from preparative SEC, debranched by catalytic action of pullulanase; (- - -) mass distribution from DRI-detection of analytical SEC of debranched glucans; (———) number distribution according eq.(1). Results of branching analysis in Tab.3b.

The short-chain-branched glucans of large granules are quite homogeneous in their branching characteristics over the total range of elution on the preparative SEC-system: an expected short average-distance between two branching positions was found with bp→bp=18.6 monomers for all debranched glucan pools (Fr.IImet_a, _b, _c: Fig.10, Tab.2b). A similar value of bp→bp-value of 20.3 monomers was found for the midrange fraction (Fr.IImet_b: Fig.12a, Tab.3b), but a significantly higher branched structure for the final fraction of preparative SEC (Fr.IImet_c: Fig.12b, Tab.3b) with bp→bp=12.0 monomers for the scb-glucans from small granules.

For a cross-check of these results methylation/GC-MS-analysis was applied to determine average branching characteristics. By means of this technique an average number of monomers between two branching points was determined as the ratio of the integrals of 1,4,5-tri-O-Ac 2,3,6-tri-O-Me-D-sorbit deriving from α1-4-linked glucose and 1,4,5,6-tetra-O-Ac 2,3-di-O-Me-D-sorbit deriving from α1-4 linked glucose with α1-6-linked branches. Obtained results can be judged to be reliable for scb-glucans, those for the nb/lcb-glucans better should be taken as trend, because the huge excess of α1-4-linked glucose over α1-4-linked glucose with α1-6-branching positions introducef high deviations in the calculated ratios. But even with this restriction a quite good agreement of GC-MS-results and results from analytical SEC was found (Tab.4).

Summarizing, differences in the branching-structure of glucans from starch granules with different biological history were identified and could be quantified as the lack of extremely high-dp glucan chains in the constituting glucan-chain distribution of starch from small granules. Obvious dissimilarities in mass- and number-distributions between glucans from large and small granules were found again, diminished but still significant, as different values of average distance between two branching points (bp→bp) and average percentage of branching (b%). In general, the majority of glucans from small granules show a higer average degree of branching than glucans from large granules, a fact that most likely is

Table 4

Branching Characteristics of Glucan Fractions from Starch-granules of Tubers of Potato Species Ukomo according to Table 1.

glucan-fraction	branching characteristics				
	SEC: av_b	SEC: b%	SEC bp→bp	GC-MS: bp→bp	iodine E_{640}/E_{525}
Fr.Ibut_a	10.58	1.06	94.5	70	2.2
Fr.Ibut_b	5.80	0.58	172.5	100	1.9
Fr.Imet_a	53.76	5.38	18.6	24	0.8
Fr.Imet_b	53.76	5.38	18.6	26	0.8
Fr.Imet_c	53.76	5.38	18.6	n.d.	0.8
Fr.IIbut_a	52.63	5.26	19.0	60	1.6
Fr.IIbut_b	19.23	1.92	52.0	119	2.2
Fr.IIbut_c	27.03	2.70	37.0	n.d.	2.0
Fr.IImet_b	49.38	4.94	20.3	18	0.8
Fr.IImet_c	83.33	8.33	12.0	n.d.	0.6

due to changing activities of (1-4)-α-D-glucan-branching 6-glycosyltransferase (EC 2.4.1.18) during biogenesis of starch in the investigated potato tubers.

ACKNOWLEDGEMENTS

This work was supported by the Austrian Fonds zur Förderung wissenschaftlicher Forschung, project P9059-CHE. Special thanks to Dipl.Ing.Martin Fischl for excellent experimental work.

REFERENCES

1. W.J.Freeman, "Characterization of Polymers," In Polymers - Polymer Characterization and Analysis, J.I.Kroschwitz, ed., John Wiley & sons, New York., 1990, pp 1-38.

2. W.Burchard, Polysaccharide, Springer Verlag, Berlin Heidelberg, 1985

3. E.D.T.Atkins, Polysaccharides - Topic in Structure and Morphology, vol 8 In Topics in Molecular and Structural Biology, VCH, Weinheim, 1985

4. A.R.Cooper, Determination of Molecular Weight, vol 103 in Chemical Analysis, John Wiley & Sons, New York, 1989

5. H.G.Barth, Modern Methods of Particle Size Analysis, John Wiley & Sons, New York, 1984

6. R.H.F.Beck, W.Praznik, Stärke/Starch, **38**: 391-394 (1986

7. O.Marclin, L.Saulnier, J.-M.Brillouet, Carbohydr.Res., **212**: 159-167 (1991)

8. F.Will, H.Dietrich, Carbohydr.Polym., **18**: 109-117 (1992)

9. W.W.Yau, J.J.Kirkland, D.D.Bly, Modern Size Exclusion Chromatography, John Wiley & Sons, New York, 1979

10. H.G.Barth, J.W.Mays, Modern Methods of Polymer Characterization, John Wiley Publishers, New York, 1990

11. S.Mori, J.Chromatogr., **411**: 355-362 (1997)

12. M.Fischl, Diploma Thesis, Universität für Bodenkultur, Vienna/Austria, 1990

13. W.Praznik, G.Rammesmayer, T.Spies, A.Huber, Carbohydr.Res., **227**: 171-182 (1992)

14. T.J.Schoch, Adv.Carbohydr.Chem., **1**: 247-277 (1945)

15. G.R.Noggele, "The Identification and the Quantitative Determination of Carbohydrates," In The Carbohydrates, W.Pigman, ed., Academic Press Inc., 1957, pp 602-640.

16. W.Praznik, R.Beck, J.Chromatogr., **387**: 467-472 (1987)

17. W.Banks, C.T.Greenwood, K.M.Khan, Carbohydr.Res., **17**: 25-33 (1971)

18. T.Handa, H.Yajima, T.Ishii, T.Nishimura, "Deep Blueing Mechanism of TGriiodide Ions in Amylose Being Associated with Its Conformation," In Solution Properties of Polysaccharides, D.A.Brant, ed., ACS Symposium Series 150, 1981, pp 455-475.

19. B.Pfannemüller, G.Ziegast, "Properties of Aqueous Amylose and Amylose-Iodine Solutions," In Solution Properties of Polysaccharides, D.A.Brant, ed., ACS Symposium Series 150, 1981, pp 529-548.

20. S.V.Bhide, M.S.Karve, N.R.Kale, "The Interaction of Sodium Dodecyl Sulfate, a Competing Ligand, with Iodine Complexes of Amylose and Amylopectin," In Solution Properties of Polysaccharides, D.A.Brant, ed., ACS Symposium Series 150, 1981, pp 491-511.

21. I.Ciucanu, F.Kerek, Carbohydr.Res., **131**: 209-217 (1984)

22. M.Durindova, P.Jurasek, I.Klbik, V.Kovacik, Chem.Papers, **47**: 3, 198-201 (1993)

23. Y.Takeda, N.Maruta, S.Hizukuri, Carbohydr.Res., **227**: 113-120 (1992)

24. K.Koizumi, M.Fukuda, S.Hizukuri, J.Chromatogr., **2**: 233-238 (1991)

25. D.W.Shortt, J.Liqu.Chromatogr., **16**: 3371-3391 (1993)

26. A.T.Czaja, Stärke/Starch, **34**: 181-183 (1982)

27. R.E.Cameron, A.M.Donald, Polymer, **33**: 12, 2628-2635 (1992)

JOURNAL OF LIQUID CHROMATOGRAPHY, 17(18), 4057-4058 (1994)

THE BOOK CORNER

DIODE ARRAY DETECTION IN HPLC, edited by L. Huber & S. A. George, Chromatographic Science Series, J. Cazes Editor, Volume 62, Marcel Dekker, Inc. New York, Basel, Hongkong, 1993, vii + 400 pp., $150.00; ISBN: 042474947-4

This book represents Volume 62 in the Chromatographic Science Series published by Marcel Dekker. The book is well presented and discusses the principles and techniques of diode array detection and its application in high performance liquid chromatography. The advantages of diode array detection over conventional absorbance detectors are also well presented. Diode array detection offers high selectivity and sensitivity as it is coupled by modern software which can evaluate and process a large amount of data, provided in a very short time. The most significant improvements made in optics of the diode array detector is also discussed.

The book is written by eight contributors, who are experienced in this technique. It also is well illustrated, as it contains 239 figures, 22 tables, and each chapter ends with references; however, the most recent references are cited in 1990.

The volume consists of 14 chapters, classified into four parts, with the following topics:

I. Theory and Design:

* Historical Developments

* Modern Developments

II. Advantages of Diode Array Detectors to Chromatographers:

* Diode Array Detection Advantages for the Chromatographer

* Spectral Matching and Peak Purity

* Chemometrics and Photodiode Array Detection

III. Applications of Diode Array Detectors:

* The Use of Diode Array Detectors in the Pharmaceutical Industry

* Clinical Applications

* Toxicological Applications

* Applications in the Analysis of Amino Acids, Peptides and Proteins

* Food and Beverages

* Environmental Applications

* Chemical, Petrochemical, and Polymer Applications

IV. Guidelines on how to optimize Sensitivity, Selectivity, Automation:

* Optimization of Diode Array Detection, and

* Using Diode Array Detectors for Automated Routine Analysis.

This book is highly recommended to analytical, pharmaceutical and environmental chemists and also for biochemists, and graduate students.

Reviewed by
Hassan Y. Aboul-Enein, PhD, FRSC
Bioanalytical and Drug Development Laboratory
Biological and Medical Research Department
King Faisal Specialist Hospital
and Research Centre
P.O. Box3354
Riyadh 11211. Saudi Arabia

JOURNAL OF LIQUID CHROMATOGRAPHY, 17(18), 4059-4064 (1994)

LIQUID CHROMATOGRAPHY CALENDAR

1994

NOVEMBER 2 - 5: 29th Midwestern Regional Meeting, ACS, Kansas City, Kansas. Contact: M. Wickham-St. Germain, Midwest Res. Inst, 425 Volker Blvd, Kansas City, MO 64110, USA.

NOVEMBER 3: Anachem Symposium, Dearborn, Michigan. Contact: Paul Beckwith, Program Chairman, Detroit Edison Co., 6100 W. warren, Detroit, MI 48210, USA.

NOVEMBER 7 - 10: 13th Int'l Conference on the Application of Accelerators in Research & Industry, Denton, Texas. Contact: J. L. Duggan, Univ. of N. Texas, Dept. of Physics, P. O. Box 5368, Denton, TX 76203, USA.

NOVEMBER 10 - 11: 17th Int'l Conference on Chemistry, Biosciences, Pharmacy & Environmental Pollution, New Delhi, India. Contact: V. M. Bhatnagar, Alena Chem of Canada, P. O. Box 1779, Cornwall, Ont., Canada K6H 5V7.

NOVEMBER 11 - 12: 3rd Conference on Current Trends in Computational Chemistry, Jackson, Mississippi. Contact: J. Leszczynski, Jackson State University, Dept. of Chem., 1400 J. R. Lynch St., Jackson, MS 39217, USA.

NOVEMBER 13 - 16: 50th Southwest Regional Meeting, ACS, Fort Worth, Texas. Contact: H. C. Kelly, Texas Christian Univ, Chem Dept, Ft. Worth, TX 76129, USA.

NOVEMBER 13 - 18: Annual Meeting of the A.I.Ch.E., San Francisco, California. Contact: AIChE Express Service Center, 345 East 47th St., New York, NY 10017, USA.

NOVEMBER 14 - 17: 33rd Eastern Analytical Symposium, Somerset, New Jersey. Contact: Sheri Gold, EAS, P. O. Box 633, Montchanin, DE 19710, USA.

NOVEMBER 16 - 18: Envirosoft'94, 5th Int'l Conference on Development and Application of Computer Techniques to Environmental Studies, San Francisco, California. Contact: Computational Mechanics, Inc., 25 Bridge St., Billerica, MA 01821, USA.

DECEMBER 4 - 6: IBEX'94, International Biotechnology Expo & Scientific Conference, Moscone Center, San Francisco, California. Contact: Cartlidge & Associates, Inc., 1070 Sixth Avenue, Suite 307, Belmont, CA 94002, USA.

1995

MARCH 6 - 10: PittCon'95: Pittsburgh Conference on Analytical Chemistry & Applied Spectroscopy, New Orleans, Louisiana. Contact: Pittsburgh Conference, Suite 332, 300 Penn Center Blvd., Pittsburgh, PA 15235-9962, USA.

APRIL 2 - 7: 209th ACS National Meeting, Anaheim, Calif. Contact: ACS Meetings, ACS, 1155 16th Street, NW, Washington, DC 20036-4899, USA.

APRIL 25 - 28: Biochemische Analytik '95, Leipzig. Contact: Prof. Dr. H. feldmann, Inst. fur Physiologische Chemie der Universitat, Goethestrasse 33, D-80336 Munchen, Germany.

MAY 28 - JUNE 2: HPLC'95, 19th International Symposium on Column Liquid Chromatography, Convention Center, Innsbruck, Austria. Contact: HPLC'95 Secretariat, Tyrol Congress, Marktgraben 2, A-6020 Innsbruck, Austria.

MAY 31 - JUNE 2: 27th Central regional Meeting, ACS, Akron Section. Contact: J. Visintainer, Goodyear Research, D415A, 142 Goodyear Blvd, Akron, OH 44236, USA.

JUNE 6 - 8: 28th Great Lakes Regional ACS Meeting, LaCrosse-Winona Section. Contact: M. Collins, Chem. Dept., Viterbo College, La Crosse, WI 54601, USA.

JUNE 14 - 16: 50th Northwest/12th Rocky Mountain Regional Meeting, ACS, Park City, Utah. Contact: J. Boerio-Goates, Chem Dept, 139C-ESC, Brigham Young Univ, Provo, UT 84602, USA.

JULY 9 - 15: SAC'95, The University of Hull, UK, sponsored by the Analytical Division, The Royal Society of Chemistry. Contact: The Royal Society of Chemistry, Burlington House, Picadilly, London W1V 0BN, UK.

JULY 7 - 8: FFF Workshop, University of Utah, Salt Lake City, UT. Contact: Ms. Julie Westwood, FFF Research Center, Dept. of Chem., University of Utah, Salt Lake City, UT 84112, USA.

JULY 10 - 12: FFF'95, Fifth International Symposium on Field-Flow Fractionation, Park City, Utah. Contact: Ms. Julie Westwood, FFF Researcvh Center, Dept. of Chem. Univ. of Utah, Salt Lake City, UT 84112, USA.

AUGUST 20 - 25: 210th ACS National Meeting, Chicago, Illinois. Contact: ACS Meetings, ACS, 1155 16th Street, NW, Washington, DC 20036-4899, USA.

SEPTEMBER 12 - 15: 5th International Symposium on Drug Analysis, Leuven, Belgium. Contact: Prof. J. Hoogmartens, Inst. of Pharmaceutical Sciences, Van Evenstraat 4, B-3000 Leuven, Belgium.

OCTOBER 18 - 21: 31st Western Regional Meeting, ACS, San Diego, Calif. Contact: S Blackburn, General Dynamics, P. O. Box 179094, San Diego, CA 92177-2094, USA.

OCTOBER 22 - 25: 25th Northeastern Regional Meeting, ACS, Rochester, New York. Contact: T. Smith, Xerox Corp, Webster Res Center, M/S 0128-28E, 800 Phillips Rd, Webster, NY 14580, USA.

NOVEMBER 1 - 3: 30th Midwestern Regional ACS Meeting, Joplin, Missouri. Contact: J. H. Adams, 1519 Washington Dr., Miami, OK 74354-3854, USA.

NOVEMBER 1 - 4: 31st Western Regional ACS Meeting, San Diego, California. Contact: T. Lobl, Tanabe Research Labs, 4450 Town Center Ct., San Diego, CA 92121, USA.

NOVEMBER 5 - 7: 30th Midwestern Regional Meeting, ACS, Joplin, Missouri. Contact: J. H. Adams, 1519 Washington Dr, Miami, OK 74354, USA.

NOVEMBER 29 - DECEMBER 1: Joint 51st Southwestern/47th Southeastern Regional Meeting, ACS, Peabody Hotel, Memphis, Tenn. Contact: P.K. Bridson, Chem Dept, Memphis State Univ, Memphis, TN 38152, USA.

DECEMBER 17 - 22: 1995 International Chemical Congress of Pacific Basin Societies, Honolulu, Hawaii. Contact: ACS Meetings, 1155 16th Street, NW, Washington, DC 20036-4899, USA.

1996

FEBRUARY 26 - MARCH 1: PittCon'96: Pittsburgh Conference on Analytical Chemistry & Applied Spectroscopy, Chicago, Illinois. Contact: Pittsburgh

Conference, Suite 332, 300 Penn Center Blvd., Pittsburgh, PA 15235-9962, USA.

MARCH 24 - 29: 211th ACS National Meeting, New Orleans, LA. Contact: ACS Meetings, ACS, 1155 16th Street, NW, Washington, DC 20036-4899, USA.

JUNE 16 - 21: "HPLC '96: Twentieth International Symposium on High Performance Liquid Chromatography," San Francisco Marriott Hotel, San Francisco, California. Contact: Mrs. Janet Cunningham, Barr Enterprises, P. O. Box 279, Walkersville, MD 21793, USA.

AUGUST 18 - 23: 212th ACS National Meeting, Boston, Mass. Contact: ACS Meetings, 1155 16th Street, NW, Washington, DC 20036-4899, USA.

OCTOBER 16 - 19: 52nd Southwest Regional ACS Meeting, Houston, Texas. Contact: J. W. Hightower, Dept. Chem. Eng., Rice University, Houston, TX 77251, USA.

OCTOBER 24 - 26: 52nd Southwestern Regional Meeting, ACS, Houston, Texas. Contact: J. W. Hightower, Chem Eng Dept, Rice Univ, Houston, TX 77251, USA.

NOVEMBER 6 - 8: 31st Midwestern Regional Meeting, ACS, Sioux Falls, South Dakota. Contact: J. Rice, Chem Dept, S. Dakota State Univ, Shepard Hall Box 2202, Brookings, SD 57007-2202, USA.

NOVEMBER 9 - 12: 48th Southeast Regional ACS Meeting, Greenville, South Carolina. Contact: H. C. Ramsey, BASF Corp., P. O. Drawer 3025, Anderson, SC 29624-3025, USA.

1997

APRIL 6 - 11: 213th ACS National Meeting, San Antonio, Texas. Contact: ACS Meetings, ACS, 1155 16th Street, NW, Washington, DC 20036-4899, USA.

SEPTEMBER 7 - 12: 214th ACS National Meeting, Las Vegas, Nevada. Contact: ACS Meetings, 1155 16th Street, NW, Washington, DC 20036-4899, USA.

1998

MARCH 29 - APRIL 3: 215th ACS National Meeting, St. Louis, Missouri. Contact: ACS Meetings, 1155 16th Street, NW, Washington, DC 20036-4899, USA.

AUGUST 23 - 28: 216th ACS National Meeting, Orlando, Florida. Contact: ACS Meetings, 1155 16th Street, NW, Washington, DC 20036-4899, USA.

1999

MARCH 21 - 26: 217th ACS National Meeting, Anaheim, Calif. Contact: ACS Meetings, 1155 16th Street, NW, Washington, DC 20036-4899, USA.

AUGUST 22 - 27: 218th ACS National Meeting, New Orleans, Louisiana. Contact: ACS Meetings, 1155 16th Street, NW, Washington, DC 20036-4899, USA.

2000

MARCH 26 - 31: 219th ACS National Meeting, Las Vegas, Nevada. Contact: ACS Meetings, 1155 16th Street, NW, Washington, DC 20036-4899, USA.

AUGUST 20 - 25: 220th ACS National Meeting, Washington, DC. Contact: ACS Meetings, 1155 16th Street, NW, Washington, DC 20036-4899, USA.

2001

APRIL 1 - 6: 221st ACS National Meeting, San Francisco, Calif. Contact: ACS Meetings, 1155 16th Street, NW, Washington, DC 20036-4899, USA.

AUGUST 19 - 24: 222nd ACS National Meeting, Chicago, Illinois. Contact: ACS Meetings, 1155 16th Street, NW, Washington, DC 20036-4899, USA.

2002

APRIL 7 - 12: 223rd ACS National Meeting, Orlando, Florida. Contact: ACS Meetings, 1155 16th Street, NW, Washington, DC 20036-4899, USA.

SEPTEMBER 8 - 13: 224th ACS National Meeting, Boston, Mass. Contact: ACS Meetings, 1155 16th Street, NW, Washington, DC 20036-4899, USA.

The Journal of Liquid Chromatography will publish, **at no charge**, announcements of interest to liquid chromatographers in every issue of the Journal. To be listed in Meetings & Symposia, we will need to know: Name of the meeting or symposium, sponsoring organization, when and where it will be held, and whom to contact for additional details. Incomplete information will not be published. You are invited to send announcements to **Dr. Jack Cazes, Editor, Journal of Liquid Chromatography, P.O. Box 2180, Cherry Hill, NJ 08034-0162, USA.**

ELECTRONIC MANUSCRIPT SUBMISSION

Effective immediately, manuscripts will be accepted on computer diskettes. A printed manuscript must accompany the diskette. For approximately one year, the diskettes will be used, on an experimental basis, to produce typeset-quality papers for publication in the Journal of Liquid Chromatography. Diskettes must be in an IBM-compatible format with MS-DOS Version 3.0 or greater. The following word processing formats can be accommodated:

ASCII	DisplayWrite Native
EBCDIC	Enable 1.0, 2.0, 2.15
Framework III 1.0, 1.1	IBM Writing Assistant
Microsoft Word 3.0, 3.1, 4.0, 5.0	Multimate 3.3
Multimate Advantage 3.6	Multimate Advantage II 3.7
Navy DIF	Office Writer 4.0, 5.0, 6.0, 6.1
PeachText 5000 2.12	PFS:First Choice 1.0, 2.0
PFS:Write Ver C	Professional Write 1.0, 2.0, 2.1
Q&A Write 3.0	RapidFile (Memo Writer) 1.2
Samna Word IV & IV+ 1.0, 2.0	Total Word 1.2, 1.3
Volkswriter 3, 4	Volkswriter Deluxe 2.2
Wang PC Ver 3	WordPerfect 4.1, 4.2, 5.0, 5.1*
WordStar 3.3, 3.31, 3.45, 4.0, 5.0, 5.5, 6.0	XyWrite III
	XyWrite III+

* The **preferred** word processor is **WordPerfect 5.1.**

Manuscripts and diskettes should be prepared in accordance with the **Instructions for Authors** given at the back of this issue of the Journal. They should be sent to the Editor:

Dr. Jack Cazes
Journal of Liquid Chromatography
P. O. Box 2180
Cherry Hill, NJ 08034

INSTRUCTIONS TO AUTHORS

Journal of Liquid Chromatography is published in the English language for the rapid communication of research in liquid chromatography and its related sciences and technologies.

Directions for Submission

One typewritten manuscript, suitable for direct reproduction, and two (2) clear copies with figures must be submitted. Since the Journal is produced by direct photography of the manuscripts, typing and format instructions must be strictly followed. Non-compliance will result in return of the manuscript to the author and will delay its publication. To avoid creasing, manuscripts should be placed between heavy cardboards before mailing.

Manuscripts may also be submitted on **computer diskettes**. A printed manuscript must also be submitted with diskettes because, at the present time, we are experimenting with manuscripts on diskettes. Diskettes must be readable with an IBM-compatible computer (Macintosh or other type not acceptable) and must be formatted with MS-DOS 3.1 or greater. Be sure to indicate the word processing software that was used to prepare the manuscript diskette.

Manuscripts and computer diskettes should be mailed to the Editor:

Dr. Jack Cazes
Journal of Liquid Chromatography
P. O. Box 2180
Cherry Hill, NJ 08034

Reprints

Due to the short production time for papers in this journal, it is essential to order reprints immediately upon receiving notification of acceptance of the manuscript. A reprint order form will be sent to the author with the letter of acceptance for the manuscript. Reprints are available in quantities of 100 and multiples thereof. Twenty (20) free reprints will be included with orders of 100 or more reprints.

Format of the Manuscript

1. The general format of the manuscript should be:
   Title
   Author(s)' names and full addresses
   Abstract
   Text Discussion
   References

2. **Title & Authors:** The entire title should be in capital letters and centered within the width of the typing area, located at least 2 inches (5.1 cm) from the top of the page. This should be followed by 3 lines of space, then by the names and addresses of the authors, also centered, in the following manner:

A SEMI-AUTOMATIC TECHNIQUE FOR THE SEPARATION AND DETERMINATION OF BARIUM AND STRONTIUM IN WATER BY ION EXCHANGE CHROMATOGRAPHY AND ATOMIC EMISSION SPECTROMETRY

F. D. Pierce and H. R. Brown
Utah Biomedical Test Laboratory
520 Wakara Way
Salt Lake City, Utah 84108

3. **Abstract:** The title **ABSTRACT** should be typed, capitalized and centered, 3 lines below the addresses. This should be followed by a **single-spaced,** concise abstract. Allow 3 lines of space below the abstract before beginning the text of the manuscript.

4. **Text Discussion:** Whenever possible, the text discussion should be divided into major sections such as

INTRODUCTION
MATERIALS
METHODS
RESULTS
DISCUSSION
ACKNOWLEDGEMENTS
REFERENCES

These **major headings** should be separated from the text by two lines of space above and one line of space below. Each major heading should be typed in capital letters, centered and underlined.

Secondary headings, if any, should be placed flush with the left margin, underlined and have the first letter of main words capitalized. Leave two lines of space above and one line of space below secondary headings.

5. The first word of each **paragraph** within the body of the text should be indented five spaces.

6. **Acknowledgements**, sources of research funds and address changes for authors should be listed in a separate section at the end of the manuscript, immediately preceding the references.

7. **References** should be numbered consecutively and placed in a separate section at the end of the manuscript. They should be typed single-spaced, with one line space between each reference. Each reference should contain names of all authors (with initials of their first and middle names); do not use *et al.* for a list of authors. Abbreviations of journal titles will follow the American Chemical Society's Chemical Abstracts List of Periodicals. The word **REFERENCES** should be capitalized and centered above the reference list.

Following are acceptable reference formats:

Journal:

1. D. K. Morgan, N. D. Danielson, J. E. Katon, Anal. Lett., 18: 1979-1998 (1985)

Book:

1. L. R. Snyder, J. J. Kirkland, Introduction to Modern Liquid Chromatography, John Wiley & Sons, Inc., New York, 1979.

2. C. T. Mant, R. S. Hodges, "HPLC of Peptides," in HPLC of Biological Macromolecules, K. M.

Gooding, F. E. Regnier, eds., Marcel Dekker, Inc., New York, 1990, pp. 301-332.

8. Each page of manuscript should be numbered lightly, with a light blue pencil, at the bottom of the page.

9. Only standard symbols and nomenclature, approved by the International Union of Pure and Applied Chemistry (IUPAC) should be used.

10. Material that cannot be typed, such as Greek symbols, script letters and structural formulae, should be drawn carefully with dark black India ink. Do not use any other color ink.

Additional Typing Instructions

1. The manuscript must be prepared on good quality **white bond paper**, measuring approximately 8½ x 11 inches (21.6 cm x 27 9 cm). The typing area of the first page, including the title and authors, should be 5½ inches wide by 7 inches high (14 cm x 18 cm). The typing area of all other pages should be no more than 5½ inches wide by 8½ inches high (14 cm x 21.6 cm).

2. The **title, abstract, tables and references** are typed single-spaced. All other text should be typed 1½-line spaced or double line spaced.

3. It is essential to use **dark black** typewriter or printer ribbon so that clean, clear, **solid characters** are produced. Characters produced with a dot/matrix printer are not acceptable, even if they are "near letter quality" or "letter quality." Erasure marks, smudges, hand-drawn corrections and creases are not acceptable.

4. **Tables** should be typed on separate pages, one table to a page. A table may not be longer than one page. If a table is larger than one page, it should be divided into more than one table. The word **TABLE** (capitalized and followed by an Arabic number) should precede the table and should be centered above the table. The title of the table should have the first letters of all main words in capitals. Table titles should be typed single line spaced, across the full width of the table.

5. **Figures (drawings, graphs, etc.)** should be professionally drawn in **black** India ink on separate sheets of **white** paper, and should be placed at the end of the text. They should not be inserted in the body of the text. They should not be reduced to a small size. Preferred size for figures is from 5 inches x 7 inches (12.7 cm x 17.8 cm) to 8½ inches by 11 inches (21.6 cm x 27.9 cm). **Photographs** should be professionally prepared *glossy* prints. A typewriter or lettering set should be used for all labels on the figures or photographs; they may not be hand drawn.

Captions for figures should be typed single-spaced on a separate sheet of white paper, along the full width of the type page, and should be preceded with the word FIGURE and an Arabic numeral. All figures and lettering must be of a size that will remain legible after a 20% reduction from the original size. Figure numbers, name of senior author and an arrow indicating "top" should be written in light blue pencil on the back of the figure. Indicate the approximate placement for each figure in the text with a note written with a light blue pencil in the margin of the manuscript page.

6. The **reference list** should be typed single-spaced. A single line space should be inserted after each reference. The format for references should be as given above.

Keep abreast of the **latest** *theoretical and applied research developments in the field with...*

Contains over 340 equations, tables, drawings, and photographs!

Advances in Chromatography

Volume 34

edited by
PHYLLIS R. BROWN, *University of Rhode Island, Kingston*
ELI GRUSHKA, *The Hebrew University of Jerusalem, Israel*

May, 1994 / 456 pages, illustrated / $165.00

Reviewer praise for this valuable series...

"...the articles [are] of high scientific standard, up to date, very well written, and interesting to read... well presented and edited."
—Journal of Chromatography

"...a valuable contribution to the chromatography literature...belongs in every library used by chromatographers." *—Liquid Chromatography*

"...maintains the high quality that chromatographers have come to expect from this invaluable series." *—Journal of Pharmaceutical Sciences*

The rapidly expanding growth of the literature on chromatography and capillary electrophoresis makes it difficult for any single individual to maintain a coherent view of progress in the field. Rather than attempt to read the avalanche of original research papers, investigators trying to preserve even a modest awareness of advances must rely upon **authoritative** surveys.

Featuring reliable, **up-to-the-minute** reviews of major developments in chromatography, this critically praised series separates the most important advances from an overabundance of supplementary materials.

Internationally acclaimed experts analyze the most current *innovations in their areas of specialization!*

Furnishing more than **800** literature citations, allowing for further, in-depth study of recent trends in research, **Volume 34** examines timely subjects such as

- high performance capillary electrophoresis—*of particular interest to engineers, chemists, biotechnologists, and environmental scientists*
- gas chromatography, matrix isolation, and infrared spectrometry—*geared toward the needs of food scientists, medical professionals, and agriculturalists*
- statistical theories of peak overlap in chromatography —*especially applicable to quality control engineers*
- capillary electrophoresis of carbohydrates and proteins —*expressly for pharmacologists, biochemists, biologists, and medical professionals*
- supercritical fluid chromatography—*essential for chemists, environmental scientists, engineers, and biologists*
- and much more!

Advances in Chromatography is an indispensable resource for all researchers who need to use separation methods effectively—especially analytical, organic, inorganic, clinical, and physical chemists; chromatographers; biochemists and biological chemists; agrochemists; chemical, materials, and quality control engineers; biotechnologists; toxicologists; pharmacologists; pharmacists; physiologists; zoologists; botanists; food, cosmetic, polymer, and environmental scientists; oceanographers; research and quality control scientists in academia, government, hospitals, and industry; and upper-level undergraduate and graduate students in these disciplines.

Contents

ISBN: 0—8247—9087—1

This book is printed on acid-free paper.

Marcel Dekker, Inc.

270 Madison Avenue, New York, NY 10016
(212) 696-9000

Hutgasse 4, Postfach 812, CH-4001 Basel, Switzerland
Tel. 061-261-8482

JOURNAL OF LIQUID CHROMATOGRAPHY, 17(18), (1994)

Contents Continued

GENERAL PAPERS

JOURNAL OF LIQUID CHROMATOGRAPHY

Volume 17, Number 18, 1994

Special Section on
Capillary Zone Electrophoresis
and Related Techniques

CONTENTS

(continued on inside back cover)

MARCEL DEKKER, INC. New York, Basel, Hong Kong
Contributions to this journal are published free of charge